August 2020

Role of CYP2B in Unsaturated Fatty Acid Metabolism, Obesity, and Non-Alcoholic Fatty Liver Disease

Melissa Heintz
Clemson University, mheintz@g.clemson.edu

ROLE OF CYP2B IN UNSATURATED FATTY ACID METABOLISM, OBESITY, AND NON-ALCOHOLIC FATTY LIVER DISEASE

A Dissertation
Presented to
the Graduate School of
Clemson University

In Partial Fulfillment
of the Requirements for the Degree
Doctor of Philosophy
Environmental Toxicology

---

by
Melissa Marie Heintz
August 2020

Accepted by:
Dr. William S. Baldwin, Committee Chair
Dr. Saurabh Chatterjee
Dr. Charles Rice
Dr. Christopher Saski

ABSTRACT

Obesity is closely linked to the development of nonalcoholic fatty liver disease (NAFLD). The prevalence of obesity is increasing in the United States, and the most recent 2017-2018 National Health and Nutrition Examination Survey recorded 42.4% of adults are obese. Cytochrome P450s (CYPs) play a primary role in phase I detoxification pathways, which in humans, includes over 90% of phase I-dependent metabolism of clinically used drugs, especially within CYP families 1-3. These enzymes also metabolize a vast number of environmental pollutants including industrial and agricultural chemicals, as well as endogenous compounds such as steroids, bile acids, and fatty acids. Hepatic CYP activity has been associated with fatty liver and the main regulator of CYP2B, the constitutive androstane receptor (CAR), has been identified as an anti-obesity transcription factor as its activation improved hepatic glucose and fatty acid metabolism in leptin-deficient mice. Thus, indicating a role for CAR in recognizing and Cyp2b in metabolizing hepatic lipids. Initial studies determined male Cyp2b-null mice are diet-induced obese with increased liver triglycerides. Cyp2b-null male mice fed a normal diet also showed hepatic gene expression and phospholipid profiles similar to wild-type mice fed a high fat diet (HFD), indicating progression to NAFLD even in the absence of a high-fat diet. Based on these results, we hypothesized that Cyp2bs are crucial in the hepatic metabolism and elimination of unsaturated fatty acids and continued to study the role of Cyp2b in the progression to nonalcoholic steatohepatitis (NASH) using our Cyp2b-null mouse model. Unexpectedly, the lack of Cyp2b in female mice was moderately protective from diet-induced NASH, while male Cyp2b-null mice were more

susceptible to NAFLD, with few significant changes in NASH development. Therefore, murine Cyp2b enzymes are anti-obesogenic in males; however, there are some important interspecies differences between mouse and human CYPs. Therefore, PUFA metabolites of human CYP2B6 were identified from CYP2B6 containing baculosomes by LC-MS/MS. Results indicate human CYP2B6 primarily metabolizes PUFAs in the 9- and 13-positions with a preference for □-linolenic acid in vitro. To increase relevance to humans, we produced a humanized CYP2B6 transgenic mouse and tested whether CYP2B6 could reverse diet-induced obesity when compared to Cyp2b-null mice. CYP2B6 partially reverses diet-induced obesity observed in Cyp2b-null mice, but with unexpected sexually dimorphic effects on obesity in females and fatty liver disease in males. Metabolic disease was also associated with oxylipin profiles and gene expression. Surprisingly, linoleic acid and arachidonic acid – based oxylipins were primarily altered in vivo; probably due to higher concentrations of these PUFAs in the mouse diet. Differential gene expression revealed changes in gene ontology terms associated with circadian rhythm, protein processing and lipid metabolism in humanized CYP2B6 transgenic mice. In conclusion, the changes in expression or inhibition of CYP2B6 may perturb lipid homeostasis, utilization, and metabolism and lead to adverse outcomes, primarily in males.

DEDICATION

To my dearest family and friends,

especially to my parents, Wendy and David Heintz,

for their steadfast love and support in all my endeavors.

ACKNOWLEDGMENTS

I am sincerely grateful to my advisor Dr. Bill Baldwin for being an excellent mentor throughout my PhD degree. Dr. Baldwin's constant encouragement and support to challenge myself as scientist is what helped me to develop into the toxicologist that I am today. I would also like to extend my thanks to my committee members, Dr. Charlie Rice, Dr. Chris Saski, and Dr. Saurabh Chatterjee for their guidance and support, as well as Dr. Rooksie Noorai for being a wonderful teacher and turning me on to genomics and bioinformatics.

Furthermore, I am thankful for all of my peers that have helped me throughout this process, including all of my past and present lab mates, Allison Schmidt, Chad Mansfield, Matt Hamilton, and Jazmine Eccles, and especially Dr. Ramiya Kumar for taking me under her wing and training me in the lab. I would also like to particularly thank Emily Olack and Emily Gessner, two great undergraduate students that assisted me with numerous experiments throughout my time at Clemson. I would also like to extend my thanks and gratitude to all my fellow 3rd floor Jordan Hall neighbor lab members, especially in Dr. Bain's, Dr. Rice's and Dr. Feliciano's lab, all who have become dear friends and colleagues.

Many thanks to my parents, family, and friends that have been so supportive in my decision to pursue a PhD. I am also thankful that I had my dearest partner, Fred Giffels, by my side the entire way. His patience, encouragement, love, and support from beginning to end made the journey that much better.

TABLE OF CONTENTS

Table of Contents (Continued)

Page

LIST OF TABLES

LIST OF FIGURES

List of Figures (Continued)

List of Figures (Continued)

Figure Page

List of Figures (Continued)

Figure Page

List of Figures (Continued)

Figure Page

CHAPTER ONE

INTRODUCTION

The purpose of this study was to investigate the potential for chemical inhibition of the detoxification enzyme cytochrome P450 2B (CYP2B), and the subsequent effects on fatty acid metabolism, obesity, and nonalcoholic fatty liver disease. Previous research found hepatic cytochrome P450 oxidoreductase-null mice, lacking all hepatic CYP activity, develop fatty liver disease with increased amounts of polyunsaturated fatty acids (PUFAs) in the liver, and induction of Cyp2b10 via activation of the constitutive androstane receptor (CAR) (Finn, Henderson, Scott, & Wolf, 2009). In addition, an RNAi-mediated Cyp2b-knockdown mouse model previously generated in our lab to study the function of Cyp2b *in vivo* (B. Damiri, Holle, Yu, & Baldwin, 2012), found male Cyp2b-knockdown mice showed increased weight and adiposity with age, and had difficulty clearing lipids in their liver (Basma Damiri & Baldwin, 2018). In order to provide a more stable drop in hepatic Cyp2b levels in the mouse, a Cyp2b9/10/13-null (Cyp2b-null) mouse model was also produced in our lab by eliminating a cluster of *Cyp2b* genes on chromosome 7 using Crispr/Cas9. This model was used to further investigate the role of Cyp2b in hepatic lipid metabolism. Initial studies determined male Cyp2b-null mice are diet-induced obese and develop weak nonalcoholic fatty liver disease (NAFLD) (Data by R. Kumar; (Heintz, Kumar, Rutledge, & Baldwin, 2019). Based on these results, we hypothesized that Cyp2bs are crucial in the hepatic metabolism and elimination of unsaturated fatty acids and continued to study the role of Cyp2b in the progression to nonalcoholic steatohepatitis (NASH). Lastly, CYP2B6

containing baculosomes and a newly generated humanized-CYP2B6-Tg mouse model were used to determine the metabolic role of human CYP2B6 *in vitro* and *in vivo*, respectively.

1.1. Obesity and progression to nonalcoholic fatty liver disease (NAFLD)

Obesity is a chronic disease, defined as an abnormal or excessive accumulation of fat that may impair health (Bray & Ryan, 2000). The prevalence of obesity in adults aged 20 and over is increasing in the United States, from 30.5% in 1999-2000 to 42.4% in the most recent 2017-2018 National Health and Nutrition Examination Survey (Hales, Carroll, Fryar, & Ogden, 2020). Obesity occurs when energy intake exceeds energy expenditure over an extended time, and is confounded by lifestyle changes (Church & Martin, 2018), food environment (Hall, 2018), genetics (Levian, Ruiz, & Yang, 2014), and environmental and behavioral factors (Keith et al., 2006). Some of these environmental factors include exposure to environmental toxicants that perturb metabolic homeostasis leading to obesity (Hoffman, Petriello, & Hennig, 2017). Individuals with obesity often further develop diseases such as hypertension, type II diabetes, cardiovascular diseases, and certain types of cancer (Must et al., 1999).

NAFLD is closely linked to obesity (Pallayova & Taheri, 2014) and is the result of the hepatic manifestation of the metabolic syndrome (Marchesini et al., 2001). Abdominal obesity, hyperglycemia, insulin resistance, hypertension and atherogenic dyslipidemia make up the cluster of risk factors that form metabolic syndrome (Gallagher, LeRoith, & Karnieli, 2008). The hepatic intracellular accumulation of lipids

in fatty liver disease can develop into NASH as inflammation, injury and fibrosis progresses (Singh et al., 2015).

Nuclear receptors are master regulators of metabolic homeostasis, that activate or inhibit key metabolic processes and transcription factors in response to dietary intake or environmental stressors. Several nuclear receptors are implicated in obesity or NAFLD. These receptors often work by forming heterodimers with the retinoid X receptor (RXR) before binding to promoter regions of target genes (Swanson et al., 2013). The hepatic lipid regulator, peroxisome proliferator-activated receptor alpha (PPARα), is protective from fatty liver and NASH, as PPARα-null mice fed a high fat diet (HFD) developed oxidative stress, steatosis and inflammation (Abdelmegeed et al., 2011). Additionally, the hepatoprotective effects of bile acids are farnesoid X receptor (FXR)-dependent (Kunne et al., 2014), and as FXR activity decreases with age, fatty liver increases in mice (Xiong et al., 2014). The xenobiotic receptors, pregnane X receptor (PXR) and constitutive androstane receptor (CAR) also have endobiotic roles in glucose and lipid metabolism and the development of metabolic diseases (Gao & Xie, 2010); however, their functions oppose one another, as PXR causes obesity (Spruiell et al., 2014) while CAR is protective from obesity (Dong et al., 2009).

Furthermore, the Organization for Economic Cooperative Development (OECD) identified obesity and diabetes as one of three areas of toxicological concern in addition to autism spectral disorders and testicular dysgenesis (LeBlanc et al., 2012). Xenobiotic activation of the neonatal estrogen receptor, PPARγ:RXR receptor complex, and glucocorticoid receptor all stimulate weight gain (via adipocyte differentiation) and

associated metabolic conditions (Dallman et al., 2004; Grun & Blumberg, 2006; Newbold, Padilla-Banks, & Jefferson, 2009). Chemicals established as "obesogens" bind and activate these receptors, perturbing lipid homeostasis and causing obesity (Grun et al., 2006).

1.2. Polyunsaturated fatty acid (PUFA) metabolism

During inflammation, PUFAs found in hepatic membrane phospholipids are cleaved by phospholipase A2 (Quach, Arnold, & Cummings, 2014). These available PUFAs are then oxidized by cyclooxygenase (COX), lipoxygenase (LOX), or cytochrome P450 (CYP) pathways to form physiologically significant metabolites. The COX pathway primarily leads to the formation of pain and inflammation mediators, such as prostanoids and resolvins. Consequently, the COX pathway is a therapeutic target of several anti-inflammatory drugs. The LOX pathway produces proinflammatory leukotrienes and hydroxyl fatty acids which have an important role in inflammatory diseases such as asthma (Funk, 2001; Wiktorowska-Owczarek, Berezinska, & Nowak, 2015). Individual CYP enzymes differ in their PUFA substrate specificities in addition to positional- and stereo-selectivity. The CYP4A and CYP4F subfamilies mainly function as PUFA hydroxylases (Fer et al., 2008), while CYP2C and CYP2J are well studied PUFA epoxygenases (Zhang, Kodani, & Hammock, 2014). Additionally, CYPs including CYP1A, CYP1B, CYP2B, CYP2C, CYP2D, CYP2J, CYP3A, CYP4A, and CYP4F have all demonstrated PUFA metabolism (Hankinson, 2016; Palacharla et al., 2017; Zeldin, 2001; Zhang et al., 2014). CYP lipid metabolites are important mediators of

inflammation and metabolic disease, as fatty acid epoxide metabolites have anti-inflammatory, cardioprotective, and vasodilative effects (Zeldin, 2001; Zhang et al., 2014). Conversely, the bioactivity of lipid metabolites produced via CYP hydroxylation are not as well known, with the exception of arachidonic acid metabolite 20-hydroxyeicosatetraenoic acid (HETE), which is synthesized by the CYP4 family and plays an important role in vascular inflammation and injury (Hoopes, Garcia, Edin, Schwartzman, & Zeldin, 2015).

1.3. Cytochrome P450s (CYPs)

In addition to PUFAs such as arachidonic acid (Zhang et al., 2014) and linoleic acid (Finn et al., 2009), CYPs also metabolize other endobiotics including steroids and bile acids (Finn et al., 2009; Nebert & Russell, 2002; Wang & Tompkins, 2008). CYPs play a primary role in phase I detoxification pathways, which in humans, includes over 90% of phase I-dependent metabolism of clinically used drugs (Purnapatre, Khattar, & Saini, 2008), especially CYP families 1-3 (Hernandez, Mota, & Baldwin, 2009). These enzymes also metabolize a vast number of environmental xenobiotics including industrial and agricultural chemicals (Hernandez, Mota, & Baldwin, 2009). There are 57 CYP genes in humans, organized into 18 families and 42 subfamilies (Nelson & Nebert, 2011), and 102 murine CYP genes, with 18 families and 43 subfamilies (Nelson et al., 2004). CYP expression is regulated by nuclear receptors including CAR, pregnane X receptor (PXR), aryl hydrocarbon receptor (AhR), and peroxisome proliferator activated receptor-alpha (PPARα). Examples of important CYPs and their respective receptors are as

follows: Ahr predominantly regulates the CYP1A subfamily (Qiang, 2001), CAR and PXR regulate both CYP2B and CYP3A, with CAR primarily inducing CYP2B and PXR inducing CYP3A (Hernandez, Mota, & Baldwin, 2009), and PPARα regulates CYP4A (Cheng & Klaassen, 2008; Kroetz, Yook, Costet, Bianchi, & Pineau, 1998). Other CYP subfamilies not listed such as CYP1B, CYP2A, and CYP2C are also regulated by these receptors (Chen et al., 2012; Hernandez, Mota, & Baldwin, 2009; Wortham, Czerwinski, He, Parkinson, & Wan, 2007).

1.4. Constitutive androstane receptor (CAR)

CAR is a member of the "adopted" orphan nuclear receptor subfamily, as it shares many of the structural features found in the nuclear receptor family but is activated by numerous xeno- and endobiotic chemicals (Chang & Waxman, 2006; Evans, 2005; Kretschmer & Baldwin, 2005). This nuclear receptor regulates phase I-III enzymes and transporters that are imperative for detoxification and elimination of environmental toxicants, steroids, and bile acids. Detoxification genes induced by CAR include phase I detoxification CYPs (e.g. CYP2B and CYP3A) (P. Wei, Zhang, Egan-Hafley, Liang, & Moore, 2000), phase II sulfotransferases (Saini et al., 2004) and uridine diphospho-glucuronosyltransferases (Sugatani et al., 2001), and phase III transporters such as multidrug resistance proteins (Assem et al., 2004) and multidrug resistance associated proteins (Kast et al., 2002). Direct ligand binding to CAR, such as by 1,4-bis[2-(3,5-dichloropyridyloxy)]benzene (TCPOBOP) in the cytoplasm causes cytoplasmic retention proteins including heat shock protein 90 (hsp90) and cytoplasmic CAR retention protein

(CCRP) to release (Kobayashi, Sueyoshi, Inoue, Moore, & Negishi, 2003; Yoshinari, Kobayashi, Moore, Kawamoto, & Negishi, 2003), allowing for subsequent translocation of CAR to the nucleus and heterodimerization with RXR. This complex then binds to direct repeats-4 (DR-4) and inverted repeats-6 (IR-6) in the phenobarbital response element module (PBREM) of the *CYP2B* promoter, and recruits histone acetylases and co-activators to activate transcription and induce target genes (Sueyoshi & Negishi, 2001). Phenobarbital and other chemicals can also indirectly activate CAR through formation of reactive oxygen species or other stressors that cause a phosphorylation cascade resulting in a conformational change and translocation of CAR into the nucleus (Blattler, Rencurel, Kaufmann, & Meyer, 2007; Shindo, Numazawa, & Yoshida, 2007).

Recent studies investigating the regulation of CYPs by CAR indicate that CAR is involved in regulating the metabolism of fats. Dong et al. (Dong et al., 2009) found that the activation of CAR by TCPOBOP in leptin-deficient (ob/ob) mice improved glucose metabolism, suppressed lipogenesis and induced β-oxidation, whereas these antidiabetic effects were lost in double mutant ob/ob CAR-/- mice. Additional studies have also shown the role of CAR in recognizing endogenous compounds and stressors as seen by CAR's involvement with fatty acid metabolism (Finn et al., 2009), caloric restriction (Maglich et al., 2004), obesity (Maglich, Lobe, & Moore, 2009), and bile acid homeostasis (Saini et al., 2004). Finn et al (Finn et al., 2009) demonstrated that a loss of hepatic CYP activity in the hepatic P450 oxidoreductase (POR)-null mouse model led to hepatic steatosis and the induction of Cyp2b primarily through the activation of CAR,

thus indicating a major role for CAR in recognizing hepatic lipids and Cyp2b in metabolizing lipids.

1.5. CYP2B

In the liver, CAR regulates both human and murine *CYP2B* genes (Finn et al., 2009; Hernandez, Mota, & Baldwin, 2009; Hoek-van den Hil et al., 2014). *Cyp2b9*, *Cyp2b10*, and *Cyp2b13* make up the hepatic Cyp2b genes in mice, and *CYP2B6* is the main hepatic CYP2B isoform in humans. While all three murine hepatic Cyp2b members are constitutively regulated by CAR (Kumar et al., 2017; Mota, Hernandez, & Baldwin, 2010), *Cyp2b10* is the member that is highly induced by exposure to xenobiotic chemicals (Cheng & Klaassen, 2008; Hernandez, Mota, Huang, Moore, & Baldwin, 2009). Previously, the CYP2B subfamily was thought to have a negligible role in drug metabolism, but due to more sensitive and specific detection methods, the number of endobiotic and xenobiotic substrates of CYP2B6 is increasing; in addition to the interindividual variability in expression of CYP2B6 (Wang & Tompkins, 2008). CYP2B6 is primarily expressed in the liver and constitutes 2-10% of the total hepatic CYP content (Wang & Tompkins, 2008). This enzyme has many substrates, including over 60 clinical drugs such as artemisinin, propofol, ketamine, ifosfamide, nevirapine, efavirenz, mephobarbital, bupropion, and tamoxifen (Mo et al., 2009). Many important environmental toxicants are also metabolized by CYP2B6 including chlorpyrifos (Tang et al., 2001), carbaryl (Hodgson & Rose, 2007), parathion (Foxenberg, McGarrigle, Knaak, Kostyniak, & Olson, 2007), triclosan (Wu et al., 2017), perfluorocarboxylic acids (Abe et

al., 2017), as well as insect repellant *N,N*-diethyl-*m*-toluamide (DEET) (Hodgson & Rose, 2007). Additionally, endogenous compounds such as estrone, testosterone, arachidonic acid, and lauric acid are also metabolized by this enzyme (Mo et al., 2009).

Unlike the centrilobular distribution of other major hepatic CYPs such as CYP3A4 and CYP2E1, CYP2B6 is widely expressed throughout hepatic lobules across zone 1 and 3 in parenchymal cells (Murray et al., 1990). CYP2B6 is also expressed in several extrahepatic tissues including the kidney, brain, intestine, endometrium, bronchoalveolar macrophages, peripheral blood lymphocytes and skin (Ding & Kaminsky, 2003). As mentioned earlier, CYP2B6 expression is closely regulated and activated by CAR upon ligand binding (P. Wei et al., 2000). In addition, this enzyme can be regulated directly by PXR (Goodwin, Moore, Stoltz, McKee, & Kliewer, 2001) and indirectly by the glucocorticoid receptor (Dvorak et al., 2003).

The hepatic murine Cyp2b members, *Cyp2b9* and *Cyp2b13* are highly sexually dimorphic (Hernandez, Mota, Huang, et al., 2009; Renaud, Cui, Khan, & Klaassen, 2011; Wiwi, Gupte, & Waxman, 2004), and CAR regulation of several genes including *Cyp2b10* is also sexually dimorphic (Ledda-Columbano et al., 2003). Signal transducer and activator of transcription 5b (Stat5b) mediates growth hormone (GH)-dependent sexually dimorphic gene expression in the male liver (Clodfelter et al., 2006). The male GH secretion profile suppresses the GH-STAT5b pathway (Holloway et al., 2007; Sakuma et al., 2004); however in females, through the regulation of HNF4α, CAR, and FoxA2, this pathway is responsible for the female predominant expression of Cyp2b (Hashita et al., 2008; Hernandez, Mota, Huang, et al., 2009; Wiwi et al., 2004). These

gender differences are also seen in human CYP2B6, as it is also predominantly expressed in females although to a much lesser extent (Lamba et al., 2003).

Several studies implicate Cyp2b's role in hepatic fatty acid metabolism. Foxa2 is activated by fasting and fatty acids, and induces transcription of β-oxidation, ketogenesis, and glycolysis genes in mice, including *Cyp2b9* (Hashita et al., 2008; Wolfrum, Asilmaz, Luca, Friedman, & Stoffel, 2004). Additionally, Cyp2b is induced via CAR activation due to increased hepatic fatty acids in POR-null mice (Finn et al., 2009). Furthermore, two recent studies demonstrate that Cyp2b9 exhibited the highest increased expression following a HFD in mice (Hoek-van den Hil et al., 2015; Leung, Trac, Du, Natarajan, & Schones, 2016). Previous research in our lab using RNAi-mediated Cyp2b-knockdown mice found older males had increased weight, adiposity, and difficulty eliminating PUFA-rich corn oil (Basma Damiri & Baldwin, 2018). This research suggests mice lacking hepatic Cyp2b members are highly susceptible to obesity and accumulate lipids in their liver.

1.6. Mouse models

House mice, *Mus musculus*, have long served as models of human biology and disease due to their genetic and physiological similarities to humans (Morse, 2007). As a model organism, the mouse genome is very similar to the human genome (99%), and the animal's small size and relatively short lifecycle makes it a cost-efficient model. C57Bl/6J mice are the most extensively used inbred strain, as a result, their genetic

similarities and differences to humans are well-studied and are employed in a wide variety of biomedical research areas, including diabetes and obesity (Bryant, 2011).

To investigate the role of Cyp2b in diet-induced obesity and NASH, our lab developed a novel triple knockout mouse model lacking the hepatic Cyp2b members, *Cyp2b9*, *Cyp2b10* and *Cyp2b13* using CRISPR/Cas9 technology on C57Bl/6J background (Kumar et al., 2017). These three Cyp2b genes are found in a cluster on murine chromosome seven. Three short guide RNAs (sgRNA) were co-injected to mediate out of frame modifications within each gene, ultimately producing a large 287 kb deletion between the sgRNA Cyp2b10 and Cyp2b9 target sites. Five genes apart from this Cyp2b cluster are *Cyp2b19* and *Cyp2b23* which are still retained in this mouse model. Cyp2b19 is expressed in fetal mouse keratinocytes (Keeney et al., 1998), while Cyp2b23 is only expressed in adolescent mice (from birth until 20 days old) (Peng et al., 2012); therefore, neither of these Cyp2b genes make a significant contribution to hepatic Cyp2b expression.

In order to study the role of human CYP2B6 in diet-induced obesity and PUFA metabolism *in vivo*, our lab also generated a humanized-CYP2B6-transgenic (Tg) mouse model. *CYP2A13/CYP2B6/CYP2F1*-Tg mice from Dr. Xinxin Ding's laboratory containing a bacterial artificial chromosome (BAC) of 210 kb from human chr19 (Y. Wei et al., 2012) were bred to Cyp2b-null mice from our laboratory (Kumar et al., 2017) to produce humanized-CYP2B6-Tg (hCYP2B6-Tg) mice lacking the hepatic murine Cyp2b members. These mice also express CYP2A13, which is primarily expressed in the nasal

mucosa and lung and CYP2F1, which is primarily expressed in the lung (Y. Wei et al., 2012).

1.7. Specific aims

CYP2B6 makes up 2-10% of the total hepatic CYP content (Wang & Tompkins, 2008) and metabolizes both xeno- and endobiotic compounds including clinical drugs (Zanger & Klein, 2013), environmental toxicants (Hernandez, Mota, & Baldwin, 2009; Hodgson & Rose, 2007), fatty acids (Palacharla et al., 2017), steroids, and bile acids (Mo et al., 2009). *In vitro* data indicates that PUFAs such as arachidonic acid and linoleic acid are metabolized by Cyp2b (Finn et al., 2009; Mo et al., 2009; Palacharla et al., 2017). In addition, our lab previously determined that mice lacking hepatic Cyp2b members are highly susceptible to obesity and accumulate lipids in their liver (Basma Damiri & Baldwin, 2018). We hypothesize that Cyp2bs play an important role in hepatic metabolism and the elimination of unsaturated fatty acids. We will continue to study the role of Cyp2b in fatty acid metabolism and in the development of NAFLD and the progression to NASH using our previously developed Cyp2b-null mouse model (Kumar et al., 2017). A humanized-CYP2B6-transgenic mouse model will also be produced to determine the role of human CYP2B6 in obesity and the metabolism of fatty acids *in vivo*.

Aim 1: Identify differentially expressed genes involved in energy and fatty acid metabolism in high fat diet (HFD)-fed Cyp2b-null mice compared to WT mice.

Aim 1a: RNA sequencing (RNAseq) will be used to detect changes in global hepatic gene expression and to test whether Cyp2b-null mice fed either a normal diet (ND) or high-fat diet (HFD) have perturbed regulation of genes involved in fatty acid metabolism, gluconeogenesis, lipogenesis, insulin signaling, and inflammation.

Aim 2: Test whether a lack of Cyp2b worsens or remediates the pathological effects of non-alcoholic steatohepatitis (NASH).

Aim 2a: Cyp2b-null and WT mice will be fed a ND or choline-deficient, L-amino acid defined, high fat diet (CDAHFD) for 8 weeks. Mouse weight, tissue weights, lipid serum panel, fasting serum glucose, glucose tolerance, and pathological staining for steatosis and fibrosis will be measured for each treatment.

Aim 2b: RNAseq will be used to determine changes in genes involved in regulating fatty acid metabolism, inflammation, and liver fibrosis development in Cyp2b-null mice compared to WT mice. Differentially expressed genes identified by RNAseq will be confirmed by qPCR.

Aim 2c: Changes in serum and liver biomarkers of fatty liver, fibrosis, inflammation, and stress will also be measured for each treatment group.

Aim 3: Determine changes in the hepatic phospholipid profile of healthy, obese, and old Cyp2b-null male mice.

Aim 3a: Phospholipid species will be identified and quantified from the livers of male Cyp2b-null and WT young (4.5 mo) ND and HFD-fed mice and old (9 mo) mice by LC-MS/MS. Changes in lipid species content will be compared between genotypes within and across treatment groups.

Aim 3b: Changes in serum and liver lipids and biomarkers will be determined between healthy, diet-induced obese, and old Cyp2b-null and WT mice. Correlations between treatment groups, Cyp2b-null mice, adverse physiological effects, serum lipids, and lipid profiles will be assessed by Principal Component Analysis (PCA).

Aim 4: Investigate the role of human CYP2B6 in PUFA metabolism *in vitro* and *in vivo*.

Aim 4a: Endogenous inhibitors of CYP2B6 will be determined using CYP2B6 containing baculosomes.

Aim 4b: Metabolites of PUFAs produced by CYP2B6 will be identified and quantified following incubation with control and CYP2B6 containing baculosomes using LC-MS/MS.

Aim 4c: A humanized-CYP2B6-transgenic (hCYP2B6-Tg) mouse model will be created by crossing the C57Bl/6J background, Cyp2b-null mouse model with a human

CYP2A13/2B6/2F1-Tg mouse model. The purpose of the humanized model is to reduce uncertainty when estimating effects in humans.

Aim 4d: Cyp2b-null and hCYP2B6-Tg female and male mice will be fed a high-fat diet for 16 weeks. Mouse weight, tissue weights, lipid serum panel, fasting serum glucose, glucose tolerance, and pathological staining for steatosis will be measured for each treatment group.

Aim 4e: Serum and liver PUFA metabolites will be identified and quantified by LC-MS/MS from HFD-fed Cyp2b-null and hCYP2B6-Tg mice.

Aim 4f: RNAseq will be used to determine changes in global hepatic gene expression in mice with human CYP2B6 compared to mice lacking all hepatic Cyp2b members under HFD conditions and to test whether genes involved in fatty acid metabolism, lipogenesis, and insulin signaling are differentially expressed in hCYP2B6-Tg mice.

References

Abdelmegeed, M. A., Yoo, S.-H., Henderson, L. E., Gonzalez, F. J., Woodcroft, K. J., & Song, B.-J. (2011). PPARα Expression Protects Male Mice from High Fat–Induced Nonalcoholic Fatty Liver. *The Journal of Nutrition, 141*(4), 603-610. doi:10.3945/jn.110.135210

Abe, T., Takahashi, M., Kano, M., Amaike, Y., Ishii, C., Maeda, K., . . . Yoshinari, K. (2017). Activation of nuclear receptor CAR by an environmental pollutant

perfluorooctanoic acid. *Arch Toxicol, 91*(6), 2365-2374. doi:10.1007/s00204-016-1888-3

Assem, M., Schuetz, E. G., Leggas, M., Sun, D., Yasuda, K., Reid, G., . . . Schuetz, J. D. (2004). Interactions between hepatic Mrp4 and Sult2a as revealed by the constitutive androstane receptor and Mrp4 knockout mice. *J Biol Chem, 279*(21), 22250-22257. doi:10.1074/jbc.M314111200

Blattler, S. M., Rencurel, F., Kaufmann, M. R., & Meyer, U. A. (2007). In the regulation of cytochrome P450 genes, phenobarbital targets LKB1 for necessary activation of AMP-activated protein kinase. *Proc Natl Acad Sci U S A, 104*(3), 1045-1050. doi:10.1073/pnas.0610216104

Bray, G. A., & Ryan, D. H. (2000). Clinical evaluation of the overweight patient. *Endocrine, 13*(2), 167-186. doi:10.1385/endo:13:2:167

Bryant, C. D. (2011). The blessings and curses of C57BL/6 substrains in mouse genetic studies. *Annals of the New York Academy of Sciences, 1245*, 31-33. doi:10.1111/j.1749-6632.2011.06325.x

Chang, T. K., & Waxman, D. J. (2006). Synthetic drugs and natural products as modulators of constitutive androstane receptor (CAR) and pregnane X receptor (PXR). *Drug metabolism reviews, 38*(1-2), 51-73. doi:10.1080/03602530600569828

Chen, H.-S., Chiang, P.-H., Wang, Y.-C., Kao, M.-C., Shieh, T.-H., Tsai, C.-F., & Tsai, E.-M. (2012). Benzyl butyl phthalate induces necrosis by AhR mediation of CYP1B1 expression in human granulosa cells. *Reproductive Toxicology, 33*(1), 67-75. doi:https://doi.org/10.1016/j.reprotox.2011.11.004

Cheng, X., & Klaassen, C. D. (2008). Perfluorocarboxylic Acids Induce Cytochrome P450 Enzymes in Mouse Liver through Activation of PPAR-α and CAR Transcription Factors. *Toxicological Sciences, 106*(1), 29-36. doi:10.1093/toxsci/kfn147

Church, T., & Martin, C. K. (2018). The Obesity Epidemic: A Consequence of Reduced Energy Expenditure and the Uncoupling of Energy Intake? *Obesity (Silver Spring), 26*(1), 14-16. doi:10.1002/oby.22072

Clodfelter, K. H., Holloway, M. G., Hodor, P., Park, S.-H., Ray, W. J., & Waxman, D. J. (2006). Sex-Dependent Liver Gene Expression Is Extensive and Largely Dependent upon Signal Transducer and Activator of Transcription 5b (STAT5b): STAT5b-Dependent Activation of Male Genes and Repression of Female Genes Revealed by Microarray Analysis. *Molecular Endocrinology, 20*(6), 1333-1351. doi:10.1210/me.2005-0489

Dallman, M. F., la Fleur, S. E., Pecoraro, N. C., Gomez, F., Houshyar, H., & Akana, S. F. (2004). Minireview: glucocorticoids--food intake, abdominal obesity, and wealthy nations in 2004. *Endocrinology, 145*(6), 2633-2638. doi:10.1210/en.2004-0037

Damiri, B., & Baldwin, W. S. (2018). Cyp2b-Knockdown Mice Poorly Metabolize Corn Oil and Are Age-Dependent Obese. *Lipids, 53*(9), 871-884. doi:10.1002/lipd.12095

Damiri, B., Holle, E., Yu, X., & Baldwin, W. S. (2012). Lentiviral-mediated RNAi knockdown yields a novel mouse model for studying Cyp2b function. *Toxicol Sci, 125*(2), 368-381. doi:10.1093/toxsci/kfr309

Ding, X., & Kaminsky, L. S. (2003). Human extrahepatic cytochromes P450: function in xenobiotic metabolism and tissue-selective chemical toxicity in the respiratory and gastrointestinal tracts. *Annu Rev Pharmacol Toxicol, 43*, 149-173. doi:10.1146/annurev.pharmtox.43.100901.140251

Dong, B., Saha, P. K., Huang, W., Chen, W., Abu-Elheiga, L. A., Wakil, S. J., . . . Moore, D. D. (2009). Activation of nuclear receptor CAR ameliorates diabetes and fatty liver disease. *PNAS, 106*(44), 18831-18836.

Dvorak, Z., Modriansky, M., Pichard-Garcia, L., Balaguer, P., Vilarem, M. J., Ulrichova, J., . . . Pascussi, J. M. (2003). Colchicine down-regulates cytochrome P450 2B6, 2C8, 2C9, and 3A4 in human hepatocytes by affecting their glucocorticoid receptor-mediated regulation. *Mol Pharmacol, 64*(1), 160-169. doi:10.1124/mol.64.1.160

Evans, R. M. (2005). The nuclear receptor superfamily: a rosetta stone for physiology. *Mol Endocrinol, 19*(6), 1429-1438. doi:10.1210/me.2005-0046

Fer, M., Corcos, L., Dréano, Y., Plée-Gautier, E., Salaün, J.-P., Berthou, F., & Amet, Y. (2008). Cytochromes P450 from family 4 are the main omega hydroxylating enzymes in humans: CYP4F3B is the prominent player in PUFA metabolism. *J Lipid Res, 49*(11), 2379-2389. doi:10.1194/jlr.M800199-JLR200

Finn, R. D., Henderson, C. J., Scott, C. L., & Wolf, C. R. (2009). Unsaturated fatty acid regulation of cytochrome P450 expression via a CAR-dependent pathway. *Biochem. J., 417*, 43-54.

Foxenberg, R. J., McGarrigle, B. P., Knaak, J. B., Kostyniak, P. J., & Olson, J. R. (2007). Human hepatic cytochrome p450-specific metabolism of parathion and chlorpyrifos. *Drug Metab Dispos, 35*(2), 189-193. doi:10.1124/dmd.106.012427

Funk, C. D. (2001). Prostaglandins and leukotrienes: advances in eicosanoid biology. *Science, 294*(5548), 1871-1875. doi:10.1126/science.294.5548.1871

Gallagher, E. J., LeRoith, D., & Karnieli, E. (2008). The Metabolic Syndrome—from Insulin Resistance to Obesity and Diabetes. *Endocrinology and Metabolism Clinics of North America, 37*(3), 559-579. doi:https://doi.org/10.1016/j.ecl.2008.05.002

Gao, J., & Xie, W. (2010). Pregnane X receptor and constitutive androstane receptor at the crossroads of drug metabolism and energy metabolism. *Drug metabolism and disposition: the biological fate of chemicals, 38*(12), 2091-2095. doi:10.1124/dmd.110.035568

Goodwin, B., Moore, L. B., Stoltz, C. M., McKee, D. D., & Kliewer, S. A. (2001). Regulation of the human CYP2B6 gene by the nuclear pregnane X receptor. *Mol Pharmacol, 60*(3), 427-431.

Grun, F., & Blumberg, B. (2006). Environmental obesogens: organotins and endocrine disruption via nuclear receptor signaling. *Endocrinology, 147*(6 Suppl), S50-55. doi:10.1210/en.2005-1129

Grun, F., Watanabe, H., Zamanian, Z., Maeda, L., Arima, K., Cubacha, R., . . . Blumberg, B. (2006). Endocrine-disrupting organotin compounds are potent inducers of adipogenesis in vertebrates. *Mol Endocrinol, 20*(9), 2141-2155. doi:10.1210/me.2005-0367

Hales, C. M., Carroll, M. D., Fryar, C. D., & Ogden, C. L. (2020). *Prevalence of obesity and severe obesity among adults: United States, 2017–2018*.

Hall, K. D. (2018). Did the Food Environment Cause the Obesity Epidemic? *Obesity, 26*(1), 11-13. doi:10.1002/oby.22073

Hankinson, O. (2016). The role of AHR-inducible cytochrome P450s in metabolism of polyunsaturated fatty acids. *Drug metabolism reviews, 48*(3), 342-350. doi:10.1080/03602532.2016.1197240

Hashita, T., Sakuma, T., Akada, M., Nakajima, A., Yamahara, H., Ito, S., . . . Nemoto, N. (2008). Forkhead Box A2–Mediated Regulation of Female-Predominant Expression of the Mouse Cyp2b9 Gene. *Drug Metabolism and Disposition, 36*(6), 1080. doi:10.1124/dmd.107.019729

Heintz, M. M., Kumar, R., Rutledge, M. M., & Baldwin, W. S. (2019). Cyp2b-null male mice are susceptible to diet-induced obesity and perturbations in lipid homeostasis. *The Journal of Nutritional Biochemistry, 70*, 125-137. doi:https://doi.org/10.1016/j.jnutbio.2019.05.004

Hernandez, J. P., Mota, L. C., & Baldwin, W. S. (2009). Activation of CAR and PXR by Dietary, Environmental and Occupational Chemicals Alters Drug Metabolism,

Intermediary Metabolism, and Cell Proliferation. *Current Pharmacogenomics Personal Medicine, 7*(2), 81-105. doi:10.2174/187569209788654005

Hernandez, J. P., Mota, L. C., Huang, W., Moore, D. D., & Baldwin, W. S. (2009). Sexually dimorphic regulation and induction of P450s by the constitutive androstane receptor (CAR). *Toxicology, 256*(1), 53-64. doi:https://doi.org/10.1016/j.tox.2008.11.002

Hodgson, E., & Rose, R. L. (2007). The importance of cytochrome P450 2B6 in the human metabolism of environmental chemicals. *Pharmacology & Therapeutics, 113*(2), 420-428. doi:https://doi.org/10.1016/j.pharmthera.2006.10.002

Hoek-van den Hil, E. F., van Schothorst, E. M., van der Stelt, I., Swarts, H. J., van Vliet, M., Amolo, T., . . . Keijer, J. (2015). Direct comparison of metabolic health effects of the flavonoids quercetin, hesperetin, epicatechin, apigenin and anthocyanins in high-fat-diet-fed mice. *Genes Nutr, 10*(4), 469. doi:10.1007/s12263-015-0469-z

Hoek-van den Hil, E. F., van Schothorst, E. M., van der Stelt, I., Swarts, H. J. M., Venema, D., Sailer, M., . . . Keijer, J. (2014). Quercetin decreases high-fat diet induced body weight gain and accumulation of hepatic and circulating lipids in mice. *Genes & Nutrition, 9*(5), 418. doi:10.1007/s12263-014-0418-2

Hoffman, J. B., Petriello, M. C., & Hennig, B. (2017). Impact of nutrition on pollutant toxicity: an update with new insights into epigenetic regulation. *Reviews on Environmental Health, 32*(1-2), 65-72.

Holloway, M. G., Cui, Y., Laz, E. V., Hosui, A., Hennighausen, L., & Waxman, D. J. (2007). Loss of sexually dimorphic liver gene expression upon hepatocyte-specific deletion of Stat5a-Stat5b locus. *Endocrinology, 148*(5), 1977-1986. doi:10.1210/en.2006-1419

Hoopes, S. L., Garcia, V., Edin, M. L., Schwartzman, M. L., & Zeldin, D. C. (2015). Vascular actions of 20-HETE. *Prostaglandins & Other Lipid Mediators, 120*, 9-16. doi:https://doi.org/10.1016/j.prostaglandins.2015.03.002

Kast, H. R., Goodwin, B., Tarr, P. T., Jones, S. A., Anisfeld, A. M., Stoltz, C. M., . . . Edwards, P. A. (2002). Regulation of multidrug resistance-associated protein 2 (ABCC2) by the nuclear receptors pregnane X receptor, farnesoid X-activated receptor, and constitutive androstane receptor. *J Biol Chem, 277*(4), 2908-2915. doi:10.1074/jbc.M109326200

Keeney, D. S., Skinner, C., Travers, J. B., Capdevila, J. H., Nanney, L. B., King, L. E., Jr., & Waterman, M. R. (1998). Differentiating keratinocytes express a novel

cytochrome P450 enzyme, CYP2B19, having arachidonate monooxygenase activity. *J Biol Chem, 273*(48), 32071-32079.

Keith, S. W., Redden, D. T., Katzmarzyk, P. T., Boggiano, M. M., Hanlon, E. C., Benca, R. M., . . . Allison, D. B. (2006). Putative contributors to the secular increase in obesity: exploring the roads less traveled. *International Journal Of Obesity, 30*, 1585. doi:10.1038/sj.ijo.0803326

Kobayashi, K., Sueyoshi, T., Inoue, K., Moore, R., & Negishi, M. (2003). Cytoplasmic accumulation of the nuclear receptor CAR by a tetratricopeptide repeat protein in HepG2 cells. *Mol Pharmacol, 64*(5), 1069-1075. doi:10.1124/mol.64.5.1069

Kretschmer, X. C., & Baldwin, W. S. (2005). CAR and PXR: xenosensors of endocrine disrupters? *Chem Biol Interact, 155*(3), 111-128. doi:10.1016/j.cbi.2005.06.003

Kroetz, D. L., Yook, P., Costet, P., Bianchi, P., & Pineau, T. (1998). Peroxisome Proliferator-activated Receptor α Controls the Hepatic CYP4A Induction Adaptive Response to Starvation and Diabetes. *Journal of Biological Chemistry, 273*(47), 31581-31589. doi:10.1074/jbc.273.47.31581

Kumar, R., Mota, L. C., Litoff, E. J., Rooney, J. P., Boswell, W. T., Courter, E., . . . Baldwin, W. S. (2017). Compensatory changes in CYP expression in three different toxicology mouse models: CAR-null, Cyp3a-null, and Cyp2b9/10/13-null mice. *PLOS ONE, 12*(3), e0174355. doi:10.1371/journal.pone.0174355

Kunne, C., Acco, A., Duijst, S., de Waart, D. R., Paulusma, C. C., Gaemers, I., & Oude Elferink, R. P. J. (2014). FXR-dependent reduction of hepatic steatosis in a bile salt deficient mouse model. *Biochimica et Biophysica Acta (BBA) - Molecular Basis of Disease, 1842*(5), 739-746. doi:https://doi.org/10.1016/j.bbadis.2014.02.004

Lamba, V., Lamba, J., Yasuda, K., Strom, S., Davila, J., Hancock, M. L., . . . Schuetz, E. G. (2003). Hepatic CYP2B6 Expression: Gender and Ethnic Differences and Relationship to CYP2B6 Genotype and CAR (Constitutive Androstane Receptor) Expression. *Journal of Pharmacology and Experimental Therapeutics, 307*(3), 906. doi:10.1124/jpet.103.054866

LeBlanc, G. A., Kullman, S. W., Norris, D. O., Baldwin, W. S., Kloas, W., & Greally, J. M. (2012). Detailed review paper state of the science on novel in vitro and in vivo screening and testing methods and endpoints for evaluating endocrine disruptors. *ENV/JM/MONO, 23*(6), 1-213.

Ledda-Columbano, G. M., Pibiri, M., Concas, D., Molotzu, F., Simbula, G., Cossu, C., & Columbano, A. (2003). Sex difference in the proliferative response of mouse

hepatocytes to treatment with the CAR ligand, TCPOBOP. *Carcinogenesis, 24*(6), 1059-1065. doi:10.1093/carcin/bgg063

Leung, A., Trac, C., Du, J., Natarajan, R., & Schones, D. E. (2016). Persistent Chromatin Modifications Induced by High Fat Diet. *J Biol Chem, 291*(20), 10446-10455. doi:10.1074/jbc.M115.711028

Levian, C., Ruiz, E., & Yang, X. (2014). The pathogenesis of obesity from a genomic and systems biology perspective. *Yale J Biol Med, 87*(2), 113-126.

Maglich, J. M., Lobe, D. C., & Moore, J. T. (2009). The nuclear receptor CAR (NR1I3) regulates serum triglyceride levels under conditions of metabolic stress. *J Lipid Res, 50*(3), 439-445. doi:10.1194/jlr.M800226-JLR200

Maglich, J. M., Watson, J., McMillen, P. J., Goodwin, B., Willson, T. M., & Moore, J. T. (2004). The nuclear receptor CAR is a regulator of thyroid hormone metabolism during caloric restriction. *J Biol Chem, 279*(19), 19832-19838. doi:10.1074/jbc.M313601200

Marchesini, G., Brizi, M., Bianchi, G., Tomassetti, S., Bugianesi, E., Lenzi, M., . . . Melchionda, N. (2001). Nonalcoholic Fatty Liver Disease. *A Feature of the Metabolic Syndrome, 50*(8), 1844-1850. doi:10.2337/diabetes.50.8.1844

Mo, S. L., Liu, Y. H., Duan, W., Wei, M. Q., Kanwar, J. R., & Zhou, S. F. (2009). Substrate specificity, regulation, and polymorphism of human cytochrome P450 2B6. *Curr Drug Metab, 10*(7), 730-753.

Morse, H. (2007). *Building a better mouse: one hundred years of genetics and biology*. Amsterdam: Elsevier.

Mota, L. C., Hernandez, J. P., & Baldwin, W. S. (2010). Constitutive androstane receptor -null mice are sensitive to the toxic effects of parathion: association with reduced cytochrome p450-mediated parathion metabolism *Drug Metabolism Disposition, 38*(9), 1582-1588. doi:10.1124/dmd.110.032961

Murray, G. I., Taylor, A., Barnes, T. S., Weaver, R., Ewen, S. W., Melvin, W. T., & Burke, M. D. (1990). The distribution of different forms of cytochrome P-450 in human liver. *Biochem Soc Trans, 18*(6), 1202.

Must, A., Spadano, J., Coakley, E. H., Field, A. E., Colditz, G., & Dietz, W. H. (1999). The disease burden associated with overweight and obesity. *JAMA, 282*(16), 1523-1529. doi:10.1001/jama.282.16.1523

Nebert, D. W., & Russell, D. W. (2002). Clinical importance of the cytochromes P450. *The Lancet, 360*(9340), 1155-1162. doi:https://doi.org/10.1016/S0140-6736(02)11203-7

Nelson, D. R., & Nebert, D. W. (2011). Cytochrome P450 (CYP) Gene Superfamily. *eLS*.

Nelson, D. R., Zeldin, D. C., Hoffman, S. M., Maltais, L. J., Wain, H. M., & Nebert, D. W. (2004). Comparison of cytochrome P450 (CYP) genes from the mouse and human genomes, including nomenclature recommendations for genes, pseudogenes and alternative-splice variants. *Pharmacogenetics, 14*(1), 1-18.

Newbold, R. R., Padilla-Banks, E., & Jefferson, W. N. (2009). Environmental estrogens and obesity. *Mol Cell Endocrinol, 304*(1-2), 84-89. doi:10.1016/j.mce.2009.02.024

Palacharla, R. C., Uthukam, V., Manoharan, A., Ponnamaneni, R. K., Padala, N. P., Boggavarapu, R. K., . . . Nirogi, R. (2017). Inhibition of cytochrome P450 enzymes by saturated and unsaturated fatty acids in human liver microsomes, characterization of enzyme kinetics in the presence of bovine serum albumin (0.1 and 1.0% w/v) and in vitro – in vivo extrapolation of hepatic clearance. *European Journal of Pharmaceutical Sciences, 101*, 80-89. doi:https://doi.org/10.1016/j.ejps.2017.01.027

Pallayova, M., & Taheri, S. (2014). Non-alcoholic fatty liver disease in obese adults: clinical aspects and current management strategies. *Clinical Obesity, 4*(5), 243-253. doi:10.1111/cob.12068

Peng, L., Yoo, B., Gunewardena, S. S., Lu, H., Klaassen, C. D., & Zhong, X. B. (2012). RNA sequencing reveals dynamic changes of mRNA abundance of cytochromes P450 and their alternative transcripts during mouse liver development. *Drug Metab Dispos, 40*(6), 1198-1209. doi:10.1124/dmd.112.045088

Purnapatre, K., Khattar, S. K., & Saini, K. S. (2008). Cytochrome P450s in the development of target-based anticancer drugs. *Cancer Letters, 259*(1), 1-15. doi:10.1016/j.canlet.2007.10.024

Qiang, M. (2001). Induction of CYP1A1. The AhR / DRE Paradigm Transcription, Receptor Regulation, and Expanding Biological Roles. *Current Drug Metabolism, 2*(2), 149-164. doi:http://dx.doi.org/10.2174/1389200013338603

Quach, N. D., Arnold, R. D., & Cummings, B. S. (2014). Secretory phospholipase A2 enzymes as pharmacological targets for treatment of disease. *Biochemical Pharmacology, 90*(4), 338-348. doi:https://doi.org/10.1016/j.bcp.2014.05.022

Renaud, H. J., Cui, J. Y., Khan, M., & Klaassen, C. D. (2011). Tissue Distribution and Gender-Divergent Expression of 78 Cytochrome P450 mRNAs in Mice. *Toxicological Sciences, 124*(2), 261-277. doi:10.1093/toxsci/kfr240

Saini, S. P., Sonoda, J., Xu, L., Toma, D., Uppal, H., Mu, Y., . . . Xie, W. (2004). A novel constitutive androstane receptor-mediated and CYP3A-independent pathway of bile acid detoxification. *Mol Pharmacol, 65*(2), 292-300. doi:10.1124/mol.65.2.292

Sakuma, T., Kitajima, K., Nishiyama, M., Mashino, M., Hashita, T., & Nemoto, N. (2004). Suppression of female-specific murine Cyp2b9 gene expression by growth or glucocorticoid hormones. *Biochem Biophys Res Commun, 323*(3), 776-781. doi:10.1016/j.bbrc.2004.08.158

Shindo, S., Numazawa, S., & Yoshida, T. (2007). A physiological role of AMP-activated protein kinase in phenobarbital-mediated constitutive androstane receptor activation and CYP2B induction. *Biochem J, 401*(3), 735-741. doi:10.1042/bj20061238

Singh, S., Allen, A. M., Wang, Z., Prokop, L. J., Murad, M. H., & Loomba, R. (2015). Fibrosis Progression in Nonalcoholic Fatty Liver vs Nonalcoholic Steatohepatitis: A Systematic Review and Meta-analysis of Paired-Biopsy Studies. *Clinical Gastroenterology and Hepatology, 13*(4), 643-654.e649. doi:10.1016/j.cgh.2014.04.014

Spruiell, K., Richardson, R. M., Cullen, J. M., Awumey, E. M., Gonzalez, F. J., & Gyamfi, M. A. (2014). Role of pregnane X receptor in obesity and glucose homeostasis in male mice. *J Biol Chem, 289*(6), 3244-3261. doi:10.1074/jbc.M113.494575

Sueyoshi, T., & Negishi, M. (2001). Phenobarbital response elements of cytochrome P450 genes and nuclear receptors. *Annu Rev Pharmacol Toxicol, 41*, 123-143. doi:10.1146/annurev.pharmtox.41.1.123

Sugatani, J., Kojima, H., Ueda, A., Kakizaki, S., Yoshinari, K., Gong, Q. H., . . . Sueyoshi, T. (2001). The phenobarbital response enhancer module in the human bilirubin UDP-glucuronosyltransferase UGT1A1 gene and regulation by the nuclear receptor CAR. *Hepatology, 33*(5), 1232-1238. doi:10.1053/jhep.2001.24172

Swanson, H. I., Wada, T., Xie, W., Renga, B., Zampella, A., Distrutti, E., . . . Chiang, J. Y. L. (2013). Role of nuclear receptors in lipid dysfunction and obesity-related diseases. *Drug metabolism and disposition: the biological fate of chemicals, 41*(1), 1-11. doi:10.1124/dmd.112.048694

Tang, J., Cao, Y., Rose, R. L., Brimfield, A. A., Dai, D., Goldstein, J. A., & Hodgson, E. (2001). Metabolism of chlorpyrifos by human cytochrome P450 isoforms and human, mouse, and rat liver microsomes. *Drug Metab Dispos, 29*(9), 1201-1204.

Wang, H., & Tompkins, L. M. (2008). CYP2B6: New Insights into a Historically Overlooked Cytochrome P450 Isozyme. *Current Drug Metabolism, 9*, 598-610.

Wei, P., Zhang, J., Egan-Hafley, M., Liang, S., & Moore, D. D. (2000). The nuclear receptor CAR mediates specific xenobiotic induction of drug metabolism. *Nature, 407*(6806), 920-923. doi:10.1038/35038112

Wei, Y., Wu, H., Li, L., Liu, Z., Zhou, X., Zhang, Q., . . . Ding, X. (2012). Generation and Characterization of a CYP2A13/2B6/2F1-Transgenic Mouse Model. *Drug Metabolism and Disposition, 40*(6), 1144-1150. doi:10.1124/dmd.112.044826

Wiktorowska-Owczarek, A., Berezinska, M., & Nowak, J. Z. (2015). PUFAs: Structures, Metabolism and Functions. *Adv Clin Exp Med, 24*(6), 931-941. doi:10.17219/acem/31243

Wiwi, C. A., Gupte, M., & Waxman, D. J. (2004). Sexually dimorphic P450 gene expression in liver-specific hepatocyte nuclear factor 4alpha-deficient mice. *Mol Endocrinol, 18*(8), 1975-1987. doi:10.1210/me.2004-0129

Wolfrum, C., Asilmaz, E., Luca, E., Friedman, J. M., & Stoffel, M. (2004). Foxa2 regulates lipid metabolism and ketogenesis in the liver during fasting and in diabetes. *Nature, 432*, 1027. doi:10.1038/nature03047 https://www.nature.com/articles/nature03047#supplementary-information

Wortham, M., Czerwinski, M., He, L., Parkinson, A., & Wan, Y.-J. Y. (2007). Expression of Constitutive Androstane Receptor, Hepatic Nuclear Factor 4α, and P450 Oxidoreductase Genes Determines Interindividual Variability in Basal Expression and Activity of a Broad Scope of Xenobiotic Metabolism Genes in the Human Liver. *Drug Metabolism and Disposition, 35*(9), 1700. doi:10.1124/dmd.107.016436

Wu, Y., Chitranshi, P., Loukotkova, L., Gamboa da Costa, G., Beland, F. A., Zhang, J., & Fang, J. L. (2017). Cytochrome P450-mediated metabolism of triclosan attenuates its cytotoxicity in hepatic cells. *Arch Toxicol, 91*(6), 2405-2423. doi:10.1007/s00204-016-1893-6

Xiong, X., Wang, X., Lu, Y., Wang, E., Zhang, Z., Yang, J., . . . Li, X. (2014). Hepatic steatosis exacerbated by endoplasmic reticulum stress-mediated downregulation of FXR in aging mice. *Journal of Hepatology, 60*(4), 847-854. doi:https://doi.org/10.1016/j.jhep.2013.12.003

Yoshinari, K., Kobayashi, K., Moore, R., Kawamoto, T., & Negishi, M. (2003). Identification of the nuclear receptor CAR:HSP90 complex in mouse liver and recruitment of protein phosphatase 2A in response to phenobarbital. *FEBS Lett, 548*(1-3), 17-20. doi:10.1016/s0014-5793(03)00720-8

Zanger, U. M., & Klein, K. (2013). Pharmacogenetics of cytochrome P450 2B6 (CYP2B6): advances on polymorphisms, mechanisms, and clinical relevance. *Front Genet, 4*, 24. doi:10.3389/fgene.2013.00024

Zeldin, D. C. (2001). Epoxygenase Pathways of Arachidonic Acid Metabolism. *Journal of Biological Chemistry, 276*(39), 36059-36062. doi:10.1074/jbc.R100030200

Zhang, G., Kodani, S., & Hammock, B. D. (2014). Stabilized epoxygenated fatty acids regulate inflammation, pain, angiogenesis and cancer. *Prog Lipid Res, 53*, 108-123. doi:10.1016/j.plipres.2013.11.003

CHAPTER TWO

CYP2B-NULL MALE MICE ARE SUSCEPTIBLE TO DIET-INDUCED OBESITY AND PERTURBATIONS IN LIPID HOMEOSTASIS

Melissa M. Heintz, Ramiya Kumar, Meredith M. Rutledge, William S. Baldwin

**Dr. Ramiya Kumar conducted the mouse study and initial physiological and biochemical measurements described in this chapter.

Data presented in this chapter was published in the *Journal of Nutritional Biochemistry*:

Heintz, M. M., Kumar, R., Rutledge, M. M., & Baldwin, W. S. (2019). Cyp2b-null male mice are susceptible to diet-induced obesity and perturbations in lipid homeostasis. *The Journal of Nutritional Biochemistry, 70*, 125-137.

2.0 Abstract

Obesity is an endemic problem in the United States and elsewhere, and data indicate that in addition to overconsumption, exposure to specific chemicals enhances obesity. CYP2B metabolizes multiple endo- and xenobiotics, and recent data suggests that repression of Cyp2b activity increases dyslipidemia and age-onset obesity, especially in males. To investigate the role played by Cyp2b in lipid homeostasis and obesity, we treated wildtype and Cyp2b-null mice with a normal (ND) or 60% high-fat diet (HFD) for 10 weeks and determined metabolic and molecular changes. Male HFD-fed Cyp2b-null mice weigh 15% more than HFD-fed wildtype mice, primarily due to an increase in white adipose tissue (WAT); however, Cyp2b-null female mice did not demonstrate greater body mass or WAT. Serum parameters indicate increased ketosis, leptin and cholesterol in HFD-fed Cyp2b-null male mice compared to HFD-fed wildtype mice. Liver triglycerides and liver:serum triglyceride ratios were higher than their similarly treated wildtype counterparts in Cyp2b-null male mice, indicating a role for Cyp2b in fatty acid metabolism regardless of diet. Furthermore, RNAseq demonstrates that hepatic gene expression in ND-fed Cyp2b-null male mice is similar to HFD-fed WT male mice, suggestive of fatty liver disease progression and a role for Cyp2b in lipid homeostasis. Females did not show as demonstrative changes in liver health, and significantly fewer changes in gene expression, as well as gene expression associated with liver disease. Overall our data indicates that the repression or inhibition of CYP2B may exacerbate metabolic disorders and cause obesity by perturbing fatty acid metabolism, especially in males.

Keywords: Non-alcoholic fatty liver disease (NAFLD); P450; Cyp2b; Triglycerides; RNAseq; Obesity

2.1 Introduction

According to the National Center for Health Statistics (NCHS) more than 40% of adults and 18.5% youth are obese in United States as of 2015-2016 (Hales, Carroll, Fryar, & Ogden, 2017). Factors that cause obesity include poor diet, changes in lifestyle, genetics, and the environment (Choquet & Meyre, 2011; Grun & Blumberg, 2009; Romieu et al., 2017). The primary problem is excess food coupled with inactivity. However, data indicates there are other anthropogenic factors, including environmental toxicants that exacerbate obesity by modulating the use and allocation of nutrient resources leading to increased white adipose tissue and obesity (Grun & Blumberg, 2009; Hatch, Nelson, Stahlhut, & Webster, 2010; Sharp, 2009; Wahlang et al., 2013). The terms "obesogen" or "metabolic disruptor" (Grun & Blumberg, 2009; Hatch et al., 2010; Wahlang et al., 2013) refer to a new subclass of endocrine disruptors that perturb metabolic signaling, energy, and lipid homeostasis (LeBlanc et al., 2012; Riu et al., 2011). In turn, the Organization for Economic Cooperation and Development (OECD) considers metabolic disorders one of three critical areas in toxicology in addition to testicular dysgenesis and autism spectral disorders (LeBlanc et al., 2012).

Chemical exposures shown to cause obesity include perinatal exposure to bisphenol A that increases lipogenic gene expression and hepatic steatosis in male mice (Marmugi et al., 2012). Tributyltin activation of PPARγ-RXR induces obesity primarily through increased adipocyte differentiation (Chamorro-García et al., 2013; le Maire et al., 2009), and TCDD activation of AhR induces obesity and steatosis through increased uptake of fatty acids (Angrish, Mets, Jones, & Zacharewski, 2012; Chang, Chen, Su, & Lee, 2016; Lee et al., 2010). Inactivation of the xenobiotic receptor, the constitutive androstane receptor (CAR), and activation of the pregnane X-receptor (PXR) are also associated with obesity (Dong et al., 2009; K Spruiell et al., 2014; K. Spruiell et al., 2014). Perturbations in hepatic Cytochrome P450 (CYP) activity were recently associated with lipid accumulation (Robert D. Finn, Henderson, Scott, & Wolf, 2009; Hoek-van den Hil et al., 2015; Hoek-van den Hil et al., 2014; Wang, Chamberlain, Vassieva, Henderson, & Wolf, 2005; Zong, Armoni, Harel, Karnieli, & Pessin, 2012) and the inhibition of all hepatic CYP activity was associated with increased hepatic lipid accumulation (Robert D. Finn et al., 2009). In constrast, knockouts of Cy2e1 and Cyp3a members were associated with reduced lipid accumulation and weight gain (only in females in Cyp3a-null mice) (R. Kumar, Litoff, Boswell, & Baldwin, 2018; Zong et al., 2012).

CYPs, primarily in families 1-3, metabolize pharmaceuticals (Zanger & Schwab, 2013), environmental pollutants (Foxenberg, McGarrigle, Knaak, Kostyniak, & Olson, 2007) and endobiotics such as fatty acids (Arnold et al., 2010), bile acids and steroids (D J Waxman, 1988). Several CYP1-3 members are crucial in fatty acid metabolism. For

example, CYP3A4 metabolizes arachidonic acid to 13-hydroxyeicosatrienoic acid (HETE), 10-HETE and 7-HETE (Bylund, Kunz, Valmsen, & Oliw, 1998), and anandamide to several metabolites including 5,6-epoxyeicosatrienoic acid ethanolamide, with high affinity for the cannabinoid-2 (CB-2) receptor (Pratt-Hyatt, Zhang, Snider, & Hollenberg, 2010). CYP2J2 metabolizes arachidonic acid to epoxyecosatrienoic acid (EET) in cardiomyocytes (Wu, Moomaw, Tomer, Falck, & Zeldin, 1996), and some Cyp2b members metabolize arachidonic acid with high affinity (Capdevila et al., 1990; Keeney et al., 1998). For example, Cyp2b19 expressed in mouse keratinocytes, epoxygenate arachidonic acid to 11,12- and 14,15-EET that play a vital role in cornification of epidermal cells (Du et al., 2005; Ladd, Du, Capdevila, Mernaugh, & Keeney, 2003).

Several recent studies implicate Cyp2b in obesity. For example, Cyp2b members are inducible by anti-obesity transcription factors (CAR; FoxA2) (Hashita et al., 2008; Hernandez, Mota, & Baldwin, 2009; Wei, Zhang, Egan-Hafley, Liang, & Moore, 2000). CAR is a key regulator of Cyp2b, including Cyp2b9 and Cyp2b10 (J. P. Hernandez, L. C. Mota, W. Huang, D. D. Moore, & W. S. Baldwin, 2009; Mota, Hernandez, & Baldwin, 2010; Oshida et al., 2015), and CAR activation by TCPOBOP ameliorates obesity, diabetic activity and fatty liver disease in ob/ob mice, but not ob/ob mice null for CAR (Dong et al., 2009). FoxA2, which is activated by fasting and fatty acids and inhibited by insulin, is a potent inducer of Cyp2b9 (Bochkis et al., 2008; Hashita et al., 2008; Wolfrum, Asilmaz, Luca, Friedman, & Stoffel, 2004). FoxA2-null mice are age-dependent obese (Bochkis, Shin, & Kaestner, 2013). Thus, Cyp2b expression is induced

by CAR and Foxa2 during nutritional or metabolic stress, potentially as a protective mechanism from NAFLD. Furthermore, cytochrome P450 oxidoreductase (HRN-null) conditional knockout mice that lack all liver CYP activity, activate CAR and induce Cyp2b mRNA during treatment with polyunsaturated fatty acid (PUFA)-rich sunflower oil (Robert D. Finn et al., 2009). Similarly, treatment with soybean oil (rich in 51% linoleic acid) resulted in weight gain, increased white adipose tissue and glucose intolerance in association with a significant increase in Cyp2b9 and 13 (Deol et al., 2015). *Cyp2b9* is also the most highly induced gene in a couple of diet-induced obesity studies (Hoek-van den Hil et al., 2015; Leung, Trac, Du, Natarajan, & Schones, 2016). Last, observations in our laboratory following production of a Cyp2b RNAi-based knockdown mouse model on a FVB strain background (B. Damiri, Holle, Yu, & Baldwin, 2012) show increases in body weight and adiposity with age and a reduced propensity to eliminate PUFA-rich corn oil (B Damiri & Baldwin, 2018). Taken together, the Cyp2b enzymes are responsive to high-fat diets and associated with obesity. Therefore, we predict that lack of Cyp2b either by gene knockout (as described here) or repression by inhibitors coupled with a high-fat diet will perturb lipid metabolism, increase body weight and lead to the development of obesity.

Murine Cyp2b members are expressed in several tissues (B. Damiri et al., 2012). For example, Cyp2b19 is primarily expressed in the skin and involved in keratinocyte development (Du et al., 2005; Keeney et al., 1998). Cyp2b23 is primarily expressed in neonate liver (L. Peng et al., 2012), Cyp2b13 is primarily expressed in adult liver (L. Peng et al., 2012), Cyp2b10 is primarily expressed in adult liver and highly inducible (J.

P. Hernandez, L. C. Mota, & W. S. Baldwin, 2009; L. Peng et al., 2012), and Cyp2b9 is expressed in several tissues including liver, brain, and to a lesser degree kidney and lungs (Hersman & Bumpus, 2014; L. Peng et al., 2012). In addition, both Cyp2b9 and Cyp2b13 are highly female predominant due to sexually dimorphic regulation by HNF4α and growth hormone (R Kumar et al., 2017; Wiwi, Gupte, & Waxman, 2004)}(J. P. Hernandez, L. C. Mota, W. Huang, et al., 2009; D J Waxman, Pampori, Ram, Agrawal, & Shapiro, 1991).

We used our newly developed Cyp2b9/10/13-null (Cyp2b-null) mice missing the primarily hepatic Cyp2b members, *Cyp2b9*, *Cyp2b10* and *Cyp2b13* to demonstrate the significance of Cyp2b on diet-induced obesity and hepatic lipid metabolism. We treated Cyp2b-null mice with a 60% high-fat diet for 10-weeks, and examined their susceptibility to diet-induced obesity compared to wild-type (WT) mice. Physiological changes such as body weight, organ weight, glucose tolerance, serum lipids, and specific metabolic hormones were examined. In addition, RNAseq was performed to determine differential gene expression and investigate which gene ontologies and pathways were perturbed. Our data demonstrates a role for perturbations in Cyp2b activity in obesity and lipid metabolism.

2.2 Materials and Methods

2.2.1 High-fat diet treatment of Cyp2b-null mice

All mice studies followed National Institute of Health guidelines for humane use of research animals and were pre-approved by Clemson University's Institutional Animal

Care and Use Committee (IACUC). Cyp2b-null mice were developed using Crispr/Cas9 technology on C57Bl6/J (B6) background mice as described earlier (R Kumar et al., 2017). Briefly, the liver predominant Cyp2b genes, Cyp2b10, Cyp2b13 and Cyp2b9 present as tandem repeat sequences on chromosome seven and were targeted individually using small guide RNA sequences (sgRNA). This led to the deletion of 287 kb lacking these three primarily hepatic Cyp2b genes (**Suppl. Material 2.1; S2.1**). Homozygous knock-out mice were verified using primers published previously (R Kumar et al., 2017).

Wildtype C57BL/6J were purchased from The Jackson Laboratory at 3 weeks of age (Bar Harbor, ME, USA), and acclimated for 6-weeks prior to the dietary treatments. Nine-ten week old male and female mice (n=9) from WT and Cyp2b-null mice were divided into normal diet (ND; 2018S-Envigo Teklad Diet, Madison, WI) and high-fat diet (HFD; Envigo, TD.06414 Adjusted calorie diet) groups. ND provided 3.1 Kcal/g with 18% of kilocalories from fat, 24% protein, and 58% carbohydrate. HFD provided 5.1 Kcal/g with 60.3% of kilocalories from fat (37% saturated, 47% monounsaturated, 16% polyunsaturated fat), 18.4% protein, and 21.3% carbohydrates.

Feed consumption was measured every other day and mice were weighed every week to determine their weight gain. At the end of the study, mice were anesthetized, blood was collected by heart puncture, and mice euthanized by carbon dioxide asphyxiation (B Damiri & Baldwin, 2018). Organs such as liver, kidney, inguinal and renal white adipose tissue, and brain were excised and weighed. Livers were dissected into five fractions and snap frozen in liquid nitrogen for microsome preparation and RNA extraction. Frozen liver fractions were stored at -80^{o}C. A portion of the liver was stored

in 10% formalin (Fisher, Fair Lawn NJ USA) for histopathological analyses. A timeline of experimental procedures performed on the mice is provided (**S2.2**).

2.2.2 RNA sequencing (RNAseq)

Liver samples were stored in RNAlater stabilization solution (Invitrogen) at -80°C. RNA was extracted from mouse livers using an RNeasy Plus Universal kit (Qiagen) per the manufacturer's instructions and quantified on a NanoDrop 8000 Spectrophotometer. An Agilent 2100 Bioanalyzer was used to assess the RNA integrity number (RIN). Samples with a RIN > 8 were determined to be of high quality and used for next generation sequencing. Libraries were prepared with the TruSeq Total RNA Library Prep kit. Samples were sequenced to an average sequencing depth of 20,000,000 read pairs with a 2 x 125 paired-end module using an Illumina HiSeq2500 for males and a 2 x 150 paired-end module using a NovaSeq 6000 for females. Quality metrics were checked using FastQC on all samples sequenced, and Trimmomatic was used to trim low quality bases. Trimmed reads were aligned to the *Mus musculus* reference genome (GCF_000001635.25_GRCm38.p5) using GSNAP, and 99.7% of the trimmed reads aligned. Subread feature counts software found reads that aligned with known genes. Raw read counts and EdgeR were used to determine differential gene expression (Huber et al., 2015). Genes in which the lowest replicate number of samples have less than one count per million of expression were ascertained to be low coverage genes and were filtered out of the analysis. Samples were then normalized to the scale of their library sizes. Genes were considered differentially expressed if their adjusted p-value and false

discovery rate were less than 0.05 and 0.1 respectively as performed previously (Park & Mori, 2010). Series GSE120761 containing the RNAseq data has been uploaded to GEO.

Heatmap hierarchical cluster analysis by Euclidiean distance using Ward's method was performed with Heatmap.2 in R (http://www.r-project.org/). Venn diagrams were created using Venn Diagram Plotter (omics.pnl.gov). GOSeq, a GO term enrichment analysis program was used to adjust for gene length and expression bias (Young, Wakefield, Smyth, & Oshlack, 2010). Significantly ($p < 0.05$) enriched GO terms were visualized in Revigo, which reduces enriched term redundancy and displays the remaining enriched GO terms in a scatterplot (Supek, Bo snjak, Skunca, & Smuc, 2011). Differentially expressed genes were annotated using InterPro (R D Finn et al., 2017), and genes with a $\log_2FC > 1.0$ were entered into KEGG Mapper (http://www.genome.jp/kegg/) to determine and visualize biochemical pathways perturbed by a HFD or a lack of Cyp2b enzymes (Kanehisa, Furumichi, Tanabe, Sato, & Morishima, 2017).

2.2.3 Histopathological analysis

Following necropsy, a clean slice of liver was placed in 10% formalin (Fisher). Hematoxylin and Eosin (H&E) staining was performed at Colorado Histoprep (Fort Collins, CO USA) and Oil Red O staining was performed with frozen samples at Baylor College of Medicine's Comparative Pathology Laboratory (Houston, TX USA) using standard protocols (Acevedo et al., 2005; Dong et al., 2009). Histopathological scoring

was performed blind by a veterinary pathologist at Colorado Histoprep (Fort Collins, CO USA).

2.2.4 Serum lipid panel

Blood samples were collected by heart puncture and incubated at room temperature for 30 min followed by centrifugation at 6000 rpm for 10 minutes. Serum samples were transferred into fresh tubes and 100µl aliquots were shipped on dry ice to Baylor College of Medicine's Comparative Pathology Laboratory (Houston, TX) for determination of nonfasting serum cholesterol, triglycerides, alanine aminotransferase (ALT), high density lipoprotein (HDL), low density lipoprotein (LDL), and very low density lipoprotein (VLDL) with a Beckman-Coulter AU480 analyzer and the appropriate Beckman-Coulter biochemical kits according to the manufacturer's instructions.

2.2.5 Serum concentrations of free fatty acids, β-hydroxybutyrate and liver triglycerides

Serum free fatty acids (FFA) and β-hydroxybutyrate (B-OHB) concentrations were determined using fluorescent and colorimetric kits, respectively, from Cayman Chemical Co (Ann Arbor, MI). Liver triglyceride concentrations were quantified following organic extraction (R. Kumar et al., 2018) with a colorimetric kit (Cayman Chemical).

2.2.6 Tests of Statistical Significance

Data are presented as mean ± SEM (n = 9) except serum lipids (n = 5). Statistical analysis was performed by one-way ANOVA followed by Fisher's LSD as the post-hoc test when comparing more than two groups. Student's t-tests were used when comparing two groups. Statistical analysis was performed using Graphpad Prism version 6 (La Jolla, CA USA). A p-value ≤ 0.05 was considered statistically significant.

2.3 Results

2.3.1 High-fat diet increases body and white adipose tissue weight

HFD-fed Cyp2b-null male mice weighed significantly more than HFD-fed WT male mice (**Fig. 2.1A**). The weight of HFD-fed Cyp2b-null male mice was significantly greater than HFD-fed WT mice after only 4-weeks and these mice stayed heavier for the rest of the study period (**Fig. 2.1A**). Much of this weight gain is from increased white adipose tissue, which increased 55% more in HFD-fed Cyp2b-null mice than HFD-fed WT mice (**Table 2.1A**). Cyp2b-null mice had similar caloric intake compared to their WT counterparts when examined by diet (HFD or ND) (**S2.3**). Therefore, alterations in dietary intake do not explain increased weight gain in Cyp2b-null mice.

Cyp2b-null and WT female mice fed a HFD gained significantly more weight and had higher white adipose tissue mass compared to mice fed a ND. However, the Cyp2b-null genotype had no significant effect on body weight gain or WAT mass in females (**Fig. 2.1B; Table 2.1B**). Overall, the loss of *Cyp2b9*, *Cyp2b10*, and *Cyp2b13* led to diet-induced obesity in male, but not female mice.

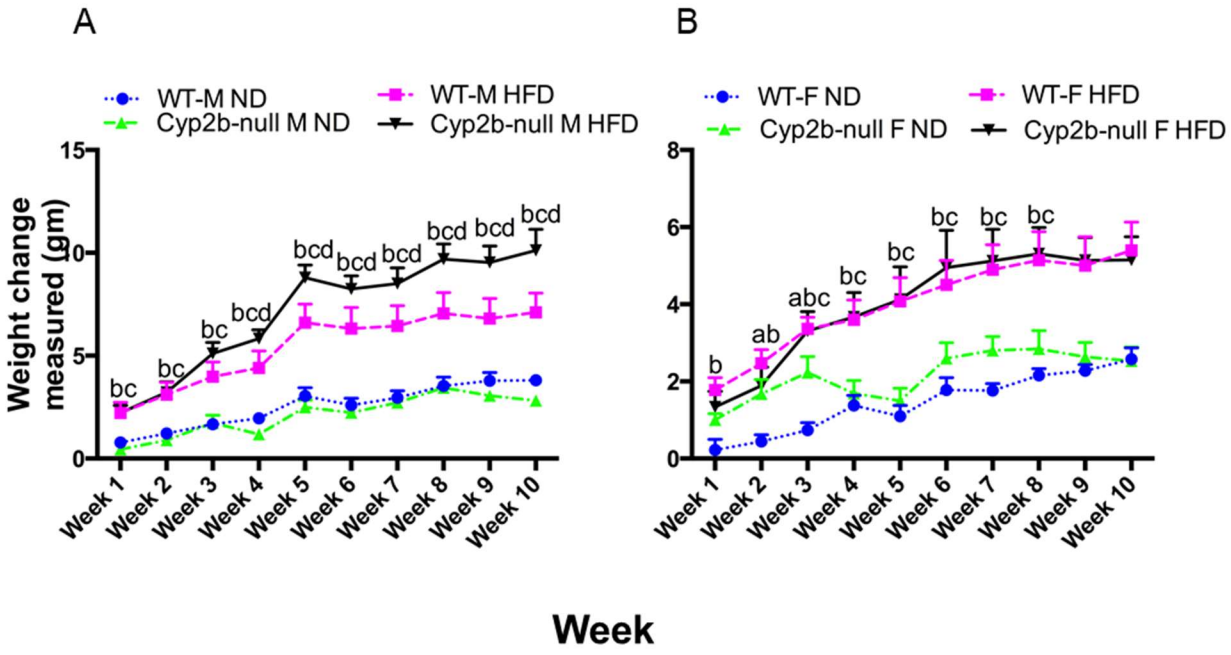

Fig. 2.1: Changes in body weight during the 10-weeks of dietary treatments. Body weight of A) male and B) female, WT, and Cyp2b-null mice were monitored during the 10-week feeding study. Male but not female Cyp2b-null mice show increased weight during HFD treatments. Data are represented as mean ± SEM. Statistical significance was determined by one-way ANOVA followed by Fisher's LSD as the post-hoc test (n= 8-9). An 'a' indicates WT-ND are different than Cyp2b-null-ND, 'b' indicates WT-ND are different than WT-HFD, 'c' indicates Cyp2b-null-ND are different than Cyp2b-null-HFD, 'd' indicates WT-HFD are different than Cyp2b-null-HFD.

Table 2.1: Organ weights determined in WT and Cyp2b9/10/13-null mice after 10-weeks of dietary treatment in male (A) and female (B) mice.

A

Mouse model	Body weight	WAT	Liver	Kidney	Brain
WT-ND M	26.48±0.57	0.51±0.06	1.23±0.03	0.34±0.01	0.48±0.03
WT-HFD M	30.43±0.92^{b**}	1.96±0.22^{b***}	1.06±0.04^{b*}	0.37±0.01	0.44±0.00
Cyp2b-null ND M	25.75±0.39	0.69±0.06	1.08±0.03^{a*}	0.31±0.01	0.46±0.01
Cyp2b-null HFD M	34.12±0.88^{c***d*}	3.04±0.19^{c***d***}	1.08±0.04	0.37±0.02^{c**}	0.43±0.01

B

Mouse model	Body weight	WAT	Liver	Kidney	Brain
WT-ND F	20.47±0.44	0.36±0.06	0.87±0.03	0.26±0.01	0.44±0.00
WT-HFD F	23.17±0.87[b*]	0.95±0.15[b*]	0.84±0.03	0.26±0.01	0.45±0.00
Cyp2b-null ND F	20.29±0.22	0.33±0.03	0.83±0.02	0.25±0.01	0.45±0.00
Cyp2b-null HFD F	24.15±0.93[c**]	1.22±0.24[c**]	0.87±0.04	0.28±0.01[c]	0.45±0.01

Data represented as mean (g) +/- SEM (n = 8/9). Statistical significance determined by one-way ANOVA followed by Fisher's LSD as the post-hoc test.
'a' indicates WT ND different than Cyp2b9/10/13-null ND
'b' indicates WT ND different than WT HFD
'c' indicates Cyp2b9/10/13-null ND different than Cyp2b9/10/13-null HFD
'd' indicates WT HFD different than Cyp2b9/10/13-null HFD,
No asterisk indicates a p-value ≤ 0.05, * indicates a p-value ≤ 0.01,** indicates a p-value ≤ 0.0001 and *** indicates a p-value ≤ 0.00001.

2.3.2 Increased hepatic triglycerides in Cyp2b-null mice

Total liver triglycerides increased 2.3X in the ND-fed Cyp2b-null male mice compared to ND-fed WT males (**Fig. 2.2A**). HFD exacerbated liver triglyceride concentrations; however, there was no significant difference between HFD-fed Cyp2b-null male mice and HFD-fed WT male mice (**Fig. 2.2A**). HFD-fed female mice showed significant increases in liver triglycerides compared to ND-fed mice; however, genotype did not significantly alter liver triglycerides in females (**Fig. 2.2B**). Despite increased liver triglycerides in both HFD-fed groups and ND-fed Cyp2b-null males, liver weight was decreased in all of these groups compared to ND-fed WT mice for unknown reasons (**Table 2.1A**). Histopathological analysis indicated mild morphological changes indicative of fat deposition in male ND-fed Cyp2b-null, HFD-fed WT, and HFD-fed Cyp2b-null mice either by H&E or Oil Red O. H&E staining showed mild vacuolization in some HFD-fed male mice of both genotypes with slightly greater vacuolization in some HFD-fed Cyp2b-null mice than HFD-fed WT mice, but no significant changes

within the female mice (**Fig. 2.2C-D**). Oil Red O staining was absent or weak in male and female ND treatments with minimal staining in ND-fed Cyp2b-null males, which corroborates the total liver triglyceride data. HFD-fed Cyp2b-null male mice showed mildly greater Oil Red O staining than HFD-fed WT mice (**Fig. 2.2E**). Female mice only showed mild staining following a HFD with no difference between genotypes (**Fig. 2.2F**). Overall, the data suggests that liver triglycerides are slightly higher in Cyp2b-null male mice than correspondingly treated WT male mice.

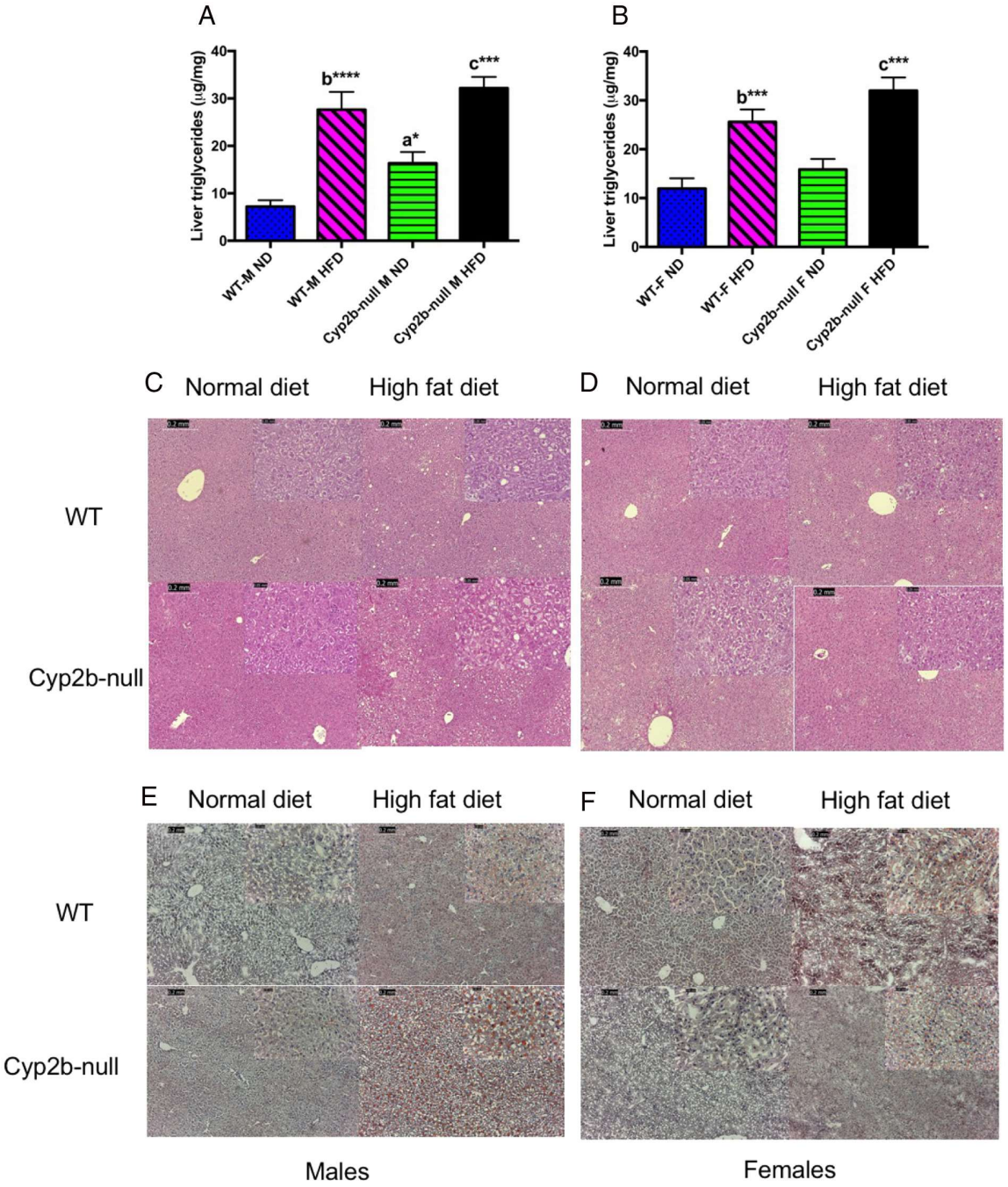

Fig. 2.2: Liver triglyceride concentrations are significantly increased in Cyp2b-null mice. Liver triglycerides were extracted and determined as described in the Materials and Methods using commercial kits. Data are presented as mean ± SEM for males (A) and females (B). Statistical significance was determined by one-way ANOVA followed by Fisher's LSD as the post-hoc test (n= 8-9). * indicates a p-value $\leq$ 0.05, *** indicates p-value $\leq$ 0.001 and **** indicates p-value $\leq$ 0.0001. An 'a' indicates WT-ND are different

than Cyp2b-null-ND, ‘b’ indicates WT-ND are different than WT-HFD, ‘c’ indicates Cyp2b-null-ND are different than Cyp2b-null-HFD, ‘d’ indicates WT-HFD different than Cyp2b-null-HFD. H&E staining was performed in male (C) and female (D) mice with increases in vacuolization in HFD-fed males. Oil Red O staining was also performed in male (E) and female (F) mice and indicate weak liver lipid staining in all ND treatments and greater triglyceride staining in HFD-fed Cyp2b-null males relative to their HFD-fed WT counterparts.

2.3.3 Serum lipids were perturbed in Cyp2b-null mice

Serum triglyceride levels were significantly decreased in Cyp2b-null male mice compared to WT mice following ND (28%) or HFD (25%) treatments (**Table 2.2**), in contrast to increased liver triglyceride concentrations (**Fig. 2.2**). The ratio of liver:serum triglycerides was 3X greater in ND-fed Cyp2b-null males than ND-fed WT males, 4X greater in HFD-fed WT males than ND-fed WT males, and 1.54X greater in HFD-fed Cyp2b-null males than HFD-fed WT males (**Fig. 2.3**), demonstrating that a Cyp2b-null genotype or a HFD increased the retention of liver triglycerides, and the Cyp2b-null genotype enhanced liver triglyceride retention induced by a HFD. This indicates either decreased metabolism and distribution of hepatic lipids or increased uptake of lipids into the liver.

Table 2.2: Serum lipid levels in Cyp2b9/10/13-null compared to WT mice treated with normal diet (ND) or high fat diet (HFD) in male (A) and female (B) mice.

A

Lipid panel	WT ND M	WT HFD M	Cyp2b-null ND M	Cyp2b-null HFD M
ALT	17.00 ± 1.48	15.00 ± 0.55	17.80 ± 0.97	14.00 ± 1.00
β-OHB	0.188 ± 0.015	0.162 ± 0.022	0.120 ± 0.015	0.365 ± 0.087^{c***d**}
Cholesterol	103.80 ± 1.63	170.4 ± 7.00^{b**}	118.60 ± 6.27^{a*}	182.75 ± 3.61^{c**d}
Fatty acids	833.7 ± 97.3	740.2 ± 93.0	739.3 ± 36.6	751.4 ± 43.2
HDL	97.00 ± 2.21	150.76 ± 6.24^{b**}	114.02 ± 4.45^{a*}	168.60 ± 4.94^{c**d*}
LDL	10.98 ± 0.58	26.34 ± 2.46^{b*}	16.34 ± 1.09	30.20 +/- 1.57^{c}
Triglycerides	80.40 ± 7.88	69.60 ± 3.96^{b}	58.00 ± 5.93^{a**}	52.25 ± 3.15^{d*}
VLDL	16.04 ±1.59	13.94 ± 0.80	11.56 ± 1.19^{a}	10.45 ± 0.61

B

Lipid panel	WT ND F	WT HFD F	Cyp2b-null ND F	Cyp2b-null ND F
ALT	20.20 ± 1.69	37.20 ± 8.49	17.80 ± 0.80	17.80 ± 0.80
β-OHB	0.325 ± 0.076	0.360 ± 0.061	0.328 ± 0.098	0.268 ± 0.046
Cholesterol	76.40 ± 3.70	98.00 ± 12.63	77.40 ± 1.94	77.40 ± 1.94
Fatty acids	374.0 ± 8.19	380.4 ± 27.2	343.9 ± 20.5	366.5 ± 30.6
HDL	72.48 ± 4.09	54.18 ± 22.92	77.36 ± 2.57	77.36 ± 2.57
LDL	8.68 ± 1.82	8.58 ± 3.24	10.20 ± 1.46	10.20 ± 1.46
Triglycerides	80.80 ± 17.74	78.40 ± 18.58	57.40 ± 12.70	57.40 ± 12.70
VLDL	16.16 ± 3.53	11.46 ± 2.52	15.68 ± 3.75	20.48 ± 3.55

Data represented as mean +/- SEM (n = 5). All units expressed as mg/dl except β-OHB (mM), fatty acids (μM) and ALT (U/L). Statistical significance was determined by one-way ANOVA followed by Fisher's LSD as the post-hoc test.
'a' indicates WT ND different than Cyp2b9/10/13-null ND.
'b' indicates WT ND different than WT HFD
'c' indicates Cyp2b9/10/13-null ND different than Cyp2b9/10/13-null HFD.
'd' indicates WT HFD different than Cyp2b9/10/13-null HFD,
No asterisk indicates a p-value ≤ 0.05 and * indicates a p-value ≤ 0.01, ** indicates a p-value of ≤ 0.0001.

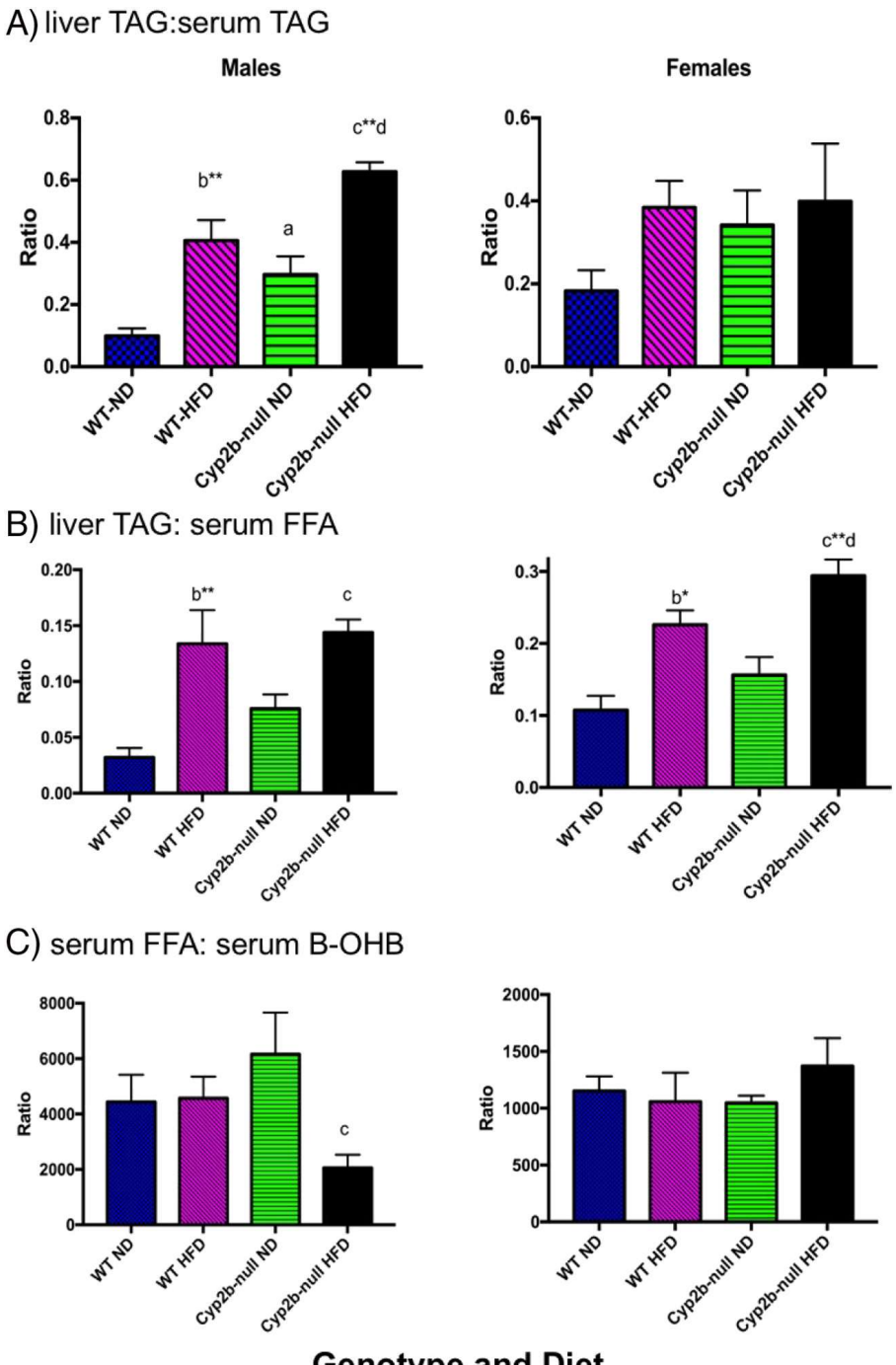

Fig. 2.3: Liver triglyceride:serum triglyceride (A), liver triglyceride:serum free fatty acid (B), and serum free fatty acid:serum b-hydroxybutyrate (C) ratios in ND and HFD-fed mice. Data are presented as mean ± SEM. Statistical significance was determined by one-way ANOVA followed by Fisher's LSD as the post-hoc test (n= 8-9). * indicates a p-value ≤ 0.05, *** indicates p-value ≤ 0.001 and **** indicates p-value ≤ 0.0001. An 'a' indicates WT-ND are different than Cyp2b-null-ND, 'b' indicates WT-ND

are different than WT-HFD, ‘c’ indicates Cyp2b-null-ND are different than Cyp2b-null-HFD, ‘d’ indicates WT-HFD different than Cyp2b-null-HFD.

Female mice showed a similar decrease (29%) to males in serum triglycerides in ND-fed Cyp2b-null mice compared to ND-fed WT mice **(Table 2.2)**; however, this was not statistically significant. In contrast to males, HFD-fed Cyp2b-null female mice showed a 31% increase in serum triglycerides compared to HFD-fed WT mice. Changes in liver and serum triglycerides were proportional in females, which is different than males, and this was further demonstrated by the liver:serum triglyceride ratios that were not different between WT and Cyp2b-null female mice (**Fig. 2.3A**).

In contrast to serum triglycerides, free fatty acids (FFA) were not perturbed significantly across groups (**Table 2.2**). This relative stability ensured that serum TAG:serum FFA ratios were not altered across groups (data not shown). However, the relative stability of FFA provides another example of the differences in liver triglyceride to serum lipid ratios across treatment groups as both males and females show large increases in liver TAG:serum FFA ratio with females showing greater relative increases in HFD-fed Cyp2b-null mice (**Fig. 2.3B**).

Serum cholesterol and HDL increased 14% and 18%, respectively, in ND-fed Cyp2b-null male mice compared to ND-fed WT male mice. Serum cholesterol and HDL increased 8% and 12%, respectively, in HFD-fed Cyp2b-null male mice compared to HFD-fed WT male mice (**Table 2.2A**); thus Cyp2b-null male mice consistently present higher cholesterol concentrations. For example, HFD-fed Cyp2b-null male mice had 2X higher cholesterol than HFD-fed male WT mice, indicating a significant role Cyp2b in

serum cholesterol concentrations. Despite lower weight gain and white adipose tissue mass, females showed greater changes in serum cholesterol and HDL concentrations. Most changes were associated with a combination of diet and the loss of Cyp2b (**Table 2.2B**). There were no significant changes in LDL or VLDL serum levels; only in HDL serum concentrations. In addition, ALT, a biomarker of liver damage, was increased only in Cyp2b-null females fed a HFD, indicating that these mice suffered some liver damage such as apoptosis or necrosis in addition to the abnormally high serum cholesterol. It is interesting that the HFD-fed Cyp2b-null female mice are not showing greater obesity than HFD-fed WT mice, but several other parameters are perturbed.

β-hydroxybutyate (B-OHB) is generated by the liver from fatty acids during prolonged exercise or starvation to meet energy requirements and compensate for lower carbohydrate levels. B-OHB can be utilized as an energy source by active tissues such as brain and muscles. HFD-fed Cyp2b-null males showed a 2.3-fold increase in B-OHB levels compared to HFD-fed WT males and a 3-fold increase compared to ND-fed Cyp2b-null males (**Table 2.2A**). The increase in B-OHB also fueled the decrease in the serum FFA/B-OHB ratio observed in HFD-fed Cyp2b-null male mice as serum fatty acid levels were relatively stable between groups, but ketones were increased by the combination of genotype and a HFD (**Fig. 2.3C**). Serum triglyceride/B-OHB ratio followed the same pattern (data not shown).

2.3.4 ND-fed Cyp2b-null mice have similar gene expression profiles compared to HFD-fed WT mice

RNAseq was performed on male and female liver samples to compare and test why only male Cyp2b-null mice showed both significant weight gain and significantly increased hepatic lipids (**Fig. 2.1, 2.2**). Analysis of global gene expression using hierarchical clustering demonstrates that male samples cluster into two different groups: one cluster consisting of WT-ND mice, and the other cluster consisting of Cyp2b-null ND and WT-HFD mice grouped among each other with Cyp2b-null HFD mice in their own subgroup. The clustering of HFD-fed WT mice and ND-fed Cyp2b-null male mice into the same clade (**Fig. 2.4A**) suggests similar changes in gene expression. Venn diagrams (**Fig. 2.4B**) confirm that within the liver the Cyp2b-null genotype with no change in diet causes comparable transcriptional effects to that of WT mice fed a HFD. Cyp2b-null ND and WT HFD mice share the same 217 significantly ($p < 0.05$) up-regulated genes and 111 down-regulated when compared to WT ND mice as the control. These two experimental groups share over 40% of each group's total number of differentially expressed genes, indicating that the Cyp2b-null genotype causes effects similar to that of a HFD-treatment potentially due to increased liver triglycerides in the ND-fed Cyp2b-null male mice (**Fig. 2.2**).

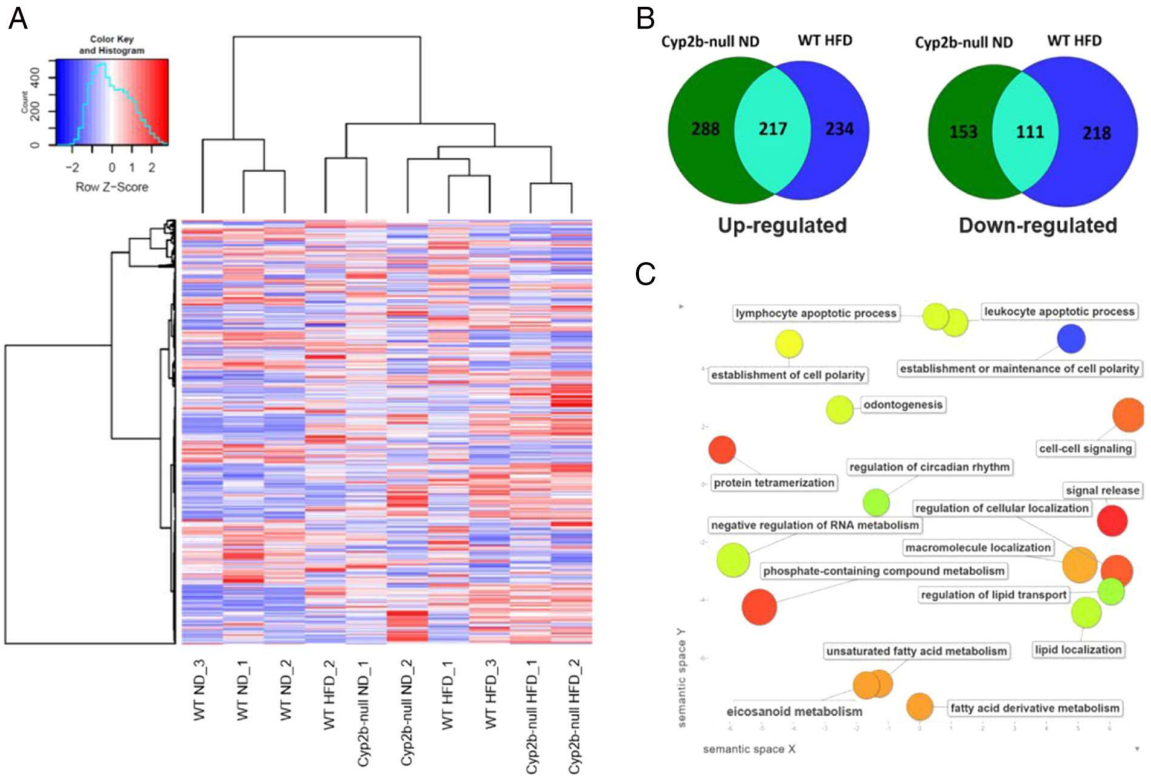

Fig. 2.4: Cyp2b-null male mice fed a ND display a similar gene expression profile to WT mice fed a HFD. RNAseq was performed on liver samples from WT and Cyp2b-null mice fed either a ND or HFD. (A) Heat map showing log2-transformed, Z-score scaled RNA-Seq expression of 500 genes with the highest variance between treatment groups. Red and blue color intensity indicate gene up- or down-regulation, respectively. Dendrogram clustering on the x-axis indicates sample similarity, whereas dendrogram clustering on the y-axis groups genes by expression profile across samples. (B) Venn diagrams of shared up- and down-regulated differentially expressed genes ($p<0.05$) between Cyp2b-null ND-fed and WT HFD-fed mice compared to WT ND mice. (C) GO term enrichment analysis summary using Revigo (Supek et al., 2011) for significantly up-regulated genes in Cyp2b-null ND mice compared to WT ND mice. The scatterplot contains enriched GO terms from the biological process class that remain after term redundancy is reduced and are displayed in a two-dimensional space where semantically similar GO terms are positioned closer together within the plot. Each circle represents an enriched GO term; the cooler the color of a term, the more significantly ($p < 0.05$) associated that term is with the group of genes being studied. Circle size indicates the frequency of the GO term in the underlying GO database, i.e. circles of more general terms are larger.

Female samples clustered in a different fashion than males. ND-fed WT and Cyp2b-null mice clustered together and separately from most of the HFD-fed mice (**Fig. 2.5A**) instead of ND-fed Cyp2b-null mice clustering with HFD-fed WT mice as seen in male groups (**Fig. 2.4B**). There is little gene expression overlap between ND-fed Cyp2b-null and HFD-fed WT female mice (**Fig. 2.5B**), in part because there are very few differentially expressed genes in HFD-fed WT female mice compared to ND-fed WT female mice (only 7; **S2.4**) and a significant drop in differentially expressed genes between ND-fed WT and ND-fed Cyp2b-null female mice compared to males (**Fig. 2.5B, S2.4-S2.7**). For example, in ND-fed groups, 506 genes were induced in Cyp2b-null male mice, but only 65 in Cyp2b-null female mice when compared to ND-fed WT mice with 15 genes overlapping between males and females. 264 genes were down-regulated in Cyp2b-null male mice, but only 73 were down-regulated in females with 19 overlapping (**S2.6, S2.8**). Most of the differences in hierarchical clustering are due to diet in females (**S2.4**). This demonstrates the lack of response to the Cyp2b knockout and HFD in female mice compared to male mice (**Fig. 2.5; S2.4-S2.6**), similar to our physiological data.

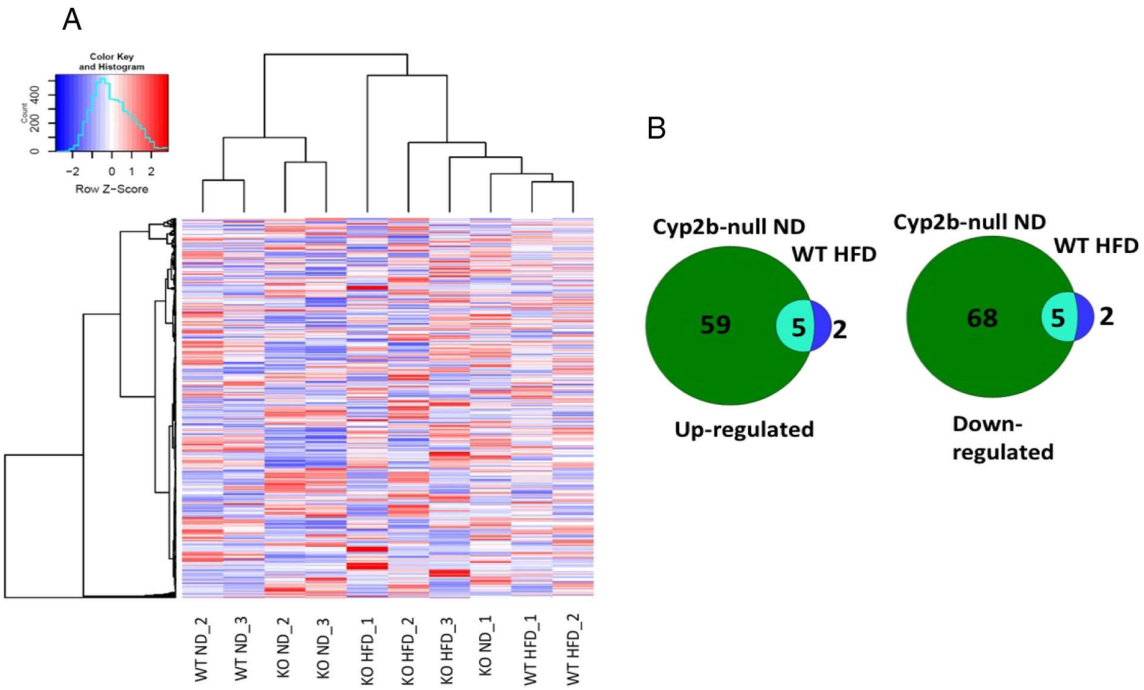

Fig. 2.5: Cyp2b-null female mice demonstrate relatively fewer gene expression changes. RNAseq was performed on liver samples from WT and Cyp2b-null mice fed either a ND or HFD. (A) Heat map showing log2-transformed, Z-score scaled RNA-Seq expression of 500 genes with the highest variance between treatment groups. Red and blue color intensity indicate gene up- or down-regulation, respectively. Dendrogram clustering on the x-axis indicates sample similarity, whereas dendrogram clustering on the y-axis groups genes by expression profile across samples. (B) Venn diagrams of shared up- and down-regulated differentially expressed genes ($p<0.05$) between Cyp2b-null ND-fed and WT HFD-fed mice compared to WT ND mice.

Interestingly, the most highly induced gene by the HFD in WT male mice was Cyp2b9 (**S2.4**). Previous diet-induced obesity (DIO) studies have also shown Cyp2b9 to be the most highly induced gene (Leung et al., 2016; McGregor et al., 2013). Among the list of shared genes by Cyp2b-null ND and WT HFD male mice, up-regulated genes with the highest logFC in both groups include Cyp2a4 (logFC: Cyp2b-null ND 6.99, WT HFD 1.53), Cyp2b9 (LogFC: Cyp2b-null ND 3.60, WT HFD 6.65), and NADH-ubiquinone oxidoreductase chain 3 (ND3) (logFC: Cyp2b-null ND 3.33, WT HFD 3.67) (**S2.5)**.

Cyp2b9 is probably highly induced in Cyp2b-null mice as a compensatory mechanism as the latter half of the Cyp2b9 gene was not eliminated by Crispr/Cas9 and is therefore most likely under control of the CAR promoter found at the front of the Cyp2b gene cluster (**S2.1**)(R Kumar et al., 2017). A Western blot confirmed that no Cyp2b's were induced and instead deleted in the Cyp2b-null mice as expected (**S2.9**). Genes down-regulated in males and females when comparing the various treatments are also available in **Supplementary Material (S2.4-S2.7)** under a separate tab.

Significantly ($p < 0.05$) enriched up-regulated gene ontology (GO) terms for male ND-fed Cyp2b-null mice in comparison to ND-fed WT mice were visualized in Revigo (**Fig. 2.4C**). Within the biological process class, ND-fed Cyp2b-null mice have enriched terms such as regulation of lipid transport, lipid localization, unsaturated fatty acid metabolism, eicosanoid metabolism, cell-cell signaling, circadian rhythms, and establishment or maintenance of cell polarity. Many of these terms are associated with NAFLD and perturbations in lipid metabolism (Berlanga, Guiu-Jurado, Porras, & Auguet, 2014; Leung et al., 2016; Sookoian & Pirola, 2013). Down-regulated GO terms for this group were mainly associated with protein stability and folding (**S2.10)**, possibly indicating endoplasmic reticulum stress via lipotoxicity from intermediate lipid metabolites or perturbations in the endoplasmic reticulum due to the loss of CYPs (Mantzaris, Tsianos, & Galaris, 2011). There were no significantly enriched GO terms when comparing ND-fed Cyp2b-null and ND-fed WT mice in females (**S2.10**).

There are not as many differentially expressed genes when comparing HFD-fed Cyp2b-null to HFD-fed WT mice in males or females (**S2.7**). In males, there are several

genes involved in triglyceride accumulation and lipid metabolism, including circadian genes associated with liver lipid metabolism, which is expected given the greater obesity and liver triglycerides in the HFD-fed Cyp2b-null mice than the HFD-fed WT mice. In addition, genes involved in tissue growth and repair and cytoskeletal remodeling are perturbed that when combined with excess serum leptin suggests that HFD-fed Cyp2b-null mice are more susceptible to tissue damage or in the early stages or fibrosis (Battaller & Brenner, 2005; Pace, Corrado, Missero, & Byers, 2003; Sanchez-Antolín et al., 2015). In females, estrogen and thyroid metabolism, steroid hormone biosynthesis, endoplasmic reticulum protein processing, and pancreatic secretion were primarily perturbed, and only a few of these are directly linked to obesity, energy metabolism, and none of the multigene pathways perturbed are linked to fibrosis.

There were 646 KEGG pathway perturbations caused by a lack of Cyp2b (comparing WT-ND to Cyp2b-null-ND) in male mice, but only 190 in female mice (**Table 2.3**). KEGG pathway analysis for both up- and down-regulated differentially expressed genes in ND-fed Cyp2b-null ND compared to ND-fed WT mice ($log_2FC > 1.0$) revealed 42 metabolic genes with altered expression in males, but only 14 in females. Pathways perturbed include PI3K-Akt signaling, protein processing in the endoplasmic reticulum, retinol metabolism, arachidonic acid metabolism, insulin resistance, glycerolipid metabolism, and fatty acid elongation within the endoplasmic reticulum (**S2.11; Table 2.3**). Many of these pathways are also crucial in fatty acid metabolism and the development of NAFLD (Berlanga et al., 2014; Naa et al., 2018). The greater transcriptional (numbers of genes and pathways) effects perturbed in ND-fed Cyp2b-null

and HFD-fed WT male mice compared to female mice provides a clue as to why males are more susceptible, and females more resistant, to obesity (**Table 2.4, 2.5**).

Table 2.3: Comparison of the number of up- and down-regulated genes within specific KEGG pathways of male and female Cyp2b-null ND-fed mice.

KEGG Pathway	Male Cyp2b-null ND vs WT ND	Female Cyp2b-null ND vs WT ND
PI3K-Akt signaling	11	5
Protein processing in endoplasmic reticulum	10	4
Retinol metabolism	7	2
MAPK signaling	7	3
Glycerophospholipid metabolism	7	2
Apoptosis	6	4
Drug metabolism	6	1
Thyroid hormone signaling	6	1
Insulin resistance/signaling	5	4
PUFA metabolism	5	1
Circadian rhythm	4	3
NAFLD	4	1
Calcium signaling	3	1
FoxO signaling	2	3
Cholesterol metabolism	1	3
Sphingolipid metabolism	1	2
Total Perturbations	646	190

Table 2.4: Comparison of the number of up- and down-regulated genes within specific KEGG pathways.

KEGG Pathway	Cyp2b-null ND vs WT ND	WT HFD vs WT ND	Cyp2b-null HFD vs WT HFD
PI3K-Akt signaling	11	12	2
Protein processing in endoplasmic reticulum	10	1	0
Retinol metabolism	7	13	1
MAPK signaling	7	12	1
Glycerophospholipid metabolism	7	1	1
Hepatocellular carcinoma	6	11	1
Drug metabolism	6	9	0
Thyroid hormone signaling	6	5	1
Apoptosis	6	1	0
PUFA metabolism	5	10	3
Insulin signaling/resistance	5	3	2
Circadian rhythm	4	2	3
NAFLD	4	2	0
Phospholipase D signaling	4	0	0
Glutathione metabolism	2	12	0
Cholesterol metabolism	1	4	2
Total Perturbations	646	620	75

Table 2.5: Comparison of the number of up- and down-regulated genes in female mice within specific KEGG pathways.

KEGG Pathway	Cyp2b-null ND vs WT ND	WT HFD vs WT ND	Cyp2b-null HFD vs WT HFD
PI3K-Akt signaling	5	0	0
Protein processing in endoplasmic reticulum	4	0	6
Insulin resistance/signaling	4	0	0
Apoptosis	4	0	0
FoxO signaling	3	0	0
Circadian rhythm	3	0	0
Cholesterol metabolism	3	1	0
MAPK signaling	3	0	1
Sphingolipid metabolism	2	0	0
Glycerophospholipid metabolism	2	0	0
Retinol metabolism	2	0	1
Calcium signaling	1	0	2
Drug metabolism	1	1	0
NAFLD	1	0	0
Total Perturbations	190	13	49

2.4 Discussion

Male, but not female Cyp2b-null mice are diet-induced obese. Male Cyp2b-null mice fed a HFD gained 15% more body weight than male WT mice fed a HFD primarily due to a 55% increase in WAT mass. Diet-induced obesity and genotype-specific diet-induced obesity are more difficult to measure in B6 female mice than male mice because the female mice are much less susceptible to obesity and diabetes than male mice (or human females) (Hong, Stubbins, Smith, Harvey, & Nunez, 2009; Wade, Gray, &

Bartness, 1985). Previous observations indicated that Cyp2b-KD mice developed age-onset obesity in males with a significant lesser effect in females. However, this work was an observation from aging mice (age-onset obesity); not a tightly planned experiment examining diet-induced obesity (B Damiri & Baldwin, 2018). Furthermore, the loss of Cyp2b, through either RNAi or Crispr/Cas9 (B. Damiri et al., 2012; R Kumar et al., 2017), causes obesity independent of strain as it occurs in FVB (Cyp2b-KD) and B6 (Cyp2b-null) mice. Overall, the loss of the primarily hepatic Cyp2b members increases WAT that in turn leads to obesity in males and suggests that inhibition of these enzymes by environmental chemicals or pharmaceuticals may have similar consequences.

Liver triglyceride concentrations were significantly increased in ND-fed Cyp2b-null mice compared to their WT male counterparts. Increases in liver triglycerides were accompanied by decreases in serum triglycerides in ND- and HFD-fed Cyp2b-null mice. In turn, both liver:serum triglyceride ratios and liver TAG:serum FFA ratios were greatly perturbed, and this includes comparisons between HFD-fed WT and HFD-fed Cyp2b-null mice. which indicates a crucial role for Cyp2b in liver triglyceride levels or distribution. Overall, triglyceride distribution was greatly perturbed in ND-fed Cyp2b-null mice, HFD-fed WT mice, and even more so in HFD-fed Cyp2b-null mice.

It is noteworthy that ND-fed Cyp2b-null male mice retain triglycerides in their liver and display a similar gene expression profile to the HFD-fed WT male mice, indicating similar early stage liver disease and compensatory changes due to increased lipids. A survey of the key biomarker genes altered in ND-fed Cyp2b-null mice such as Cyps and transporters suggests activation of transcription factors such as Foxa2, LXR,

FXRb, and potentially Rev-Erb, RAR, ROR and CAR/PXR in males (Bochkis et al., 2008; Hashita et al., 2008; J. P. Hernandez, L. C. Mota, & W. S. Baldwin, 2009; Sakai, Fukushima, Yamamoto, & Ikeuchi, 2017; Thatcher & Isoherranen, 2009; Urquhart, Tirona, & Kim, 2007). All of these transcription factors response to changes in lipid distribution or energy allocation. Hierarchical clustering, direct comparisons by Venn diagrams, shared GO terms, and similarly perturbed KEGG pathways all present evidence that ND-fed Cyp2b-null male mice have similar gene expression changes to HFD-fed WT mice. For example, both HFD-fed WT and ND-fed Cyp2b-null male mice show enriched terms for lipid transport, lipid localization, unsaturated fatty acid metabolism, and eicosanoid metabolism, clearly indicating perturbations in lipid utilization and metabolism. However, it should be noted that there are also some differences based on KEGG pathway analysis. For example, ND-fed Cyp2b-null male mice show perturbations in glycerolipid metabolism, apoptosis, and endoplasmic reticulum protein processing that are not manifested in WT-HFD mice; whereas WT-HFD mice show perturbed hepatocellular carcinoma and glutathione metabolism that is not manifested in Cyp2b-null-ND mice. Cyp2b induction by CAR is partially responsible for subsequent CAR-initiated Nrf2 activation (Rooney, Oshida, Kumar, Baldwin, & Corton, 2019), and therefore Cyp2b-null mice may not activate protective mechanisms from oxidative stress such as glutathione metabolism as well as WT mice. It is also interesting that the apoptotic and hepatocellular carcinoma responses are reversed, suggesting Cyp2b-null mice may be less susceptible to cancer even with the increase in liver triglycerides. Overall, the similarities in differential gene expression outweigh the

differences, and provide data associating the loss of hepatic Cyp2b members to liver triglycerides and obesity in males.

This was not the case in females. Significantly fewer genes were altered in females, especially following a HFD and in turn ND-fed Cyp2b-null females did not cluster with HFD-fed WT females. Female mice are generally considered partially resistant to obesity except post-menopausal (Hong et al., 2009; K Spruiell et al., 2014). This resistance was also observed during this study and demonstrates that Cyp2b enzymes such as Cyp2b9 and Cyp2b13 ,expressed at much greater levels in females (R Kumar et al., 2017; Wiwi et al., 2004)}(J. P. Hernandez, L. C. Mota, W. Huang, et al., 2009), are not the reason for the sexual dimorphism in obesity. It is still possible that some of the transcription factors that regulate Cyp2b and are predominantly expressed in females such as CAR, PXR, and FoxA2 (Hashita et al., 2008; J. P. Hernandez, L. C. Mota, W. Huang, et al., 2009; Ledda-Columbano et al., 2003; K Spruiell et al., 2014) are in part responsible for the murine female resistance to obesity.

HFD-fed Cyp2b-null females were the only mice with increased serum triglycerides and these mice also present with higher ALT levels, suggesting that the combination of a HFD and Cyp2b-knockout caused some liver damage in females. In contrast to males, Cyp2b-null females did not show significant perturbations in liver:serum ratios probably because neither serum nor liver triglycerides were perturbed as much in females, but also because both serum and liver triglycerides went up in HFD-fed Cyp2b-null female mice. Ratios are often used to increase the sensitivity of data from two physiological systems (liver:serum; TAG:HDL) or sexually dimorphic comparison

(steroid metabolites)(Di Bonito et al., 2015; R Kumar et al., 2017). Therefore, we also examined liver triglyceride:serum FFA ratios, and found they varied significantly in HFD-fed Cyp2b-null female mice.

Serum cholesterol and HDL were also significantly increased in Cyp2b-null male mice compared to WT male mice. Increased serum cholesterol coupled with decreased serum triglycerides was observed previously in diet induced obesity studies performed in B6 mice (Eisinger et al., 2014), and recent studies indicate that high cholesterol is associated with progressive NAFLD and a potential marker for NASH (Kerr & Davidson, 2012; Walenbergh & Shiri-Sverdlov, 2015). ALT is also associated with HDL, NAFLD and metabolic syndrome in men, but not women (Chen, Chen, Dai, Chen, & Fang, 2008). Overall, multiple serum and liver lipid parameters that are associated with NAFLD and NASH were perturbed (Arguello, Balboa, Arrese, & Zanlungo, 2015; K. Peng, Mo, & Tian, 2017), indicating that Cyp2b-null male mice are progressing towards hepatic steatosis and NASH. However, the lack of changes in LDL and VLDL suggest that accompanying cardiovascular disease may not be a chronic issue (Di Bonito et al., 2015; Kawano & Cohen, 2013). Histopathology did not show any pathological changes indicative of significant liver injury, although liver lipids were increased by a HFD and exacerbated by Cyp2b-knockout as measured by Oil Red O. However, our research was performed for only 10-weeks and recent work indicates B6 mice are relatively resistant to fatty liver disease and take upwards of 22-weeks to develop NAFLD (Asgharpour et al., 2016). Therefore this study was not performed for long enough to fully assess progressive NAFLD or NASH, but primarily obesity and early stage steatosis. Long-term (22-weeks)

or better yet, methionine-choline deficient dietary studies are needed to determine if the Cy2b-null mice may be susceptible to NASH.

B-OHB is increased from the breakdown of fatty acids in response to starvation and consistent with higher WAT weight (Jastreboff et al., 2014). Taken together, WAT, liver triglycerides, serum cholesterol, and B-OHB levels were all increased in Cyp2b-null mice, primarily in males, indicating an unhealthy lipid state with increased ketosis and β-oxidation sometimes regardless of dietary treatment. This combined with perturbations in transcription associated with lipid metabolism, distribution and homeostasis demonstrates a role for Cyp2b members in lipid metabolism and obesity.

Several unsaturated fatty acids are metabolized by Cyp2b members including arachidonic acid (Bishop-Bailey, Thomson, Askari, Faulkner, & Wheeler-Jones, 2014; Du et al., 2005), anandamide (Sridar, Snider, & Hollenberg, 2011), and potentially linoleic acid (Bylund et al., 1998; Robert D. Finn et al., 2009). Some data indicates high affinity for fatty acids (Du et al., 2005); however, most Cyp2b-mediated metabolism likely occurs under high fat diet conditions or directly after a meal high in PUFA (Robert D. Finn et al., 2009; Sridar et al., 2011). It is interesting to consider that a Cyp2b-mediated product of PUFA metabolism such as an epoxyecosatrienoic acid produced from AA or anandamide, may perform signaling functions that mediate lipid uptake, distribution, or metabolism in the liver, WAT, or other tissues following a diet high in PUFAs.

In summary, the data presented indicates that the hepatic Cyp2b genes are important in fatty acid metabolism. Cyp2b-null mice are diet-induced obese and show

greater susceptibility to obesity than WT mice. HFD-fed Cyp2b-null male mice present increased WAT mass, liver triglycerides, serum cholesterol, and B-OHB. In addition, the increased accumulation of liver triglycerides and decreased serum triglycerides in ND- and HFD-fed Cyp2b-null male mice suggests difficulty in allocating and utilizing fatty acids. The ND-fed Cyp2b-null male mice also showed a similar gene expression profile to the HFD-fed WT male mice as demonstrated by RNAseq, indicating increased lipids and perturbed lipid signaling regardless of diet in the Cyp2b-null mice. Taken together, this data indicates a role of Cyp2b in fatty acid metabolism and obesity, and therefore, it is certainly possible that chemical inhibition of Cyp2b members by dietary fats, pesticides, plasticizers, and pharmaceuticals could elicit similar effects on lipid metabolism and elicit obesity.

Acknowledgements

This work was supported by NIEHS grant R15ES017321. Transcriptomoic support was provided by Dr. Rooksana E. Noorai through the Clemson University Genomics and Bioinformatics Facility, NIH COBRE grant P20GM109094.

Conflict of Interest

The authors declare that they have no conflicts of interest with the contents of this article.

References

Acevedo, R., Villanueva, H., Parnell, P. G., Chapman, L. M., Gimenez, T., Gray, S. L., & Baldwin, W. S. (2005). The contribution of hepatic steroid metabolism to serum

estradiol and estriol concentrations in nonylphenol treated MMTVneu mice and its potential effects on breast cancer incidence and latency. *J Appl Toxicol, 25*, 339-353.

Angrish, M. M., Mets, B. D., Jones, A. D., & Zacharewski, T. R. (2012). Dietary fat is a lipid source in 2,3,7,8-tetrachlorodibenzo-ρ-dioxin (TCDD)-elicited hepatic steatosis in C57BL/6 mice. *Toxicol Sci, 128*(2), 377-386.

Arguello, G., Balboa, E., Arrese, M., & Zanlungo, S. (2015). Recent insights on the role of cholesterol in non-alcoholic fatty liver disease. *Biochim Biophys Acta, 1852*(9), 1765-1778.

Arnold, C., Markovic, M., Blossey, K., Wallukat, G., Fischer, R., Dechend, R., . . . Schunck, W. H. (2010). Arachidonic acid-metabolizing cytochrome P450 enzymes are targets of {omega}-3 fatty acids. *J Biol Chem, 285*(43), 32720-32733.

Asgharpour, A., Cazanave, S. C., Pacana, T., Seneshaw, M., Vincent, R., Banini, B. A., . . . Sanyal, A. J. (2016). A diet-induced animal model of non-alcoholic fatty liver disease and hepatocellular cancer. *J Hepatol, 66*(3), 579-588.

Battaller, R., & Brenner, D. A. (2005). Liver fibrosis. *J Clin Invest, 115*, 209-218.

Berlanga, A., Guiu-Jurado, E., Porras, J. A., & Auguet, T. (2014). Molecular pathways in non-alcoholic fatty liver disease. *Clin Exp Gastroenterol, 7*, 221-239.

Bishop-Bailey, D., Thomson, S., Askari, A., Faulkner, A., & Wheeler-Jones, C. (2014). Lipid-metabolizing CYPs in the regulation and dysregulation of metabolism. *Annu Rev Nutr, 34*, 261-279.

Bochkis, I. M., Rubins, N. E., White, P., Furth, E. E., Friedman, J. R., & Kaestner, K. H. (2008). Hepatocyte-specific ablation of Foxa2 alters bile acid homeostasis and results in ER stress. *Nat Med, 14*(8), 828-836.

Bochkis, I. M., Shin, S., & Kaestner, K. H. (2013). Bile acid-induced inflammatory signaling in mice lacking Foxa2 in the liver leads to activation of mTOR and age-onset obesity. *Mol Metab, 2*, 447-456.

Bylund, J., Kunz, T., Valmsen, K., & Oliw, E. H. (1998). Cytochromes P450 with bisallylic hydroxylation activity on arachidonic and linoleic acids studied with human recombinant enzymes and with human and rat liver microsomes. *J Pharmacol Exp Ther, 284*, 51-60.

Capdevila, J. H., Karara, A., Waxman, D. J., Martin, M. V., Falck, J. R., & Guengerich, F. P. (1990). Cytochrome P-450 enzyme-specific control of the regio- and

enantiofacial selectivity of the microsomal arachidonic acid epoxygenase. *J Biol Chem, 265*(19), 10865-10871.

Chamorro-García, R., Sahu, M., Abbey, R. J., Laude, J., Pham, N., & B, B. (2013). Transgenerational inheritance of increased fat depot size, stem cell reprogramming, and hepatic steatosis elicited by prenatal exposure to the obesogen tributyltin in mice. *Environ Health Perspect, 121*(3), 359-366.

Chang, J. W., Chen, H. L., Su, H. J., & Lee, C. C. (2016). Abdominal Obesity and Insulin Resistance in People Exposed to Moderate-to-High Levels of Dioxin. *PLOS One, 11*(1), e0145818.

Chen, Z.-w., Chen, L.-y., Dai, H.-l., Chen, J.-h., & Fang, L.-z. (2008). Relationship between alanine aminotransferase levels and metabolic syndrome in nonalcoholic afatty liver disease. *J Zhejiang Univ Sci B, 9*(8), 616-622.

Choquet, H., & Meyre, D. (2011). Genetics of Obesity: What have we Learned? *Current genomics, 12*(3), 169-179. doi:10.2174/138920211795677895

Damiri, B., & Baldwin, W. S. (2018). Cyp2b-knockdown Mice Poorly Metabolize Corn Oil and are Age-Dependent Obese. *Lipids, 53*(9), 871-884.

Damiri, B., Holle, E., Yu, X., & Baldwin, W. S. (2012). Lentiviral-mediated RNAi knockdown yields a novel mouse model for studying Cyp2b function. *Toxicol Sci, 125*(2), 368-381. doi:10.1093/toxsci/kfr309

Deol, P., Evans, J. R., Dhahbi, J., Chellappa, K., Han, D. S., Spindler, S., & Sladek, F. M. (2015). Soybean oil is more obesogenic and diabetogenic than coconut oil and fructose in mouse: potential role for the liver. *PLOS One, 10*(7), e0132672. doi:doi:10.1371/journal.pone.0132672

Di Bonito, P., Valerio, G., Grugni, G., Licenziati, M. R., Maffeis, C., Manco, M., . . . Baroni, M. G. (2015). CARdiometabolic risk factors in overweight and obese children in ITALY (CARITALY) Study Group. Comparison of non-HDL-cholesterol versus triglycerides-to-HDL-cholesterol ratio in relation to cardiometabolic risk factors and preclinical organ damage in overweight/obese children: the CARITALY study. *Nutr Metab Cardiovas Dis, 25*(5), 489-494.

Dong, B., Saha, P. K., Huang, W., Chen, W., Abu-Elheiga, L. A., Wakil, S. J., . . . Moore, D. D. (2009). Activation of nuclear receptor CAR ameliorates diabetes and fatty liver disease. *PNAS, 106*(44), 18831-18836.

Du, L., Yermalitsky, V., Ladd, P. A., Capdevila, J. H., Mernaugh, R., & Keeney, D. S. (2005). Evidence that cytochrome P450 CYP2B19 is the major source of

epoxyeicosatrienoic acids in mouse skin. *Arch Biochem Biophys, 435*(1), 125-133.

Eisinger, K., Krautbauer, S., Hebel, T., Schmitz, G., Aslanidis, C., Liebisch, G., & Buechler, C. (2014). Lipidomic analysis of the liver from high-fat diet induced obese mice identifies changes in multiple lipid classes. *Exp Mol Pathol, 97*(1), 37-43.

Finn, R. D., Attwood, T. K., Babbitt, P. C., Bateman, A., Bork, P., Bridge, A. J., . . . L, M. A. (2017). InterPro in 2017—beyond protein family and domain annotations. *Nucl Acids Res, 45(Database issue)*, D190-D199.

Finn, R. D., Henderson, C. J., Scott, C. L., & Wolf, C. R. (2009). Unsaturated fatty acid regulation of cytochrome P450 expression via a CAR-dependent pathway. *Biochem. J., 417*, 43-54.

Foxenberg, R. J., McGarrigle, B. P., Knaak, J. B., Kostyniak, P. J., & Olson, J. R. (2007). Human hepatic cytochrome p450-specific metabolism of parathion and chlorpyrifos. *Drug Metab Dispos, 35*(2), 189-193. doi:10.1124/dmd.106.012427

Grun, F., & Blumberg, B. (2009). Minireview: the case for obesogens. *Mol Endocrinol, 23*(8), 1127-1134. doi:10.1210/me.2008-0485

Hales, C. M., Carroll, M. D., Fryar, C. D., & Ogden, C. L. (2017). Prevalence of Obesity Among Adults and Youth: United States, 2015-2016. *NCHS Data Brief*(288), 1-8.

Hashita, T., Sakuma, T., Akada, M., Nakajima, A., Yamahara, H., Ito, S., . . . Nemoto, N. (2008). Forkhead box A2-mediated regulation of female-predominant expression of the mouse Cyp2b9 gene. *Drug Metab Dispos, 36*, 1080-1087.

Hatch, E. E., Nelson, J. W., Stahlhut, R. W., & Webster, T. F. (2010). Association of endocrine disruptors and obesity: Perspectives from epidemiologic studies. *Int J Androl, 33*(2), 324-332.

Hernandez, J. P., Mota, L. C., & Baldwin, W. S. (2009). Activation of CAR and PXR by Dietary, Environmental and Occupational Chemicals Alters Drug Metabolism, Intermediary Metabolism, and Cell Proliferation. *Current Pharmacogenomics Personal Medicine, 7*(2), 81-105. doi:10.2174/187569209788654005

Hernandez, J. P., Mota, L. C., Huang, W., Moore, D. D., & Baldwin, W. S. (2009). Sexually dimorphic regulation and induction of P450s by the constitutive androstane receptor (CAR). *Toxicology, 256*(1), 53-64. doi:https://doi.org/10.1016/j.tox.2008.11.002

Hernandez, J. P., Mota, L. C., Huang, W., Moore, D. D., & Baldwin, W. S. (2009). Sexually dimorphic regulation and induction of P450s by the constitutive androstane receptor (CAR). *Toxicology, 256*, 53-64.

Hersman, E. M., & Bumpus, N. N. (2014). A Targeted Proteomics Approach for Profiling Murine Cytochrome P450 Expression. *J Pharmacol Exp Ther, 349*(2), 221-228.

Hoek-van den Hil, E. F., van Schothorst, E. M., van der Stelt, I., Swarts, H. J., van Vliet, M., Amolo, T., . . . Keijer, J. (2015). Direct comparison of metabolic health effects of the flavonoids quercetin, hesperetin, epicatechin, apigenin and anthocyanins in high-fat-diet-fed mice. *Genes Nutr, 10*(4), 469. doi:10.1007/s12263-015-0469-z

Hoek-van den Hil, E. F., van Schothorst, E. M., van der Stelt, I., Swarts, H. J. M., Venema, D., Sailer, M., . . . Keijer, J. (2014). Quercetin decreases high-fat diet induced body weight gain and accumulation of hepatic and circulating lipids in mice. *Genes & Nutrition, 9*(5), 418. doi:10.1007/s12263-014-0418-2

Hong, J., Stubbins, R. E., Smith, R. R., Harvey, A. E., & Nunez, N. P. (2009). Differential susceptibility to obesity between male, female and ovariectomized female mice. *Nutr J, 8*, 11.

Huber, W., Carey, V. J., Gentleman, R., Anders, S., Carlson, M., Carvalho, B. S., . . . Morgan, M. (2015). Orchestrating high-throughput genomic analysis with Bioconductor. *Nat Methods, 12*, 115-121.

Jastreboff, A. M., Lacadie, C., Seo, D., Kubat, J., Van Name, M. A., Giannini, C., . . . Sinha, R. (2014). Leptin Is Associated With Exaggerated Brain Reward and Emotion Responses to Food Images in Adolescent Obesity. *Diabetes Care, 37*, 3061-3068.

Kanehisa, M., Furumichi, M., Tanabe, M., Sato, Y., & Morishima, K. (2017). KEGG: new perspectives on genomes, pathways, diseases and drugs. *Nucleic Acids Res, 45*, D353-D361.

Kawano, Y., & Cohen, D. E. (2013). Mechanisms of hepatic triglyceride accumulation in non-alcoholic fatty liver disease. *J Gastroenterol, 48*(4), 434-441.

Keeney, D. S., Skinner, C., Travers, J. B., Capdevila, J. H., Nanney, L. B., King, L. E., Jr. , & Water, M. R. (1998). Differentiating keratinocytes express a novel cytochrome P450 enzyme, Cyp2b19, having arachidonate monoxygenase activity. . *J Biol Chem, 273*(48), 32071-32079.

Kerr, T. A., & Davidson, N. O. (2012). Cholesterol and NAFLD: Renewed focus on an old villain. *Hepatology, 56*(5), 1995-1998.

Kumar, R., Litoff, E. J., Boswell, W. T., & Baldwin, W. S. (2018). High fat diet induced obesity is mitigated in Cyp3a-null female mice. *Chem Biol Interact, 289*, 129-140. doi:10.1016/j.cbi.2018.05.001

Kumar, R., Mota, L. C., Litoff, E. J., Rooney, J. P., Boswell, W. T., Courter, E., . . . Baldwin, W. S. (2017). Compensatory changes in CYP expression in three different toxicology mouse models: CAR-null, Cyp3a-null, and Cyp2b9/10/13-null mice. *PLOS One, 12*(3), e0174355.

Ladd, P. A., Du, L., Capdevila, J. H., Mernaugh, R., & Keeney, D. S. (2003). Epoxyeicosatrienoic acids activate transglutaminases in situ and induce cornification of epidermal keratinocytes. *J Biol Chem, 278*(37), 35184-35192.

le Maire, A., Grimaldi, M., Roecklin, D., Dagnino, S., Vivat-Hannah, V., Balaguer, P., & Bourguet, W. (2009). Activation of RXR-PPAR heterodimers by organotin environmental endocrine disruptors. *EMBO Reports, 10*(4), 367-373.

LeBlanc, G. A., Kullman, S. W., Norris, D. O., Baldwin, W. S., Kloas, W., & Greally, J. M. (2012). Detailed review paper state of the science on novel in vitro and in vivo screening and testing methods and endpoints for evaluating endocrine disruptors. *ENV/JM/MONO, 23*(6), 1-213.

Ledda-Columbano, G. M., Pibiri, M., Concas, D., Molotzu, F., Simbula, G., Cossu, C., & Columbano, A. (2003). Sex difference in the proliferative response of mouse hepatocytes to treatment with the CAR ligand, TCPOBOP. *Carcinogenesis, 24*(6), 1059-1065.

Lee, J. H., Wada, T., Febbraio, M., He, J., Matsubara, T., Lee, M. J., . . . Xie, W. (2010). A novel role for the dioxin receptor in fatty acid metabolism and hepatic steatosis. *Gastroenterology, 139*(2), 653-663.

Leung, A., Trac, C., Du, J., Natarajan, R., & Schones, D. E. (2016). Persistent chromatin modifications induced by a high fat diet. *J Biol Chem, 291*(20), 10446-10455.

Mantzaris, M. D., Tsianos, E. V., & Galaris, D. (2011). Interruption of triacylglycerol synthesis in the endoplasmic reticulum is the initiating event for saturated fatty acid-induced lipotoxicity in liver cells. *FEBS J, 278*(3), 519-530.

Marmugi, A., Ducheix, S., Lasserre, F., Polizzi, A., Paris, A., Priymenko, N., . . . Mselli-Lakhal, L. (2012). Low doses of bisphenol A induce gene expression related to lipid synthesis and trigger triglyceride accumulation in adult mouse liver. *Hepatology, 55*(2), 395-407.

McGregor, R. A., Kwon, E.-Y., Shin, S.-K., Jung, U. J., Kim, E., Park, J. H. Y., . . . Choi, M.-S. (2013). Time-course microarrays reveal modulation of developmental, lipid metabolism and immune gene networks in intrascapular brown adipose tissue during the development of diet-induced obesity. *Int J Obes, 37*, 1524-1531.

Mota, L. C., Hernandez, J. P., & Baldwin, W. S. (2010). CAR-null mice are sensitive to the toxic effects of parathion: Association with reduced Cytochrome P450-mediated parathion metabolism. *Drug Metab Dispos, 38*(9), 1582-1588.

Naa, A.-Y., Joa, J. J., Kwona, O. K., Shresthaa, R., Choa, P. J., Kimb, K. M., . . . Leea, S. (2018). Investigation of nonalcoholic fatty liver disease-induced drug metabolism by comparative global toxicoproteomics. *Toxicol Appl Pharmacol, 352*, 28-37.

Oshida, K., Vasani, N., Jones, C., Moore, T., Hester, S., Nesnow, S., . . . Corton, J. C. (2015). Identification of chemical modulators of the constitutive activated receptor (CAR) in a gene expression compendium. *Nucl Recept Signal, 13*, e002.

Pace, J. M., Corrado, M., Missero, C., & Byers, P. H. (2003). Identification, characterization and expression analysis of a new fibrillar collagen gene, COL27A1. *Matrix Biol, 22*(1), 3-14.

Park, B. S., & Mori, M. (2010). Balancing false discovery and false negative rates in selection of differentially expressed genes in microarrays. *Open Access Bioinformatics, 2*, 1-9. doi:doi: 10.2147/OAB.S7181

Peng, K., Mo, Z., & Tian, G. (2017). Serum lipid abnormalities and nonalcoholic fatty liver disease in adult males. *Am J Med Sci, 353*(3), 236-241.

Peng, L., Yoo, B., Gunewardena, S. S., Lu, H., Klaassen, C. D., & Zhong, X.-b. (2012). RNA sequencing Reveals Dynamic Changes of mRNA Abundance of Cytochromes P450 and Their Alternative Transcripts during Mouse Liver Development. *Drug Metab Dispos, 40*, 1198-1209.

Pratt-Hyatt, M., Zhang, H., Snider, N. T., & Hollenberg, P. F. (2010). Effects of a commonly occurring genetic polymorphism of human CYP3A4 (I118V) on the metabolism of anandamide. *Drug Metab Dispos, 38*(11), 2075-2082.

Riu, A., Grimaldi, M., le Maire, A., Bey, G., Phillips, K., Boulahtouf, A., . . . Balaguer, P. (2011). Peroxysome proliferator-activated receptor γ is a target for halogenated analogues of bisphenol-A. *Environ Health Perspect, 119*(9), 1227-1232.

Romieu, I., Dossus, L., Barquera, S., Blottiere, H. M., Franks, P. W., Gunter, M., . . . Willett, W. C. (2017). Energy balance and obesity: what are the main drivers? *Cancer Causes Control, 28*(3), 247-258. doi:10.1007/s10552-017-0869-z

Rooney, J. P., Oshida, I., Kumar, R., Baldwin, W. S., & Corton, J. C. (2019). Chemical Activation of the Constitutive Androstane Receptor Leads to Activation of Oxidant-Induced Nrf2. *Toxicol Sci, 167*(1), 172-189.

Sakai, K., Fukushima, H., Yamamoto, Y., & Ikeuchi, T. (2017). A fourth subtype of retinoic acid receptor-related orphan receptors is activated by oxidized all-trans retinoic acid in medaka (Oryzias latipes). *Zool Lett, 3*, 11. doi:https://doi.org/10.1186/s40851-017-0074-7

Sanchez-Antolín, G., Almohalla-Alvarez, C., Bueno, P., Almansa, R., Iglesias, I., Rico, L., . . . Bermejo-Martin, J. F. (2015). Evidence of Active Pro-Fibrotic Response in Blood of Patients with Cirrhosis. *PLOS One, 10*(8), e0137128. doi:doi:10.1371/journal.pone.0137128

Sharp, D. (2009). Environmental toxins, a potential risk factor for diabetes among Canadian Aboriginals. *Int J Circumpolar Health, 68*(4), 316-326.

Sookoian, S., & Pirola, C. J. (2013). Systems Biology Elucidates Common Pathogenic Mechanisms between Nonalcoholic and Alcoholic-Fatty Liver Disease. *PLOS One, 8*(3), e58895.

Spruiell, K., Jones, D. Z., Cullen, J. M., Awumey, E. M., Gonzalez, F. J., & Gyamfi, M. A. (2014). Role of human pregnane X receptor in high fat diet-induced obesity in pre-menopausal female mice. *Biochem Pharmacol, 89*(3), 399-412.

Spruiell, K., Richardson, R. M., Cullen, J. M., Awumey, E. M., Gonzalez, F. J., & Gyamfi, M. A. (2014). Role of pregnane X receptor in obesity and glucose homeostasis in male mice. *J Biol Chem, 289*(6), 3244-3261. doi:10.1074/jbc.M113.494575

Sridar, C., Snider, N. T., & Hollenberg, P. F. (2011). Anandamide oxidation by wild-type and polymorphically expressed CYP2B6 and CYP2D6. *Drug Metab Dispos, 39*(5), 782-788.

Supek, F., Bo snjak, M., Skunca, N., & Smuc, T. (2011). Revigo summarizes and visualizes long lists of gene ontology terms. *PLOS One, 6*(7), e21800.

Thatcher, J. E., & Isoherranen, N. (2009). The role of CYP26 enzymes in retinoic acid clearance. *Expert Opin Drug Metab Toxicol, 5*(8), 875-886.

Urquhart, B. L., Tirona, R. G., & Kim, R. B. (2007). Nuclear receptors and the regulation of drug-metabolizing enzymes and drug transporters: implications for interindividual variability in response to drugs. *J Clin Pharmacol, 47*(5), 566-578.

Van der Hoeven, T. A., & Coon, M. J. (1974). Preparation and properties of partially purified cytochrome P450 and NADPH-cytochrome P450 reductase from rabbit liver microsomes. *J Biol Chem, 249*, 6302-6310.

Wade, G. N., Gray, J. M., & Bartness, T. J. (1985). Gonadal influences on adiposity. *Int J Obes, 9(Suppl 1)*, 83-92.

Wahlang, B., Falkner, K. C., Gregory, B., Ansert, D., Young, D., Conklin, D. J., . . . Cave, M. (2013). Polychlorinated biphenyl 153 is a diet-dependent obesogen that worsens nonalcoholic fatty liver disease in male C57BL6/J mice. *J Nutr Biochem, 24*, 1587-1595.

Walenbergh, S. M. A., & Shiri-Sverdlov, R. (2015). Cholesterol is a significant risk factor for non-alcoholic steatohepatitis. *Exp Rev Gastronentrol Hepatol, 9*(11), 1343-1346.

Wang, X. J., Chamberlain, M., Vassieva, O., Henderson, C. J., & Wolf, C. R. (2005). Relationship between hepatic phenotype and changes in gene expression in cytochrome P450 reductase (POR) null mice. *Biochem J, 388*(Pt 3), 857-867. doi:10.1042/BJ20042087

Waxman, D. J. (1988). Interactions of hepatic cytochromes P-450 with steroid hormones: Regioselectivity and stereoselectivity of steroid metabolism and hormonal regulation of rat P-450 enzyme expression. *Biochem Pharmcol, 37*, 71-84.

Waxman, D. J., Pampori, N. A., Ram, P. A., Agrawal, A. K., & Shapiro, B. H. (1991). Interpulse interval in circulating growth hormone patterns regulates sexually dimorphic expression of hepatic cytochrome P450. *Proc Natl Acad Sci U S A, 88*(15), 6868-6872.

Wei, P., Zhang, J., Egan-Hafley, M., Liang, S., & Moore, D. D. (2000). The nuclear receptor CAR mediates specific xenobiotic induction of drug metabolism. *Nature, 407*(6806), 920-923.

Wiwi, C. A., Gupte, M., & Waxman, D. J. (2004). Sexually dimorphic P450 gene expression in liver-specific hepatocyte nuclear factor 4a-deficient mice. *Mol Endocrinol, 18*(8), 1975-1987.

Wolfrum, C., Asilmaz, E., Luca, E., Friedman, J. M., & Stoffel, M. (2004). Foxa2 regulates lipid metabolism and ketogenesis in the liver during fasting and in diabetes. *Nature, 432*, 1027-1032.

Wu, S., Moomaw, C. R., Tomer, K. B., Falck, J. R., & Zeldin, D. C. (1996). Molecular Cloning and Expression of CYP2J2, a Human Cytochrome P450 Arachidonic Acid Epoxygenase Highly Expressed in Heart. *J Biol Chem, 271*(7), 3460-3468.

Young, M. D., Wakefield, M. J., Smyth, G. K., & Oshlack, A. (2010). Gene ontology analysis for RNA-seq: accounting for selection bias. *Genome Biol, 11*, R14.

Zanger, U. M., & Schwab, M. (2013). Cytochrome P450 enzymes in drug metabolism: Regulation of gene expression, enzyme activities, and impact of genetic variation. *Pharmacol Ther, 138*(1), 103-141. doi:10.1016/j.pharmthera.2012.12.007

Zong, H., Armoni, M., Harel, C., Karnieli, E., & Pessin, J. E. (2012). Cytochrome P-450 CYP2E1 knockout mice are protected against high-fat diet-induced obesity and insulin resistance. *American journal of physiology. Endocrinology and metabolism, 302*(5), E532-539. doi:10.1152/ajpendo.00258.2011

Supplementary Material

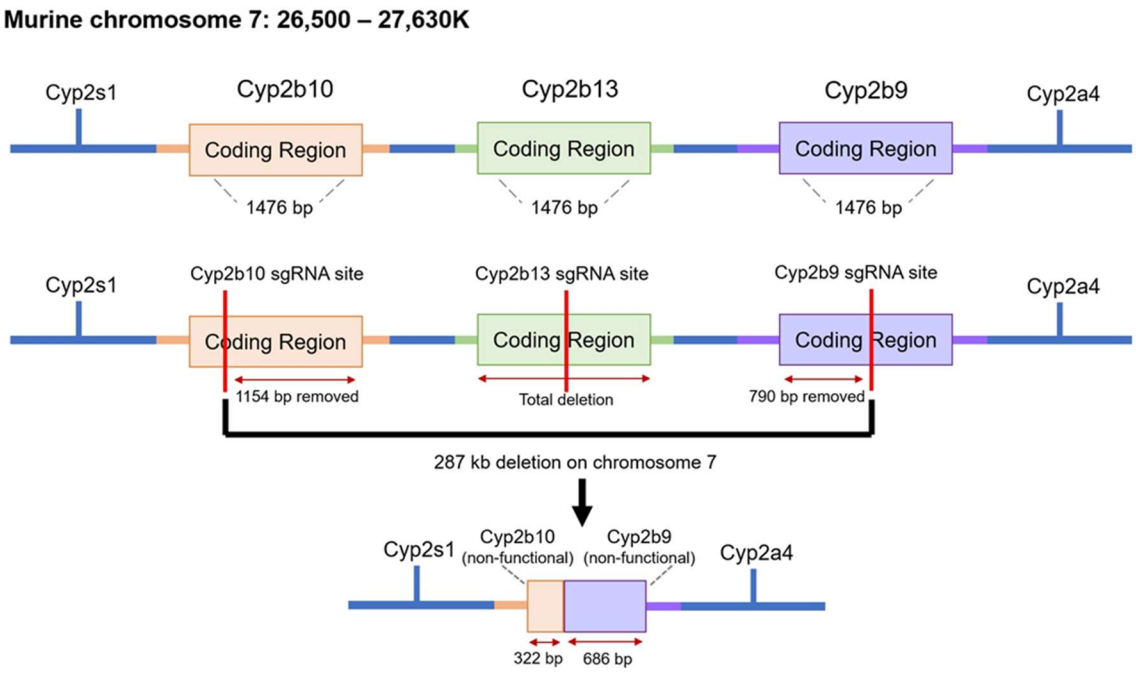

Supplementary Material 2.1: Crispr/Cas9-mediated partial chromosome deletion was used to produce a Cyp2b9/10/13-null mouse.

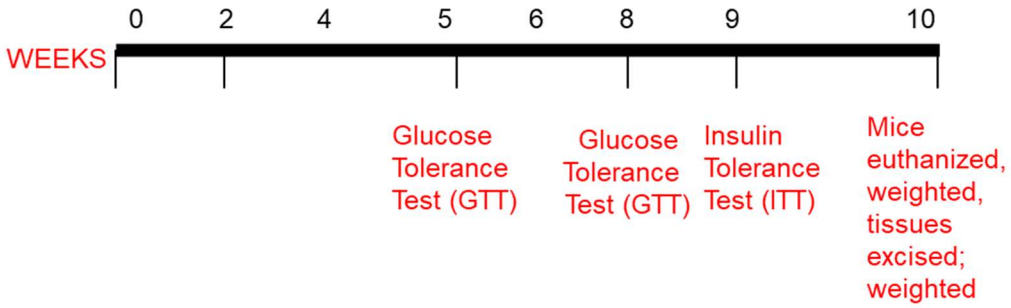

Supplementary Material 2.2: Timeline of the different procedures performed during a 10-week treatment of 9-10 week old WT and Cyp2b-null mice with either a normal diet (ND; 6.2%) or a high-fat diet (HFD; 60% fat).

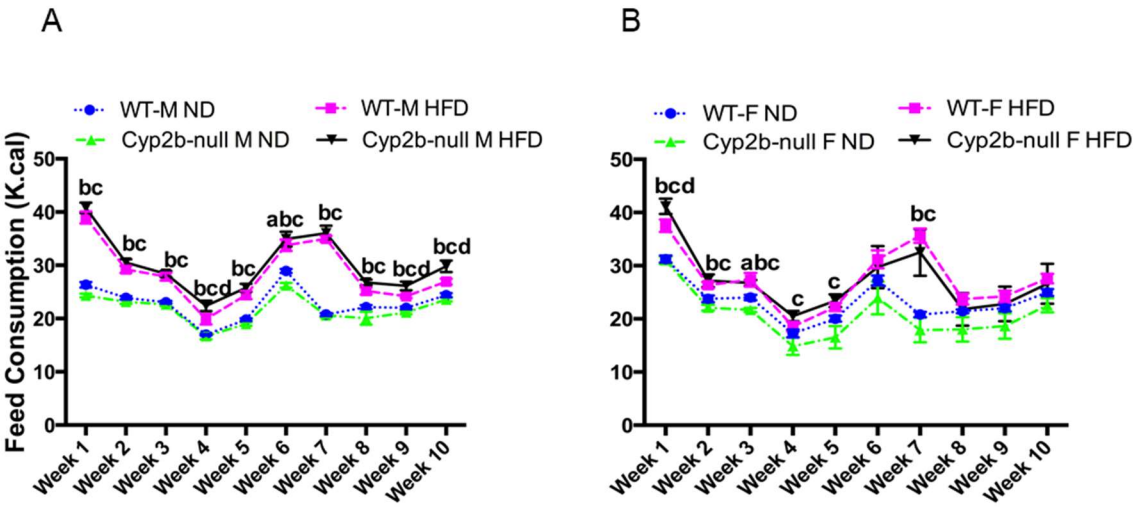

Supplementary Material 2.3: Feed consumption of WT and Cyp2b-null mice during 10-weeks of diet-induced obesity treatment. Feed consumption was measured by weighing the food every alternate day. Data are presented as mean calories ± SEM.Statistical significance was determined by one-way ANOVA followed by Fisher's LSD as post-hoc test (n= 8-9).'a' indicates WT ND are different than Cyp2b9/10/13-null ND, 'b' indicates WT ND are different than WT HFD, 'c' indicates Cyp2b9/10/13-null ND are different than Cyp2b9/10/13-null HFD, 'd' indicates WT HFD different than Cyp2b9/10/13-null HFD.

Supplementary Material 2.4: Differentially expressed gene list of WT HFD mice compared to WT ND mice. Up- and down-regulated differentially expressed genes from raw read counts in WT HFD male mice were determined using EdgeR ($p < 0.05$, FDR < 0.1). *Data published in Heintz et al. 2019, J Nutr Biochem.*

Supplementary Material 2.5: Shared differentially expressed gene list between Cyp2b-null ND and WT HFD mice compared to WT ND mice. Up- and down-regulated differentially expressed genes from raw read counts in Cyp2b-null ND and WT HFD male mice were determined using EdgeR ($p < 0.05$, FDR < 0.1) and differentially expressed genes present in both treatment groups are listed. *Data published in Heintz et al. 2019, J Nutr Biochem.*

Supplementary Material 2.6: Differentially expressed gene list of Cyp2b-null ND mice compared to WT ND mice. Up- and down-regulated differentially expressed genes from raw read counts in Cyp2b-null ND male mice were determined using EdgeR ($p < 0.05$, FDR < 0.1). *Data published in Heintz et al. 2019, J Nutr Biochem.*

Supplementary Material 2.7: Differentially expressed gene list of WT HFD mice compared to Cyp2b-null HFD mice. Up- and down-regulated differentially expressed genes from raw read counts in HFD-fed Cyp2b-null male mice compared to HFD-fed WT mice were determined using EdgeR ($p < 0.05$, FDR < 0.1). *Data published in Heintz et al. 2019, J Nutr Biochem.*

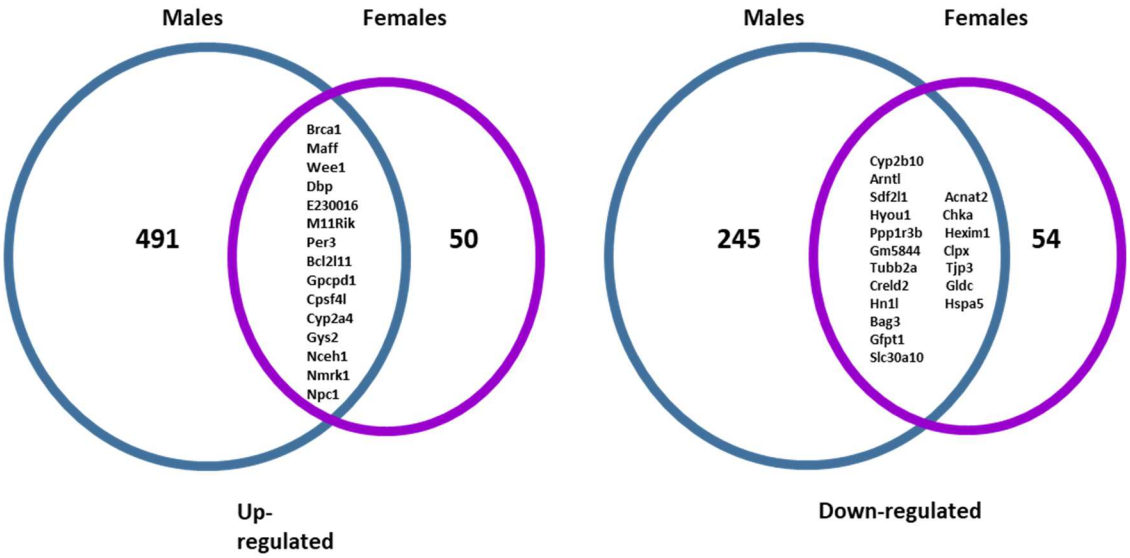

Supplementary Material 2.8: Venn Diagram showing shared differentially expressed genes between male and female Cyp2b-null ND mice compared to WT-ND mice.

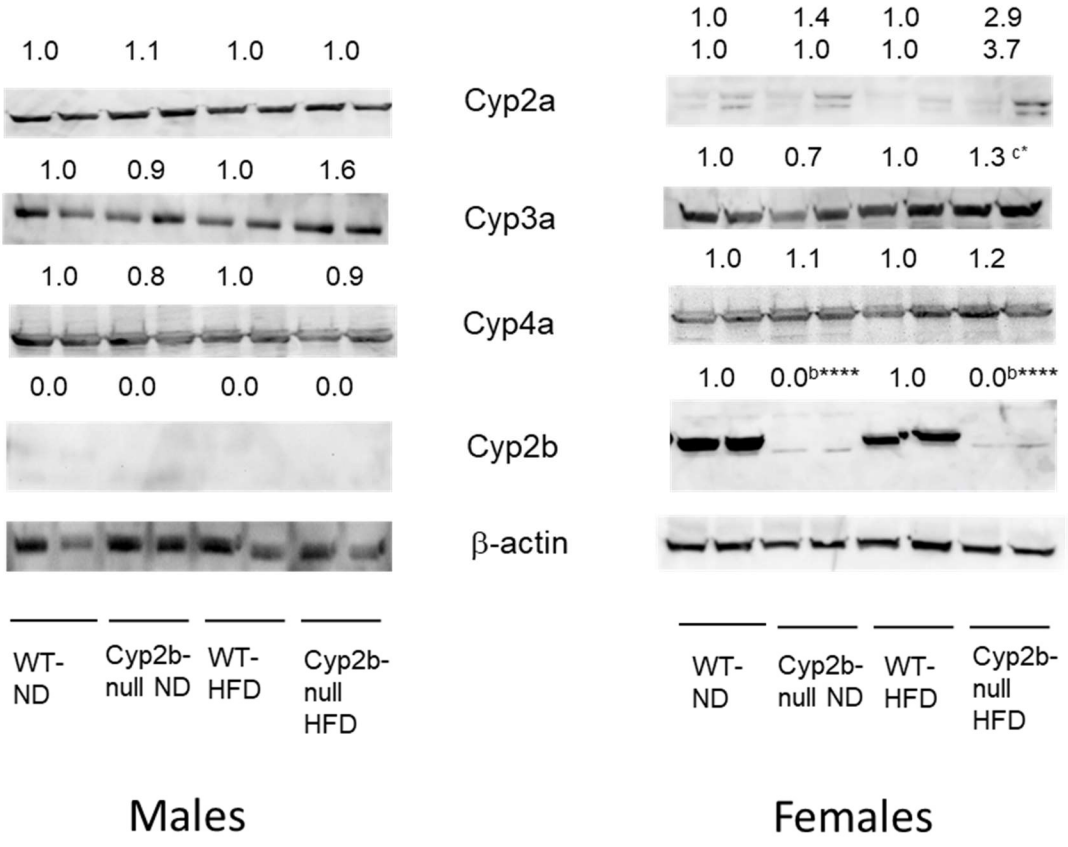

Supplementary Material 2.9: Western blots show changes in Cyp2b protein expression between WT and Cyp2b9/10/13-null mice. Microsomes were prepared by homogenizing frozen livers followed by differential centrifugation as described previously (Van der Hoeven & Coon, 1974). Protein concentrations were determined using Bradford reagent (Bio-Rad). Immunoblots were performed using 30 µg of microsomal protein separated on 12% SDS-polyacrylamide gels (BioRad). Protein was transferred onto 0.2µm polyvinylidene difluoride (PVDF) membrane and were recognized using polyclonal antibodies to to Cyp2a (Invitrogen, Carlsbad, CA USA), Cyp3a (Chemicon International, Temecula CA USA), Cyp2b (previously developed in house)(J P Hernandez, L C Mota, W Huang, D D Moore, & W S Baldwin, 2009; Mota et al., 2010), Cyp4a (Thermofisher Scientific, Rockford IL USA). β-actin (Sigma Aldrich, St.Louis MO USA) was used as the reference protein. Chemiluminescent western blot detection was done using alkaline phosphatase conjugated secondary antibodies, where in anti-mouse IgG (Immunostar, Bio-Rad) was used to visualize β-actin and anti-rabbit IgG (Immunostar, Bio-Rad) was used to visualize CYPs. Protein was quantified by densitometry (Quality One, BioRad, Hercules, CA). Relative density is shown as the average of two samples using □-actin as the reference gene. Data represents relative mean of WT compared to Cyp2b-null mice of the same gender and dietary teatment.

Statistical differences were determined by Student's t-tests (n = 2) (* $p \leq 0.05$ ** $p \leq 0.01$).

Supplementary Material 2.10: GO term enrichment analysis list of up and down-regulated genes in Cyp2b-null ND mice compared to WT ND mice. GOSeq, a GO term enrichment analysis program was used to adjust for gene length and expression bias of differentially expressed up- and down-regulated genes in Cyp2b-null ND male and female mice. *Data published in Heintz et al. 2019, J Nutr Biochem.*

Supplementary Material 2.11: Lists of altered KEGG pathways between different treatment groups. Up- and down-regulated differentially expressed genes were annotated to NCBI Gene IDs using InterPro and genes with $\log_2FC > 1.0$ were uploaded into KEGG Mapper (http://www.genome.jp/kegg/). *Data published in Heintz et al. 2019, J Nutr Biochem.*

CHAPTER THREE

GENDER DIFFERENCES IN DIET-INDUCED STEATOTIC DISEASE IN CYP2B-NULL MICE

Melissa M Heintz, Rebecca McRee, Ramiya Kumar, and William S Baldwin

Data presented in this chapter was published in *PLoS One*:

Heintz, M. M., McRee, R., Kumar, R., & Baldwin, W. S. (2020). Gender differences in diet-induced steatotic disease in Cyp2b-null mice. *PLoS One,* 15(3): e0229896.

3.0 Abstract

Nonalcoholic fatty liver disease (NAFLD) is the most common liver disease; however, progression to nonalcoholic steatohepatitis (NASH) is associated with most adverse outcomes. CYP2B metabolizes multiple xeno- and endobiotics, and male Cyp2b-null mice are diet-induced obese (DIO) with increased NAFLD. However, the DIO study was not performed long enough to assess progression to NASH. Therefore, to assess the role of Cyp2b in fatty liver disease progression from NAFLD to NASH, we treated wildtype (WT) and Cyp2b-null mice with a normal diet (ND) or choline-deficient, L-amino acid-defined high fat diet (CDAHFD) for 8 weeks and determined metabolic and molecular changes. CDAHFD-fed WT female mice gained more weight and had greater liver and white adipose tissue mass than their Cyp2b-null counterparts; males experienced diet-induced weight loss regardless of genotype. Serum biomarkers of liver injury increased in both CDAHFD-fed female and male mice; however CDAHFD-fed Cyp2b-null females exhibited significantly lower serum ALT, AST, and ASP concentrations compared to WT mice, indicating Cyp2b-null females were protected from liver injury. In both genders, hierarchical clustering of RNA-seq data demonstrates several gene ontologies responded differently in CDAHFD-fed Cyp2b-null mice compared to WT mice (lipid metabolism > fibrosis > inflammation). Oil Red O staining and direct triglycerides measurements confirmed that CDAHFD-fed Cyp2b-null females were protected from NAFLD. CDAHFD-fed Cyp2b-null mice showed equivocal changes in fibrosis with transcriptomic and serum markers suggesting less inflammation due to glucocorticoid-mediated repression of immune responses. In contrast to females,

CDAHFD-fed Cyp2b-null males had higher triglyceride levels. Results indicate that female Cyp2b-null mice are protected from NAFLD while male Cyp2b-null mice are more susceptible to NAFLD, with few significant changes in NASH development. This study confirms that increased NAFLD development does not necessarily lead to progressive NASH. Furthermore, it indicates a role for Cyp2b in fatty liver disease that differs based on gender.

Keywords: nonalcoholic fatty liver disease (NAFLD); corticosterone; P450; Cyp2b; RNAseq

3.1 Introduction

Liver disease often progresses from nonalcoholic fatty liver disease (NAFLD) to more severe diseases such as nonalcoholic steatohepatitis (NASH), fibrosis including cirrhosis, and liver cancer (Vernon, Baranova, & Younossi, 2011). NAFLD is the most common liver disease and increasing in prevalence, with 10-30% of U.S. citizens and 25% of people worldwide diagnosed (Younossi et al., 2016). NAFLD is closely linked to obesity (Pallayova & Taheri, 2014) and is the result of the hepatic manifestation of the metabolic syndrome (Chalasani et al., 2012). NAFLD is defined as the presence of $\geq$ 5% hepatic steatosis in the absence of other liver diseases (Younossi et al., 2016), yet less than 25% of patients with NAFLD develop NASH (Singh et al., 2015). In some cases the hepatic intracellular accumulation of lipids in fatty liver disease can develop into NASH

as inflammation, injury and fibrosis progress due to anti-lipotoxic protection failure (Singh et al., 2015). NASH is recognized as one of the primary causes of cirrhosis in adults and is currently the second most prominent cause for liver transplants in the United States (Wong et al., 2015). Studies have shown that steatosis may not affect NASH development (Tilg & Moschen, 2010); therefore, the pathogenesis of NASH remains controversial. However, fibrosis progression occurs in most patients with NASH and cirrhosis is the main histological feature associated with mortality of NASH patients (Angulo et al., 2015).

Regardless of how these diseases progress, dietary factors are the primary source for both NAFLD and NASH (Tilg & Moschen, 2010). A rise in consumption of foods high in polyunsaturated fatty acids (PUFAs) including vegetable and soybean oil parallels the increase in obesity in the United States and worldwide since the 1970s (Blasbalg, Hibbeln, Ramsden, Majchrzak, & Rawlings, 2011). During inflammation, PUFAs found in hepatic membranes, are released by phospholipase A2. These free PUFAs are then oxidized by cyclooxygenase, lipoxygenase, or cytochrome P450s (CYPs) to form physiologically significant metabolites. CYP-derived epoxides include the epoxyeicosatrienoic acids (EETs) produced from the metabolism of arachidonic acid (AA) (Fer et al., 2008; Funk, 2001); the epoxyoctadecenoic acids (EpOMEs) from linoleic acid; the epoxyoctadecadienoic acids from α-linolenic acid; the epoxyeicosatetraenoic acids from eicosapentaenoic acid (EPA); and the epoxydocosapentaenoic acids from docosahexaenoic acid (DHA)(Bishop-Bailey, Thomson, Askari, Faulkner, & Wheeler-Jones, 2014; Konkel & Schunck, 2011). Some

PUFAs regulate CYP activity, such as DHA which binds to the retinoid X receptor (RXR) (Urquiza et al., 2000) and prevents constitutive androstane receptor (CAR) translocation to the nucleus and subsequent transcription of Cyp2b and other CAR biomarker proteins (C.-C. Li, Lii, Liu, Yang, & Chen, 2007). Conversely, linoleic acid induces Cyp2b expression via activation of CAR (Finn, Henderson, Scott, & Wolf, 2009).

In the liver, CAR regulates both human and murine Cyp2b genes (Hernandez, Mota, & Baldwin, 2009; Hoek-van den Hil et al., 2014; Wei, Zhang, Egan-Hafley, Liang, & Moore, 2000). *Cyp2b9, Cyp2b10*, and *Cyp2b13* make up the primary hepatic Cyp2b genes in mice, and *CYP2B6,* the only *CYP2B* member in humans is highly expressed in the liver (Wang & Tompkins, 2008). Several studies indicate a role for Cyp2b in metabolizing fatty acids. Murine Cyp2b19, found in keratinocytes, metabolizes arachidonic acid to 11,12- and 14,15-EET that are important for a functional epidermis (Keeney et al., 1998). However, human CYP2B6 does not produce significant arachidonic acid metabolites (Bylund, Kunz, Valmsen, & Oliw, 1998). Interestingly, anandamide, an arachidonic acid-derived endogenous cannabinoid, is metabolized by CYP2B6 into four EET metabolites (Sridar, Snider, & Hollenberg, 2011), including 5,6-epoxyeicosatetraenoic acid ethanolamide, which has been found to be a potent agonist of the peripheral cannabinoid receptor, CB2 (Snider, Nast, Tesmer, & Hollenberg, 2009).

Finn et al (Finn et al., 2009) found that loss of all hepatic CYP activity in the hepatic P450 oxidoreductase (POR)-null mouse model led to hepatic steatosis and the induction of Cyp2b10 through the activation of CAR, a putative anti-obesity receptor

(Gao, He, Zhai, Wada, & Xie, 2009; Hernandez, Mota, & Baldwin, 2009). The authors hypothesized that Cyp2b and to a lesser extent Cyp3a enzymes play a backup role in the metabolism and protection from the build-up of fatty acids in the liver (Finn et al., 2009). Additional studies show CAR's important role in recognizing hepatic lipids via fat metabolism regulation (Dong et al., 2009), caloric restriction (Maglich et al., 2004), obesity (Maglich, Lobe, & Moore, 2009), and bile acid homeostasis (Saini et al., 2004). Furthermore, several studies performed in mice demonstrated that *Cyp2b9* exhibited the highest increased expression by RNAseq following a high fat diet (HFD) (Hoek-van den Hil et al., 2015; Leung, Trac, Du, Natarajan, & Schones, 2016).

In addition, RNAi-based Cyp2b-knockdown mice on an FVB/NJ background display increased adiposity and body weight with age as well as a decreased ability to eliminate PUFA-rich corn oil, primarily in males (Damiri, Holle, Yu, & Baldwin, 2012). In our recently published research, C57Bl/6J (B6)-Cyp2b9/10/13-null (Cyp2b-null) mice lacking the predominantly hepatic Cyp2b members, *Cyp2b9*, *Cyp2b10*, and *Cyp2b13,* are diet-induced obese in males with moderate increases in steatosis. Interestingly, the Cyp2b-null male mice developed some steatosis regardless of diet; however, they showed very little hepatic inflammation, which is unusual, suggesting Cyp2b-null mice may be protected from developing NASH (Heintz, Kumar, Rutledge, & Baldwin, 2019). This study was only carried out for 10 weeks and new research indicates that B6 mice fed a high fructose + 42% Kcal HFD for up to 22-weeks failed to form NASH following NAFLD development. Therefore, the previous study was not equipped to investigate NASH development in Cyp2b-null mice. Based on the lack of inflammation in HFD-fed

Cyp2b-null mice, we predict that diet-induced NASH will increase hepatic triglycerides in Cyp2b-null mice. This increase in triglycerides will provide protection from liver inflammation and injury compared to their WT counterparts, as free fatty acids and their metabolites are more lipotoxic than inert triglycerides (Alkhouri, Dixon, & Feldstein, 2009).

We used our previously developed Cyp2b-null mouse model (Heintz et al., 2019; Kumar et al., 2017) to test whether a lack of Cyp2b plays a role in the progression of liver disease. Cyp2b-null and WT mice (n = 9) were fed either a choline-deficient, L-amino acid-defined, high fat diet (CDAHFD) or normal diet (ND) for 8 weeks. The CDAHFD is similar to a methionine-choline deficient (MCD) diet model for the determination of NAFLD/NASH. However, the MCD diet exhibits severe body weight loss which makes long term studies difficult (Rizki et al., 2006). CDAHFD-fed mice do not lose weight, but instead gradually gain weight and develop steatohepatitis and fibrosis more rapidly (Matsumoto et al., 2013). Both physiological and biochemical changes, including differential gene expression via RNA sequencing were examined in treated WT and Cyp2b-null mice. Results from this study show that a lack of Cyp2b causes gender-based differences in response to diet-induced NASH treatment.

3.2 Materials and Methods

3.2.1 Choline-deficient, L-amino acid-defined high-fat diet (CDAHFD):

Animal care and associated procedures were approved by Clemson University's Institutional Animal Care and Use committee. Cyp2b9/10/13-null (Cyp2b-null) mice were developed using CRISPR/Cas9 technology on the C57Bl/6J (B6) background mice as previously described (Heintz et al., 2019; Kumar et al., 2017). Wildtype (WT) B6 mice were purchased from The Jackson Laboratory (Bar Harbor, ME, USA) at 6 weeks of age and were acclimated for 4 weeks prior to treatment. WT and Cyp2b-null male and female (10 weeks old) mice were divided into groups (n=9) and fed either a normal chow diet (ND; Harlan, 3.1 Kcal/g: 18.6% protein, 6.2 % fat, 44.2% carbohydrates; Madison, WI USA) or a CDAHFD (Research Diets, 5.2 Kcal/g: 18% protein, 62% fat, 20% carbohydrates, 0.1% methionine; New Brunswick, NJ, USA) for 8 weeks (Matsumoto et al., 2013). Weight gain was monitored weekly and feed consumption was measured every other day. Fasting blood glucose levels were determined during weeks 4 and 6. Glucose tolerance tests (GTT) were performed during week 6. At the end of the study, mice were anesthetized and blood collected by heart puncture prior to euthanasia. Liver, kidney, white adipose tissue (WAT), and brown adipose tissue (BAT) were excised and weighed. All tissues were immediately snap frozen with liquid nitrogen and stored at -80°C or placed in 10% formalin (Fisher, Fairlawn, NJ USA) for further studies. A timeline of procedures is provided in **Supplementary Material** (**S3.1**).

3.2.2 Fasting Blood Glucose and Glucose tolerance tests:

During weeks 4 and 6, mice were fasted for 4 hours and fasting blood glucose was determined using an Alphatrak 2 (AlphaTRAK, Chicago, IL USA) blood glucose meter

following tail bleed. During week 6, glucose tolerance was determined following an intraperitoneal injection of 1g/kg of their body weight of D-glucose (Sigma Ultra, St. Louis, MO USA) with blood glucose readings every 20 min for the first hour and every 30 min for the second hour as described previously (Ayala et al., 2010; Heintz et al., 2019).

3.2.3 Serum biomarker panel:

Blood samples were collected by heart puncture and incubated at room temperature for 30 min followed by centrifugation at 6000 rpm for 10 min. Serum from each sample was transferred into a fresh tube and aliquots shipped on dry ice to Baylor College of Medicine's Comparative Pathology Laboratory (Houston, TX USA) for determination of tissuse damage serum marker concentrations including alanine aminotransferase (ALT), aspartate aminotransferase (AST), alkaline phosphatase (ALP), and creatine kinase (CK), and lactate dehydrogenase (LDH). In addition, serum glucose, cholesterol, triglycerides, high density lipoprotein (HDL), low density lipoprotein (LDL), very low density lipoprotein (VLDL), phosphorus, calcium, and direct, indirect, and total bilirubin were quantified. Serum parameters were determined using a Beckman Coulter AU480 chemistry analyzer (Atlanta, GA, USA) and the appropriate Beckman Coulter biochemical kits according to the manufacturer's instructions.

3.2.4 Serum concentrations of leptin, adiponectin, corticosterone, β-hydroxybutyrate, and C-reactive protein:

Serum leptin, adiponectin and β-hydroxybutyrate concentrations were determined using EIA or colorimetric kits from Cayman Chemical (Ann Arbor, MI), and serum corticosterone and C-reactive protein (CRP) from Abcam (Cambridge, MA USA) according to the manufacturer's instructions.

3.2.5 Liver triglyceride, cholesterol, and hydroxyproline:

Liver triglycerides, cholesterol and hydroxyproline were extracted and quantified as described previously (R. Kumar, E. J. Litoff, W. T. Boswell, & W. S. Baldwin, 2018) using colorimetric kits from Cayman Chemical (triglycerides only) and Abcam according to the manufacturer's instructions.

3.2.6 Histopathological analysis:

During necropsy, clean liver slices were placed in 10% formalin (Fisher) or snap frozen in liquid nitrogen for staining. Slices placed in 10% formalin were stained with Hematoxylin and Eosin (H&E) or Masson's trichrome at Colorado Histoprep (Fort Collins, CO USA). Slices snap frozen in liquid nitrogen were stained with Oil Red O at Baylor College of Medicine's Comparative Pathology Laboratory using standard protocols (Dong et al., 2009). The liver lipid droplets stained by Oil Red O were quantified by total area of each sample imaged (400x magnification) using ImageJ Fiji (Schindelin et al., 2012). In Fiji, the scale bar was set to equal 0.05 mm and threshold color to red, with red pass selected and green/blue pass deselected. Red coverage of

particles was set to 130-255 and size (mm^2) equals 0.00001-infinity for all images measured.

3.2.7 Immunoblots:

Nuclear protein extracts were prepared by homogenizing frozen livers followed by differential centrifugation using a Nuclear Protein Extraction kit (Cayman Chemical). Protein concentrations were determined using Bradford reagent (Bio-Rad). Immunoblots were performed using 30 μg of nuclear protein separated on a 12% SDS-polyacrylamide gel (BioRad) and then protein was transferred onto a 0.2μm polyvinylidene difluoride (PVDF) membrane. Specific proteins were recognized using polyclonal antibodies to Proliferating Cell Nuclear Antigen (PCNA) (ThermoFisher, Waltham, MA) and β-actin (Sigma Aldrich, St.Louis MO USA) as the reference protein. Chemiluminescent immunoblot detection was done using alkaline phosphatase conjugated secondary antibodies where anti-rabbit IgG (Immunostar, Bio-Rad) was used to visualize PCNA and anti-mouse IgG (Immunostar, Bio-Rad) was used to visualize β-actin. Protein bands were quantified by densitometry (Image Lab 6.0.1, BioRad, Hercules, CA). Relative density is shown as the average of two samples using β-actin as the reference gene. Data are presented as relative mean of WT ND compared to each treatment group.

3.2.8 RNA sequencing (RNAseq):

Liver samples were stored in RNAlater Stabilization Solution (Invitrogen, Carlsbad, CA USA) at -80°C. Total RNA was extracted from mouse livers of each

treatment group using TRIzol (Ambion, Carlsbad, CA USA) and quantified on a Qubit 2.0 Fluorometer. RNA integrity number (RIN) was determined with an Agilent 2100 Bioanalyzer (place) to assess RNA quality, and samples with a RIN > 8.0 were determined to be of high quality and used for next generation sequencing. Libraries were prepared using NEB Next Ultra RNA Library Prep kit. Samples were sequenced to an average sequencing depth of 20,000,000 read pairs with a 2x150 paired-end module using a NovaSeq 6000. Quality metrics were checked using FastQC on all samples sequenced, and Trimmomatic was used to trim low quality bases. Trimmed reads were aligned to the *Mus musculus* reference genome (GCF_000001635.25_GRCm38.p6) using GSNAP, and 99.8% of the trimmed reads aligned. Subread feature counts software found reads that aligned with known genes. Raw read counts and EdgeR were used to determine differential gene expression (Huber et al., 2015). Series GSE137449 containing the RNAseq data has been uploaded to the Gene Expression Omnibus (GEO).

Differential gene expression by multiple comparisons for all treatment groups was determined by EdgeR. Results were filtered for p- and FDR values < 0.05. Normalized counts from the remaining genes post-filtering were compared between groups by Student's t-tests to determine significantly different ($p < 0.05$) expressed genes. Heatmap hierarchical cluster analysis by Euclidean distance using Ward's method was performed with Heatmap.2 in R (https://www.r-project.org/) using significant differentially expressed genes with a $\log_2FC > 1.0$ between CDAHFD-fed Cyp2b-null and CDAHFD-fed WT groups. GOSeq, a gene ontology (GO) term enrichment analysis program was

used to adjust for gene length and expression bias, and create GO term lists for the significant differentially expressed genes between CDAHFD-fed groups in female and male mice(Young, Wakefield, Smyth, & Oshlack, 2010). Significantly ($p < 0.05$) enriched GO terms were visualized in Revigo, which reduces enriched term redundancy and displays the remaining GO terms in a scatterplot (Supek, Bošnjak, Škunca, & Šmuc, 2011). Differentially expressed genes acoss treatment groups were annotated using PANTHER (http://www.pantherdb.org/) and InterPro (Finn et al., 2017), and differentially expressed genes between CDAHFD-fed Cyp2b-null and CDAHFD-fed WT mice were entered into KEGG Mapper (Kanehisa, Furumichi, Tanabe, Sato, & Morishima, 2017) to determine and visualize biochemical pathways perturbed by diet-induced NASH and/or a lack of Cyp2b enzymes (Heintz et al., 2019).

3.2.9 Quantitative Real-time Polymerase Chain Reaction (qPCR):

cDNA was prepared from RNA with MMLV reverse transcriptase, a dNTP mixture, and random hexamers (Promega Corporation, Madison WI). qPCR was used to quantify changes in gene expression using previously published primers (R Kumar, E J Litoff, W T Boswell, & W S Baldwin, 2018) and newly developed primers for genes involved in inflammation, fibrosis, and lipid metabolism (**S3.1 Table**). PCR efficiency was determined based on a standard curve preparedusing a sample mixture containing all the cDNA samples diluted at 1:1, 1:4, 1:16, 1:64, 1:256 and 1:1024 in triplicate with 0.25X RT_2 SybrGreen (Qiagen Frederick, MD USA) on a CFX 96-well Real-Time PCR detection system (Bio-Rad). 18S was used as the reference gene and Muller's inverted

equation was used to quantify differences in gene expression (Muller, Janovjak, Miserez, & Dobbie, 2002; Roling, Bain, & Baldwin, 2004).

3.2.10 Tests of statistical significance:

Data are presented as mean ± SEM (n = 8-9). Statistical analyses were performed by one-way ANOVA followed by Fisher's LSD as the post-hoc using Graphpad Prism version 7 (GraphPad Software, San Diego, CA). A p-value < 0.05 was considered statistically significant.

3.3 Results

3.3.1 Changes in body mass following a CDAHFD:

CDAHFD-fed WT female mice gained the most weight; significantly more than CDAHFD-fed Cyp2b-null female mice after only two weeks and this trend continued throughout the study. This indicates the lack of Cyp2b enzymes had a substantial repressive effect on CDAHFD-mediated weight gain in females (**Fig 3.1A**). In contrast, CDAHFD-fed male mice weighed significantly less than their normal diet counterparts, indicating that diet was the primary modifier of weight in males, not genotype (**Fig 3.1B**). Previous research indicated one of the benefits of a CDAHFD is no weight loss (Matsumoto et al., 2013); nevertheless, there was little weight gain in male mice fed a CDAHFD (**Fig 3.1B**). Mice fed a CDAHFD consumed more calories compared to their ND counterparts; however, genotype did not effect calorie intake (**S3.2**). Therefore, the

differences in weight between CDAHFD-fed WT and CDAHFD-fed Cyp2b-null female mice cannot be explained by alterations in caloric uptake.

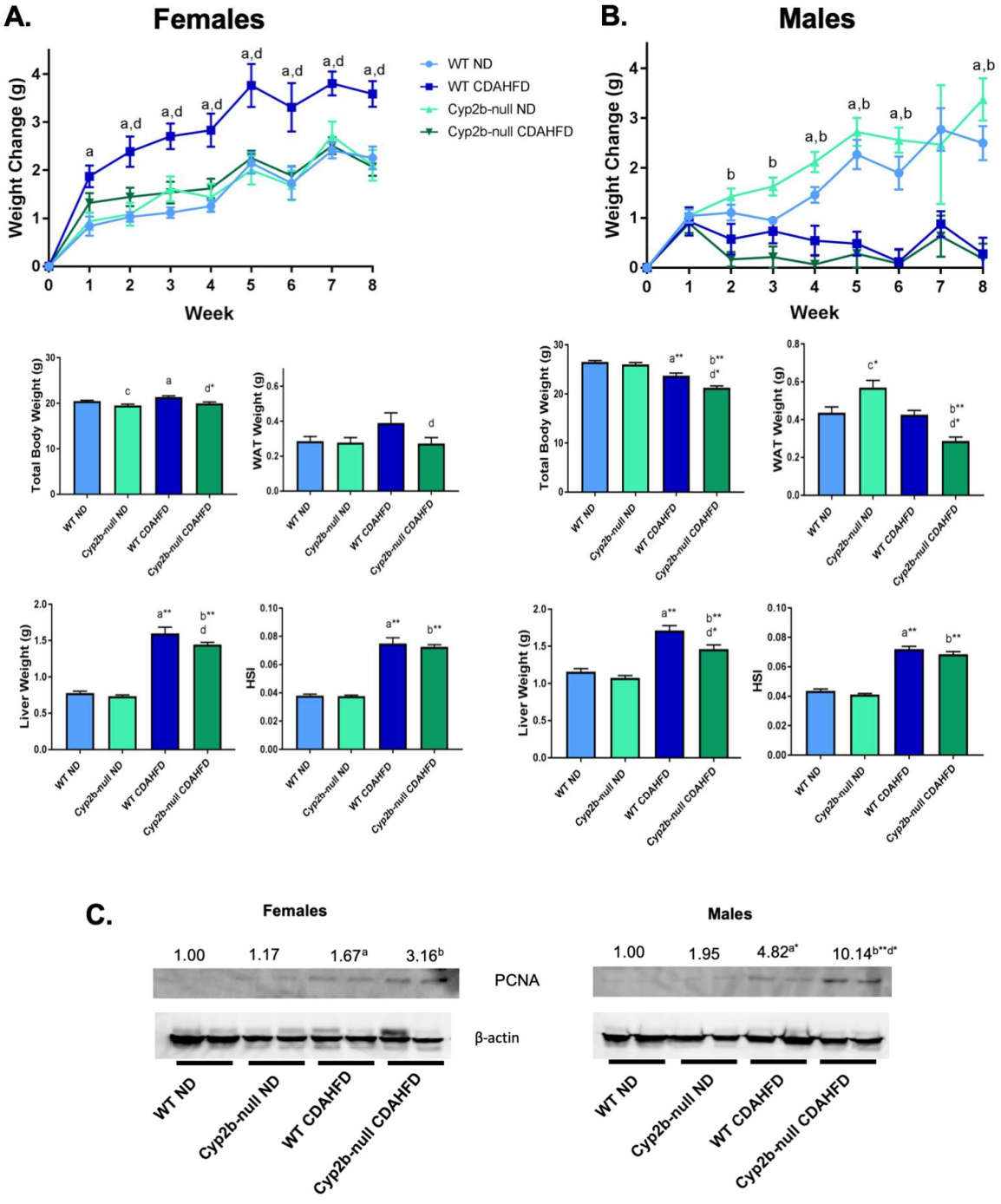

Figure 3.1. Changes in body weight and organ weight over the 8 weeks of diet-induced NASH treatment. Body and select organ weights of female (A) and male (B) WT and Cyp2b-null mice were monitored during the 8 weeks of treatment. (C) Immunoblots of PCNA in female and male mice with b-actin as the reference gene. Data are presented as mean ± SEM. Statistical significance was determined by one-way ANOVA followed by Fisher's LSD as the post-hoc test (n=9; n=2 for immunoblots). An 'a' indicates ND-fed WT different than CDAHFD-fed WT, 'b' indicates ND-fed Cyp2b-null different than CDAHFD-fed Cyp2b-null, 'c' indicates ND-fed WT different than ND-fed Cyp2b-null, 'd' indicates CDAHFD-fed WT different than CDAHFD-fed Cyp2b-null.

The weight gain in CDAHFD-fed WT female mice was in part attributed to greater liver and white adipose tissue (WAT) mass than CDAHFD-fed Cyp2b-null mice (**Fig 3.1A**). The lower liver mass in Cyp2b-null females following a CDAHFD suggests a protective effect of Cyp2b loss on liver proliferation or the development of fatty liver disease; however, liver weight decreased in relative proportion to body weight based on the hepatosomatic index (HSI). In contrast to females, ND-fed Cyp2b-null male mice accumulated more white adipose tissue than all other groups (**Fig 3.1B**). The increase in white adipose tissue in ND-fed Cyp2b-null males is consistent with previous results in Cyp2b-null mice (Heintz et al., 2019). Similar to females, CDAHFD-fed Cyp2b-null male livers and WAT weighed less than CDAHFD-fed WT mice; however, liver weight

was altered in proportion to body weight (HSI) (**Fig 3.1B**). To determine if liver weight or HSI was more indicative of cell proliferation, we examined proliferative cell nuclear antigen (PCNA) protein levels by immunoblotting (**Fig 3.1C**). PCNA levels increased in response to a CDAHFD. This response was significantly greater in the male CDAHFD-fed Cyp2b-null mice than the male CDAHFD-fed WT mice, indicating that at least in Cyp2b-null males liver weight was likely increased due to greater proliferation.

3.3.2 Serum glucose and glucose tolerance in response to a CDAHFD are gender-dependent:

Fasting serum glucose levels measured during weeks 4 and 6 were significantly decreased by the CDAHFD diet in males, but not females (**Fig 3.2AB**). Fasting serum glucose was not effected by the combination of diet and genotype in either sex. However, fasting serum glucose was increased in ND-fed Cyp2b-null female (25%) and male (32%) mice at week 6 (**Fig 3.2B**), consistent with previous findings (Heintz et al., 2019). Glucose tolerance tests (GTT) were performed to determine if Cyp2b-null mice have reduced ability to respond to glucose, a biomarker of metabolic disease. ND-fed Cyp2b-null female mice were slower to clear serum glucose compared to ND-fed WT females; however, there were no differences attributed to diet or a combination of genotype and diet (**Fig 3.2CD**). In contrast to females, ND-fed Cyp2b-null males showed no difference in glucose tolerance compared to WT mice; CDAHFD-fed males exhibited a significantly faster response to glucose (better glucose tolerance) than ND-fed males regardless of

genotype (**Fig 3.2CD**). In general, poor glucose tolerance was genotype dependent in females and weight or diet dependent in males.

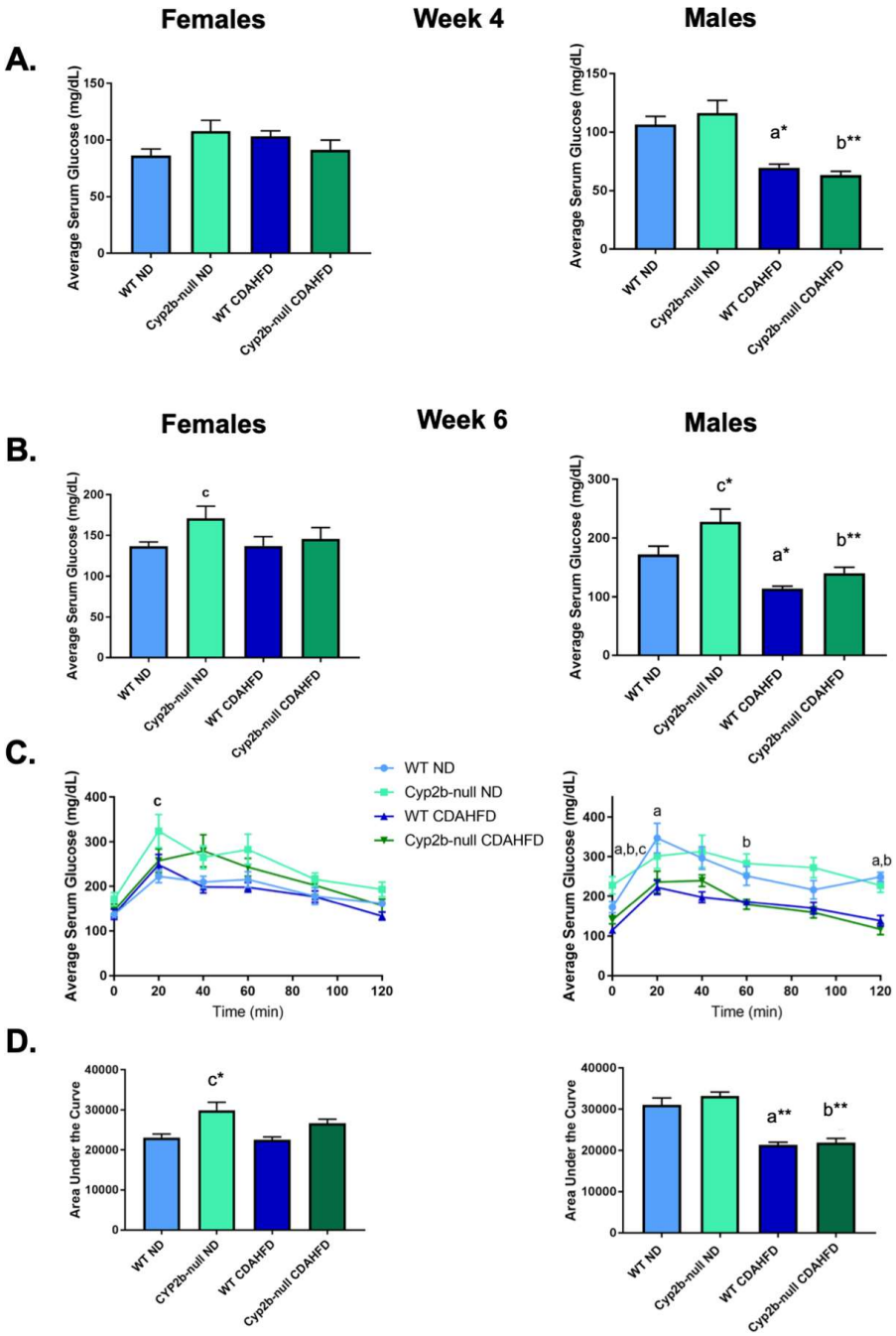

Figure 3.2. Gender-dependent differences in serum glucose and glucose tolerance in response to CDAHFD. Fasting blood glucose levels were measured during weeks 4 (A)

and 6 (B) in female and male mice. During week 6 glucose tolerance tests were performed on all treatment groups (C) and glucose measured at 20, 40, 60, 90, and 120 minutes after the glucose challenge. Results are also represented as area under the curve (D). Data are presented as mean serum glucose ± SEM. Statistical significance was determined by one-way ANOVA followed by Fisher's LSD as the post-hoc test (n= 9). An 'a' indicates ND-fed WT different than CDAHFD-fed WT, 'b' indicates ND-fed Cyp2b-null different than CDAHFD-fed Cyp2b-null, 'c' indicates ND-fed WT different than ND-fed Cyp2b-null. No asterisk indicates a p-value < 0.05, * indicates a p-value < 0.01, and ** indicates a p-value < 0.0001.

3.3.3 Serum biomarkers indicate Cyp2b-loss is protective against liver injury in females:

Common serum biomarkers of liver injury such as ALT, AST, and ALP increased in female mice fed a CDAHFD; however, CDAHFD-fed Cyp2b-null females exhibited significantly lower serum levels of these enzymes (28%, 42%, 29% lower respectively) compared to their WT counterparts, indicating Cyp2b-null female mice are protected from diet-induced NASH (**Fig 3.3A**). H&E staining revealed cytoplasmic vacuolization, a marker of cell death (Shubin, Demidyuk, Komissarov, & Rafieva, 2016) caused by the CDAHFD; however, no significant differences in pathology were observed between WT and Cyp2b-null mice (Fig 3AB). Male mice fed a CDAHFD showed increased levels of serum ALT, AST, and ALP regardless of genotype (**Fig 3.3B**). CDAHFD-fed Cyp2b-null males had higher levels of creatine kinase (CK) (1.5-fold) compared to all other treatment

groups including their WT counterparts, suggesting that Cyp2b-null males are more susceptible to CDAHFD-induced damage in other tissues such as cardiac and skeletal muscle (Yen et al., 2017), the opposite of females (**Fig 3.3B**).

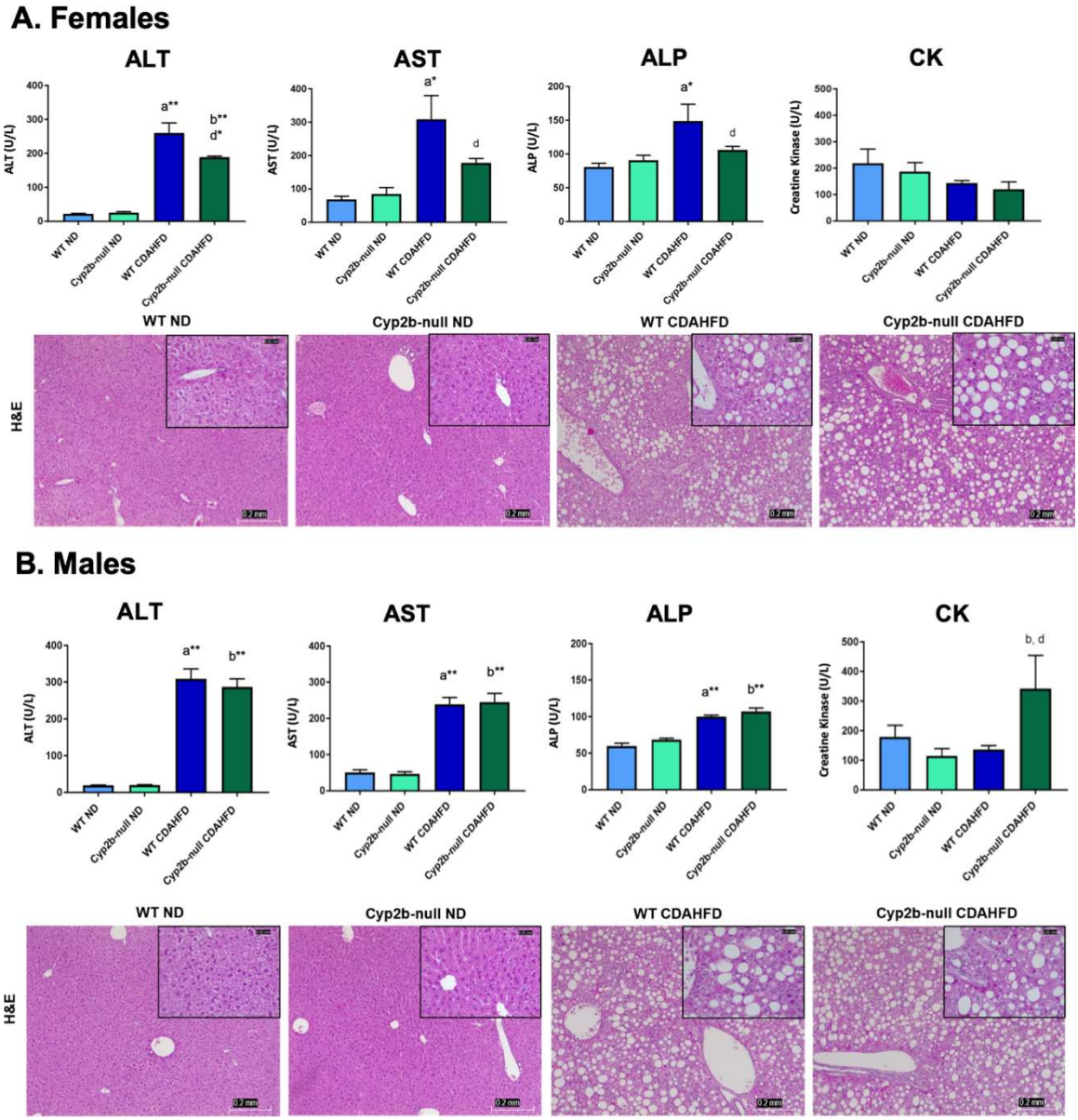

Figure 3.3. Biomarkers of liver tissue damage in ND and CDAHFD-fed WT and Cyp2b-null mice. Serum ALT, AST, ALP, and CK concentrations were measured, and

histopathological changes were evaluated by H&E staining of liver tissues from female (A) and male (B) mice. Images were taken at 100x (0.2 mm) and 400x (0.05 mm) magnification. Data are presented as mean ± SEM. Statistical significance was determined by one-way ANOVA followed by Fisher's LSD as the post-hoc test (n=5). An 'a' indicates ND-fed WT different than CDAHFD-fed WT, 'b' indicates ND-fed Cyp2b-null different than CDAHFD-fed Cyp2b-null, 'c' indicates ND-fed WT different than ND-fed Cyp2b-null, 'd' indicates CDAHFD-fed WT different than CDAHFD-fed Cyp2b-null. No asterisk indicates a p-value < 0.05, * indicates a p-value < 0.01, and ** indicates a p-value < 0.0001.

3.3.4 Perturbed gene expression in Cyp2b-null mice fed a CDAHFD:

RNA-seq was performed on liver samples from all treatment groups to further investigate the role of Cyp2b in the development and progression of NASH because of the observed changes in serum markers of liver injury in the CDAHFD-treated groups, especially within the relatively resistant Cyp2b-null female mice. A CDAHFD caused numerous changes in gene expression relative to a ND (**S3.3**). Analysis of the differentially expressed genes between CDAHFD-fed Cyp2b-null and WT groups ($log_2FC > 1.0$; **S3.4**) by hierarchical clustering revealed numerous CDAHFD-induced changes in gene expression in both female and male WT mice (**Fig 3.4**). Several genes that were altered by a CDAHFD in WT mice were regulated in the opposite direction in CDAHFD-fed Cyp2b-null mice (**Fig 3.4AB**). Associated immune system genes, *Cd8*

antigen beta chain 1 (*Cd8b1*) and nuclear factor of activated T-cells cytoplasmic 2 (*Nfatc2*), as well as the upstream cortisol synthesis calmodulin-like protein 4 (*Calml4*) gene had very low expression or down-regulation (blue) in CDAHFD-fed WT females but up-regulation (yellow) in Cyp2b-null counterparts (**Fig 3.4A**). Oppositely regulated genes between CDAHFD-fed WT and Cyp2b-null male mice included feeding behavior regulation and insulin signaling genes, hypocretin receptor 2 (*Hcrtr2*) and protein phosphatase 1 regulatory subunit 3C (*Ppp1r3c*), respectively. These genes had low expression or up-regulation (yellow) in CDAHFD-fed WT males but down-regulation (blue) in Cyp2b-null counterparts (**Fig. 3.4B**).

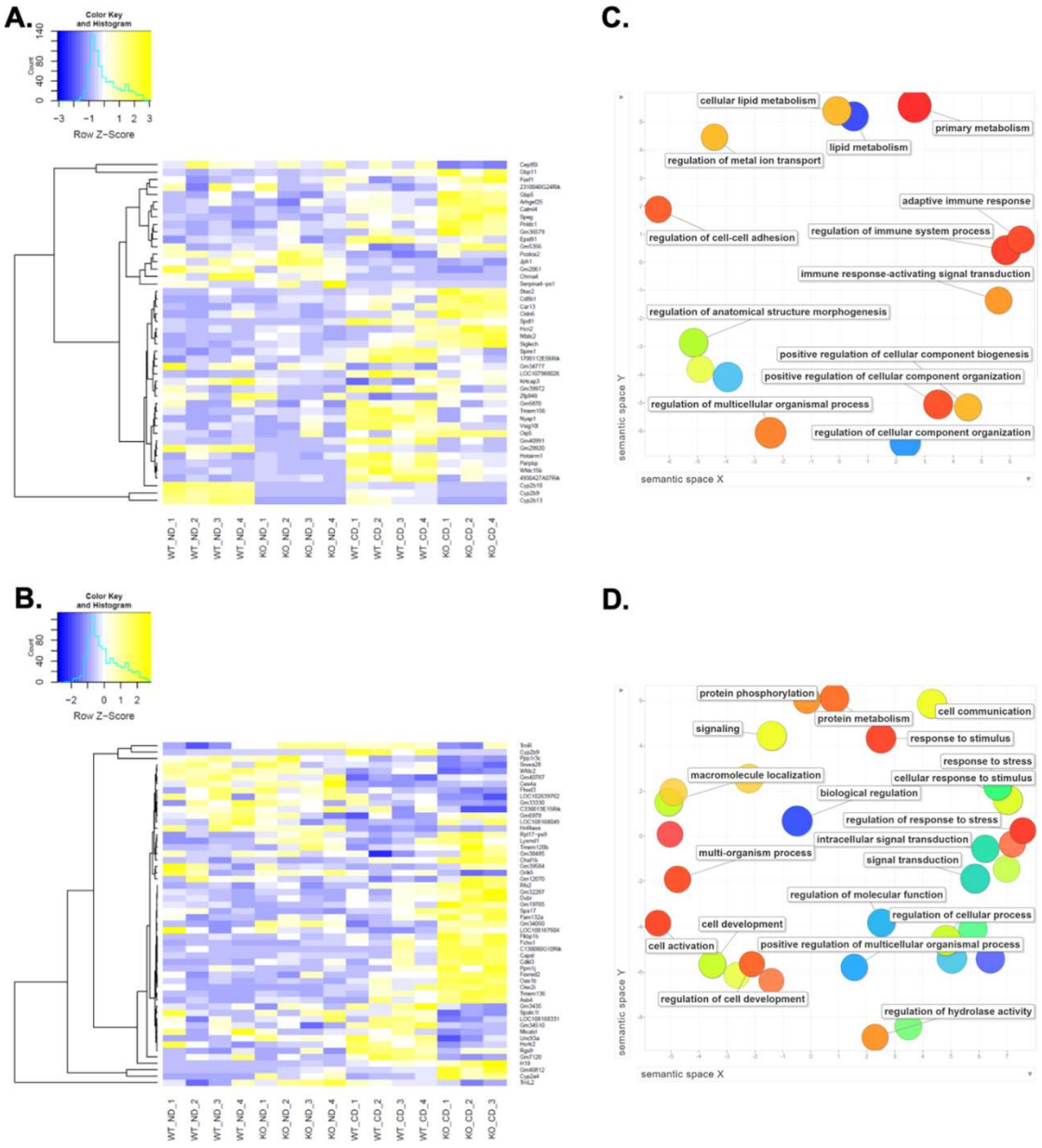

Figure 3.4. RNAseq demonstrates changes in gene expression in livers of CDAHFD-fed Cyp2b-null mice. Heat maps showing log2-transformed, Z-score scaled RNA-seq expression of significant differentially expressed genes ($log_2FC > 1.0$) between CDAHFD-fed Cyp2b-null and CDAHFD-fed WT groups in female (A) and male (B) mice. Yellow and blue color intensity indicate gene up- or down-regulation, respectively.

Dendrogram clustering on the y-axis groups genes by expression profile across samples. GO term enrichment analysis summary using Revigo (Supek et al., 2011) for up-regulated GO terms in CDAHFD-fed Cyp2b-null female (C) and male (D) mice compared to CDAHFD-fed WT mice. Each scatterplot contains enriched GO terms from the biological process class that remain after term redundancy is reduced and are displayed in a two-dimensional space where semantically similar GO terms are positioned closer together within the plot. Each circle represents an enriched GO term; the cooler the color of a term, the greater significance ($p < 0.05$) of that term with measured changes in gene expression. Circle size indicates the frequency of the GO term in the underlying GO database, i.e. circles of more general terms are larger.

Gene ontology (GO) enrichment analysis (**S3.5**) demonstrates significant ($p < 0.05$) increases in terms associated with lipid metabolism and immune system regulation in CDAHFD-fed Cyp2b-null female mice, and increases in stimulus/stress response, cell communication, and signal transduction terms in CDAHFD-fed Cyp2b-null male mice compared to CDAHFD-fed WT mice (**Fig 3.4CD**). Both female and male CDAHFD-fed Cyp2b-null mice had down-regulated GO terms related to xenobiotic metabolism (**S3.6**). Fatty liver and NASH are known to mediate the down-regulation of detoxification enzymes, especially CYPs (Deol et al., 2015; H. Li, Toth, & Cherrington, 2017). *Cyp2b9*, *Cyp2b10*, and *Cyp2b13* were all significantly down-regulated in CDAHFD-fed WT females; conversely, *Cyp2b9* was significantly up-regulated in WT CDAHFD-fed males

compared to their ND-fed counterparts (**S3.7**). Immunoblotting confirmed that CYP2B protein was reduced in female but increased in male CDAHFD-fed WT mice compared to WT ND-fed mice (**S3.8**). Overall, there is substantial sexual dimorphism in gene expression with Cyp2b-null females showing changes in lipid metabolism, energy metabolism, and inflammation; Cyp2b-null males showing changes related to stress responses and cell signaling (**Fig 3.4**).

3.3.5 Analysis of fibrosis, inflammation, and stress associated biomarkers in CDAHFD-fed Cyp2b-null mice:

Gene markers associated with fibrosis and inflammation were up-regulated in CDAHFD-fed WT female mice (**Fig 3.5A; S3.7**). When comparing CDAHFD-fed Cyp2b-null mice to CDAHFD-fed WT mice, expression of several fibrosis-related genes were slightly down-regulated or unchanged (**S3.4**). However, the pro-inflammatory interleukin-6 receptor (*Il6ra*) was significantly down-regulated, while other apoptotic and immune response genes such as immunosuppressive transforming growth factor beta 2 (*Tgfb2*) (Yoshimura & Muto, 2011) and chemokine receptor 7 (*Ccr7*) were up-regulated in CDAHFD-fed Cyp2b-null female mice (**S3.9**). Furthermore, the tumor necrosis factor receptor superfamily member 18 (*Tnfrsf18*) also known as the glucocorticoid-induced TNFR-related protein and calmodulin-like 4 (Calml4), a calcium-binding messenger protein involved in upstream signaling of steroid hormone biosynthesis, were significantly up-regulated (logFC = 1.70 and logFC = 1.28, respectively) in CDAHFD-

fed Cyp2b-null females compared to WT counterparts (**Fig 3.5A**), suggesting a potential role for glucocorticoid mediated suppression of inflammation and immune response.

A.

Gene Name	CDAHFD-fed WT vs ND-fed WT F logFC	CDAHFD-fed Cyp2b-null vs CDAHFD-fed WT F log FC	P-value	Biomarkers/KEGG Pathway
Acta2 (a-Sma)	4.1569*	-0.4753	8.82×10^{-27}	Fibrosis
Col1a1	3.2968*	0.0362	3.22×10^{-44}	Fibrosis
Col3a1	3.2267*	-0.0054	9.3×10^{-100}	Fibrosis
Col4a1	1.7838*	-0.3732	8.49×10^{-43}	Fibrosis
Tgfb1	1.2314*	0.0075	1.18×10^{-12}	Fibrosis
Tgfb2	0.6624*	0.6397*	1.12×10^{-6}	Fibrosis
Il1a	0.6223	0.0308	0.13349	Inflammatory/ apoptosis markers
Ccl2 (Mcp-1)	3.6837*	0.3393	6.43×10^{-30}	Inflammatory/ apoptosis markers
Ccl9	0.3635*	0.0693	3.93×10^{-5}	Inflammatory/ apoptosis markers
Ifngr2	1.2964*	0.0826	7.66×10^{-16}	Inflammatory/ apoptosis markers
Acvrl1	1.2157*	-0.4741*	9.58×10^{-8}	Inflammatory/ apoptosis markers
Ccr7	1.6611*	0.6367*	6.25×10^{-5}	Inflammatory/ apoptosis markers
Il6ra	-0.7958	-0.5366*	1.97×10^{-6}	Inflammatory/ apoptosis markers
Il10ra	1.5479*	0.0394	2.06×10^{-10}	Inflammatory/ apoptosis markers
Il10rb	0.9131*	0.1011	1.24×10^{-11}	Inflammatory/ apoptosis markers
Il16	-0.1295	0.0107	0.92787	Inflammatory/ apoptosis markers
Tnfrsf18	0.8610	1.6997*	0.01743	Inflammatory/ apoptosis markers
Il17rb	0.5321	-0.0683	0.11009	Inflammatory/ apoptosis markers
Tnfaip3	1.7860*	-0.0815	7.88×10^{-23}	Inflammatory/ apoptosis markers
Cd68	2.5171*	-0.1120	3.36×10^{-52}	Inflammatory/ apoptosis markers
Cyp17a1	-2.5188*	-0.0024	3.39×10^{-9}	Cortisol synthesis/ secretion
Camk2b	0.4739	-0.2605	0.01423	Cortisol synthesis/ secretion
Calml4	1.5243*	1.2768*	3.58×10^{-12}	Cortisol synthesis/ secretion

Color Key
-2 -1 0 1 2
logFC

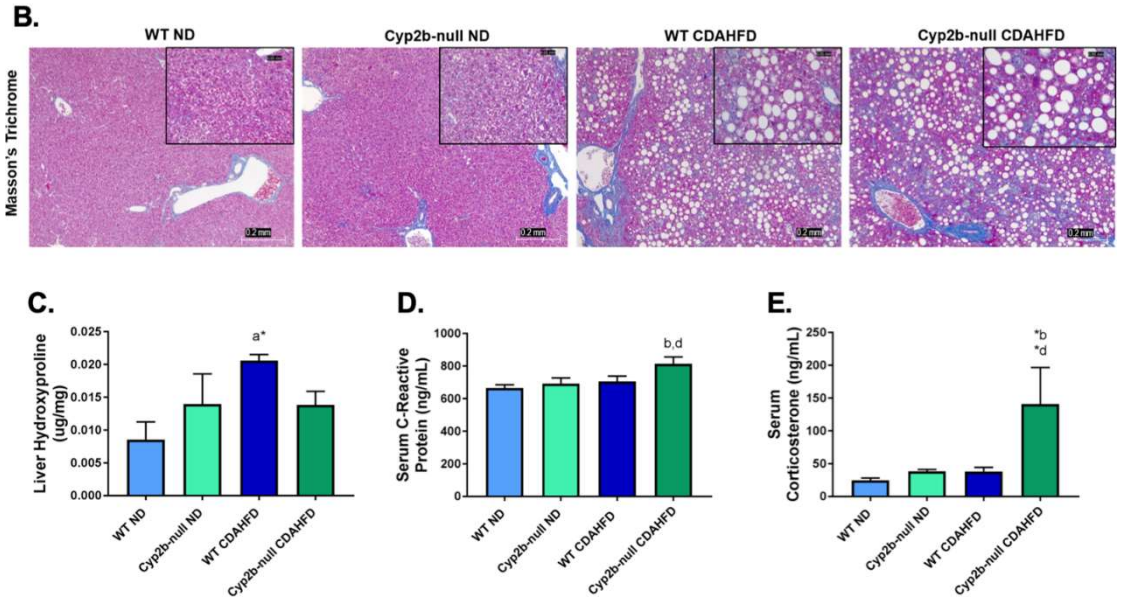

Figure 3.5. Measured liver fibrosis and inflammatory markers in CDAHFD-treated Cyp2b-null female mice. Changes in the expression of fibrosis, inflammation and stress response-associated genes were investigated and grouped by respective biomarkers and/or KEGG pathways (A). LogFC values with an asterisk indicates a significant difference ($p < 0.05$) between two groups, e.g. CDAHFD-fed versus ND-fed WT mice, and no asterisk denotes significance by one-way ANOVA across all treatment groups. Histopathological changes were evaluated by Masson's trichrome staining of female liver tissues (B). Images were taken at 100x (0.2 mm) and 400x (0.05 mm) magnification. Liver hydroxyproline (C), as well as serum C-reactive protein (D) and corticosterone (E) were measured in all treatment groups. Graph data are presented as mean ± SEM. Statistical significance was determined by one-way ANOVA followed by Fisher's LSD as the post-hoc test (n=5). An 'a' indicates ND-fed WT different than CDAHFD-fed WT, 'b' indicates ND-fed Cyp2b-null different than CDAHFD-fed Cyp2b-null, 'c' indicates ND-fed WT different than ND-fed Cyp2b-null, 'd' indicates CDAHFD-fed WT different than CDAHFD-fed Cyp2b-null. No asterisk indicates a p-value < 0.05, * indicates a p-value < 0.01, and ** indicates a p-value < 0.0001.

Liver histopathology along with markers of NASH were examined because of gene expression profile differences found between CDAHFD-fed WT and Cyp2b-null mice. Masson's Trichrome confirmed the development of cytoplasmic vacuolization and and revealed the progresion of fibrosis from CDAHFD treatment; however, the difference

in severity was not significant between genotypes (**Fig 3.5B**). Liver hydroxyproline, a major component of collagen and marker for fibrosis development, was significantly increased in female CDAHFD-fed WT mice compared to ND-fed WT mice. Hydroxyproline concentrations were 33% lower in female CDAHFD-fed Cyp2b-null mice than CDAHFD-fed WT mice; however, this was not statistically significant ($p = 0.18$) (**Fig 3.5C**). Overall, liver fibrosis was induced by a CDAHFD and some expression markers of liver fibrosis and inflammation were higher in female CDAHFD-fed WT mice than CDAHFD-fed Cyp2b-null mice; however, perturbation was often either minimal to moderate or not significant.

Liver inflammation was determined by serum levels of C-reactive protein (CRP). CDAHFD-fed Cyp2b-null females had higher (15%) CRP concentrations over WT counterparts (**Fig 3.5D**). Corticosterone, the main glucocorticoid in rodents, was also measured due to induction of immune system regulation-associated GO terms and inflammatory markers in CDAHFD-fed Cyp2b-null females (**Fig 3.4C and 3.5A**). Corticosterone increased in CDAHFD-fed Cyp2b-null females by 2.7X compared to WT mice (**Fig 3.5E**). These results concur with the up-regulation of glucocorticoid-mediated KEGG pathways including *Tnfrsf18* and *Calml4* in CDAHFD-fed Cyp2b-null females. Overall, gene expression, inflammatory markers, and corticosterone levels indicate Cyp2b-null mice differed in their response to a CDAHFD than WT mice; however, there were no significant changes in fibrosis (**Fig 3.5**).

CDAHFD-fed male mice show significant adverse changes compared to ND-fed mice, with expression markers associated with increased fibrosis and inflammation up-

regulated in CDAHFD-fed WT male mice and greater up-regulation of fibrosis marker genes in CDAHFD-fed Cyp2b-null males, (**Fig 3.6A; S3.4, S3.7, & S3.9**) especially when compared to females (**Fig 3.5A**). Masson's Trichrome staining also confirmed the development of cytoplasmic vacuolization and revealed the progression of fibrosis from CDAHFD treatment regardless of genotype (**Fig 3.6BC**). Contrary to females, CDAHFD-fed male mice had unexpectedly lower concentrations of CRP and corticosterone in CDAHFD-treated mice (**Fig** 3.**6DE**). Taken together, gene expression suggests only minor differences between CDAHFD-fed WT and Cyp2b-null males, and these changes did not manifest themselves in the histopathology or hydroxyproline results, indicating few to no differences between WT and Cyp2b-null male mice regarding susceptibility to NASH.

A.

Gene Name	CDAHFD-fed WT vs ND-fed WT M logFC	CDAHFD-fed Cyp2b-null vs CDAHFD-fed WT M log FC	P-value	Biomarkers/KEGG Pathway
Acta2 (a-Sma)	3.1597*	0.1015	3.14×10^{-24}	Fibrosis
Col1a1	4.7061*	0.3787	4.31×10^{-69}	
Col3a1	3.2378*	0.3183	2.53×10^{-82}	
Col4a1	1.6091*	0.1719	9.59×10^{-61}	
Tgfb1	2.5763*	0.2037*	5.61×10^{-46}	
Tgfb2	1.5342*	0.4569	1.7×10^{-8}	
Il1a	1.3383*	-0.0386*	0.00719	Inflammatory/ apoptosis markers
Ccl2 (Mcp-1)	3.5689*	-0.2165	1.83×10^{-24}	
Ccl9	0.3639*	0.3575*	9.94×10^{-11}	
Ifngr2	1.2562*	0.3253*	1.01×10^{-33}	
Acvrl1	1.4440*	0.2076	2.87×10^{-11}	
Ccr7	2.2748*	0.4319	0.000269	
Il6ra	0.0307	-0.1835	0.8522	
Il10ra	2.3400*	0.3879	2.91×10^{-19}	
Il10rb	1.9809*	0.0797	7.57×10^{-29}	
Il16	0.3195*	0.4684*	0.000298	
Tnfrsf18	1.2974*	-0.8389	0.01751	
Il17rb	0.6294*	-0.3773*	0.012776	
Tnfaip3	3.1989*	0.2152*	6.21×10^{-41}	
Cd68	3.6980*	0.1955	4.32×10^{-83}	
Cyp17a1	-1.8610	0.6690*	1.04×10^{-5}	Cortisol synthesis/ secretion
Camk2b	0.7377*	0.9889*	2.84×10^{-10}	
Calml4	2.4764*	0.0939	0.00017	

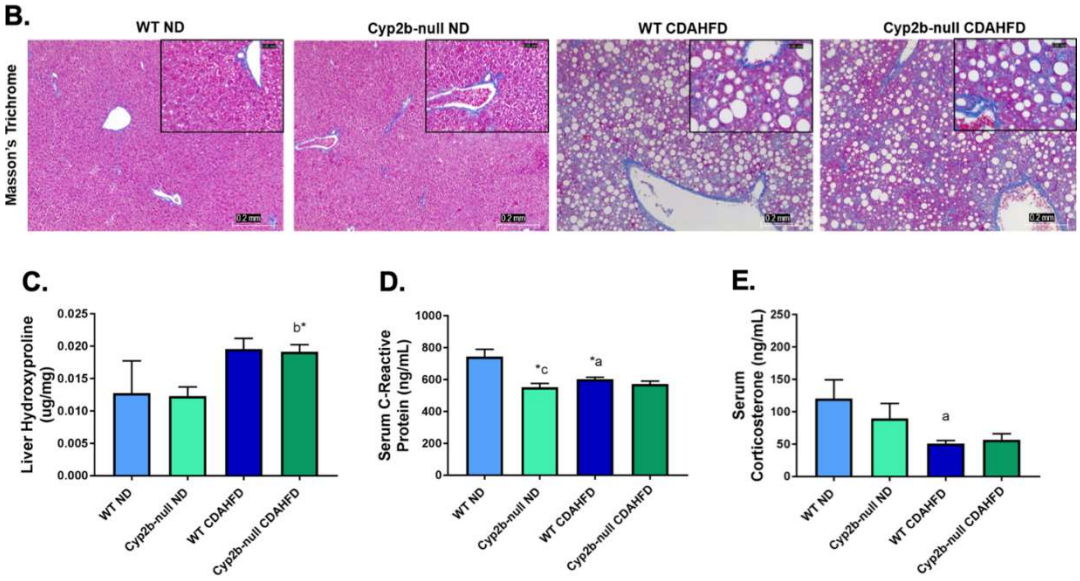

Figure 3.6. Measured liver fibrosis and inflammatory markers in CDAHFD-treated Cyp2b-null male mice. Changes in the expression of fibrosis, inflammation and stress response-associated genes were investigated and grouped by respective biomarkers and/or KEGG pathways (A). LogFC values with an asterisk indicates a significant

difference ($p < 0.05$) between two groups, e.g. CDAHFD-fed versus ND-fed WT mice, and no asterisk denotes significance by one-way ANOVA across all treatment groups. Histopathological changes were evaluated by H&E, and Masson's trichrome staining of male liver tissues (B). Images were taken at 100x (0.2 mm) and 400x (0.05 mm) magnification. Liver hydroxyproline (C), as well as serum C-reactive protein (D) and corticosterone (E) were measured in all treatment groups. Graph data are presented as mean ± SEM. Statistical significance was determined by one-way ANOVA followed by Fisher's LSD as the post-hoc test (n=5). An 'a' indicates ND-fed WT different than CDAHFD-fed WT, 'b' indicates ND-fed Cyp2b-null different than CDAHFD-fed Cyp2b-null, 'c' indicates ND-fed WT different than ND-fed Cyp2b-null, 'd' indicates CDAHFD-fed WT different than CDAHFD-fed Cyp2b-null. No asterisk indicates a p-value < 0.05, * indicates a p-value < 0.01, and ** indicates a p-value < 0.0001.

3.3.6 Cyp2b-null mice show gender differences in CDAHFD-induced liver triglyceride accumulation:

NAFLD is often a precursor to NASH and therefore differences in NAFLD were also investigated. GO analysis indicated an up-regulation of lipid metabolism-related terms in CDAHFD-fed Cyp2b-null females. In contrast, several genes associated with fatty acid metabolism were down-regulated in CDAHFD-fed WT female mice (**Fig 3.7A; S3.7**). Genes that reversed direction of regulation from down- to up-regulation in CDAHFD-fed Cyp2b-null female mice compared to CDAHFD-fed WT mice include

Ndufa4-mitochondrial complex associated protein (*Ndufa4*) and *Cyp27a1*, which breaks down cholesterol to bile acids (**S3.4 & S3.9**). Pathological analysis of Oil Red O staining established increased steatosis in CDAHFD-treated female mice, with less lipid accumulation in CDAHFD-fed Cyp2b-null females than CDAHFD-fed WT females (**Fig 3.7B**). Total lipid area quantified by ImageJ Fiji confirmed the pathological findings (Schindelin et al., 2012) that CDAHFD-fed Cyp2b-null female mice had significantly less hepatic lipids than CDAHFD-fed WT mice (**Fig 3.7C**) and this was verified by total triglyceride concentrations measured colorimetrically (**Fig 3.7D**). Despite smaller droplets (data not shown), CDAHFD-fed Cyp2b-null mice did not appear to present with microsteatosis. To make sure, serum β-hydroxybutyrate levels were also measured because impaired mitochondrial β-oxidation can cause microvesicular steatosis development (Fromenty & Pessayre, 1997). Serum β-hydroxybutyrate increased in both CDAHFD-fed groups with no significant difference between genotypes (**Fig 3.7E**).

A.

Gene Name	CDAHFD-fed WT vs ND-fed WT F logFC	CDAHFD-fed Cyp2b-null vs CDAHFD-fed WT F logFC	P-value	Biomarkers/KEGG Pathway
Ndufa4	-0.5580	0.1695*	0.000656	NAFLD
Ppara	-0.1065	0.0704	0.00044	
Mlxipl (Chrebp)	-0.6088	-0.1258	0.000313	
Srebf1 (Srebp1)	-0.8219	-0.0176	8.16×10^{-9}	
Irs1	-0.5325	-0.2342*	0.000117	
Cpt1a	0.5985*	0.1573	0.00082	Insulin resistance/ signaling
Fasn	-2.5476*	0.0796	4.02×10^{-20}	
Slc27a1 (Fatp)	0.7529*	-0.2072	0.001285	
Ppp1r3b	-1.9414*	-1.0183	6.19×10^{-31}	
Ppp1r3c	-0.5787	-0.3619	0.0922	
G6pc	-2.3073*	-0.4026	7.08×10^{-20}	
Hk1	0.3041*	0.3970*	0.006591	Galactose metabolism
Akr1b10	1.4395*	0.1696	0.00531	
Gla	0.4480*	0.4003*	0.0015	
Angptl8	0.0888	-1.1243	0.00265	Lipid metabolism
Cyp27a1	-1.3083*	0.2274*	2.17×10^{-35}	
Cyp2b10	-3.0119*	-6.0151*	1.4×10^{-142}	
Elovl2	-0.5930	-0.0364	5.36×10^{-10}	
Pparg	0.9523*	0.1445	5.95×10^{-9}	Pathways in cancer
Egfr	-0.2820	0.4423*	0.002123	

Color Key

-2 -1 0 1 2

logFC

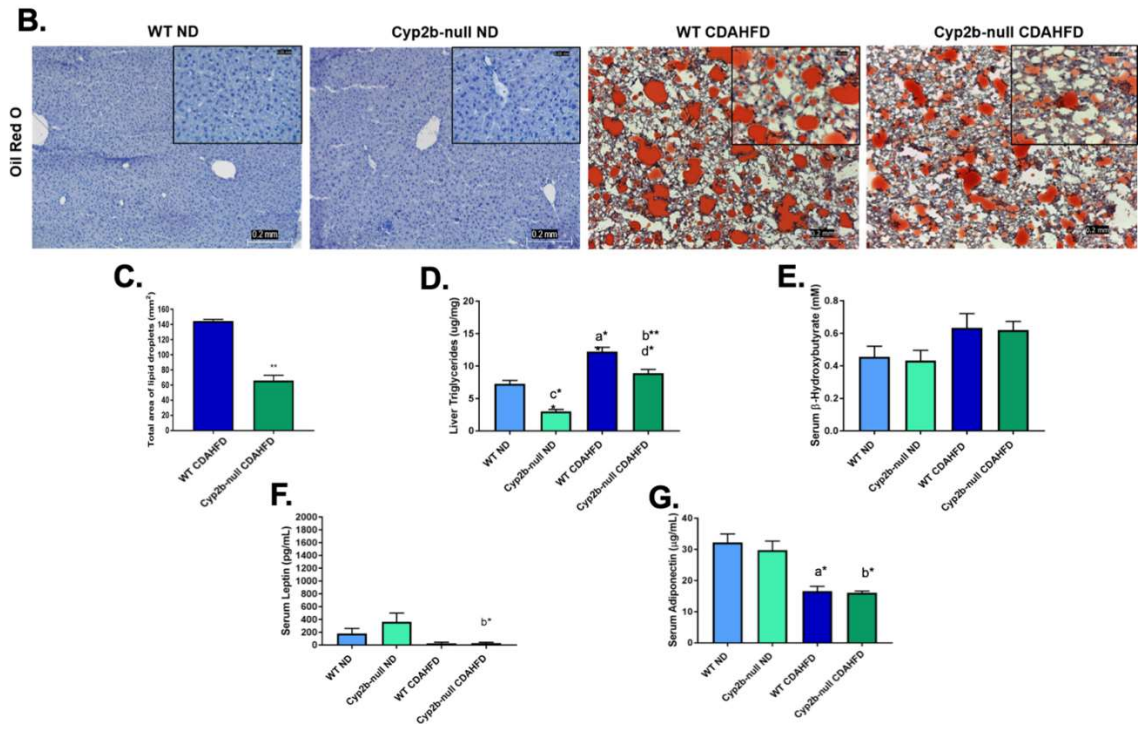

Figure 3.7. Steatosis and markers of steatosis in CDAHFD-fed WT and CDAHFD-fed Cyp2b-null female mice. Changes in the expression of nonalcoholic fatty liver

disease-related genes were investigated and grouped by respective biomarkers and/or KEGG pathways (A). LogFC values with an asterisk indicates a significant difference ($p < 0.05$) between two groups, e.g. CDAHFD-fed versus ND-fed WT mice, and no asterisk denotes significance by one-way ANOVA across all treatment groups. Fatty liver histopathological changes were evaluated by Oil red O staining in female mice (B). Images were taken at 100x (0.2 mm) and 400x (0.05 mm) magnification. Total liver triglycerides (C) were measured in female mice to confirm Oil Red O staining results. Liver lipid droplets were also quantified by total area (D) using ImageJ Fiji from Oil Red O slides (400x). Serum levels of β-hydroxybutyrate (E), leptin (F), and adiponectin (G) were also determined. Graphed data are presented as mean ± SEM. Statistical significance was determined by one-way ANOVA followed by Fisher's LSD as the post-hoc test (n=5). An 'a' indicates ND-fed WT different than CDAHFD-fed WT, 'b' indicates ND-fed Cyp2b-null different than CDAHFD-fed Cyp2b-null, 'c' indicates ND-fed WT different than ND-fed Cyp2b-null, 'd' indicates CDAHFD-fed WT different than CDAHFD-fed Cyp2b-null. No asterisk indicates a p-value < 0.05, * indicates a p-value < 0.01, and ** indicates a p-value < 0.0001.

There were changes in the serum lipid levels of female mice (**Table 3.1A**). This includes decreased calcium and increased serum HDL and LDH in ND-fed Cyp2b-null mice compared to ND-fed WT mice consistent with previous data (Heintz et al., 2019). CDAHFD-fed female mice had lower serum glucose and HDL compared to ND-fed

counterparts. However, between CDAHFD-fed genotypes, CDAHFD-fed Cyp2b-null mice increased HDL but decreased calcium levels. LDH was consistently increased in the serum of Cyp2b-null mice regardless of diet indicating skeletal or cardiac muscular tissue damage. Liver to serum triglyceride ratios confirm reduced accumulation of triglycerides in the livers of Cyp2b-null female mice regardless of diet (**Table 3.1A**). The metabolic hormones leptin and adiponectin were measured due to changes in weight, liver lipids, and gene expression changes. Significant differences were associated with diet and not genotype (**Fig 3.7FG**).

Table 3.1. Serum biomarker levels in ND and CDAHFD-treated WT and Cyp2b-null mice.

A.

Serum Panel	ND-fed WT F	ND-fed Cyp2b-null F	CDAHFD-fed WT F	CDAHFD-fed Cyp2b-null F
Calcium (mg/dL)	9.41 ± 0.15	8.02 ± 0.20^{c**}	9.60 ± 0.14	7.72 ± 0.20^{d**}
Phosphorus (mg/dL)	5.68 ± 0.38	5.95 ± 0.36	6.92 ± 0.63	7.04 ± 0.35
Glucose (mg/dL)	181.23 ± 6.72	186.42 ± 4.25	155.07 ± 12.06^{a}	151.73 ± 5.41^{b*}
Triglycerides (mg/dL)	59.91 ± 9.23	53.34 ± 0.40	64.88 ± 4.30	57.97 ± 7.15
Cholesterol (mg/dL)	71.88 ± 4.62	119.96 ± 42.45	70.57 ± 21.29	53.13 ± 2.02
HDL (mg/dL)	46.59 ± 2.03	51.85 ± 2.28	28.26 ± 4.97^{a*}	37.60 ± 0.82^{b*d}
LDL (mg/dL)	5.6 ± 0.20	8.13 ± 2.64	6.58 ± 2.19	4.28 ± 0.98
VLDL (mg/dL)	11.98 ± 1.85	10.67 ± 1.45	12.98 ± 0.86	11.59 ± 1.43
LDH (U/L)	n.d.	260.73 ± 104.64^{c*}	n.d.	680.96 ± 96.79
Direct bilirubin (mg/dL)	0.024 ± 0.004	0.04 ± 0.01	0.16 ± 0.11	0.068 ± 0.01
Indirect bilirubin (mg/dL)	0.218 ± 0.05	0.78 ± 0.58	0.56 ± 0.24	0.21 ± 0.048
Total bilirubin (mg/dL)	0.24 ± 0.05	0.69 ± 0.47	0.71 ± 0.22	0.45 ± 0.17
Liver:Serum Triglycerides	0.139 ± 0.03	0.065 ± 0.01^{c}	0.192 ± 0.02	0.163 ± 0.02^{b*}

B.

Serum Panel	ND-fed WT M	ND-fed Cyp2b-null M	CDAHFD-fed WT M	CDAHFD-fed Cyp2b-null M
Calcium (mg/dL)	9.82 ± 0.27	8.54 ± 0.17^{c*}	9.26 ± 0.10	8.50 ± 0.39
Phosphorus (mg/dL)	5.69 ± 0.34	5.76 ± 0.37	6.72 ± 0.21	7.37 ± 0.51^{b*}
Glucose (mg/dL)	206.87 ± 15.42	212.36 ± 7.55	124.80 ± 3.55^{a**}	141.45 ± 9.21^{b*}
Triglycerides (mg/dL)	96.24 ± 5.46	66.72 ± 4.59^{c*}	53.004 ± 4.64^{a**}	55.15 ± 3.99
Cholesterol (mg/dL)	96.18 ± 4.65	105.48 ± 3.69	38.26 ± 1.78^{a**}	46.38 ± 3.078^{b**}
HDL (mg/dL)	69.76 ± 3.24	77.94 ± 2.25^{c}	18.86 ± 2.33^{a**}	29.53 ± 2.46^{b**d}
LDL (mg/dL)	3.53 ± 0.20	3.29 ± 0.22	6.19 ± 2.09	3.40 ± 0.56
VLDL (mg/dL)	19.25 ± 1.09	13.34 ± 0.92^{c*}	10.6 ± 0.93^{a**}	11.03 ± 0.80
LDH (U/L)	n.d.	187.64 ± 23.73^{c**}	n.d.	909.80 ± 55.91^{bd}
Direct bilirubin (mg/dL)	0.02 ± 0.0045	0.026 ± 0.004	0.12 ± 0.0045^{a**}	0.095 ± 0.013^{b**c}
Indirect bilirubin (mg/dL)	0.14 ± 0.014	0.15 ± 0.0097	0.22 ± 0.015^{a*}	0.3 ± 0.026^{b**d*}
Total bilirubin (mg/dL)	0.16 ± 0.012	0.18 ± 0.0073	0.34 ± 0.017^{a**}	0.41 ± 0.032^{b**d}
Liver:Serum Triglycerides	0.081 ± 0.009	0.115 ± 0.007	0.244 ± 0.012^{a**}	0.322 ± 0.034^{b**c}

Data are presented as mean ± SEM. Statistical significance was determined by one-way ANOVA followed by Fisher's LSD as the post-hoc test (n=5).
'a' indicates ND-fed WT different than CDAHFD-fed WT
'b' indicates ND-fed Cyp2b-null different than CDAHFD-fed Cyp2b-null
'c' indicates ND-fed WT different than ND-fed Cyp2b-null
'd' indicates CDAHFD-fed WT different than CDAHFD-fed Cyp2b-null.
No asterisk next to a 'letter' indicates a p-value < 0.05, * indicates a p-value < 0.01, and ** indicates a p-value < 0.0001. n.d. = not detected
Raw data from the serum panel and other measured endpoints are supplied in **S3.6 File**.

Numerous genes associated with fatty acid metabolism were also down-regulated in CDAHFD-fed WT male mice compared to ND-fed counterparts, and these genes were further down-regulated in CDAHFD-fed Cyp2b-null male mice (**Fig 3.8A; S3.4, S3.7, & S3.9**), suggesting greater steatosis in the CDAHFD-fed Cyp2b-null male mice. These genes include regulators of glycogen metabolism, Ppp1r3b and Ppp1r3c, glucose metabolism regulator, glucose-6-phosphatase (*G6pc*), serum triglyceride regulator, angiopoietin-like protein 8 (*Angptl8*), and long chain fatty acid elongase 2 (*Elovl2*). Liver steatosis also increased in CDAHFD-fed male mice, with higher liver triglyceride levels

in Cyp2b-null compared to WT mice (**Fig 3.8B-D**) corroborating the gene expression data. Serum β-hydroxybutyrate also indicates no change in ketosis in male mice similar to female mice (**Fig 3.8E**).

A.

Gene Name	CDAHFD-fed WT vs ND-fed WT M logFC	CDAHFD-fed Cyp2b-null vs CDAHFD-fed WT M logFC	P-value	Biomarkers/KEGG Pathway
Ndufa4	0.7155	0.3537	0.04985	
Ppara	-0.0804	-0.0508	0.04570	
Mlxipl (Chrebp)	-1.2900*	0.1325	1.21×10^{-25}	NAFLD
Srebf1 (Srebp1)	-1.0699*	-0.2453	1.09×10^{-10}	
Irs1	-0.8893	-0.0609	4.54×10^{-6}	
Cpt1a	0.6117*	0.0509	3.59×10^{-5}	
Fasn	-2.0685*	-0.2387	3.3×10^{-23}	
Slc27a1 (Fatp)	0.4678*	0.3091	0.000536	Insulin resistance/ signaling
Ppp1r3b	-2.3686*	-0.4803*	1.45×10^{-31}	
Ppp1r3c	-1.2091*	-1.0501*	5.68×10^{-17}	
G6pc	-1.1354*	-0.9204*	5.87×10^{-17}	
Hk1	1.3058*	0.1345	0.05129	
Akr1b10	1.4053*	0.9183*	4.16×10^{-6}	Galactose metabolism
Gla	1.1070*	0.0990	4.73×10^{-16}	
Angptl8	-1.1161	-0.4296*	5.83×10^{-9}	
Cyp27a1	-1.1796*	-0.1971	1.14×10^{-37}	Lipid metabolism
Cyp2b10	-4.1554*	-1.3091	6.24×10^{-39}	
Elovl2	-0.6402	-0.2882*	6.06×10^{-9}	
Pparg	0.6824*	0.0166	0.00573	Pathways in cancer
Egfr	-0.7567	-0.0081	0.00496	

Color Key

-2 -1 0 1 2

logFC

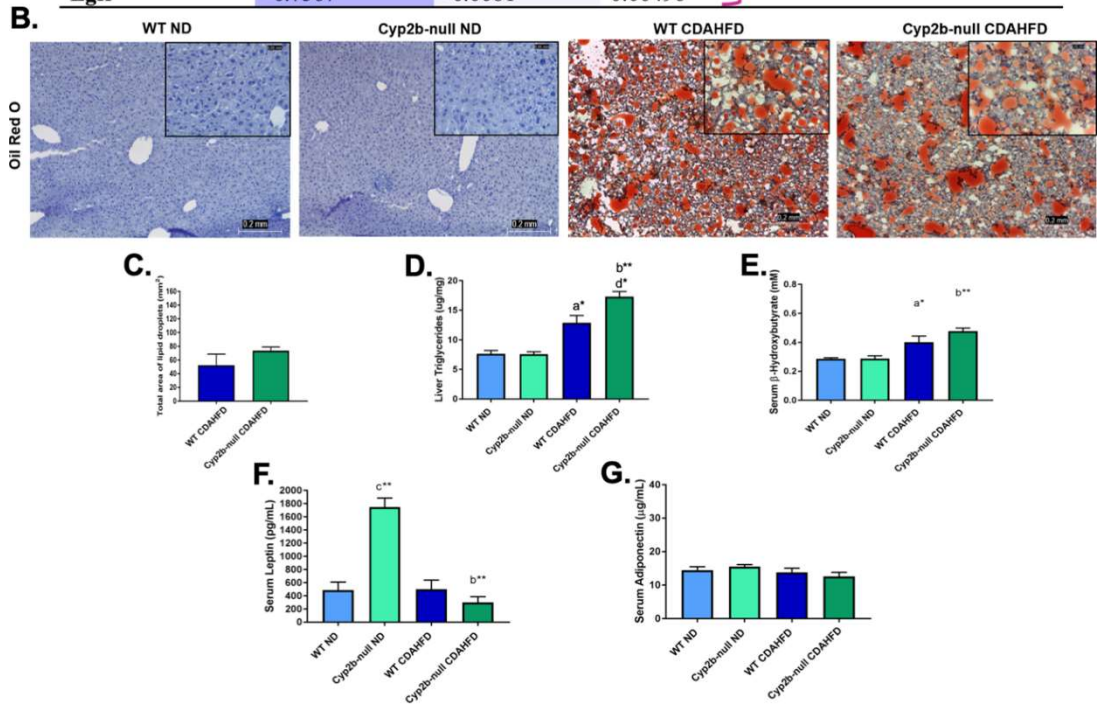

Figure 3.8. Steatosis and markers of steatosis in CDAHFD-fed WT and CDAHFD-fed Cyp2b-null male mice. Changes in the expression of nonalcoholic fatty liver disease-related genes were investigated and grouped by respective biomarkers and/or KEGG pathways (A). LogFC values with an asterisk indicates a significant difference ($p < 0.05$) between two groups, e.g. CDAHFD-fed versus ND-fed WT mice, and no asterisk denotes significance by one-way ANOVA across all treatment groups. Fatty liver histopathological changes were evaluated by Oil red O staining in female mice (B). Images were taken at 100x (0.2 mm) and 400x (0.05 mm) magnification. Total liver triglycerides (C) were measured in male mice to confirm Oil Red O staining results. Liver lipid droplets were also quantified by total area (D) using ImageJ Fiji from Oil Red O slides (400x). Serum levels of β-hydroxybutyrate (E), leptin (F), and adiponectin (G) were also determined. Graph data are presented as mean ± SEM. Statistical significance was determined by one-way ANOVA followed by Fisher's LSD as the post-hoc test (n=5). An 'a' indicates ND-fed WT different than CDAHFD-fed WT, 'b' indicates ND-fed Cyp2b-null different than CDAHFD-fed Cyp2b-null, 'c' indicates ND-fed WT different than ND-fed Cyp2b-null, 'd' indicates CDAHFD-fed WT different than CDAHFD-fed Cyp2b-null. No asterisk indicates a p-value < 0.05, * indicates a p-value < 0.01, and ** indicates a p-value < 0.0001.

ND-fed Cyp2b-null male mice showed significantly lower serum calcium and triglycerides consistent with previous data (Heintz et al., 2019), and greater HDL and

LDH similar to females. Relative to CDAHFD-fed WT mice, CDAHFD-fed Cyp2b-null mice showed greater HDL, bilirubin, serum:triglyceride ratios, and LDH. Males showed similar directional changes in HDL and LDH as females; however, their serum:triglyceride ratios were in opposing directions, which was expected because liver triglycerides went down in CDAHFD-fed Cyp2b-null females and up in CDAHFD-fed Cyp2b-null males (**Table 3.1B**). Serum leptin increased 2.6-fold in ND-fed Cyp2b-null males compared to their WT counterparts, while leptin levels remained low in CDAHFD-fed mice (**Fig 3.8F**). No differences were observed between groups for male adiponectin levels (**Fig 3.8G**). Overall, Cyp2b-null female and male mice reacted very differently to a CDAHFD pertaining to liver lipids, with protection from steatosis in Cyp2b-null females and increased steatosis in Cyp2b-null males.

3.3.7 qPCR confirmation of changes in gene expression:

qPCR was used to verify RNAseq results of genes associated with hepatic fibrosis (*Acta2; Col1a1*), inflammation (*Cd68*) and steroid metabolism associated with cortisol (*Cyp17a1*), insulin signaling and glucose metabolism (*Ppp1r3b*; *G6pc*), and cell proliferation (aldo-keto reductase 1b8, *Akr1b8*, ortholog of *AKR1B10*) in female (**Fig 3.9A)** and male (**Fig 3.9B**) mice. All genes verified by qPCR exhibited similar directional trends in terms of gene expression to the RNAseq results (**Fig 3.5-3.8; S3.3**). *Col1a1* was significantly different between CDAHFD-fed WT and CDAHFD-fed Cyp2b-null mice in both sexes, with lower *Col1a1* expression in the Cyp2b-null females (**Fig 3.9A**) and higher in the Cyp2b-null males provided a CDAHFD (**Fig 3.9B**). *Acta2* was not different

between CDAHFD-treated genotypes but showed similar trends in expression to *Col1a1*, suggesting increased fibrosis. *Cd68* also differed by genotype in CDAHFD-fed female mice only, with decreased expression in CDAHFD-fed Cyp2b-null mice, suggesting lower inflammation and macrophage infiltration in these mice. *Cyp17a1* qPCR results were similar to RNAseq, however, there was no statistical differences between CDAHFD-fed WT and Cyp2b-null mice. The insulin signaling and glucose metabolism genes, *Ppp1r3b* and *G6pc* trended in the same direction of the RNAseq results, with decreased G6pc expression in both CDAHFD-fed Cyp2b-null female and male mice compared to WT counterparts; however only males were significant by ANOVA. Females were significant by t-tests directly comparing CDAHFD-fed WT to CDAHFD-fed Cyp2b-null mice ($p = 0.04$). *Akr1b8* showed similar patterns in gene expression to RNAseq, but no differences between genotypes in CDAHFD-fed mice. In conclusion, qPCR results showed exactly the same trends as RNAseq but did not always agree statistically. qPCR also indicates an increase in fibrosis, inflammation, and fatty liver in CDAHFD-fed mice that is repressed somewhat in Cyp2b-null females.

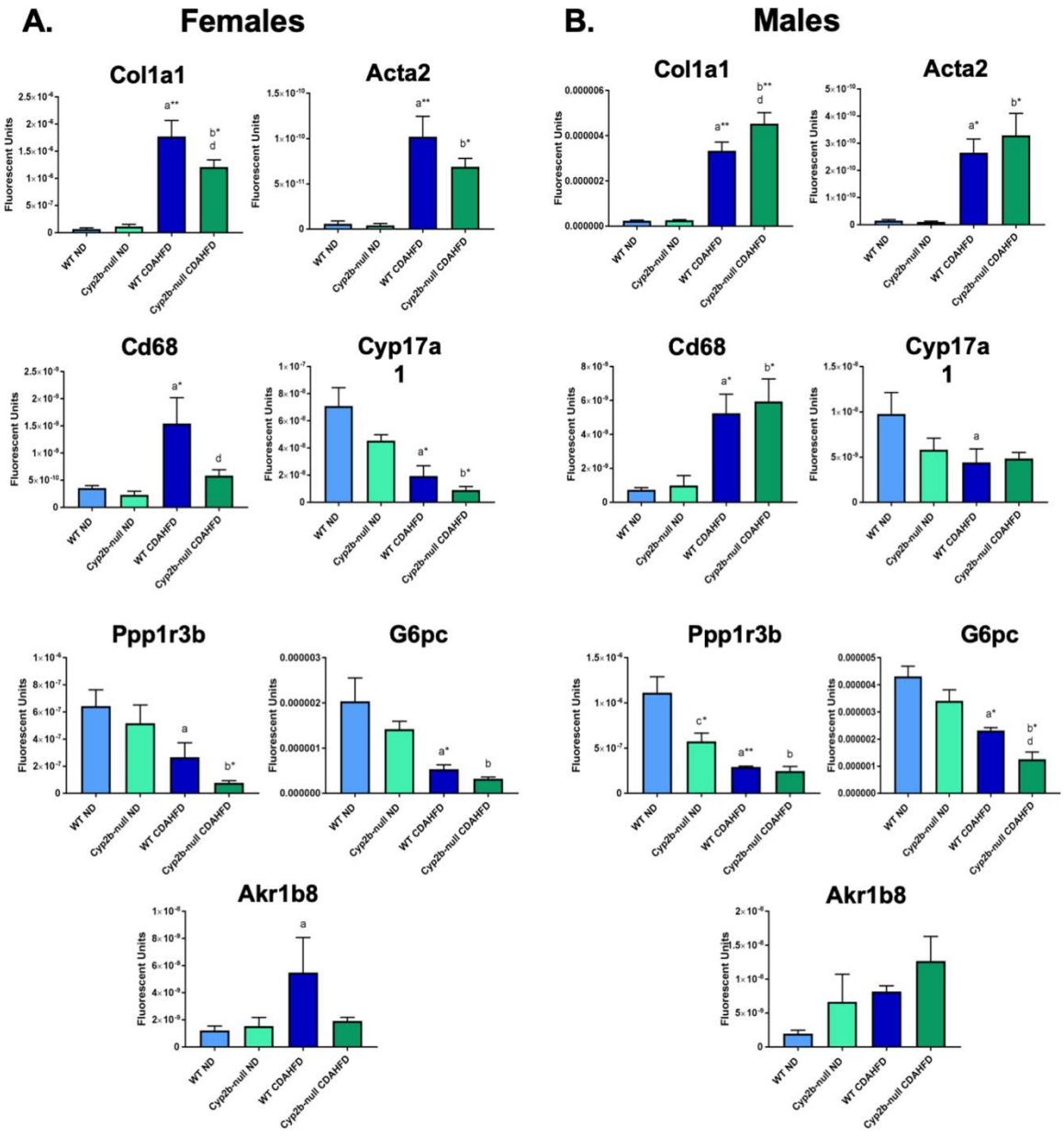

Figure 3.9. qPCR confirmation of RNAseq analysis. Changes in the expression of genes in females (A) and males (B) involved in fibrosis, inflammation, insulin signaling, fatty liver, and proliferation by qPCR confirmation. Data are presented as mean ± SEM. Statistical significance was determined by one-way ANOVA followed by Fisher's LSD as the post-hoc test (n=5). An 'a' indicates ND-fed WT different than CDAHFD-fed WT,

'b' indicates ND-fed Cyp2b-null different than CDAHFD-fed Cyp2b-null, 'c' indicates ND-fed WT different than ND-fed Cyp2b-null, 'd' indicates CDAHFD-fed WT different than CDAHFD-fed Cyp2b-null. No asterisk indicates a p-value < 0.05, * indicates a p-value < 0.01, and ** indicates a p-value < 0.0001.

3.4 Discussion

Cyp2b-null female mice weigh less, primarily due to lower white adipose tissue mass, and are protected from diet-induced steatosis and to a lesser extent diet-induced NASH. There were few differences in fibrosis markers between CDAHFD-fed WT and Cyp2b-null females, however hydroxyproline levels were slighty lower in Cyp2b-null female mice. CDAHFD caused substantial liver injury, however Cyp2b-null females had significantly lower markers of liver injury including ALT, AST, and ALP compared to their WT counterparts. Protection from liver damage in Cyp2b-null females may occur due to lower immune suppression as indicated by gene expression changes in Tgfb2, Il6ra, and activin receptor-like kinase 1 (Acvrl1), potentially due to glucocorticoid-mediated repression.

In contrast, CDAHFD-fed Cyp2b-null male mice exhibit no significant changes in serum ALT, AST, and ALP in comparison to CDAHFD-fed WT mice indicating no differences in liver damage. Fibrosis was heavily induced by a CDAHFD, but there was also no difference between CDAHFD-fed male groups except for PCNA. Cyp2b-null males also have slightly greater inflammatory responses based on RNA-seq data with no

changes in CRP or corticosterone levels. CDAHFD-fed Cyp2b-null males also showed a 1.5-fold increase of serum creatine kinase levels compared to all other treatment groups, suggesting that CDAHFD treatment causes damage to Cyp2b-null males in other tissues, such as cardiac or skeletal muscle, in addition to liver (Yen et al., 2017).

Direct measurement of liver triglycerides and histopathological staining using Oil Red O revealed less lipid accumulation in the livers of CDAHFD-fed Cyp2b-null females than CDAHFD-fed WT females. Liver to serum triglyceride ratios also indicate less triglyceride accumulation in the livers of Cyp2b-null female mice (especially when treated with CDAHFD) compared to their WT counterparts. GO enrichment analysis of RNA-seq data demonstrated significant increases in terms associated with lipid metabolism in CDAHFD-fed Cyp2b-null female mice compared to CDAHFD-fed WT female mice. Several genes involved in fatty acid metabolism were down-regulated in CDAHFD-fed WT females. When comparing gene expression of CDAHFD-fed Cyp2b-null mice to their WT counterparts, lipid metabolism genes were either minimally down-regulated but not significantly, or reversed direction and were slightly up-regulated as shown in **Figure 3.7**.

Conversely, male Cyp2b-null mice were not protected from development of fatty liver. Consistent with previous results (Heintz et al., 2019), liver steatosis increased in CDAHFD-fed male mice, with more triglyceride accumulation in CDAHFD-fed Cyp2b-null males than CDAHFD-fed WT males as demonstrated by liver triglycerides and liver to serum triglyceride ratios. CDAHFD-fed Cyp2b-null male mice also had more down-regulated lipid metabolism associated genes compared to female counterparts, with

several genes further down-regulated from CDAHFD-fed WT males, including regulators of glycogen and triglyceride metabolism. Based on these results, it is clear that a lack of hepatic Cyp2b members is not protective against fatty liver disease in male mice.

The progression of NAFLD to NASH is characterized by inflammation, fibrosis, stress responses, and hepatocellular injury (Singh et al., 2015). GO terms related to xenobiotic metabolism were down-regulated in female and male CDAHFD-fed Cyp2b-null mice in comparison to CDAHFD-fed WT mice, which is commonly seen in NASH (Deol et al., 2015; H. Li et al., 2017). Interestingly, CDAHFD decreased Cyp2b expression in WT females, but increased Cyp2b expression in WT males. This sexual dimorphism of Cyp2b gene expression in WT mice fed a CDAHFD may be associated with the gender differences observed in Cyp2b-null mice for other measured biomarkers. Markers of fibrosis and inflammation were also examined in CDAHFD-fed mice, however changes in these markers were relatively small. Histopathology revealed development of cytoplasmic vacuolization and fibrosis from CDAHFD treatment in both sexes, but no significant differences between genotypes. Of the major fibrotic markers investigated, only *Tgfb1* and *Tgfb2* were perturbed in CDAHFD-fed Cyp2b-null mice compared to CDAHFD-fed WT mice; *Tgfb1* in males and *Tgfb2* in females. Consequently, susceptibility to NASH only differed following the CDAHFD, but not by genotype despite minor respression of inflammatory markers and hydroxyproline in female mice.

The hepatic Cyp2b members, *Cyp2b9* and *Cyp2b13* are highly sexually dimorphic (Hernandez, Mota, Huang, Moore, & Baldwin, 2009; Renaud, Cui, Khan, & Klaassen,

2011; Wiwi, Gupte, & Waxman, 2004), and CAR regulation of several genes including *Cyp2b10* is also sexually dimorphic as is cell proliferation (Braeuning et al., 2006; Ledda-Columbano et al., 2003). Signal transducer and activator of transcription 5b (Stat5b) mediates growth hormone (GH)-dependent sexually dimorphic gene expression in the male liver (Clodfelter et al., 2006), and results indicate that the GH-STAT5b pathway regulates female predominant expression of *Cyp2b9*, as this pathway is suppressed by the male GH secretion profile (Holloway et al., 2007; Sakuma et al., 2004) through its regulation of HNF4a, CAR, and forkhead box A2 (FoxA2) (Hashita et al., 2008; Hernandez, Mota, Huang, et al., 2009; Wiwi et al., 2004). Female predominant regulation of these genes is crucial in their physiological responses. For example, FoxA2 increases fatty acid oxidation, decreases obesity, regulates *Cyp2b9*, and represses hepatocellular carcinoma only in female mice (Golson & Kaestner, 2016; Hashita et al., 2008; Wolfrum, Asilmaz, Luca, Friedman, & Stoffel, 2004). However, it's ability to regulate obesity in a sexually dimorphic manner has not been established (Bochkis, Shin, & Kaestner, 2013). Based on this information, it is certainly possible that the Cyp2b's play a role in lipid metabolism that decreases obesity, provides protection from liver toxicity, but increases NAFLD in female mice because of their much higher expression, greater control, and production of key but as yet not completely understood oxylipins (Keeney et al., 1998). Most NAFLD studies using mouse models have found that disease is more severe in males, however sex differences differ by model and strain (Lonardo et al., 2019). For example, a recent study found female C57Bl/6J mice fed a high-fructose diet to be more susceptible to NAFLD in terms of greater hepatic inflammation and

decreased adiponectin in visceral adipose tisse than males, with no difference in liver steatosis between genders (Spruss et al., 2012).

These gender differences are also seen in human CYP2B6, as it is also predominantly expressed in females although to a much lesser extent (Lamba et al., 2003). Current studies investigating the effects of NAFLD and NASH on CYP2B6 expression, activity and protein levels are inconclusive. A slight increase in the mRNA levels of CYP2B6 was found in steatotic and NASH human liver tissues, with no change in protein level or activity (Fisher et al., 2009). Conversely, the progression of NAFLD to hepatocellular carcinoma drastically decreased the estimated activity of CYP2B6 in hepatocellular carcinoma patients (Gao et al., 2016). To our knowledge, CYP2B6 expression in NAFLD and NASH patients based on gender has yet to be determined; however, it is established that premenopausal women are protected from dysmetabolism, and NAFLD more often affects men (Ballestri et al., 2017).

A previous diet-induced obesity study in our laboratory performed with a 60% HFD for 10-weeks increased obesity in Cyp2b-null males only (Heintz et al., 2019); however, WAT was increased in both genders. Liver weight was decreased in Cyp2b-null males regardless of diet (ND or HFD), while liver:serum triglyceride ratios increased in Cyp2b-null males. Furthermore, serum cholesterol, which is associated with progressive NAFLD and potentially NASH (Chen, Chen, Dai, Chen, & Fang, 2008; Kerr & Davidson, 2012) was increased in males, but unaffected in females (Heintz et al., 2019). Taken together, Cyp2b-null males were susceptible to obesity and NAFLD with markers indicating the potential for progressive liver disease with the exception of inflammation.

Females showed significantly fewer effects including those on the liver. It is because of this lack of inflammatory markers plus increased liver triglycerides providing protection from free fatty acid-induced oxidative stress observed in the previous study, that we hypothesized less progression to NASH. Interestingly, our hypothesis is correct although the manner of progression was not expected. In Cyp2b-null females, we observed protection from a progressive increase in NASH biomarkers, but that was associated with a decrease in NAFLD following the CDAHFD. In Cyp2b-null males, very few differences in NASH markers were observed while NAFLD increased; identical to the previous study. This suggests that the lack of Cyp2b may increase NAFLD, especially in males, but is protective from progression of the disease to NASH although the data with males is equivocal and in females is may be due to protection from initial damage and NAFLD.

In conclusion, the data presented indicates CDAHFD-fed Cyp2b-null female mice are less susceptible to the development of obesity and NAFLD than WT mice, and have less inflammation potentially due to glucocorticoid-mediated repression of immune responses. Female Cyp2b-null mice fed CDAHFD had decreased concentrations of serum liver injury biomarkers (ALT, AST, and ALP) and less liver steatosis compared to their WT CDAHFD-fed counterparts. In contrast, male Cyp2b-null mice are more susceptible to liver damage and hepatic steatosis with no changes in fibrosis or inflammation markers between CDAHFD-fed WT and Cyp2b-null mice. CDAHFD-fed Cyp2b-null male mice had more liver triglycerides accumulation, as well as significantly higher concentrations of circulating creatine kinase compared to CDAHFD-fed WT males, indicating damage

in other tissues besides the liver. Taken together, there are marked gender-based differences in the role of Cyp2b in the development of NAFLD and progression to NASH.

Acknowledgements

Transcriptomic support was provided by Dr. Rooksana E. Noorai through the Clemson University Genomics and Bioinformatics Facility. Clemson University Open Access Publishing Fund defrayed costs of publishing open access in PLoS ONE.

References

Alkhouri, N., Dixon, L. J., & Feldstein, A. E. (2009). Lipotoxicity in nonalcoholic fatty liver disease: not all lipids are created equal. *Expert review of gastroenterology & hepatology, 3*(4), 445-451. doi:10.1586/egh.09.32

Angulo, P., Kleiner, D. E., Dam-Larsen, S., Adams, L. A., Bjornsson, E. S., Charatcharoenwitthaya, P., . . . Bendtsen, F. (2015). Liver Fibrosis, but No Other Histologic Features, Is Associated With Long-term Outcomes of Patients With Nonalcoholic Fatty Liver Disease. *Gastroenterology, 149*(2), 389-397.e310. doi:10.1053/j.gastro.2015.04.043

Ayala, J. E., Samuel, V. T., Morton, G. J., Obici, S., Croniger, C. M., Shulman, G. I., . . . McGuinness, O. P. (2010). Standard operating procedures for describing and performing metabolic tests of glucose homeostasis in mice. *Disease Models & Mechanisms, 3*(9-10), 525-534. doi:10.1242/dmm.006239

Ballestri, S., Nascimbeni, F., Baldelli, E., Marrazzo, A., Romagnoli, D., & Lonardo, A. (2017). NAFLD as a Sexual Dimorphic Disease: Role of Gender and Reproductive Status in the Development and Progression of Nonalcoholic Fatty Liver Disease and Inherent Cardiovascular Risk. *Advances in Therapy, 34*(6), 1291-1326. doi:10.1007/s12325-017-0556-1

Bishop-Bailey, D., Thomson, S., Askari, A., Faulkner, A., & Wheeler-Jones, C. (2014). Lipid-Metabolizing CYPs in the Regulation and Dysregulation of Metabolism. *Annual Review of Nutrition, 34*(1), 261-279. doi:10.1146/annurev-nutr-071813-105747

Blasbalg, T. L., Hibbeln, J. R., Ramsden, C. E., Majchrzak, S. F., & Rawlings, R. R. (2011). Changes in consumption of omega-3 and omega-6 fatty acids in the United States during the 20th century. *Am J Clin Nutr, 93*(5), 950-962. doi:10.3945/ajcn.110.006643

Bochkis, I. M., Shin, S., & Kaestner, K. H. (2013). Bile acid-induced inflammatory signaling in mice lacking Foxa2 in the liver leads to activation of mTOR and age-onset obesity. *Molecular Metabolism, 2*(4), 447-456. doi:10.1016/j.molmet.2013.08.005

Braeuning, A., Ittrich, C., Kohle, C., Hailfinger, S., Bonin, M., Buchmann, A., & Schwarz, M. (2006). Differential gene expression in periportal and perivenous mouse hepatocytes. *Febs j, 273*(22), 5051-5061. doi:10.1111/j.1742-4658.2006.05503.x

Bylund, J., Kunz, T., Valmsen, K., & Oliw, E. H. (1998). Cytochromes P450 with bisallylic hydroxylation activity on arachidonic and linoleic acids studied with human recombinant enzymes and with human and rat liver microsomes. *J Pharmacol Exp Ther, 284*(1), 51-60.

Chalasani, N., Younossi, Z., Lavine, J. E., Diehl, A. M., Brunt, E. M., Cusi, K., . . . Sanyal, A. J. (2012). The diagnosis and management of non-alcoholic fatty liver disease: Practice Guideline by the American Association for the Study of Liver Diseases, American College of Gastroenterology, and the American Gastroenterological Association. *Hepatology, 55*(6), 2005-2023. doi:10.1002/hep.25762

Chen, Z.-W., Chen, L.-Y., Dai, H.-l., Chen, J.-H., & Fang, L.-Z. (2008). Relationship between alanine aminotransferase levels and metabolic syndrome in nonalcoholic afatty liver disease. *J Zhejiang Univ Sci B, 9*(8), 616-622.

Clodfelter, K. H., Holloway, M. G., Hodor, P., Park, S.-H., Ray, W. J., & Waxman, D. J. (2006). Sex-Dependent Liver Gene Expression Is Extensive and Largely Dependent upon Signal Transducer and Activator of Transcription 5b (STAT5b): STAT5b-Dependent Activation of Male Genes and Repression of Female Genes Revealed by Microarray Analysis. *Molecular Endocrinology, 20*(6), 1333-1351. doi:10.1210/me.2005-0489

Damiri, B., Holle, E., Yu, X., & Baldwin, W. S. (2012). Lentiviral-mediated RNAi knockdown yields a novel mouse model for studying Cyp2b function. *Toxicol Sci, 125*(2), 368-381. doi:10.1093/toxsci/kfr309

Deol, P., Evans, J. R., Dhahbi, J., Chellappa, K., Han, D. S., Spindler, S., & Sladek, F. M. (2015). Soybean Oil Is More Obesogenic and Diabetogenic than Coconut Oil and Fructose in Mouse: Potential Role for the Liver. *PLOS ONE, 10*(7), e0132672. doi:10.1371/journal.pone.0132672

Dong, B., Saha, P. K., Huang, W., Chen, W., Abu-Elheiga, L. A., Wakil, S. J., . . . Moore, D. D. (2009). Activation of nuclear receptor CAR ameliorates diabetes and fatty liver disease. *PNAS, 106*(44), 18831-18836.

Fer, M., Dréano, Y., Lucas, D., Corcos, L., Salaün, J.-P., Berthou, F., & Amet, Y. (2008). Metabolism of eicosapentaenoic and docosahexaenoic acids by recombinant human cytochromes P450. *Archives of Biochemistry and Biophysics, 471*(2), 116-125. doi:https://doi.org/10.1016/j.abb.2008.01.002

Finn, R. D., Attwood, T. K., Babbitt, P. C., Bateman, A., Bork, P., Bridge, A. J., . . . Mitchell, A. L. (2017). InterPro in 2017—beyond protein family and domain annotations. *Nucleic Acids Research, 45*(Database issue), D190-D199. doi:10.1093/nar/gkw1107

Finn, R. D., Henderson, C. J., Scott, C. L., & Wolf, C. R. (2009). Unsaturated fatty acid regulation of cytochrome P450 expression via a CAR-dependent pathway. *Biochem. J., 417*, 43-54.

Fisher, C. D., Lickteig, A. J., Augustine, L. M., Ranger-Moore, J., Jackson, J. P., Ferguson, S. S., & Cherrington, N. J. (2009). Hepatic cytochrome P450 enzyme alterations in humans with progressive stages of nonalcoholic fatty liver disease. *Drug metabolism and disposition: the biological fate of chemicals, 37*(10), 2087-2094. doi:10.1124/dmd.109.027466

Fromenty, B., & Pessayre, D. (1997). Impaired mitochondrial function in microvesicular steatosis effects of drugs, ethanol, hormones and cytokines. *Journal of Hepatology, 26*, 43-53. doi:https://doi.org/10.1016/S0168-8278(97)80496-5

Funk, C. D. (2001). Prostaglandins and leukotrienes: advances in eicosanoid biology. *Science, 294*(5548), 1871-1875. doi:10.1126/science.294.5548.1871

Gao, J., He, J., Zhai, Y., Wada, T., & Xie, W. (2009). The constitutive androstane receptor is an anti-obesity nuclear receptor that improves insulin sensitivity. *J Biol Chem, 284*(38), 25984-25992. doi:10.1074/jbc.M109.016808

Gao, J., Zhou, J., He, X.-P., Zhang, Y.-F., Gao, N., Tian, X., . . . Qiao, H.-L. (2016). Changes in cytochrome P450s-mediated drug clearance in patients with hepatocellular carcinoma in vitro and in vivo: a bottom-up approach. *Oncotarget, 7*(19), 28612-28623. doi:10.18632/oncotarget.8704

Golson, M. L., & Kaestner, K. H. (2016). Fox transcription factors: from development to disease. *Development, 143*(24), 4558. doi:10.1242/dev.112672

Hashita, T., Sakuma, T., Akada, M., Nakajima, A., Yamahara, H., Ito, S., . . . Nemoto, N. (2008). Forkhead Box A2–Mediated Regulation of Female-Predominant Expression of the Mouse Cyp2b9 Gene. *Drug Metabolism and Disposition, 36*(6), 1080. doi:10.1124/dmd.107.019729

Heintz, M. M., Kumar, R., Rutledge, M. M., & Baldwin, W. S. (2019). Cyp2b-null male mice are susceptible to diet-induced obesity and perturbations in lipid homeostasis. *The Journal of Nutritional Biochemistry, 70*, 125-137. doi:https://doi.org/10.1016/j.jnutbio.2019.05.004

Hernandez, J. P., Mota, L. C., & Baldwin, W. S. (2009). Activation of CAR and PXR by Dietary, Environmental and Occupational Chemicals Alters Drug Metabolism, Intermediary Metabolism, and Cell Proliferation. *Current Pharmacogenomics Personal Medicine, 7*(2), 81-105. doi:10.2174/187569209788654005

Hernandez, J. P., Mota, L. C., Huang, W., Moore, D. D., & Baldwin, W. S. (2009). Sexually dimorphic regulation and induction of P450s by the constitutive androstane receptor (CAR). *Toxicology, 256*(1), 53-64. doi:https://doi.org/10.1016/j.tox.2008.11.002

Hoek-van den Hil, E. F., van Schothorst, E. M., van der Stelt, I., Swarts, H. J., van Vliet, M., Amolo, T., . . . Keijer, J. (2015). Direct comparison of metabolic health effects of the flavonoids quercetin, hesperetin, epicatechin, apigenin and anthocyanins in high-fat-diet-fed mice. *Genes Nutr, 10*(4), 469. doi:10.1007/s12263-015-0469-z

Hoek-van den Hil, E. F., van Schothorst, E. M., van der Stelt, I., Swarts, H. J. M., Venema, D., Sailer, M., . . . Keijer, J. (2014). Quercetin decreases high-fat diet induced body weight gain and accumulation of hepatic and circulating lipids in mice. *Genes & Nutrition, 9*(5), 418. doi:10.1007/s12263-014-0418-2

Holloway, M. G., Cui, Y., Laz, E. V., Hosui, A., Hennighausen, L., & Waxman, D. J. (2007). Loss of sexually dimorphic liver gene expression upon hepatocyte-specific deletion of Stat5a-Stat5b locus. *Endocrinology, 148*(5), 1977-1986. doi:10.1210/en.2006-1419

Huber, W., Carey, V. J., Gentleman, R., Anders, S., Carlson, M., Carvalho, B. S., . . . Morgan, M. (2015). Orchestrating high-throughput genomic analysis with Bioconductor. *Nature Methods, 12*, 115. doi:10.1038/nmeth.3252

Kanehisa, M., Furumichi, M., Tanabe, M., Sato, Y., & Morishima, K. (2017). KEGG: new perspectives on genomes, pathways, diseases and drugs. *Nucleic Acids Res, 45*(D1), D353-d361. doi:10.1093/nar/gkw1092

Keeney, D. S., Skinner, C., Travers, J. B., Capdevila, J. H., Nanney, L. B., King, L. E., Jr., & Waterman, M. R. (1998). Differentiating keratinocytes express a novel cytochrome P450 enzyme, CYP2B19, having arachidonate monooxygenase activity. *J Biol Chem, 273*(48), 32071-32079.

Kerr, T. A., & Davidson, N. O. (2012). Cholesterol and NAFLD: Renewed focus on an old villain. *Hepatology, 56*(5), 1995-1998.

Konkel, A., & Schunck, W.-H. (2011). Role of cytochrome P450 enzymes in the bioactivation of polyunsaturated fatty acids. *Biochimica et Biophysica Acta (BBA) - Proteins and Proteomics, 1814*(1), 210-222. doi:https://doi.org/10.1016/j.bbapap.2010.09.009

Kumar, R., Litoff, E. J., Boswell, W. T., & Baldwin, W. S. (2018). High fat diet induced obesity is mitigated in Cyp3a-null female mice. *Chem-Biol Interact, 289*, 129-140.

Kumar, R., Litoff, E. J., Boswell, W. T., & Baldwin, W. S. (2018). High fat diet induced obesity is mitigated in Cyp3a-null female mice. *Chem Biol Interact, 289*, 129-140. doi:10.1016/j.cbi.2018.05.001

Kumar, R., Mota, L. C., Litoff, E. J., Rooney, J. P., Boswell, W. T., Courter, E., . . . Baldwin, W. S. (2017). Compensatory changes in CYP expression in three different toxicology mouse models: CAR-null, Cyp3a-null, and Cyp2b9/10/13-null mice. *PLOS ONE, 12*(3), e0174355. doi:10.1371/journal.pone.0174355

Lamba, V., Lamba, J., Yasuda, K., Strom, S., Davila, J., Hancock, M. L., . . . Schuetz, E. G. (2003). Hepatic CYP2B6 Expression: Gender and Ethnic Differences and Relationship to CYP2B6 Genotype and CAR (Constitutive Androstane Receptor) Expression. *Journal of Pharmacology and Experimental Therapeutics, 307*(3), 906. doi:10.1124/jpet.103.054866

Ledda-Columbano, G. M., Pibiri, M., Concas, D., Molotzu, F., Simbula, G., Cossu, C., & Columbano, A. (2003). Sex difference in the proliferative response of mouse hepatocytes to treatment with the CAR ligand, TCPOBOP. *Carcinogenesis, 24*(6), 1059-1065. doi:10.1093/carcin/bgg063

Leung, A., Trac, C., Du, J., Natarajan, R., & Schones, D. E. (2016). Persistent Chromatin Modifications Induced by High Fat Diet. *J Biol Chem, 291*(20), 10446-10455. doi:10.1074/jbc.M115.711028

Li, C.-C., Lii, C.-K., Liu, K.-L., Yang, J.-J., & Chen, H.-W. (2007). DHA down-regulates phenobarbital-induced cytochrome P450 2B1 gene expression in rat primary hepatocytes by attenuating CAR translocation. *Toxicology and applied pharmacology, 225*(3), 329-336. doi:https://doi.org/10.1016/j.taap.2007.08.009

Li, H., Toth, E., & Cherrington, N. J. (2017). Asking the Right Questions With Animal Models: Methionine- and Choline-Deficient Model in Predicting Adverse Drug Reactions in Human NASH. *Toxicological Sciences, 161*(1), 23-33. doi:10.1093/toxsci/kfx253

Lonardo, A., Nascimbeni, F., Ballestri, S., Fairweather, D., Win, S., Than, T. A., . . . Suzuki, A. (2019). Sex Differences in Nonalcoholic Fatty Liver Disease: State of the Art and Identification of Research Gaps. *Hepatology, 70*(4), 1457-1469. doi:10.1002/hep.30626

Maglich, J. M., Lobe, D. C., & Moore, J. T. (2009). The nuclear receptor CAR (NR1I3) regulates serum triglyceride levels under conditions of metabolic stress. *J Lipid Res, 50*(3), 439-445. doi:10.1194/jlr.M800226-JLR200

Maglich, J. M., Watson, J., McMillen, P. J., Goodwin, B., Willson, T. M., & Moore, J. T. (2004). The nuclear receptor CAR is a regulator of thyroid hormone metabolism during caloric restriction. *J Biol Chem, 279*(19), 19832-19838. doi:10.1074/jbc.M313601200

Matsumoto, M., Hada, N., Sakamaki, Y., Uno, A., Shiga, T., Tanaka, C., . . . Sudoh, M. (2013). An improved mouse model that rapidly develops fibrosis in non-alcoholic steatohepatitis. *International Journal of Experimental Pathology, 94*(2), 93-103. doi:10.1111/iep.12008

Mota, L. C., Hernandez, J. P., & Baldwin, W. S. (2010). Constitutive androstane receptor -null mice are sensitive to the toxic effects of parathion: association with reduced cytochrome p450-mediated parathion metabolism *Drug Metabolism Disposition, 38*(9), 1582-1588. doi:10.1124/dmd.110.032961

Muller, P. Y., Janovjak, H., Miserez, A. R., & Dobbie, Z. (2002). Processing of gene expression data generated by quantitative real-time RT-PCR. *Biotechniques, 32*, 1372-1379.

Pallayova, M., & Taheri, S. (2014). Non-alcoholic fatty liver disease in obese adults: clinical aspects and current management strategies. *Clinical Obesity, 4*(5), 243-253. doi:10.1111/cob.12068

Renaud, H. J., Cui, J. Y., Khan, M., & Klaassen, C. D. (2011). Tissue Distribution and Gender-Divergent Expression of 78 Cytochrome P450 mRNAs in Mice. *Toxicological Sciences, 124*(2), 261-277. doi:10.1093/toxsci/kfr240

Rizki, G., Arnaboldi, L., Gabrielli, B., Yan, J., Lee, G. S., Ng, R. K., . . . Maher, J. J. (2006). Mice fed a lipogenic methionine-choline-deficient diet develop hypermetabolism coincident with hepatic suppression of SCD-1. *J Lipid Res, 47*(10), 2280-2290. doi:10.1194/jlr.M600198-JLR200

Roling, J. A., Bain, L. J., & Baldwin, W. S. (2004). Differential gene expression in mummichogs (*Fundulus heteroclitus*) following treatment with pyrene: comparison to a creosote contaminated site. *Mar Environ Res, 57*, 377-395.

Saini, S. P., Sonoda, J., Xu, L., Toma, D., Uppal, H., Mu, Y., . . . Xie, W. (2004). A novel constitutive androstane receptor-mediated and CYP3A-independent pathway of bile acid detoxification. *Mol Pharmacol, 65*(2), 292-300. doi:10.1124/mol.65.2.292

Sakuma, T., Kitajima, K., Nishiyama, M., Mashino, M., Hashita, T., & Nemoto, N. (2004). Suppression of female-specific murine Cyp2b9 gene expression by growth or glucocorticoid hormones. *Biochem Biophys Res Commun, 323*(3), 776-781. doi:10.1016/j.bbrc.2004.08.158

Schindelin, J., Arganda-Carreras, I., Frise, E., Kaynig, V., Longair, M., Pietzsch, T., . . . Cardona, A. (2012). Fiji: an open-source platform for biological-image analysis. *Nature Methods, 9*, 676. doi:10.1038/nmeth.2019 https://www.nature.com/articles/nmeth.2019#supplementary-information

Shubin, A. V., Demidyuk, I. V., Komissarov, A. A., & Rafieva, L. M. (2016). Cytoplasmic vacuolization in cell death and survival. *Oncotarget, 7*(34), 55863-55889.

Singh, S., Allen, A. M., Wang, Z., Prokop, L. J., Murad, M. H., & Loomba, R. (2015). Fibrosis Progression in Nonalcoholic Fatty Liver vs Nonalcoholic Steatohepatitis: A Systematic Review and Meta-analysis of Paired-Biopsy Studies. *Clinical Gastroenterology and Hepatology, 13*(4), 643-654.e649. doi:10.1016/j.cgh.2014.04.014

Snider, N. T., Nast, J. A., Tesmer, L. A., & Hollenberg, P. F. (2009). A Cytochrome P450-Derived Epoxygenated Metabolite of Anandamide Is a Potent Cannabinoid Receptor 2-Selective Agonist. *Mol Pharmacol, 75*(4), 965. doi:10.1124/mol.108.053439

Spruss, A., Henkel, J., Kanuri, G., Blank, D., Püschel, G. P., Bischoff, S. C., & Bergheim, I. (2012). Female Mice Are More Susceptible to Nonalcoholic Fatty

Liver Disease: Sex-Specific Regulation of the Hepatic AMP-Activated Protein Kinase-Plasminogen Activator Inhibitor 1 Cascade, but Not the Hepatic Endotoxin Response. *Molecular Medicine, 18*(9), 1346-1355. doi:10.2119/molmed.2012.00223

Sridar, C., Snider, N. T., & Hollenberg, P. F. (2011). Anandamide Oxidation by Wild-Type and Polymorphically Expressed CYP2B6 and CYP2D6. *Drug Metabolism and Disposition, 39*(5), 782. doi:10.1124/dmd.110.036707

Supek, F., Bošnjak, M., Škunca, N., & Šmuc, T. (2011). REVIGO Summarizes and Visualizes Long Lists of Gene Ontology Terms. *PLOS ONE, 6*(7), e21800. doi:10.1371/journal.pone.0021800

Tilg, H., & Moschen, A. R. (2010). Evolution of inflammation in nonalcoholic fatty liver disease: the multiple parallel hits hypothesis. *Hepatology, 52*(5), 1836-1846. doi:10.1002/hep.24001

Urquiza, A. M. d., Liu, S., Sjöberg, M., Zetterström, R. H., Griffiths, W., Sjövall, J., & Perlmann, T. (2000). Docosahexaenoic Acid, a Ligand for the Retinoid X Receptor in Mouse Brain. *Science, 290*(5499), 2140. doi:10.1126/science.290.5499.2140

van der Hoeven, T. A., & Coon, M. J. (1974). Preparation and properties of partially purified cytochrome P-450 and reduced nicotinamide adenine dinucleotide phosphate-cytochrome P-450 reductase from rabbit liver microsomes. *J Biol Chem, 249*(19), 6302-6310.

Vernon, G., Baranova, A., & Younossi, Z. M. (2011). Systematic review: the epidemiology and natural history of non-alcoholic fatty liver disease and non-alcoholic steatohepatitis in adults. *Alimentary Pharmacology & Therapeutics, 34*(3), 274-285. doi:10.1111/j.1365-2036.2011.04724.x

Wang, H., & Tompkins, L. M. (2008). CYP2B6: New Insights into a Historically Overlooked Cytochrome P450 Isozyme. *Current Drug Metabolism, 9*, 598-610.

Wei, P., Zhang, J., Egan-Hafley, M., Liang, S., & Moore, D. D. (2000). The nuclear receptor CAR mediates specific xenobiotic induction of drug metabolism. *Nature, 407*(6806), 920-923. doi:10.1038/35038112

Wiwi, C. A., Gupte, M., & Waxman, D. J. (2004). Sexually dimorphic P450 gene expression in liver-specific hepatocyte nuclear factor 4alpha-deficient mice. *Mol Endocrinol, 18*(8), 1975-1987. doi:10.1210/me.2004-0129

Wolfrum, C., Asilmaz, E., Luca, E., Friedman, J. M., & Stoffel, M. (2004). Foxa2 regulates lipid metabolism and ketogenesis in the liver during fasting and in

diabetes. *Nature, 432*, 1027. doi:10.1038/nature03047
https://www.nature.com/articles/nature03047#supplementary-information

Wong, R. J., Aguilar, M., Cheung, R., Perumpail, R. B., Harrison, S. A., Younossi, Z. M., & Ahmed, A. (2015). Nonalcoholic steatohepatitis is the second leading etiology of liver disease among adults awaiting liver transplantation in the United States. *Gastroenterology, 148*(3), 547-555. doi:10.1053/j.gastro.2014.11.039

Yen, C.-H., Wang, K.-T., Lee, P.-Y., Liu, C.-C., Hsieh, Y.-C., Kuo, J.-Y., . . . Lam, C. S. P. (2017). Gender-differences in the associations between circulating creatine kinase, blood pressure, body mass and non-alcoholic fatty liver disease in asymptomatic asians. *PLOS ONE, 12*(6), e0179898. doi:10.1371/journal.pone.0179898

Yoshimura, A., & Muto, G. (2011). TGF-beta function in immune suppression. *Curr Top Microbiol Immunol, 350*, 127-147. doi:10.1007/82_2010_87

Young, M. D., Wakefield, M. J., Smyth, G. K., & Oshlack, A. (2010). Gene ontology analysis for RNA-seq: accounting for selection bias. *Genome Biology, 11*(2), R14. doi:10.1186/gb-2010-11-2-r14

Younossi, Z. M., Koenig, A. B., Abdelatif, D., Fazel, Y., Henry, L., & Wymer, M. (2016). Global epidemiology of nonalcoholic fatty liver disease—Meta-analytic assessment of prevalence, incidence, and outcomes. *Hepatology, 64*(1), 73-84. doi:10.1002/hep.28431

Supplementary Material

S3.1 Table. Primers and annealing temperatures for qPCR.

Gene	Forward Primer	Reverse Primer	T_a(°C)
18s	ATGGCCGTTCTTAGTTGGTG	ATGCCAGAGTCTCGTTCGTT	64
Acta2	CGAAACCACCTATAACAGCATCA	GCGTTCTGGAGGGGCAAT	57
Akr1b8	TCAGCCCACGAGGCTTCCTTC	CTCCGGAGTCGCATTTGCTCGCA	66
Cd68	CGCAGACGACAATCAACCTA	AGTGGCATGGTGAAGAGATG	59
Col1a1	GAGAGCGAGGCCTTCCCGGA	GGGAGCCAGCGGGACCTTGT	66
Cyp17a1	GATCGGTTTATGCCTGAGCG	TCCGAAGGGCAAATAACTGG	61
G6pc	CGACTCGCTATCTCCAAGTGA	GGGCGTTGTCCAAACAGAAT	56
Ppp1r3b	AGCCGTACAATGGACCAGAT	AGTAGTAGGGCCCCAGCTTT	62.4

S3.1 Figure. Timeline of procedures performed. Procedures performed during an 8-week treatment of 9-10 week old WT and Cyp2b-null mice with either a normal diet (ND; 6.2% fat) or a choline-deficient, L-amino acid-defined high fat diet (CDAHFD; 62% fat and 0.1% methionine).

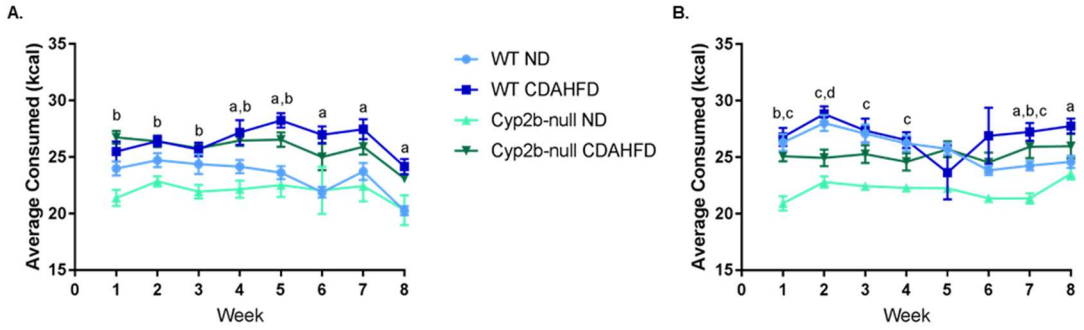

S3.2 Figure. Feed consumption of WT and Cyp2b-null mice during 8-weeks of diet-induced NASH treatment. Female (A) and male (B) feed consumption was measured by weighing the food every alternate day. Data are presented as mean calories ± SEM. Statistical significance was determined by one-way ANOVA followed by Fisher's LSD as post-hoc test (n=9 An 'a' indicates ND-fed WT different than CDAHFD-fed WT, 'b'

indicates ND-fed Cyp2b-null different than CDAHFD-fed Cyp2b-null, ‘c’ indicates ND-fed WT different than ND-fed Cyp2b-null, ‘d’ indicates CDAHFD-fed WT different than CDAHFD-fed Cyp2b-null.

S3.3 File. List of differentially expressed genes by multiple comparisons for all treatment groups. Up- and down-regulated differentially expressed genes from raw read counts were determined by multiple comparisions in EdgeR for all treatment groups ($p < 0.05$, FDR < 0.1). *Data is published in Heintz et al. 2020, PLos ONE.*

S3.4 File. Differentially expressed gene list of CDAHFD-fed Cyp2b-null mice compared to CDAHFD-fed WT mice. Normalized counts of genes from the multiple comparisions results were compared by Student’s t tests to determine significant ($p < 0.05$) differentially expressed genes between CDAHFD-fed Cyp2b-null and WT groups. *Data is published in Heintz et al. 2020, PLos ONE.*

S3.5 File. GO term enrichment analysis list of up and down-regulated genes in CDAHFD-fed Cyp2b-null mice compared to CDAHFD-fed WT mice. GOSeq (Young et al., 2010), a GO term enrichment analysis program was used to adjust for gene length and expression bias of significant differentially expressed genes between CDAHFD-fed groups in female and male mice. *Data is published in Heintz et al. 2020, PLos ONE.*

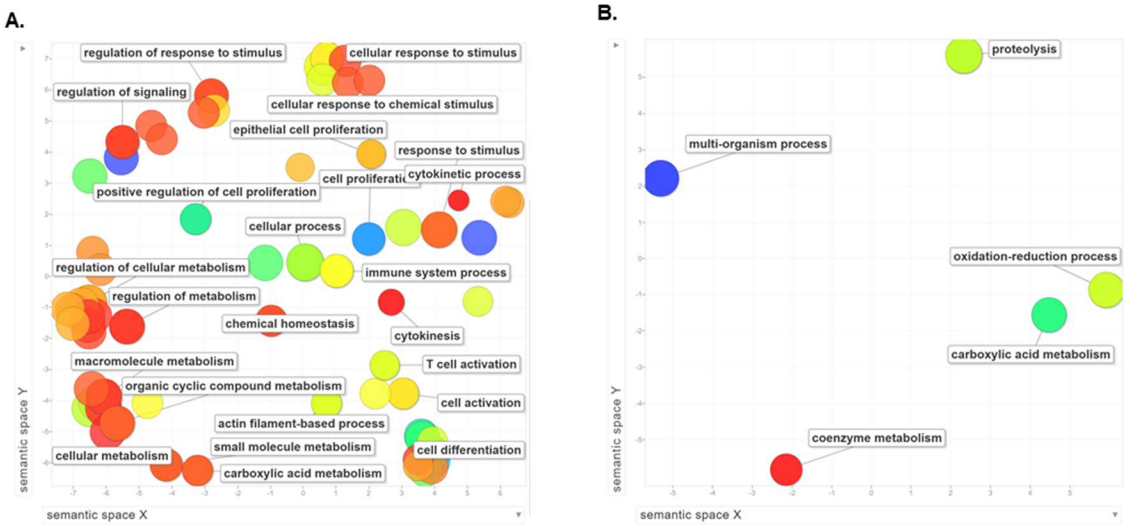

S3.6 Figure. Gene ontology (GO) term enrichment analysis summary for down-regulated GO terms in CDAHFD-fed Cyp2b-null mice. GO term enrichment analysis summary using Revigo (Supek et al., 2011) for significant down-regulated GO terms in CDAHFD-fed Cyp2b-null female (A) and male (B) mice compared to CDAHFD-fed WT mice. Each scatterplot contains enriched GO terms from the biological process class that remain after term redundancy is reduced and are displayed in a two-dimensional space where semantically similar GO terms are positioned closer together within the plot. Each circle represents an enriched GO term; the cooler the color of a term, the greater signficance ($p < 0.05$) of that term with measured changes in gene expression. Circle size indicates the frequency of the GO term in the underlying GO database, i.e. circles of more general terms are larger.

S3.7 File. Differentially expressed gene list of CDAHFD-fed WT mice compared to ND-fed WT mice. Normalized counts of genes from the multiple comparisions results

were compared by Student's t tests to determine significant ($p < 0.05$) differentially expressed genes between ND-fed and CDAHFD-fed WT groups. *Data is published in Heintz et al. 2020, PLos ONE.*

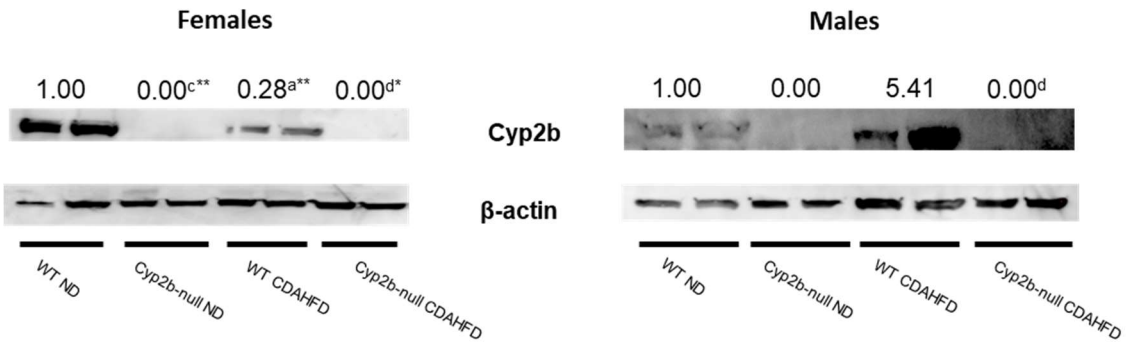

S3.8 Figure. Immunoblots of Cyp2b protein expression between ND-fed and CDAHFD-fed WT and Cyp2b-null mice. Microsomes were prepared by homogenizing frozen livers followed by differential centrifugation as described previously (van der Hoeven & Coon, 1974). Protein concentrations were determined using Bradford reagent (Bio-Rad). Immunoblots were performed using 30 µg of microsomal protein separated on 12% SDS-polyacrylamide gels (BioRad). Protein was transferred onto 0.2µm polyvinylidene difluoride (PVDF) membrane and were recognized using polyclonal antibodies to Cyp2b (previously developed in house) (Hernandez, Mota, & Baldwin, 2009; Mota, Hernandez, & Baldwin, 2010). β-actin (Sigma Aldrich, St.Louis MO USA) was used as the reference protein. Chemiluminescent immunoblot detection was done using alkaline phosphatase conjugated secondary antibodies, where in anti-mouse IgG (Immunostar, Bio-Rad) was used to visualize β-actin and anti-rabbit IgG (Immunostar,

Bio-Rad) was used to visualize Cyp2b. Protein was quantified by densitometry (Image Lab 6.0.1, BioRad, Hercules, CA). Relative density is shown as the average of two samples using β-actin as the reference gene. Data are presented as relative mean of WT ND compared to each treatment group. Statistical significance was determined by one-way ANOVA followed by Fisher's LSD as post-hoc test (n=2). An 'a' indicates WT ND are different than WT CDAHFD, 'b' indicates Cyp2b-null ND are different than Cyp2b-null CDAHFD, 'c' indicates Cyp2-null ND are different than WT ND, 'd' indicates WT CDAHFD are different than Cyp2b-null CDAHFD. No asterisk indicates a p-value < 0.05, * indicates a p-value < 0.01, and ** indicates a p-value < 0.0001.

S3.9 File. List of altered KEGG pathways in CDAHFD-fed Cyp2b-null mice compared to CDAHFD-fed WT mice. Significant differentially expressed genes between CDAHFD-fed Cyp2b-null and WT groups were annotated to NCBI Gene IDs using InterPro and entered into KEGG Mapper (Kanehisa et al., 2017). *Data is published in Heintz et al. 2020, PLos ONE.*

S3.10 Figure. Full immunoblot and gel images required by PLoS ONE. Full immunoblot images of PCNA, CYP2B, and b-actin. (A) CYP2B immunoblot: CYP2B is sexually dimorphic and expressed much higher in females than males (Hernandez, Mota, Huang, et al., 2009; Renaud et al., 2011; Wiwi et al., 2004). (B) Microsomal b-actin as the housekeeping protein. (C) PCNA. (D) Nuclear b-actin as the housekeeping protein. Left hand side of blots are often but not always stained with molecular weight

markers. Blot images are from **S3.8 Figure** (CYP2B and b-actin) and **Figure 3.1** (PCNA and b-actin). *Data is published in Heintz et al. 2020, PLos ONE.*

S3.11 File. Raw data from necropsies, glucose tolerance tests, serum and liver biomarkers, and qPCR. *Data is published in Heintz et al. 2020, PLos ONE.*

CHAPTER FOUR

AGE AND DIET-DEPENDENT CHANGES IN THE HEPATIC LIPIDOMIC PROFILES OF MALE MICE: AGE ACCELERATION IN CYP2B-NULL MICE

Melissa M Heintz, Ramiya Kumar, Kristal M. Maner-Smith, Eric A. Ortlund, and William S Baldwin

Data presented in this chapter was submitted for publication in *Nutrition Research*:

Heintz, M. M., Kumar, R., Maner-Smith, K. M., Ortlund, E. A., & Baldwin, W. S. (2020). Age and Diet-dependent Changes in the Hepatic Lipidomic Profiles of Male Mice: Age Acceleration in Cyp2b-null mice. *Nutr Res* (*In review*).

4.0 Abstract

The effects of age (9 months old), high-fat diet (4.5 months old), and the loss of the xeno- and endobiotic metabolizing enzymes *Cyp2b9*, *Cyp2b10*, and *Cyp2b13* (Cyp2b-null mice) on the male murine hepatic lipidome was compared. Hierarchical clustering and principal component analysis show that age perturbs phospholipid profiles and serum lipid markers the most compared to healthy, young mice; followed by a high-fat diet and then loss of Cyp2b. Lipid profiles from older mice followed by diet-induced obese mice contain greater n-6 fatty acids than normal diet (ND)-fed young mice that contain significantly more n-3 fatty acids. The lack of Cyp2b typically enhanced the adverse effects found in the older (9 mo) mice with increased liver injury, cluster of phospholipids, and weight gain combined with a deteriorating cholesterol profile.

Keywords: VLDL, diet-induced obesity, omega-6 fatty acids, liver, serum lipids

Highlights

- In male mice, adverse outcomes such as weight gain and VLDL are more closely associated with age than high-fat diet or lack of Cyp2b
- Age has a powerful effect on lipid profiles; more so than HFD or the lack of Cyp2b
- Male Cyp2b-null mice show an enhancement of undesireable traits and lipid markers as they age

4.1 Introduction

Obesity is a major risk factor for metabolic disorders such as cardiovascular disease, diabetes, and fatty liver disease. Data from the most recent National Health and Nutrition Examination Survey in 2015-2016 shows that 39.8% of adults and 18.5% of youth in the United States are obese (Hales, Carroll, Fryar, & Ogden, 2017). Disease susceptibility and overall health is greatly affected by changes to the lipidome (Murphy & Nicolaou, 2013; Orešič, Hänninen, & Vidal-Puig, 2008). High-fat diets, such as the Western diet, cause obesity and drastically alter the hepatic lipidome (Wang et al., 2017), and perturbed lipid profiles are associated with specific liver diseases, such as nonalcoholic fatty liver disease (NAFLD) and nonalcoholic steatohepatitis (NASH) (Chiappini, Desterke, Bertrand-Michel, Guettier, & Le Naour, 2016; Saito et al., 2015). Age also alters the phospholipid profile of mitochondria in the liver, brain, and skeletal tissue (Modi, Katyare, & Patel, 2008; Pollard, Ortori, Stöger, Barrett, & Chakrabarti, 2017). Age transcended the effect of a high fat diet on alterations to the blood lipidome in female mice (males were not investigated) (Pati et al., 2018); however, little is known about changes that occur with age to the hepatic lipidome.

Lipids provide membrane structure, energy storage, and act as signaling molecules that mediate lipid metabolism, inflammation, and progression of chronic diseases such as insulin resistance (Glass & Olefsky, 2012). For example, the polyunsaturated fatty acid (PUFA), linoleic acid is the endogenous ligand for HNF4α, a key regulator of multiple metabolic pathways (Yuan et al., 2009). Several fatty acids are peroxisome proliferator-activated receptor (PPAR) ligands (Feige, Gelman, Michalik,

Desvergne, & Wahli, 2006), and fatty acids released by lipolysis during fasting trigger hepatic PPARα-mediated β-oxidation while inhibiting lipogenesis through the liver X receptor (LXR) (Yoshikawa et al., 2003). During inflammation, PUFAs found in hepatic membrane phospholipids are cleaved by phospholipase A2 (Quach, Arnold, & Cummings, 2014). These available PUFAs are then oxidized by cyclooxygenase, lipoxygenase, or cytochrome P450s (CYP) to form physiologically significant metabolites. The CYP pathways typically metabolize PUFAs to fatty acid epoxides that have bioactive effects (G. Zhang, Kodani, & Hammock, 2014). CYPs including CYP1A, CYP1B, CYP2B, CYP2C, CYP2D, CYP2J, CYP3A, CYP4A, and CYP4F all metabolize PUFAs (Hankinson, 2016; Zeldin, 2001; G. Zhang et al., 2014).

Our lab previously produced a Cyp2b9/10/13-null (Cyp2b-null) mouse model, lacking the primary hepatic Cyp2b members: *Cyp2b9*, *Cyp2b10*, and *Cyp2b13* on a C57Bl/6J (B6) background (Ramiya Kumar et al., 2017) and Cyp2b-null males are diet-induced obese (DIO) with NAFLD development (Heintz, Kumar, Rutledge, & Baldwin, 2019). Similar lipid accumulation has also been observed in male Cyp2b-KD (RNAi-based knockdown) mice on a FVB/NJ background as the mice aged (Damiri & Baldwin, 2018). However, the hepatic phospholipid profile has not been investigated in Cyp2b-null mice. The previously referenced studies with Cyp2b-KD and Cyp2b-null mice showed few differences between genotypes in female mice, but significant differences in obesity in male mice, most likely because several strains of mice are less susceptible to obesity in females (Hong, Stubbins, Smith, Harvey, & Nunez, 2009; Wade, Gray, & Bartness,

1985). Therefore, in this study we compared the hepatic lipidome of male Cyp2b-null and WT mice in healthy, diet-induced obese, and older mice.

4.2 Materials and Methods

4.2.1 Treatment of experimental groups:

Animal care procedures were approved by Clemson University's Institutional Animal Care and Use committee. Cyp2b-null mice were developed using CRISPR/Cas9 as previously described (Ramiya Kumar et al., 2017) and wildtype (WT) B6 mice were purchased from The Jackson Laboratory (Bar Harbor, ME, USA) at 3 weeks of age and acclimated for 6 weeks prior to treatment. WT and Cyp2b-null male (9 weeks old) mice were divided into groups (n=9) and fed either a normal chow diet (ND; Harlan, 3.1 Kcal/g: 18.6% protein, 6.2 % fat, 44.2% carbohydrates; Madison, WI USA) or a high-fat diet (HFD; Envigo TD.06414, 5.1 Kcal/g: 60.3% fat (37% saturated, 47% monounsaturated, 16% polyunsaturated fat), 18.4% protein, 21.3% carbohydrates; Madison, WI USA) for 10 weeks (Heintz et al., 2019). Mice were 4.5 months old at the end of the HFD study and referred to as ND-fed young or HFD-fed young; WT or Cyp2b-null mice. An additional experimental group of WT (Jackson) and Cyp2b-null male mice (n= 5) were fed a ND until they reached 9 months (termed old WT and old Cyp2b-null mice). At the end of the studies, mice were weighed, anesthetized, and blood collected by heart puncture prior to euthanasia and serum prepared. Serum biomarkers and liver triglycerides were measured as described (Heintz et al., 2019). Liver and inguinal white adipose tissue (WAT) were excised, weighed, and divided by total body

weight to determine the hepatosomatic index (HSI) and white adipose somatic index (WSI). Tissues were immediately snap frozen in liquid nitrogen and stored at -80°C.

4.2.2 Targeted lipidomics and analysis:

Phospholipid species of arachidonic (ARA; 20:4), linoleic (LA; 18:2), α-linolenic (ALA; 18:3) and docosahexaenoic acid (DHA; 22:6) were identified and quantified from the livers of mice (n=3 for young (4.5 mo) ND and HFD-fed mice; n=5 for old (9 mo.) mice) from each experimental group by LC-MS/MS at the Emory Integrated Lipidomics Core (EILC). Livers were homogenized and extracted using a modified Bligh/Dyer chloroform/methanol lipid extraction protocol (Bligh & Dyer, 1959)(**S4.1**). Recovered lipids were reconstituted in 1:1 v/v chloroform:methanol prior to analysis by LC/MS. Targeted lipidomics were conducted using Sciex AC LC system and Sciex QTrap5500 mass spectrometer (Framingham, MA, USA). Lipids were deposited onto ThermoScientific Accucore C18 column (4.6 x 100mm, 2.6µm) and resolved on an 18 minute linear gradient using the solvents and parameters recorded in detail in **Suppl Material 4.1**. PUFAs were selectively targeted in samples by performing precursor ion scans in the negative ion mode. The resulting scans, corresponding to the molecular weights are m/z 279 (LA), m/z 277 (ALA), m/z 303 (ARA), and m/z 327 (DHA). All peaks above signal to noise ratio of 5 were fragmented for identification. The area under the curve for all scans were used to compare changes in lipid distribution between groups. For total quantification, the area under the curve is calibrated against the area of an internal standard of known concentration.

4.2.3 Statistical analysis:

Data are presented as mean ± SEM (n = 3-5). Statistical significance was determined (p-value < 0.05) by unpaired Student's t-tests when comparing two groups; one-way ANOVA followed by Fisher's LSD as the post-hoc test when comparing more than two groups with Graphpad Prism 7.0 (Graphpad Software, San Diego, CA, USA). Hierarchical cluster analysis was performed on lipidomic data and visualized in heatmaps with MetaboAnalyst 3.6 (Xia & Wishart, 2002) to compare lipid species content across treatment groups. RandomForest (http://www.r-project.org/) was used to rank phospholipid species as a prediction of the significance of an effect each lipid species has on differences between treatment groups (Breiman, 2001). The tuneRF() function was used to determine the best number of predictors (mtry) value to get the lowest out-of-bag (OOB) classification error as trees are added to the forest. The number of trees to be built (ntree) was set to 350 for all experimental groups to achieve the lowest OOB error. The larger the mean decreased accuracy (MDA) value, the more important the phospholipid species are for the accuracy of the association between variable and response. Lipid species with importance scores less than or equal to zero are likely to have no predictive ability. Principal component analysis (PCA) was performed and a biplot drawn using the ggbiplot package in R to compare the relationship between multiple variables and treatment groups. Variables included total body weight, WSI, serum lipids, and phospholipid species. The factoextra R package (https://cran.r-project.org) was used to obtain the percent contributions of each measured variable in principle components 1-3.

4.3 Results and Discussion

4.3.1 Increase in obesity due to a high-fat diet or age is exacerbated in Cyp2b-null mice:

ND-fed old Cyp2b-null male mice weigh more than all other groups (**Fig. 4.1**). Cyp2b-null mice also weigh more than their WT counterparts after a HFD (**Fig. 4.1**). WAT weight is usually associated with the increased body mass as determined by WSI. Old WT mice are the only group whose body mass rises at a greater rate than the measured WAT or WSI. Cyp2b-null mice further exacerbate the increase in WAT/WSI and liver weight/HSI (**Fig. 4.1**). Age increases obesity similar to a HFD but with a lower percentage of inguinal WAT and greater liver weight, especially in Cyp2b-null mice.

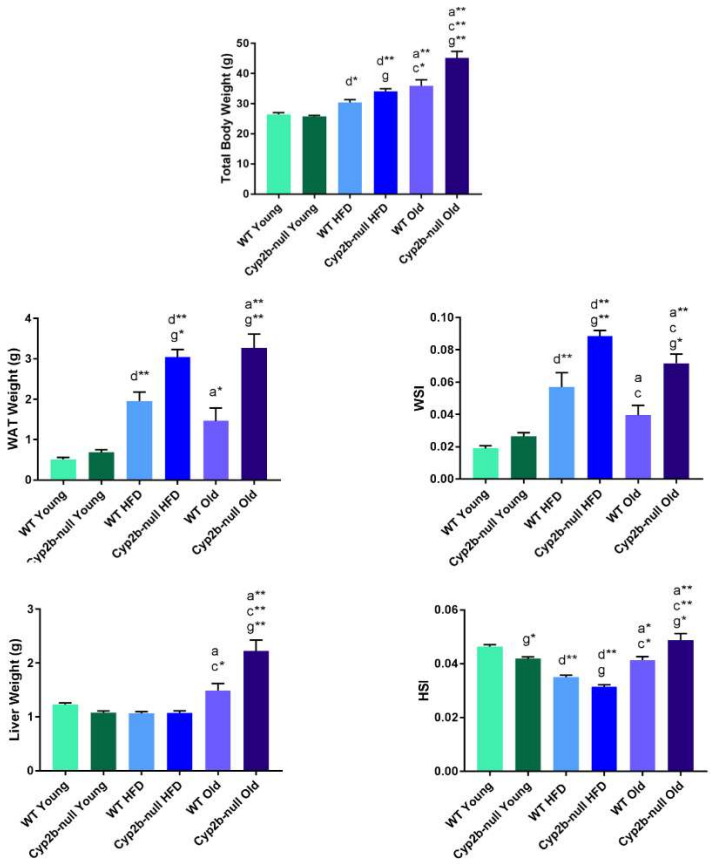

Figure 4.1. Comparison of total body, liver and WAT weights between all treatment groups. Total body weight, liver weight, hepatic somatic index (HSI), WAT weight, and WAT somatic index (WSI) were measured for all treatment groups. Data are presented as mean (g) + SEM. Statistical significance was determined by one-way ANOVA multiple comparisons test using Fisher's LSD as the post-hoc test (n = 5-9). 'a' indicates age difference between young (4.5 mo) and old (9 mo) mice within same genotype and diet group, 'c' indicates difference between HFD-fed young (4.5 mo) and ND-fed old (9 mo) mice within same genotype, 'd' indicates diet difference between ND-fed and HFD-fed mice within in same genotype and age, 'g' indicates genotype difference between WT and Cyp2b-null mice within same diet and age group. No asterisk indicates a p-value < 0.05, * indicates a p-value < 0.01, and ** indicates a p-values < 0.0001.

Serum cholesterol increased in old Cyp2b-null mice compared to old WT mice, but total cholesterol levels were highest in HFD treated groups (**Fig. 4.2a**). The relatively healthy HDL were highest following a HFD and exacerbated in Cyp2b-null mice. HDL significantly decreased as mice aged (**Fig. 4.2a**). Diets high in *cis* unsaturated fatty acids have also been found to increase HDL levels in humans in addition to serum cholesterol and LDL (Mensink, Zock, Kester, & Katan, 2003). Conversely, LDL, VLDL (**Fig. 4.2a**), and serum TAG (**Fig. 4.2b**) levels were higher in old Cyp2b-null mice compared to all other groups. Age clearly had an adverse impact on these parameters. Liver TAG increased with diet but decreased with age (**Fig. 4.2b**). Interestingly, ALT (**Fig. 4.2c**), a

marker of liver damage shows a spike with the combination of age and a Cyp2b-null genotype. Taken together, these results indicate a TAG-cholesterol profile, lower HDL, higher LDL and VLDL, that deteriorates with age and to a lesser degree, HFD. Often, this decline is greater in Cyp2b-null mice.

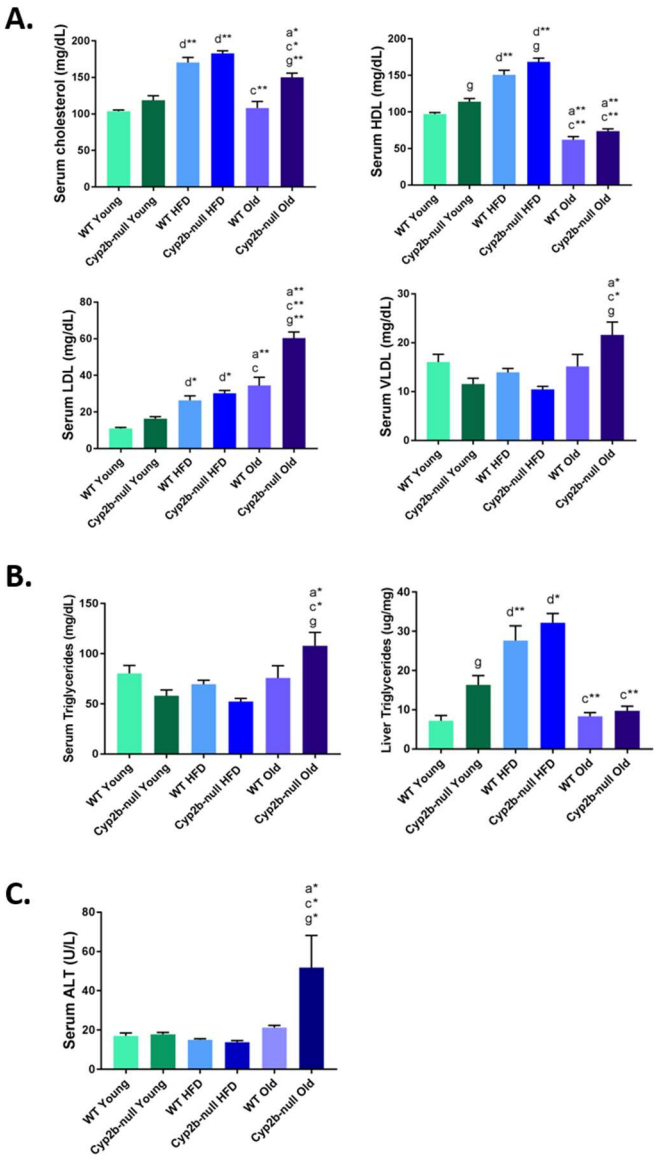

Figure 4.2. Perturbations in serum lipids, liver triglycerides, and alanine aminotransferase (ALT) with age, diet, and genotype. Serum cholesterol, HDL, LDL, and VLDL (A), serum and liver triglycerides (B), and serum ALT (C) were measured in all treatment groups using standard methods. Data are presented as mean + SEM. Statistical significance was determined by one-way ANOVA followed by Fisher's LSD as the post-hoc test (n = 5-6). 'a' indicates age difference comparing young (4.5 mo) and old (9 mo) mice within the same genotype and diet group, 'c' indicates difference between HFD-fed young (4.5 mo) and ND-fed old (9 mo) mice within same genotype, 'd' indicates diet difference between ND-fed and HFD-fed mice within in same genotype and age, 'g' indicates genotype difference between WT and Cyp2b-null mice within same diet and age group. No asterisk indicates a p-value < 0.05, * indicates a p-value < 0.01, and ** indicates a p-values < 0.0001.

4.3.2 Hepatic phospholipid data distribution and perturbations by age, diet and loss of Cyp2b:

Seventy-seven total hepatic phospholipid species were identified by LC-MS/MS from ARA, LA, ALA, and DHA. Hierarchical clustering was performed on all 77 lipid species identified to evaluate the effects of age, diet, and Cyp2b-null genotype on hepatic lipid species content (**Fig. 4.3;** data in **S4.2** with standard and abbreviated nomenclature). Age has a powerful effect on lipid profiles; more so than HFD or loss of Cyp2b based on the hierarchical cluster analyses (**Fig. 4.3**).

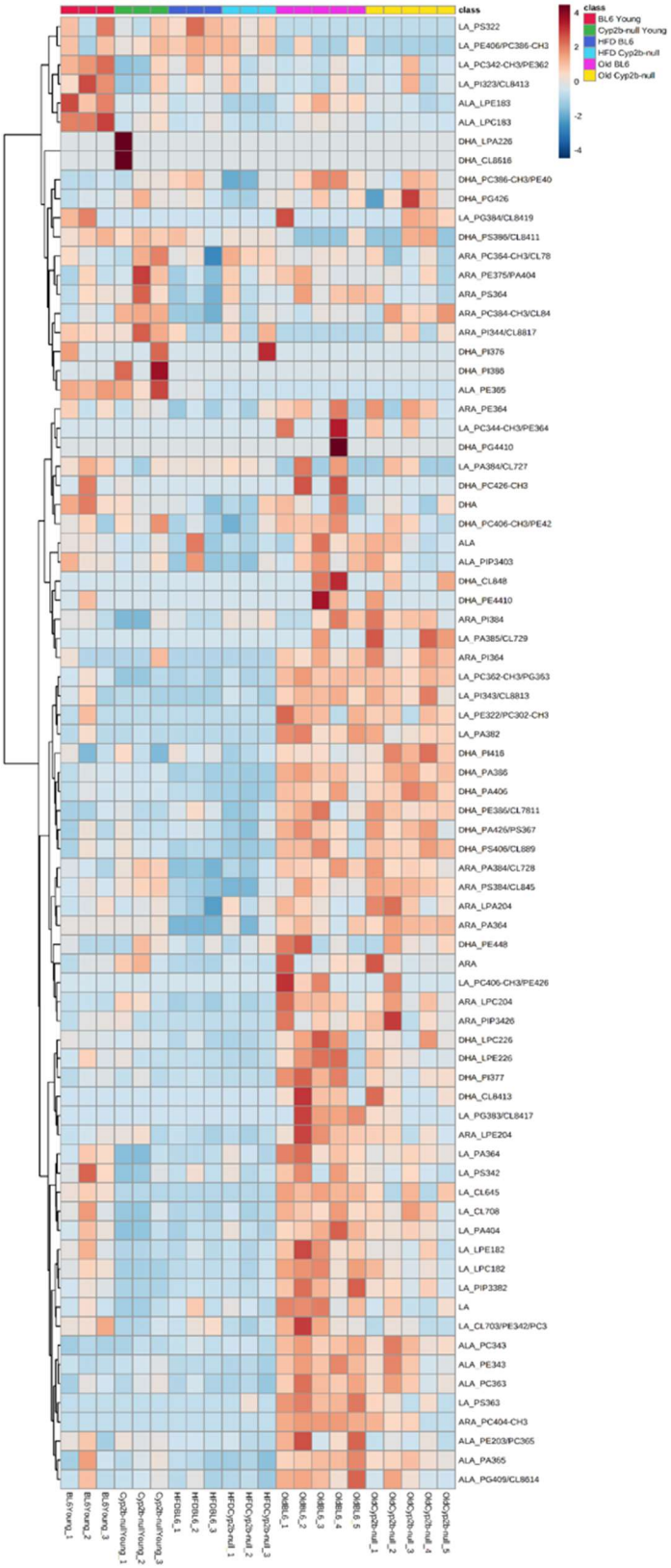
class
BL6 Young
Cyp2b-null Young
HFD BL6
HFD Cyp2b-null
Old BL6
Old Cyp2b-null
4
2
0
-2
-4
LA_PS322
LA_PE406/PC386-CH3
LA_PC342-CH3/PE362
LA_PI323/CL8413
ALA_LPE183
ALA_LPC183
DHA_LPA226
DHA_CL8616
DHA_PC386-CH3/PE40
DHA_PG426
LA_PG384/CL8419
DHA_PS386/CL8411
ARA_PC364-CH3/CL78
ARA_PE375/PA404
ARA_PS364
ARA_PC384-CH3/CL84
ARA_PI344/CL8817
DHA_PI376
DHA_PI386
ALA_PE365
ARA_PE364
LA_PC344-CH3/PE364
DHA_PG4410
LA_PA384/CL727
DHA_PC426-CH3
DHA
DHA_PC406-CH3/PE42
ALA
ALA_PIP3403
DHA_CL848
DHA_PE4410
ARA_PI384
LA_PA385/CL729
ARA_PI364
LA_PC362-CH3/PG363
LA_PI343/CL8813
LA_PE322/PC302-CH3
LA_PA382
DHA_PI418
DHA_PA386
DHA_PA406
DHA_PE386/CL7811
DHA_PA426/PS367
DHA_PS406/CL889
ARA_PA384/CL728
ARA_PS384/CL845
ARA_LPA204
ARA_PA364
DHA_PE448
ARA
LA_PC406-CH3/PE426
ARA_LPC204
ARA_PIP3426
DHA_LPC226
DHA_LPE226
DHA_PI377
DHA_CL8413
LA_PG383/CL8417
ARA_LPE204
LA_PA364
LA_PS342
LA_CL645
LA_CL708
LA_PA404
LA_LPE182
LA_LPC182
LA_PIP3382
LA
LA_CL703/PE342/PC3
ALA_PC343
ALA_PE343
ALA_PC363
LA_PS363
ARA_PC404-CH3
ALA_PE203/PC365
ALA_PA365
ALA_PG409/CL8614
BL6Young_1
BL6Young_2
BL6Young_3
Cyp2bnullYoung_1
Cyp2bnullYoung_2
Cyp2bnullYoung_3
HFDBL6_1
HFDBL6_2
HFDBL6_3
HFDCyp2bnull_1
HFDCyp2bnull_2
HFDCyp2bnull_3
OldBL6_1
OldBL6_2
OldBL6_3
OldBL6_4
OldBL6_5
OldCyp2bnull_1
OldCyp2bnull_2
OldCyp2bnull_3
OldCyp2bnull_4
OldCyp2bnull_5

Figure 4.3. Heat map of phospholipid profiles of all treatment groups. Hierarchical cluster analysis heatmap of all measured phospholipid species from ND-fed WT (BL6), ND-fed Cyp2b-null, HFD-fed WT, HFD-fed Cyp2b-null, old WT, and old Cyp2b-null mice. Seventy-seven lipid species were identified from liver samples of male mice by LC-MS/MS from arachidonic (ARA), linoleic (LA), α-linolenic (ALA) and docosahexaenoic acid (DHA).

4.3.3 Specific lipid species are associated with adverse physiological events:

To determine associations between physiological parameters, serum lipids, and hepatic phospholipid profiles in the different treatment groups (genotype, age, diet) PCA analysis was performed (**Fig. 4.4a**; data in **S4.3**) with the top 10 parameters involved in differences as determined by PCA shown in **Fig. 4.4b**. In general, treatment groups segregated primarily by age and diet; genotype caused lesser differences between groups with age combined with genotype having a greater effect than a HFD in combination with genotype. ND-fed young Cyp2b-null mice were pulled towards the HFD-fed mice in the PCA plot, which is consistent with the increased triglycerides in this group (**Fig. 4.2**). ND-fed young mice, especially WT, were associated with greater percentage of n-3 (ALA/DHA) fatty acid species than other groups. More importantly, no adverse physiological or serum parameters were associated with young ND-fed mice, concurring with previously data on the effects of ALA and DHA on healthy lipid homeostasis in humans (Amigó et al., 2020; Catapano et al., 2016) and mice (Pauter et al., 2014)(**Fig.**

4.4). HFD-fed young mice were associated with greater cholesterol, especially HDL, and along with older mice showed an association with WSI (**Fig. 4.4**). The lack of phospholipids in the HFD-fed mice is primarily caused by the dominance of phospholipids concentrations within the older mice (**S4.2, S4.3**). There was little to no separation between WT and Cyp2b-null mice following a HFD.

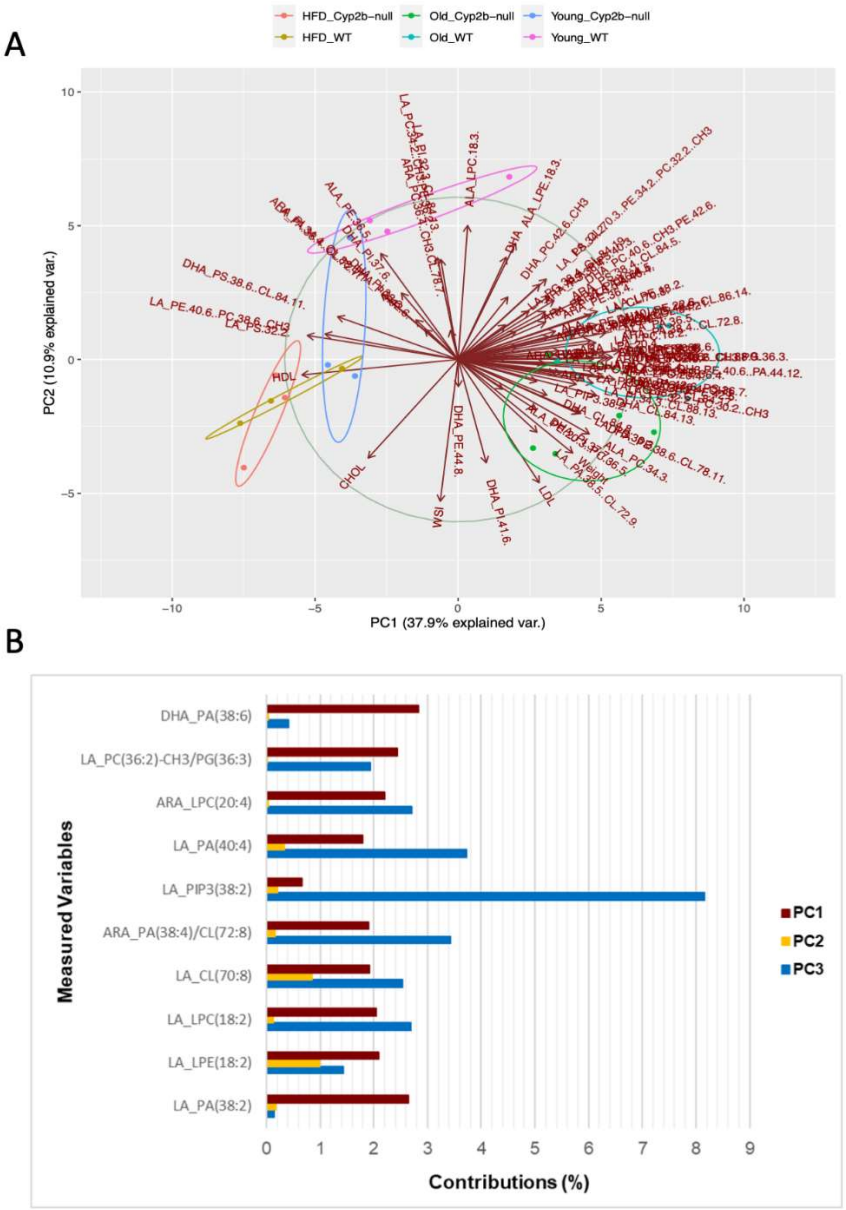

Figure 4.4. Relationship between treatment groups and measured variables. (A) Principal component analysis (PCA) biplot showing relationships between treatment groups and measured variables such as physiological parameters, serum lipids, and phospholipid species. Variables include serum lipids, WAT somatic index (WSI), body weight, and lipid species in order to associate specific biochemical parameters with different treatment groups (diet; age) and genotypes (WT; Cyp2b-null). (B) Top 10 contributing variables in the PCA plot based on loading strength expressed in percent contribution.

Old mice clearly had the unhealthiest profiles, strongest set of lipid species associations, and greatest difference between genotypes (**Fig. 4.4**). The effect of age also superseded the effect of HFD on the blood lipidome of female mice (Pati et al., 2018); therefore our work further demonstrates the adverse effect of age on hepatic lipid profiles. Age was heavily associated with more fatty acids, larger fatty acids, n-6 fatty acids, and higher serum VLDL and serum TAG concentrations. Increased hepatic PC biosynthesis, as seen in the older mice, has been proposed to stimulate the production and secretion of VLDL and TAG (Martínez-Uña et al., 2013). Greater dietary n-6:n-3 ratios have been found to increase HDL levels without suppressing atherogenesis in mice (L. Zhang et al., 2009). Somewhat more n-6 fatty acids showed greater association with older WT mice than Cyp2b-null mice. In addition, old Cyp2b-null mice were associated with weight and to a lesser extent WSI (**Fig. 4.4**). Overall, old WT and Cyp2b-null mice are

associated with unhealthy physiological, serum, and lipid profiles that contribute to an increased risk of metabolic disease and obesity (Donahue et al., 2011; Simopoulos, 2016).

4.3.4 Lipid species and outcomes associated with Cyp2b-null mice:

To better define the phospholipid species most predictive of differences between Cyp2b-null and WT mice, random forest was performed (**Fig. 4.5a**). Very few lipid species were shared among the top 6 most predictive species between the different groups (young, old, HFD) with the exception of ARA-PC(38:4) (18:0-20:4 PC(38:4)) found in ND and HFD-fed young mice. LA species were common in the top 6 of ND-fed young and old mice; ARA species were much more common in the top 6 of HFD-fed mice when comparing WT and Cyp2b-null mice. Unpaired Student's t-tests were also performed between genotypes and compared across groups (**S4.4**). One additional (DHA-38:6 PE/78:11 CL) species in HFD-fed mice and three additional species (DHA-based 41:6-PI, LA-based 40:4-PA, and ALA-based 40:9 PG/86:14 CL in older mice not detected by random forest were found to be statistically different between genotypes (**S4.4-S4.5**). Most of the species that were different between WT and Cyp2b-null mice were decreased in the Cyp2b-null mice, potentially because of the absence of Cyp2b metabolism.

A PCA biplot was used to associate different hepatic phospholipid species, serum parameters, and physiological outcomes with age, diet, and Cyp2b status in the mice (**Fig. 4.5b;** data **S4.6** also includes a top 10 PCA contribution graph) using only the altered lipid species determined by random forest and Student's t-test. This closer look at

genotypic differences confirmed that several n-3 fatty acids along with some ARA and LA phospholipid species are correlated with young ND-fed WT and Cyp2b-null mice; consistent with better health in these mice. ND-fed WT and Cyp2b-null mice show significantly different PCA profiles with no overlap potentially due to decreased metabolism; however, the ND-fed young groups are positioned next to each other within the plot. Interestingly, LA species make up 7 of the 10 most perturbed parameters as determined by PCA with ARA and WSI, a major contributor due to age and diet to age, making up the other contributors (**S4.6**).

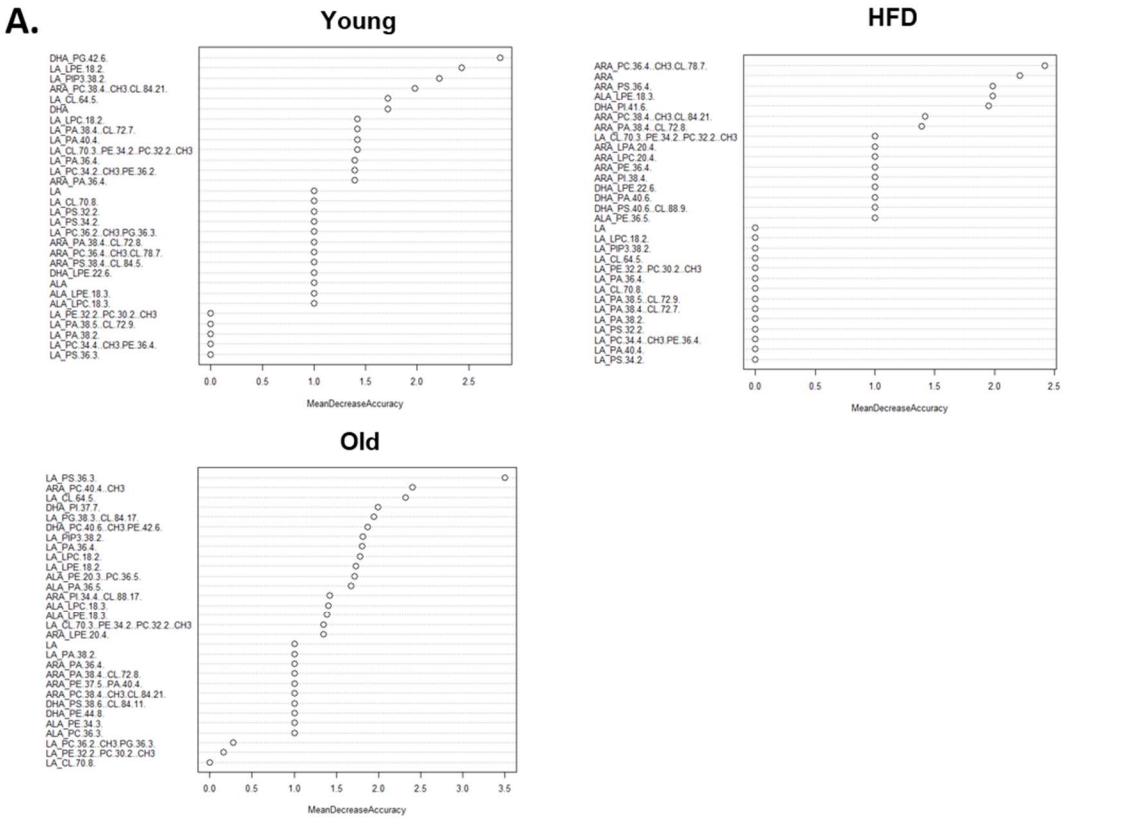
A.
Young
DHA_PG.42.6.
LA_LPE.18.2.
LA_PIP3.38.2.
ARA_PC.38.4._CH3.CL.84.21.
LA_CL.64.5.
DHA_
LA_LPC.18.2.
LA_PA.38.4._CL.72.7.
LA_PA.40.4.
LA_CL.70.3._PE.34.2._PC.32.2._CH3
LA_PA.36.4.
LA_PC.34.2._CH3.PE.36.2.
ARA_PA.36.4.
LA_
LA_CL.70.8.
LA_PS.32.2.
LA_PS.34.2.
LA_PC.36.2._CH3.PG.36.3.
ARA_PA.38.4._CL.72.8.
ARA_PC.36.4._CH3.CL.78.7.
ARA_PS.38.4._CL.84.5.
DHA_LPE.22.6.
ALA_
ALA_LPE.18.3.
ALA_LPC.18.3.
LA_PE.32.2._PC.30.2._CH3
LA_PA.38.5._CL.72.9.
LA_PA.38.2.
LA_PC.34.4._CH3.PE.36.4.
LA_PS.36.3.
0.0 0.5 1.0 1.5 2.0 2.5
MeanDecreaseAccuracy
HFD
ARA_PC.36.4._CH3.CL.78.7.
ARA_
ARA_PS.36.4.
ALA_LPE.18.3.
DHA_PI.41.6.
ARA_PC.38.4._CH3.CL.84.21.
ARA_PA.38.4._CL.72.8.
LA_CL.70.3._PE.34.2._PC.32.2._CH3
ARA_LPA.20.4.
ARA_LPC.20.4.
ARA_PE.36.4.
ARA_PI.38.4.
DHA_LPE.22.6.
DHA_PA.40.6.
DHA_PS.40.6._CL.88.9.
ALA_PE.36.5.
LA_
LA_LPC.18.2.
LA_PIP3.38.2.
LA_CL.64.5.
LA_PE.32.2._PC.30.2._CH3
LA_PA.36.4.
LA_CL.70.8.
LA_PA.38.5._CL.72.9.
LA_PA.38.4._CL.72.7.
LA_PA.38.2.
LA_PS.32.2.
LA_PC.34.4._CH3.PE.36.4.
LA_PA.40.4.
LA_PS.34.2.
0.0 0.5 1.0 1.5 2.0 2.5
MeanDecreaseAccuracy
Old
LA_PS.36.3.
ARA_PC.40.4._CH3
LA_CL.64.5.
DHA_PI.37.7.
LA_PG.38.3._CL.84.17.
DHA_PC.40.6._CH3.PE.42.6.
LA_PIP3.38.2.
LA_PA.36.4.
LA_LPC.18.2.
LA_LPE.18.2.
ALA_PE.20.3._PC.36.5.
ALA_PA.36.5.
ARA_PI.34.4._CL.88.17.
ALA_LPC.18.3.
ALA_LPE.18.3.
LA_CL.70.3._PE.34.2._PC.32.2._CH3
ARA_LPE.20.4.
LA_
LA_PA.38.2.
ARA_PA.36.4.
ARA_PA.38.4._CL.72.8.
ARA_PE.37.5._PA.40.4.
ARA_PC.38.4._CH3.CL.84.21.
DHA_PS.38.6._CL.84.11.
DHA_PE.44.8.
ALA_PE.34.3.
ALA_PC.36.3.
LA_PC.36.2._CH3.PG.36.3.
LA_PE.32.2._PC.30.2._CH3
LA_CL.70.8.
0.0 0.5 1.0 1.5 2.0 2.5 3.0 3.5
MeanDecreaseAccuracy
B.
PC2 (12.2% explained var.)
PC1 (38.4% explained var.)
4
0
−4
−8
−5
0
5
10
WBI
DHA_PI.41.6.
LDL
CHOL
ARA_PI.38.4.
LA_PIP3.38.2
Weight
DHA_PE.44.8.
DHA_PI.37.7
LA_PS.36.3.
LA_PE.38.6._CL.78.11.
ALA_PE.20.3._PC.36.5.
HDL
LA_PS.32.2.
LA_PA.38.2.
LA_PE.34.3.
ALA_
LA_PC.36.3.
LA_PS.40.6._CL.88.9.
LA_PA.38.4._CL.72.7.
DHA_PS.38.6._CL.84.11.
DHA_PG.42.6.
LA_PC.34.2._CH3.PE.36.2.
LA_PA.38.4._CL.72.8.
DHA_
ALA_LPE.18.3.
ARA_PI.34.4._CL.88.17.
ALA_PE.36.5.
LA_PC.34.2._CH3.PE.36.2.
ARA_PC.36.4._CH3.CL.78.7.
ALA_LPC.18.3.
Young_Cyp2b−null
Young_WT
HFD_Cyp2b−null
HFD_WT
Old_Cyp2b−null
Old_WT

Figure 4.5. Lipid species and measured variables associated with differences between Cyp2b-null and WT mice. (A) Random forest analysis of key lipids predictive of differences between Cyp2b-null and WT mice. (B) Principal component analysis (PCA) biplot showing relationships between treatment groups and measured variables such as physiological parameters, serum lipids, and phospholipid species. Variables include serum lipids, WAT somatic index (WSI), body weight, and lipid species in order to associate specific biochemical parameters with different treatment groups (diet; age) and genotypes (WT; Cyp2b-null). Only important or significantly perturbed lipid species between genotypes as determined by Student's t-test ($p < 0.05$) or random forest (MDA > 0) were included in this plot.

HFD-fed mice show greater separation from ND-fed mice in this plot in comparison to **Fig. 4.4**, primarily due to the positioning of ND-fed Cyp2b-null mice. Following a HFD, there were few differences between genotypes with Cyp2b-null mice showing higher association with HDL (**Fig. 4.2**). An increase in fatty acid chain length was observed in HFD-fed Cyp3a-null male mice, but this was not observed in Cyp2b-null mice (R. Kumar, Litoff, Boswell, & Baldwin, 2018). Older mice continued to show differences between genotypes with a higher association with weight, WSI, and LDL in Cyp2b-null mice, and a greater cluster of phospholipids in the old WT mice (**Fig. 4.5b**). This is consistent with lower metabolism of some PUFA species in Cyp2b-null mice

(**Fig. 4.2, 4.4 & 4.5**), which was also observed in hepatic P450 reductase- and Cyp3a-nullizygous mice (Finn, Henderson, Scott, & Wolf, 2009; R. Kumar et al., 2018).

In summary, the data indicates that age > HFD > Cyp2b-null genotype compromises the hepatic phospholipid profile the most. ND-fed old Cyp2b-null and HFD-fed young mice show significant changes in several phospholipids and physiological parameters such as serum cholesterol and WAT compared to ND-fed young mice, which have significantly lower lipids and greater n-3 fatty acids. Interestingly, the lipid profile of ND-fed Cyp2b-null mice clustered between ND-fed WT mice and HFD-fed groups, consistent with their liver triglyceride concentrations. Age was found to increase total and LDL-cholesterol in both humans and rodents (Ericsson, Berglund, FrostegÅrd, Einarsson, & Angelin, 1997; Parini, Angelin, & Rudling, 1999). Total body and liver weight, serum LDL, VLDL, TAG, and ALT levels are all significantly higher in old Cyp2b-null mice compared to their WT counterparts as well as several featured groups. The combination of age and lack of Cyp2b is more harmful than age alone, as it resulted in dyslipidemia and liver injury. Overall, aging and a HFD are associated with weight gain, WAT, LDL, VLDL, and a relative increase in n-6 species compared to n-3 species. This profile is further exacerbated in old Cyp2b-null mice, suggesting accelerated aging or metabolic disease symptoms with the lack of Cyp2b in male mice.

Acknowledgements:

This study was primarily supported by NIH grant R15ES017321 with assistance from the Emory Integrated Lipidomics Core (EILC), which is subsidized by the Emory University School of Medicine and is one of the Emory Integrated Core Facilities. Additional support was provided by the Georgia Clinical & Translational Science Alliance of the National Institutes of Health under Award Number UL1TR002378.

References

Amigó, N., Akinkuolie, A. O., Chiuve, S. E., Correig, X., Cook, N. R., & Mora, S. (2020). Habitual Fish Consumption, n‐3 Fatty Acids, and Nuclear Magnetic Resonance Lipoprotein Subfractions in Women. *Journal of the American Heart Association, 9*(5), e014963. doi:doi:10.1161/JAHA.119.014963

Bligh, E. G., & Dyer, W. J. (1959). A rapid method of total lipid extraction and purification. *Can J Biochem Physiol, 37*(8), 911-917. doi:10.1139/o59-099

Breiman, L. (2001). Random Forests. *Machine Learning, 45*(1), 5-32. doi:10.1023/A:1010933404324

Catapano, A. L., Graham, I., De Backer, G., Wiklund, O., Chapman, M. J., Drexel, H., . . . Cooney, M. T. (2016). 2016 ESC/EAS Guidelines for the Management of Dyslipidaemias. *Eur Heart J, 37*(39), 2999-3058. doi:10.1093/eurheartj/ehw272

Chiappini, F., Desterke, C., Bertrand-Michel, J., Guettier, C., & Le Naour, F. (2016). Hepatic and serum lipid signatures specific to nonalcoholic steatohepatitis in murine models. *Scientific Reports, 6*, 31587. doi:10.1038/srep31587 https://www.nature.com/articles/srep31587#supplementary-information

Damiri, B., & Baldwin, W. S. (2018). Cyp2b-Knockdown Mice Poorly Metabolize Corn Oil and Are Age-Dependent Obese. *Lipids, 53*(9), 871-884. doi:10.1002/lipd.12095

Donahue, S. M., Rifas-Shiman, S. L., Gold, D. R., Jouni, Z. E., Gillman, M. W., & Oken, E. (2011). Prenatal fatty acid status and child adiposity at age 3 y: results from a US pregnancy cohort. *Am J Clin Nutr, 93*(4), 780-788. doi:10.3945/ajcn.110.005801

Ericsson, S., Berglund, L., FrostegÅrd, J., Einarsson, K., & Angelin, B. (1997). The influence of age on low density lipoprotein metabolism: effects of cholestyramine treatment in young and old healthy male subjects. *Journal of Internal Medicine, 242*(4), 329-337. doi:10.1046/j.1365-2796.1997.00238.x

Feige, J. N., Gelman, L., Michalik, L., Desvergne, B., & Wahli, W. (2006). From molecular action to physiological outputs: Peroxisome proliferator-activated receptors are nuclear receptors at the crossroads of key cellular functions. *Progress in Lipid Research, 45*(2), 120-159. doi:https://doi.org/10.1016/j.plipres.2005.12.002

Finn, R. D., Henderson, C. J., Scott, C. L., & Wolf, C. R. (2009). Unsaturated fatty acid regulation of cytochrome P450 expression via a CAR-dependent pathway. *Biochem J, 417*, 43-54.

Glass, Christopher K., & Olefsky, Jerrold M. (2012). Inflammation and Lipid Signaling in the Etiology of Insulin Resistance. *Cell Metabolism, 15*(5), 635-645. doi:https://doi.org/10.1016/j.cmet.2012.04.001

Hales, C. M., Carroll, M. D., Fryar, C. D., & Ogden, C. L. (2017). Prevalence of Obesity Among Adults and Youth: United States, 2015-2016. *NCHS Data Brief*(288), 1-8.

Hankinson, O. (2016). The role of AHR-inducible cytochrome P450s in metabolism of polyunsaturated fatty acids. *Drug metabolism reviews, 48*(3), 342-350. doi:10.1080/03602532.2016.1197240

Heintz, M. M., Kumar, R., Rutledge, M. M., & Baldwin, W. S. (2019). Cyp2b-null male mice are susceptible to diet-induced obesity and perturbations in lipid homeostasis. *The Journal of Nutritional Biochemistry, 70*, 125-137. doi:https://doi.org/10.1016/j.jnutbio.2019.05.004

Hong, J., Stubbins, R. E., Smith, R. R., Harvey, A. E., & Nunez, N. P. (2009). Differential susceptibility to obesity between male, female and ovariectomized female mice. *Nutr J, 8*, 11. doi:10.1186/1475-2891-8-11

Kumar, R., Litoff, E. J., Boswell, W. T., & Baldwin, W. S. (2018). High fat diet induced obesity is mitigated in Cyp3a-null female mice. *Chem Biol Interact, 289*, 129-140. doi:10.1016/j.cbi.2018.05.001

Kumar, R., Mota, L. C., Litoff, E. J., Rooney, J. P., Boswell, W. T., Courter, E., . . . Baldwin, W. S. (2017). Compensatory changes in CYP expression in three different toxicology mouse models: CAR-null, Cyp3a-null, and Cyp2b9/10/13-null mice. *PLOS ONE, 12*(3), e0174355. doi:10.1371/journal.pone.0174355

Martínez-Uña, M., Varela-Rey, M., Cano, A., Fernández-Ares, L., Beraza, N., Aurrekoetxea, I., . . . Mato, J. M. (2013). Excess S-adenosylmethionine reroutes phosphatidylethanolamine towards phosphatidylcholine and triglyceride synthesis. *Hepatology, 58*(4), 1296-1305. doi:10.1002/hep.26399

Mensink, R. P., Zock, P. L., Kester, A. D., & Katan, M. B. (2003). Effects of dietary fatty acids and carbohydrates on the ratio of serum total to HDL cholesterol and on serum lipids and apolipoproteins: a meta-analysis of 60 controlled trials. *Am J Clin Nutr, 77*(5), 1146-1155. doi:10.1093/ajcn/77.5.1146

Modi, H. R., Katyare, S. S., & Patel, M. A. (2008). Ageing-induced alterations in lipid/phospholipid profiles of rat brain and liver mitochondria: implications for mitochondrial energy-linked functions. *J Membr Biol, 221*(1), 51-60. doi:10.1007/s00232-007-9086-0

Murphy, S. A., & Nicolaou, A. (2013). Lipidomics applications in health, disease and nutrition research. *Molecular Nutrition & Food Research, 57*(8), 1336-1346. doi:doi:10.1002/mnfr.201200863

Orešič, M., Hänninen, V. A., & Vidal-Puig, A. (2008). Lipidomics: a new window to biomedical frontiers. *Trends in Biotechnology, 26*(12), 647-652. doi:https://doi.org/10.1016/j.tibtech.2008.09.001

Parini, P., Angelin, B., & Rudling, M. (1999). Cholesterol and Lipoprotein Metabolism in Aging. *Arteriosclerosis, Thrombosis, and Vascular Biology, 19*(4), 832-839. doi:doi:10.1161/01.ATV.19.4.832

Pati, S., Krishna, S., Lee, J. H., Ross, M. K., de La Serre, C. B., Harn, D. A., . . . Cummings, B. S. (2018). Effects of high-fat diet and age on the blood lipidome and circulating endocannabinoids of female C57BL/6 mice. *Biochimica et Biophysica Acta (BBA) - Molecular and Cell Biology of Lipids, 1863*(1), 26-39. doi:https://doi.org/10.1016/j.bbalip.2017.09.011

Pauter, A. M., Olsson, P., Asadi, A., Herslöf, B., Csikasz, R. I., Zadravec, D., & Jacobsson, A. (2014). Elovl2 ablation demonstrates that systemic DHA is endogenously produced and is essential for lipid homeostasis in mice. *J Lipid Res, 55*(4), 718-728. doi:10.1194/jlr.M046151

Pollard, A. K., Ortori, C. A., Stöger, R., Barrett, D. A., & Chakrabarti, L. (2017). Mouse mitochondrial lipid composition is defined by age in brain and muscle. *Aging, 9*(3), 986-998. doi:10.18632/aging.101204

Quach, N. D., Arnold, R. D., & Cummings, B. S. (2014). Secretory phospholipase A2 enzymes as pharmacological targets for treatment of disease. *Biochemical Pharmacology, 90*(4), 338-348. doi:https://doi.org/10.1016/j.bcp.2014.05.022

Saito, K., Uebanso, T., Maekawa, K., Ishikawa, M., Taguchi, R., Nammo, T., . . . Saito, Y. (2015). Characterization of hepatic lipid profiles in a mouse model with nonalcoholic steatohepatitis and subsequent fibrosis. *Scientific Reports, 5*(1), 12466. doi:10.1038/srep12466

Simopoulos, A. P. (2016). An Increase in the Omega-6/Omega-3 Fatty Acid Ratio Increases the Risk for Obesity. *Nutrients, 8*(3), 128.

Wade, G. N., Gray, J. M., & Bartness, T. J. (1985). Gonadal influences on adiposity. *Int J Obes, 9 Suppl 1*, 83-92.

Wang, W., Yang, J., Qi, W., Yang, H., Wang, C., Tan, B., . . . Zhang, G. (2017). Lipidomic profiling of high-fat diet-induced obesity in mice: Importance of cytochrome P450-derived fatty acid epoxides. *Obesity, 25*(1), 132-140. doi:doi:10.1002/oby.21692

Xia, J., & Wishart, D. S. (2002). Using MetaboAnalyst 3.0 for Comprehensive Metabolomics Data Analysis. In *Current Protocols in Bioinformatics*: John Wiley & Sons, Inc.

Yoshikawa, T., Ide, T., Shimano, H., Yahagi, N., Amemiya-Kudo, M., Matsuzaka, T., . . . Yamada, N. (2003). Cross-talk between peroxisome proliferator-activated receptor (PPAR) alpha and liver X receptor (LXR) in nutritional regulation of fatty acid metabolism. I. PPARs suppress sterol regulatory element binding protein-1c promoter through inhibition of LXR signaling. *Mol Endocrinol, 17*(7), 1240-1254. doi:10.1210/me.2002-0190

Yuan, X., Ta, T. C., Lin, M., Evans, J. R., Dong, Y., Bolotin, E., . . . Sladek, F. M. (2009). Identification of an Endogenous Ligand Bound to a Native Orphan Nuclear Receptor. *PLOS ONE, 4*(5), e5609. doi:10.1371/journal.pone.0005609

Zeldin, D. C. (2001). Epoxygenase Pathways of Arachidonic Acid Metabolism. *Journal of Biological Chemistry, 276*(39), 36059-36062. doi:10.1074/jbc.R100030200

Zhang, G., Kodani, S., & Hammock, B. D. (2014). Stabilized epoxygenated fatty acids regulate inflammation, pain, angiogenesis and cancer. *Prog Lipid Res, 53*, 108-123. doi:10.1016/j.plipres.2013.11.003

Zhang, L., Geng, Y., Xiao, N., Yin, M., Mao, L., Ren, G., . . . Pan, J. (2009). High Dietary n-6/n-3 PUFA Ratio Promotes HDL Cholesterol Level, but does not Suppress Atherogenesis in Apolipoprotein E-Null Mice 1. *Journal of Atherosclerosis and Thrombosis, advpub*, 0909020086-0909020086. doi:10.5551/jat.No1347

Supplementary Material:

S4.1. Detailed methods of detection of phospholipids by LC-MS/MS.

S4.2. Lipidomic data from all treatment groups. Seventy-seven lipid species were identified from liver samples of male mice by LC-MS/MS from arachidonic (ARA), linoleic (LA), α-linolenic (ALA) and docosahexaenoic acid (DHA). Treatment groups are ND-fed young (4.5 mo), ND-fed old (9 mo), and young mice fed a HFD for 10 weeks. All data is in relative percent.

S4.3. Data used to make Figure 4 principal component analysis (PCA) biplot.

S4.4. Phospholipids identified as important by both t-tests and random forest between WT and Cyp2b-null mice. (A) Lipids that are statistically different by Student's t-tests between Cyp2b-null and WT mice in the different age and diet groups. (B) Important or significantly perturbed phospholipid species in Cyp2b-null mice compared to WT mice identified by both random forest analysis and Student's t-tests in young (4.5 mo) ND-fed, young (4.5 mo) HFD-fed, and old (9 mo) mice.

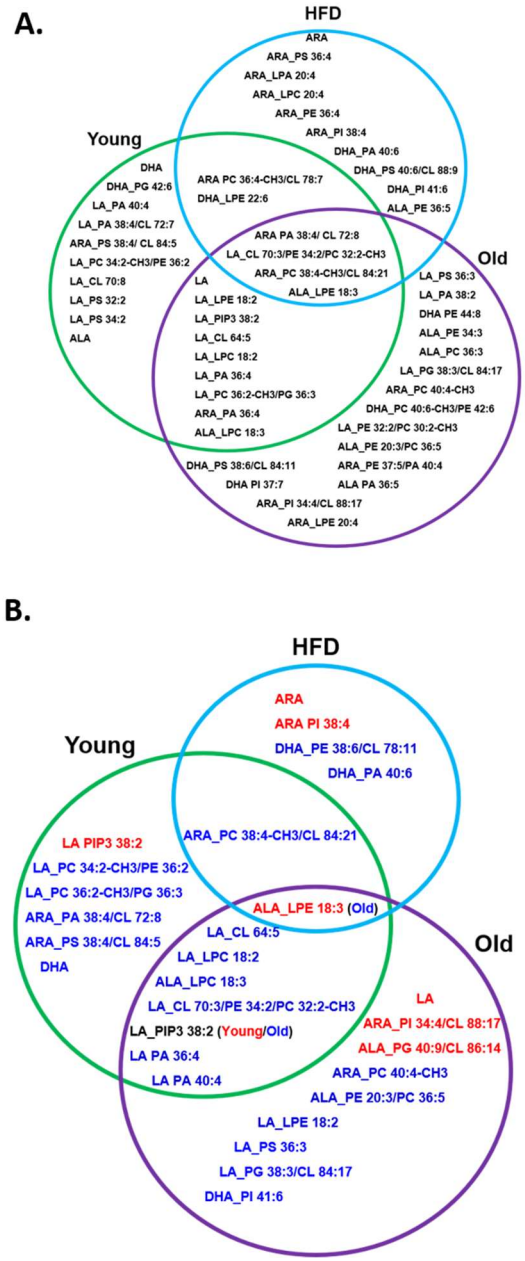

S4.5. Important perturbed hepatic phospholipid species in Cyp2b-null mice within each group. (A) Venn diagram of important lipid species between Cyp2b-null and WT mice of each featured group based on random forest analysis (MDA > 0). (B) Venn diagram of significantly increased (red) or decreased (blue) lipid species in Cyp2b-null mice of each featured group as determined by Student's t-tests ($p < 0.05$).

S4.6. Data used to make principal component analysis (PCA) biplot for Figure 4.5b. PCA contribution graph below containing the top 10 contributing variables of the PCA plot based on loading strength expressed in percent contribution. The factoextra R package (https://cran.r-project.org) was used to obtain the percent contributions of each measured variable in principle components 1-3.

CHAPTER FIVE

HUMAN CYP2B6 IS AN ANTI-OBESITY ENZYME THAT METABOLIZES POLYUNSATURATED FATTY ACIDS TO IMPORTANT OXYLIPIN METABOLITES IN THE 9- AND 13- POSITIONS

Melissa M. Heintz, Emily M. Olack, and William S. Baldwin

5.0 Abstract

Multiple factors in addition to over consumption lead to obesity and non-alcoholic fatty liver disease (NAFLD) in the United States and worldwide. CYP2B metabolizes numerous xeno- and endobiotic compounds, and male Cyp2b-null mice are diet-induced obese with increased white adipose tissue and steatosis. However, it has yet to be determined whether human CYP2B6 is anti-obesogenic and a putative mechanism. CYP2B6 containing baculosomes were used to determine endogenous inhibitors of CYP2B6. Several polyunsaturated fatty acids (PUFAs) including arachidonic acid, linoleic acid, DHA, and α-linolenic acid (ALA) were inhibitors with IC50's below 10μM. LC-MS/MS revealed that CYP2B6 metabolizes PUFAs, with a greater than 20-fold preference for metabolism of ALA to 9-HOTrE and to a lesser extent 13-HOTrE. To further study the role of CYP2B6 *in vivo*, humanized-CYP2B6-transgenic (hCYP2B6-Tg) and Cyp2b-null mice were fed a 60% high-fat diet for 16 weeks. Compared to Cyp2b-null mice, hCYP2B6-Tg mice reduced weight gain and metabolic disease as measured by glucose tolerance tests, however hCYP2B6-Tg male mice increased liver triglycerides. Serum and liver oxylipin metabolite concentrations generally increased in male hCYP2B6-Tg mice, while only serum oxylipins increased in female hCYP2B6-Tg mice. RNA-seq data also demonstrated sexually dimorphic changes in gene expression, as *Cyp2b10*/CYP2B6 was induced in male, but not female, hCYP2B6-Tg mice. Overall, our data indicates that CYP2B6 is an anti-obesity enzyme, but to a lesser extent than murine Cyp2b. Therefore, the inhibition of CYP2B6 by xenobiotics or dietary fats can

exacerbate obesity and metabolic disease through disrupted metabolism of key lipid metabolites.

Keywords: α-linolenic acid (ALA), diet-induced obesity, oxylipin, Cyp2b-null, CYP2B6, non-alcoholic fatty liver disease (NAFLD)

Highlights

- Human CYP2B6 partially reverses diet-induced obesity observed in Cyp2b-null mice
- Unlike WT mice, effects are strongest in hCYP2B6-Tg female mice
- CYP2B6 increases steatosis, which was not expected, but also reduces metabolic disease
- CYP2B6 primarily metabolizes α-linolenic acid to 9-HOTrE and 13-HOTrE *in vitro*
- However, *in vivo* CYP2B6 metabolizes several PUFAs in the 9- and 13- positions

5.1 Introduction

Obesity, in addition to insulin resistance and dyslipidemia, are the most important risk factors for development of nonalcoholic fatty liver disease (NAFLD) (Masuoka & Chalasani, 2013). The prevalence of obesity is increasing in the United States, and the most recent 2017-2018 National Health and Nutrition Examination Survey recorded 42.4% of adults are obese (Hales, Carroll, Fryar, & Ogden, 2020). The constitutive androstane receptor (CAR) has been identified as an anti-obesity transcription factor, as

its activation in leptin-deficient mice induced cytochrome P450 2b10 (Cyp2b10) and subsequently improved hepatic glucose and fatty acid metabolism (Dong et al., 2009). Additionally, a loss of hepatic CYP activity in hepatic P450 oxidoreductase (POR)-null mice led to steatosis and the induction of Cyp2b primarily through CAR activation (Finn, Henderson, Scott, & Wolf, 2009), indicating a role for CAR in recognizing and Cyp2b in metabolizing hepatic lipids. Furthermore, forkhead box protein A2 (Foxa2) regulates lipid metabolism and ketogenesis genes in mice including *Cyp2b9* (Hashita et al., 2008; Wolfrum, Asilmaz, Luca, Friedman, & Stoffel, 2004), and three recent studies found *Cyp2b9* exhibited the highest increase in gene expression following a HFD in mice (Heintz, Kumar, Rutledge, & Baldwin, 2019; Hoek-van den Hil et al., 2015; Leung, Trac, Du, Natarajan, & Schones, 2016). Our previously generated Cyp2b9/10/13-null (Cyp2b-null) mice are diet-induced obese (DIO) with increased NAFLD in males (Heintz et al., 2019). Similarly, age-dependent lipid accumulation was observed in RNAi-mediated Cyp2b-knockdown male mice (Damiri & Baldwin, 2018). These findings implicate Cyp2b's role in hepatic fatty acid metabolism and obesity.

In the liver, CAR followed by pregnane X receptor (PXR) are the primary regulators of human and murine *Cyp2b* genes (Hernandez, Mota, & Baldwin, 2009; P. Wei, Zhang, Egan-Hafley, Liang, & Moore, 2000). *CYP2B6* is the only hepatic CYP2B isoform in humans; *Cyp2b9*, *Cyp2b10*, and *Cyp2b13* are the dominant hepatic Cyp2b genes in mice. CYP2B members are also regulated by the glucocorticoid receptor (GR) and transcription factors FOXA2, hepatocyte nuclear factor 4α (HNF4α), and CCAAT/enhancer-binding protein α (C/EBPα) in humans (Benet, Lahoz, Guzmán,

Castell, & Jover, 2010; Dvorak et al., 2003; Hongbing & Masahiko, 2003; L. Li, Li, Heyward, & Wang, 2016) and rodents (Audet-Walsh & Anderson, 2009; Hashita et al., 2008; Wiwi, Gupte, & Waxman, 2004). Growth hormone-mediated regulation of these transcription factors results in the female predominant expression of murine Cyp2b (Hernandez, Mota, Huang, Moore, & Baldwin, 2009; Renaud, Cui, Khan, & Klaassen, 2011; Wiwi et al., 2004). Although there is large interindividual variation in human hepatic CYP2B6 expression, it is also primarily female expressed, but to a much lesser degree compared to rodents (Lamba et al., 2003). It is hypothesized that changes in the expression of transcription factors such as FOXA2 by fluctuations of steroids and hormones may contribute to the large interindividual variations of CYP2B6 expression in human populations (L. Li et al., 2016).

Human CYP2B6 has broad substrate specificity, playing a role in the metabolism of numerous xeno- and endobiotic compounds (Zanger & Klein, 2013). The substrate selectivity of CYP2B6 includes over 60 clinical drugs such as artemisinin, propofol, ketamine, ifosfamide, nevirapine, efavirenz, mephobarbital, bupropion, and tamoxifen (Mo et al., 2009), as well as many important environmental toxicants including chlorpyrifos (Tang et al., 2001), carbaryl (Hodgson & Rose, 2007), parathion (Foxenberg, McGarrigle, Knaak, Kostyniak, & Olson, 2007), triclosan (Wu et al., 2017), perfluorocarboxylic acids (Abe et al., 2017), and the insect repellant *N,N*-diethyl-*m*-toluamide (DEET) (Hodgson & Rose, 2007). Endogenous compounds such as steroids, bile acids, and fatty acids are also metabolized by CYP2B6 (Mo et al., 2009; Nebert & Russell, 2002).

Polyunsaturated fatty acids (PUFAs) may regulate Cyp2b transcription and act as Cyp2b substrates. For example, the omega-6 fatty acid, linoleic acid (LA), activates CAR and induces Cyp2b10 (Finn et al., 2009). The omega-3 fatty acid, docosahexaenoic acid (DHA) inhibits CAR translocation and subsequently inhibits Cyp2b transcription (C.-C. Li, Lii, Liu, Yang, & Chen, 2007). Arachidonic acid is metabolized by Cyp2b19 (mouse) and Cyp2b12 (rat) in keratinocytes, as well as Cyp2b1/2 in rat hepatic microsomes to anti-inflammatory epoxyeicosatrienoic acids (EETs) (Capdevila et al., 1990; Du et al., 2005; Keeney, Skinner, Wei, Friedberg, & Waterman, 1998). Human CYP2B6 also appears to play a role in the epoxidation of anandamide, an arachidonic acid-derived endogenous cannabinoid to bioactive hydroxyeicosatetraenoic acid (HETE) and EET metabolites (Sridar, Snider, & Hollenberg, 2011), such as 5,6-EET-ethanolamide, a potent agonist of the peripheral cannabinoid receptor, CB2 (Snider, Nast, Tesmer, & Hollenberg, 2009). However, the role of human CYP2B6 in the metabolism of most PUFAs is not well-characterized or completely untested.

Murine Cyp2b enzymes are anti-obesogenic in males. Cyp2b-null mice are diet-induced obese with an increase in NAFLD, white adipose tissue, serum cholesterol, leptin, and β-hydroxybutyrate. Furthermore, Cyp2b-null males fed a normal diet show increased liver triglycerides and a gene expression profile similar to WT mice fed a HFD, indicating progression to NAFLD even without a high-fat diet (Heintz et al., 2019). In contrast, female weight gain was not significantly different, nor was NAFLD; however, the lack of Cyp2b in female mice was moderately protective from methionine and choline-deficient diet-induced non-alcoholic steatosis (NASH) (Heintz, McRee, Kumar,

& Baldwin, 2020). However, the role of CYP2B6 as an anti-obesity gene has not been assessed. The purpose of this research is to determine the role of CYP2B6 in PUFA metabolism and test whether CYP2B6 is an anti-obesity enzyme by comparing diet-induced obesity (DIO) between Cyp2b-null mice and our newly produced humanized CYP2B6 mice to determine if CYP2B6 can reverse obesity and NAFLD in Cyp2b-null mice. PUFA metabolites of CYP2B6 were identified in vitro from CYP2B6 containing baculosomes by LC-MS/MS and in vivo from serum and liver following high-fat diet treatment. Physiological (body, tissue weights, glucose tolerance), biochemical (cholesterol, serum and liver lipids, PUFA metabolites), and transcriptomic (RNAseq) changes were measured. Results indicate human CYP2B6 primarily metabolizes PUFAs in the 9- and 13- positions and partially reverses diet-induced obesity observed in Cyp2b-null mice, but with unexpected sexually dimorphic effects.

5.2 Materials and Methods

5.2.1 CYP2B6 inhibition:

The Vivid CYP2B6 Blue Screening kit with CYP2B6-containing baculosomes was obtained from ThermoFisher (Waltham, MA, USA) and used to screen for potent PUFA inhibitors of CYP2B6. Decreased fluorescence due to chemical inhibition was quantified on a Gen5 microplate reader (Synergy H1 Hybrid Reader, BioTek, Winooski, Vermont, USA) at 415/460 nm excitation/emission at 30-second intervals for 30 minutes in kinetic assay mode in accordance with manufacturer's protocol. IC50 values were

determined as described previously using GraphPad Prism 7.0 (Graphpad Software, San Diego, CA, USA) (Baldwin & Roling, 2009; Schmidt, Sengupta, Saski, Noorai, & Baldwin, 2017). Briefly, chemical concentrations were log10 transformed, sigmoidal concentration-response curves were fit with a variable slope model with least squares ordinary fit. Confidence intervals were produced assuming asymmetrical distribution as recommended by GraphPad.

5.2.2 CYP2B6 fatty acid substrates:

CYP2B6 containing and control baculosomes™ (Thermo Fisher) were incubated with 25 µM arachidonic acid (AA), linoleic acid (LA), α-linolenic acid (ALA), or docosahexaenoic acid (DHA) (n = 3) for two hours in VIVID™ P450 reaction buffer and the NADPH-regeneration system (Thermo Fisher). Following incubation, samples were stored at -80°C and shipped on dry ice to the Emory Integrated Lipidomics Core (EILC). Oxidized lipids were selectively extracted from the samples by solid phase extraction because of their low concentrations in comparison to other high abundance lipid species. This was done by depositing homogenized samples into a C18 solid phase extraction cassette, rinsing with hexane to remove nonpolar lipid species, and eluting with methyl formate. The recovered lipids were analyzed via LC-MS/MS in a multiple reaction monitoring (MRM) based method that selectively targets oxylipins using an AB SCIEX QTrap5500 enhanced high performance hybrid triple quadrupole/linear ion trap LC/MS/MS with a mass range of m/z 5 to 1250 in triple quadrupole mode and 5-1000 in LIT mode. The LC/MS/MS is paired with an ExionLC AC HPLC/UHPLC system with

an ExionLC column oven and autosampler along with a computer workstation running LipidView software (AB SCIEX) (Naudin et al., 2020; Tillman et al., 2020). The concentration of the intracellular oxylipins were calibrated against external standards.

5.2.3 High-fat diet treatment of Cyp2b-null mice and hCYP2B6-Tg:

CYP2A13/CYP2B6/CYP2F1-transgenic mice from Dr. Qing Yu and Dr. Xinxin Ding's laboratory's containing a bacterial artificial chromosome (BAC) of 210 kb from human chr19 containing *CYP2A13, CYP2B6, and CYP2F1* genes (Y. Wei et al., 2012) were bred to Cyp2b9/10/13-null (Cyp2b-null) mice from our laboratory that lack the primarily hepatic murine Cyp2b members, *Cyp2b9, Cyp2b10*, and *Cyp2b13* (Ramiya Kumar et al., 2017) to produce humanized CYP2B6-transgenic (hCYP2B6-Tg) mice lacking the hepatic murine Cyp2b members. These mice also express CYP2A13, which is primarily expressed in the nasal mucosa and lung and CYP2F1, which is primarily expressed in the lung (Y. Wei et al., 2012). Cyp2b-null and hCYP2B6-Tg female and male mice (10 weeks old; n=8 per gender) were fed a high-fat diet (HFD; Envigo TD.06414, 5.1 Kcal/g: 60.3% fat (37% saturated, 47% monounsaturated, 16% polyunsaturated fat), 18.4% protein, 21.3% carbohydrates; Madison, WI USA) for 16 weeks. Weight gain was monitored weekly and feed consumption was measured every other day. Glucose tolerance tests (GTT) were performed during week 13. At the end of the study, mice were anesthetized and blood collected by heart puncture prior to euthanasia. Liver, kidney, inguinal white adipose tissue (WAT), brown adipose tissue

(BAT), and testes were excised and weighed. All tissues were immediately snap frozen with liquid nitrogen and stored at -80°C.

5.2.4 Fasting blood glucose and glucose tolerance tests:

Mice were fasted for 4.5 hours and fasting blood glucose was determined using an Alphatrak 2 (AlphaTRAK, Chicago, IL USA) blood glucose meter following tail bleed on week 13. Then glucose tolerance was determined following an intraperitoneal injection of 1g/kg D-glucose (Sigma Ultra, St. Louis, MO USA) with blood glucose readings from tail bleeds every 20 min for the first hour and every 30 min for the second hour as described previously (Ayala et al., 2010; Heintz et al., 2019). Results are recorded over the time and as area under the curve (AUC). Data are presented as mean blood glucose levels ± SEM. Statistical significance was determined by unpaired Student's t-tests using GraphPad Prism 7.0.

5.2.5 Serum biomarker panel:

Blood samples were collected by heart puncture and incubated at room temperature for 30 min followed by centrifugation at 6000 rpm for 10 min. Serum from each sample was transferred into a fresh tube and aliquots shipped on dry ice to Baylor College of Medicine's Comparative Pathology Laboratory (Houston, TX USA) for determination of serum biomarker concentrations including alanine aminotransferase (ALT), cholesterol, triglycerides (TAG), high density lipoprotein (HDL), low density lipoprotein (LDL), and very low density lipoprotein (VLDL). Serum parameters were

determined using a Beckman Coulter AU480 chemistry analyzer (Atlanta, GA, USA) and the appropriate Beckman Coulter biochemical kits according to the manufacturer's instructions.

5.2.6 Liver triglycerides:

Liver triglycerides were extracted and quantified as described previously (R. Kumar, Litoff, Boswell, & Baldwin, 2018) using colorimetric kits from Cayman Chemical (Ann Arbor, MI). In addition, visual confirmation was performed with Oil Red O. During necropsy, clean liver slices were snap frozen in liquid nitrogen and stained with Oil Red O at Baylor College of Medicine's Comparative Pathology Laboratory using standard protocols (Dong et al., 2009).

5.2.7 Lipidomic analysis of polyunsaturated fatty acids (PUFA) metabolites:

Serum and liver samples were shipped on dry ice to EILC for lipidomic analysis of lipid metabolites from AA, LA, ALA, DHA, and eicosapentaenoic acid (EPA). Oxidized lipids were selectively extracted from samples by solid phase extraction following ELIC methods (Naudin et al., 2020).

Random forest analyses by MetaboAnalyst 3.6 (Xia & Wishart, 2002) were performed on lipidomic data to rank PUFA metabolite species as a prediction of how large of an effect each species has between genotype (Breiman, 2001). The mtry parameter was set to 7, and the number of trees to be built was set to 500 for each analysis to achieve the lowest out-of-bag (OOB) error. The larger the mean decreased

accuracy (MDA) value, the more important the lipid metabolites are for the accuracy of the association between variable and response. Lipid metabolites with importance scores less than or equal to zero are likely to have no predictive ability. Statistical significance between genotypes was also determined by unpaired Student's t-tests using GraphPad Prism 7.0. Data are presented as mean concentration ± SEM.

5.2.8 RNA sequencing (RNAseq):

Liver samples were stored in RNAlater Stabilization Solution (Invitrogen, Carlsbad, CA USA) at -80°C. Total RNA was extracted from mouse livers of each treatment group using TRIzol (Ambion, Carlsbad, CA USA) and quantified on a Qubit 2.0 Fluorometer. RNA integrity number (RIN) was determined with an Agilent 2100 Bioanalyzer (place) to assess RNA quality, and samples with a RIN > 8.0 were determined to be of high quality and used for next generation sequencing. Libraries were prepared using NEB Next Ultra RNA Library Prep kit. Samples were sequenced to an average sequencing depth of 20,000,000 read pairs with a 2x150 paired-end module using a NovaSeq 6000. Quality metrics were checked using FastQC on all samples sequenced, and Trimmomatic was used to trim low quality bases. Trimmed reads were aligned to the *Mus musculus* reference genome (GCF_000001635.25_GRCm38.p6) using GSNAP, and 100% of the trimmed reads aligned. Subread feature counts software found reads that aligned with known genes. Raw read counts and EdgeR were used to determine differential gene expression (Huber et al., 2015). Series GSE148460 containing the RNAseq data has been uploaded to the Gene Expression Omnibus (GEO).

DAVID (Huang da, Sherman, & Lempicki, 2009a, 2009b) functional annotation tool was used to perform the analysis of enriched gene ontology (GO) terms from differentially expressed gene lists for female and male mice (adjusted p-value < 0.05). Chord plots were generated in R using GOplot (Wencke, Sánchez-Cabo, & Ricote, 2015) to display the relationship between enriched GO terms and differentially expressed genes. Hierarchical cluster analysis was performed on variables including total body weight, WSI, serum lipids, oxylipin species from liver and serum, and differentially expressed genes (logFC > 1.0 or < 1.0) and visualized in heatmaps with MetaboAnalyst 3.6 (Xia & Wishart, 2002) to compare measured variables between genotypes.

5.3 Results

5.3.1 Inhibition of CYP2B6 by endogenous compounds:

Various fatty acids and other endobiotic chemicals (10 μM) were screened to measure inhibition of CYP2B6 activity in CYP2B6 containing baculosomes (**Fig. 5.1A**), as we hypothesized many inhibitors would also be substrates. Most of the endobiotic compounds examined significantly reduced CYP2B6 activity, however, AA and DHA decreased CYP2B6 activity the most, by 78% and 89.6%, respectively. Concentration-dependent response curves from CYP2B6 containing baculosomes incubated with fatty acids, bile acids, or steroids were determined to further investigate the inhibition of CYP2B6 by PUFAs in comparison to other endobiotics and the plasticizer, nonylphenol, as a positive control (Acevedo et al., 2005). In concurrence with the CYP2B6 screening

results, AA and DHA had the lowest IC50s (1.04 μM and 2.69 μM, respectively) compared to other LA (9.19 μM) and ALA (9.53 μM) measured (**Fig. 5.1B**). However, even the strongest endogenous inhibitors have 5X times less affinity to CYP2B6 than the known xenobiotic inhibitor, nonylphenol (Acevedo et al., 2005). Most bile acids and steroids measured had much higher IC50s than the PUFAs, apart from lithocholic acid (IC50 = 2.47 μM) (**Fig. 5.1B**). Based on the low IC50 values for AA and DHA, it is expected that these PUFAs are effective inhibitors and potential substrates for CYP2B6; at least following a HFD or a diet high in those respective PUFAs.

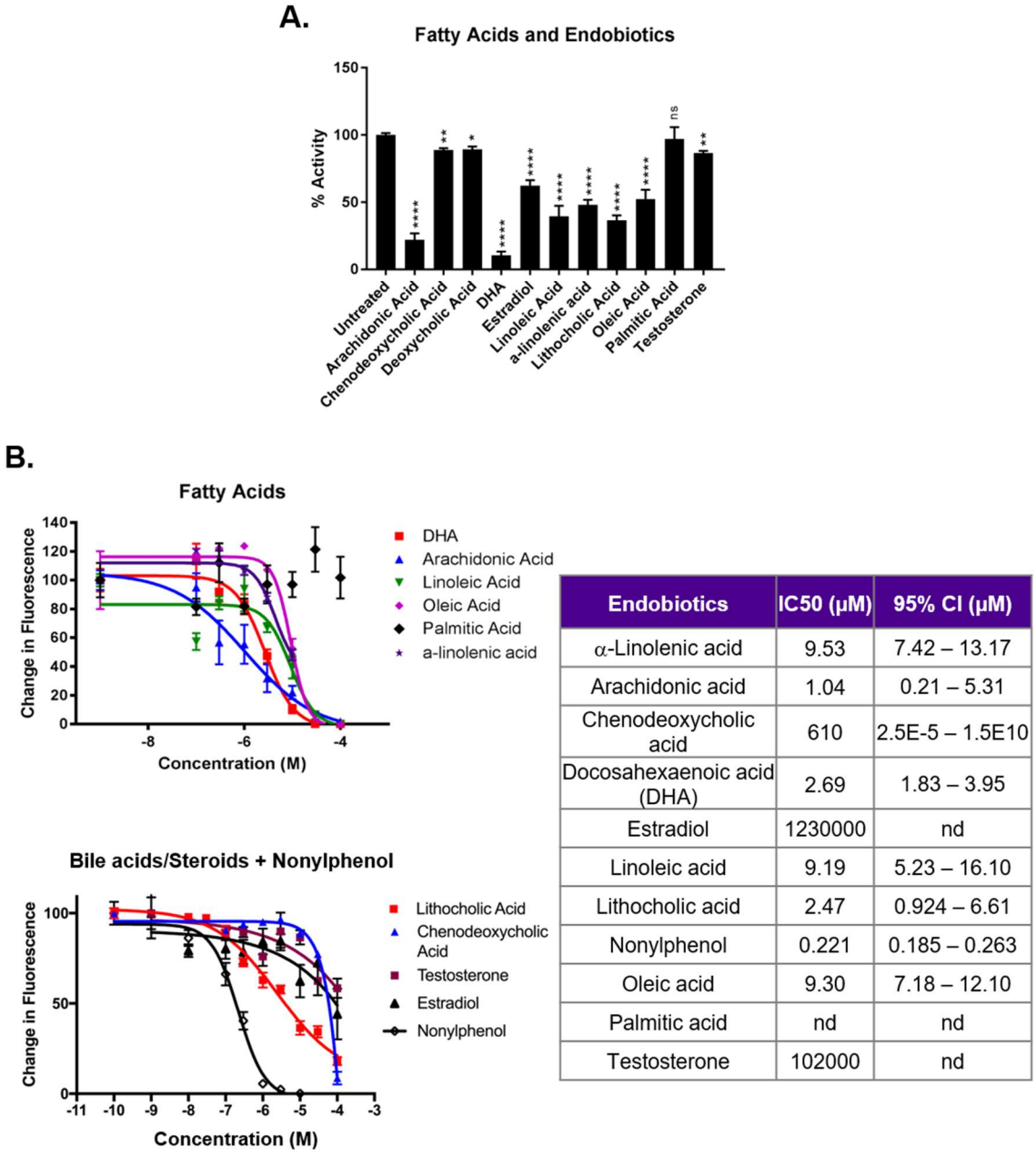

Endobiotics	IC50 (μM)	95% CI (μM)
α-Linolenic acid	9.53	7.42 – 13.17
Arachidonic acid	1.04	0.21 – 5.31
Chenodeoxycholic acid	610	2.5E-5 – 1.5E10
Docosahexaenoic acid (DHA)	2.69	1.83 – 3.95
Estradiol	1230000	nd
Linoleic acid	9.19	5.23 – 16.10
Lithocholic acid	2.47	0.924 – 6.61
Nonylphenol	0.221	0.185 – 0.263
Oleic acid	9.30	7.18 – 12.10
Palmitic acid	nd	nd
Testosterone	102000	nd

Figure 5.1. Endogenous inhibitors of CYP2B6. (A) Percent activity of CYP2B6 containing baculosomes treated with 10 μM of various fatty acids and endobiotic inhibitors. (B) Concentration-response curves of CYP2B6 containing baculosomes treated with fatty acids, bile acids, steroids, or nonylphenol (positive control). Data are

presented as mean ± SEM. Statistical significance was determined by unpaired Student's t-tests of each inhibitor treatment compared to untreated (n=4-6). * indicates p-value <0.05; ** indicates p-value <0.01; *** indicates p-value <0.001; **** indicates p-value <0.0001.

5.3.2 Preferential metabolism of ALA to 9-HOTrE by CYP2B6-containing baculosomes:

Oxylipins of AA, LA, DHA, and ALA produced by CYP2B6 were measured by LC-MS/MS to further investigate the role of CYP2B6 in PUFA metabolism. Considering their IC50s, surprisingly few AA, LA and DHA metabolites were formed (**Fig. 5.2**). Instead, the n-3 PUFA, ALA, was the most prominently metabolized PUFA with metabolite concentrations almost 20X greater than other PUFA metabolites. 9-hydroxy-10E,12Z,15Z-octadecatrienoic acid (HOTrE) and 13-HOTrE were the primary oxylipins produced. Such high concentrations suggest that CYP2B6 has a specific PUFA substrate and products, potentially as key signaling molecules. Interestingly, in addition to ALA, other n-3 and n-6 based oxylipins were also primarily metabolized at the 9 or 13 position, indicating that CYP2B6 preferentially metabolizes PUFAs in these positions.

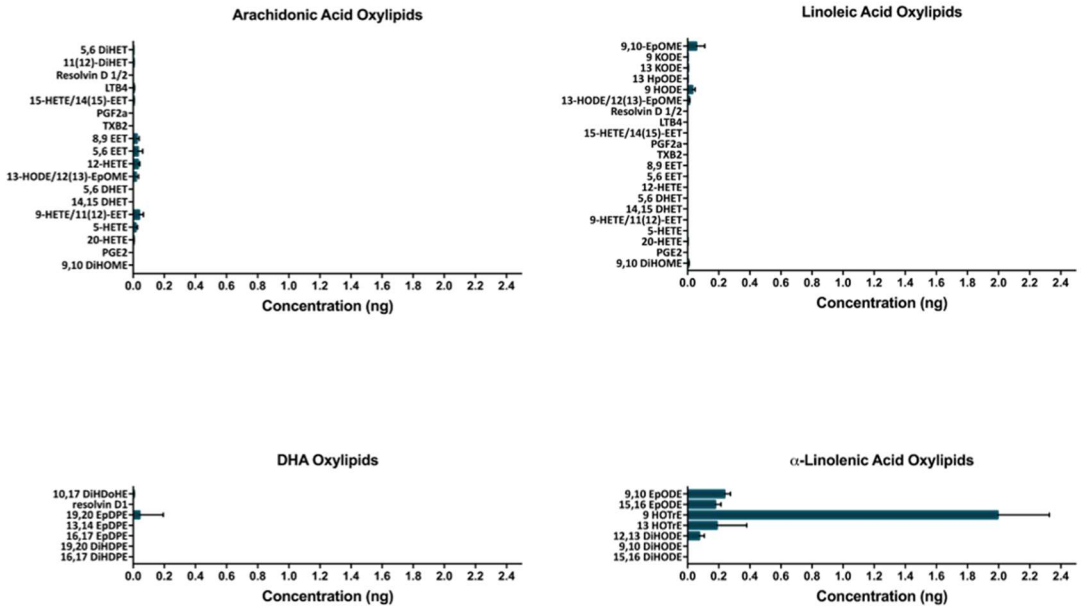

Figure 5.2. PUFA metabolites of CYP2B6. LC-MS/MS was used to measure production of oxylipid metabolites formed by CYP2B6 containing baculosomes compared to control baculosomes incubated with 25 μM arachidonic acid, linoleic acid, docosahexaenoic acid, and α-linolenic acid (n=3).

5.3.3 Humanized-CYP2B6-Tg mice have increased glucose sensitivity and decreased body mass following 16 weeks of HFD treatment:

Female hCYP2B6-Tg mice gained significantly less weight than Cyp2b-null counterparts after 16 weeks of HFD treatment. Changes in body mass were similar until about week 11 and continued to separate by genotype for the duration of the study (**Fig. 5.3A**). In contrast, male hCYP2B6-Tg mice showed no significant differences in body mass gain compared to Cyp2b-null mice over 16 weeks of HFD treatment; although male

hCYP2B6-Tg mice tended to gain a little less weight than their Cyp2b-null counterparts during the second half of the study (**Fig. 5.3A**). Both genotypes in female and male mice consumed similar amounts of calories throughout the duration of the 16-week HFD study (**Suppl. Material 5.1; S5.1**); therefore, caloric consumption does not explain the differences in body mass. The reduced weight gain in hCYP2B6-Tg female mice may be partly attributed to lower tissue weights as inguinal WAT was decreased 27% although not significantly; only kidney weights were significantly decreased (**Table 5.1**). No differences were observed in tissue weights between Cyp2b-null and hCYP2B6-Tg male mice (**Table 5.1**).

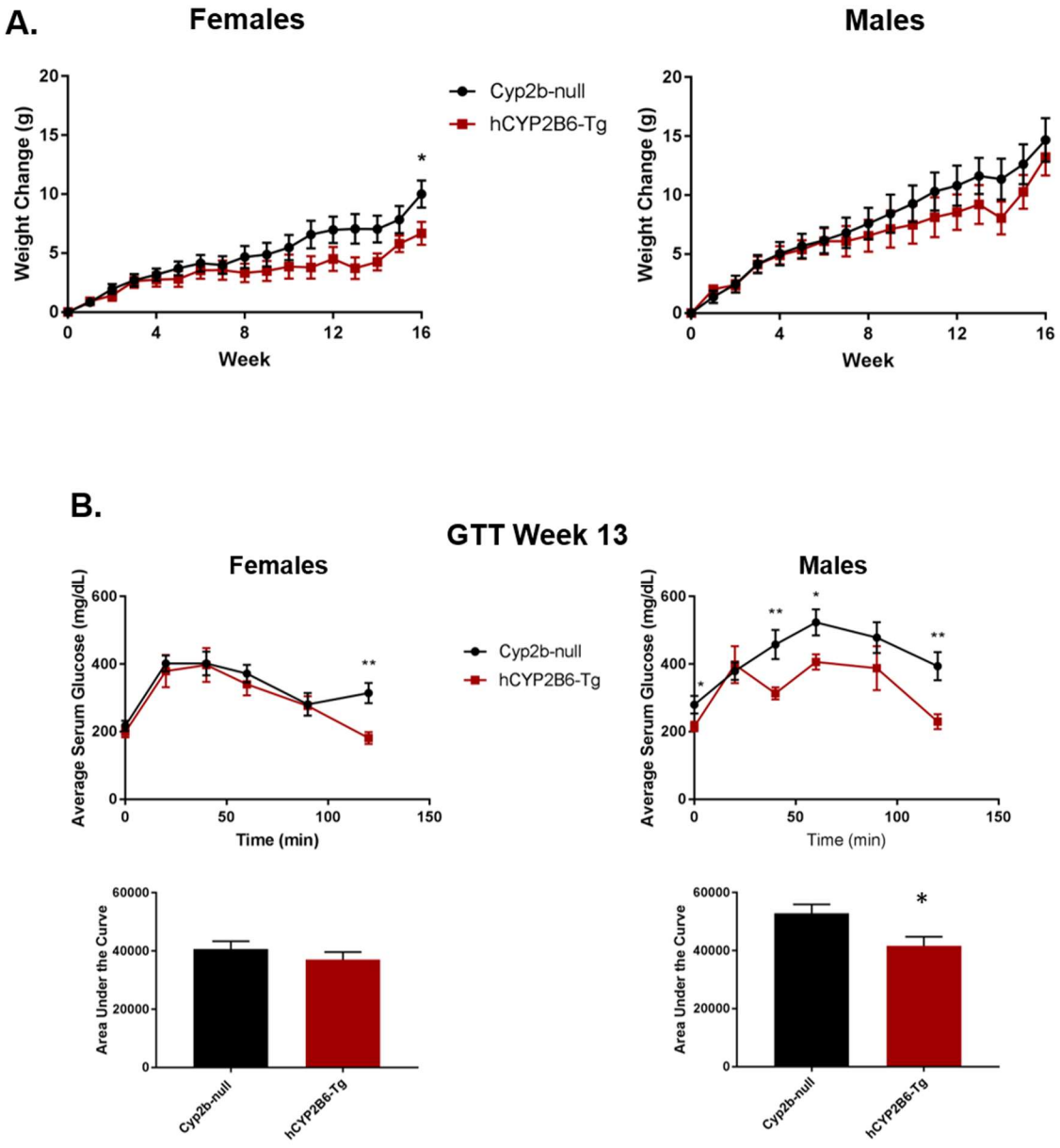

Figure 5.3. Genotypic differences in body weight gain and glucose sensitivity during 16 weeks of high-fat diet treatment. (A) Change in body weight gain over 16 weeks of HFD treatment. (B) Glucose tolerance tests (GTT) performed during week 13 on Cyp2b-null and hCYP2B6-Tg female and male mice. Results are represented as area under the curve. Data are presented as mean ± SEM. Statistical significance was determined by

unpaired Student's t-tests (n=7-8). * indicates a p-value < 0.05 and ** indicates a p-value < 0.01.

Table 5.1. Comparison of tissue weights between Cyp2b-null and hCYP2B6-Tg female (A) and male (B) mice fed a HFD for 16 weeks.

A.

Tissue Weights	Cyp2b-null F	hCYP2B6-Tg F
Total Body	29.63 ± 1.40	27.05 ± 1.21
Liver	1.02 ± 0.03	0.99 ± 0.04
Kidney	0.33 ± 0.01	0.29 ± 0.01*
WAT	2.25 ± 0.33	1.65 ± 0.31
BAT	0.13 ± 0.02	0.12 ± 0.01

B.

Tissue Weights	Cyp2b-null M	hCYP2B6-Tg M
Total Body	38.81 ± 1.99	38.93 ± 1.66
Liver	1.40 ± 0.13	1.51 ± 0.07
Kidney	0.48 ± 0.04	0.52 ± 0.02
WAT	3.41 ± 0.07	3.52 ± 0.33
BAT	0.31 ± 0.03	0.29 ± 0.07
Testes	0.33 ± 0.03	0.38 ± 0.03

Data are presented as mean (g) ± SEM. Statistical significance was determined by unpaired Student's t-tests (n=7-8). * indicates a p-value < 0.05, ** indicates a p-value < 0.01, and *** indicates a p-values < 0.0001.

GTTs were performed to determine if HFD-fed hCYP2B6-Tg mice respond better than HFD-fed Cyp2b-null mice to a glucose challenge, a biomarker of metabolic disease. Female hCYP2B6-Tg mice performed slightly better than Cyp2b-null counterparts, but only at the last time point, suggesting that this may be an outlier. However, male hCYP2B6-Tg mice exhibited a significantly faster response to a glucose challenge than Cyp2b-null males even though there was no change in weight between the genotypes

(**Fig. 5.3B**), suggesting some other physiological perturbation is protecting hCYP2B6-Tg mice from metabolic disease relative to Cyp2b-null mice.

5.3.4 Hepatic and serum lipids in HFD-fed hCYP2B6-Tg mice:

Differences in hepatic lipid accumulation between Cyp2b-null and hCYP2B6-Tg mice were examined to determine if the presence of hCYP2B6 provided protection from NAFLD as do murine Cyp2b members in male mice (Finn et al., 2009; Heintz et al., 2019). Male but not female hCYP2B6-Tg mice showed increased hepatic triglycerides compared to Cyp2b-null mice, (**Fig. 5.4a**); the opposite of what was predicted and observed in Cyp2b-null compared to WT (B6) male mice (Heintz et al., 2019). Histological analysis of Oil Red O staining was performed to confirm the chemical analysis of lipid accumulation in the liver; however, although steatosis increased as a result of HFD treatment, differences observed between genotypes were relatively small and not significant (**Fig. 5.4b**). There were also no significant differences in serum lipids between Cyp2b-null and hCYP2B6-Tg mice (**Table 5.2**). Overall, the increase of inert liver triglycerides in hCYP2B6-Tg mice may be protective based on increased glucose sensitivity although other measured physiological and biochemical parameters are equivocal.

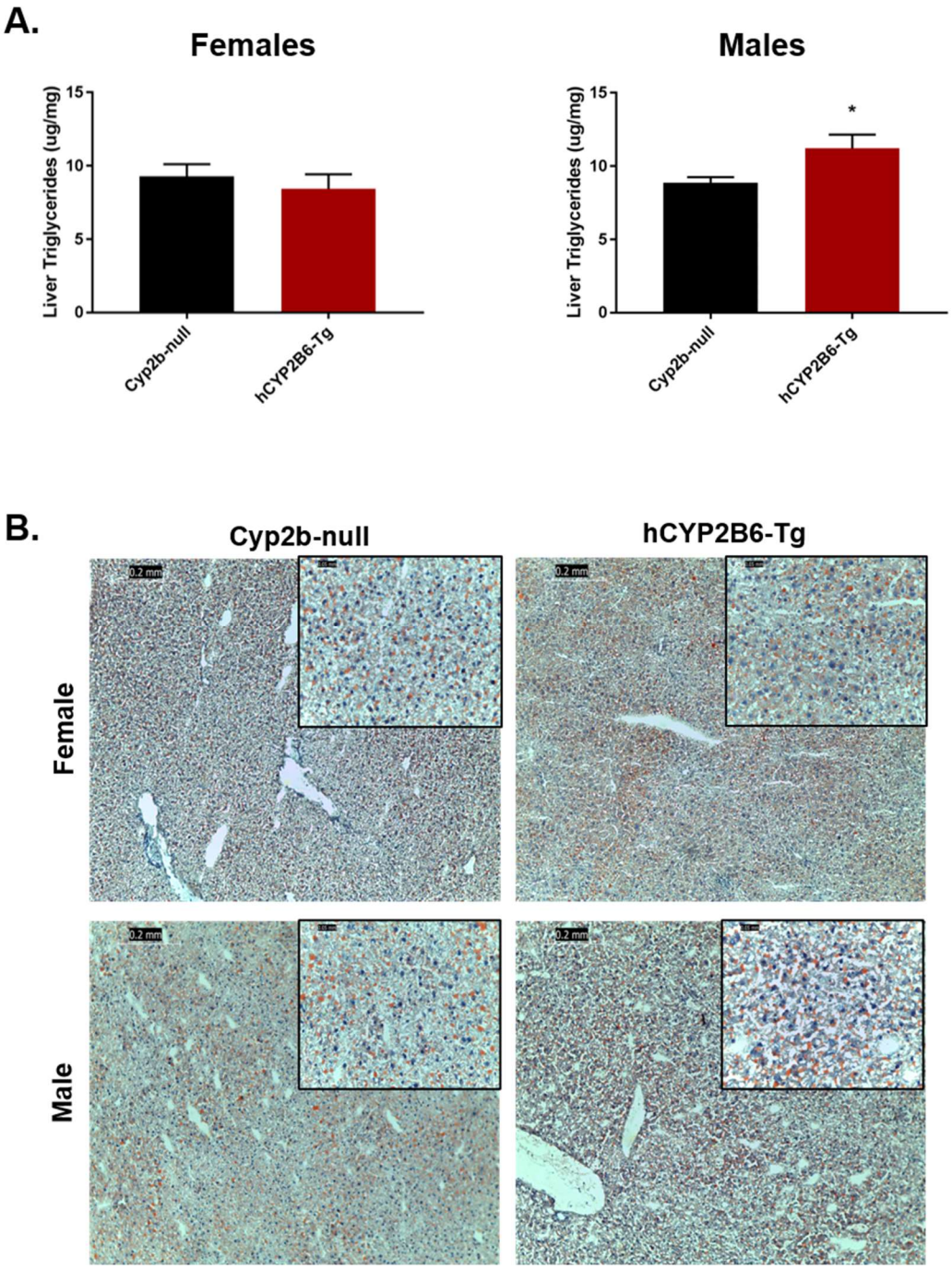

Figure 5.4. Comparison of steatosis markers in hCYP2B6-Tg and Cyp2b-null mice.

(A) Total liver triglycerides were measured in Cyp2b-null and hCYP2B6-Tg female and male mice. Data are presented as mean + SEM. Statistical significance was determined

by unpaired Student's t-tests (n=5). * indicates a p-value < 0.05. (B) Fatty liver histopathological changes were evaluated by Oil red O staining in female and male mice. Images were taken at 100x (0.2 mm) and 400x (0.05 mm) magnification.

Table 5.2. Comparison of serum biomarkers between Cyp2b-null and hCYP2B6-Tg female (A) and male (B) mice fed a HFD for 16 weeks.

A.

Serum Biomarkers	Cyp2b-null F	hCYP2B6-Tg F
ALT	21.76 ± 2.02	18.81 ± 1.14
Triglycerides	87.53 ± 15.68	71.33 ± 12.36
HDL	74.37 ± 2.88	75.26 ± 1.78
LDL	6.75 ± 0.46	7.59 ± 0.29
VLDL	17.51 ± 3.14	14.27 ± 2.47
Cholesterol	133.24 ± 7.44	127.82 ± 4.05

B.

Serum Biomarkers	Cyp2b-null M	hCYP2B6-Tg M
ALT	40.02 ± 15.89	30.65 ± 7.51
Triglycerides	88.06 ± 9.61	79.25 ± 7.31
HDL	100.76 ± 3.03	98.70 ± 1.76
LDL	10.90 ± 0.76	10.97 ± 0.76
VLDL	17.61 ± 1.92	15.85 ± 1.46
Cholesterol	213.71 ± 6.18	200.52 ± 6.56

Data are presented as mean (g) ± SEM. Statistical significance was determined by unpaired Student's t-tests (n=5).

5.3.5 Hepatic and serum oxylipin metabolites produced in HFD-fed hCYP2B6-Tg mice:

Concentrations of serum and hepatic lipid metabolites from LA, AA, ALA, DHA, and EPA were compared between HFD-fed Cyp2b-null and hCYP2B6-Tg mice to identify lipid metabolites metabolized by human CYP2B6 *in vivo*. The oxylipin species most predictive of differences between Cyp2b-null and hCYP2B6-Tg mice in serum or

liver tissue are primarily AA and LA-species as determined by random forest analysis (**Fig. 5.5**).

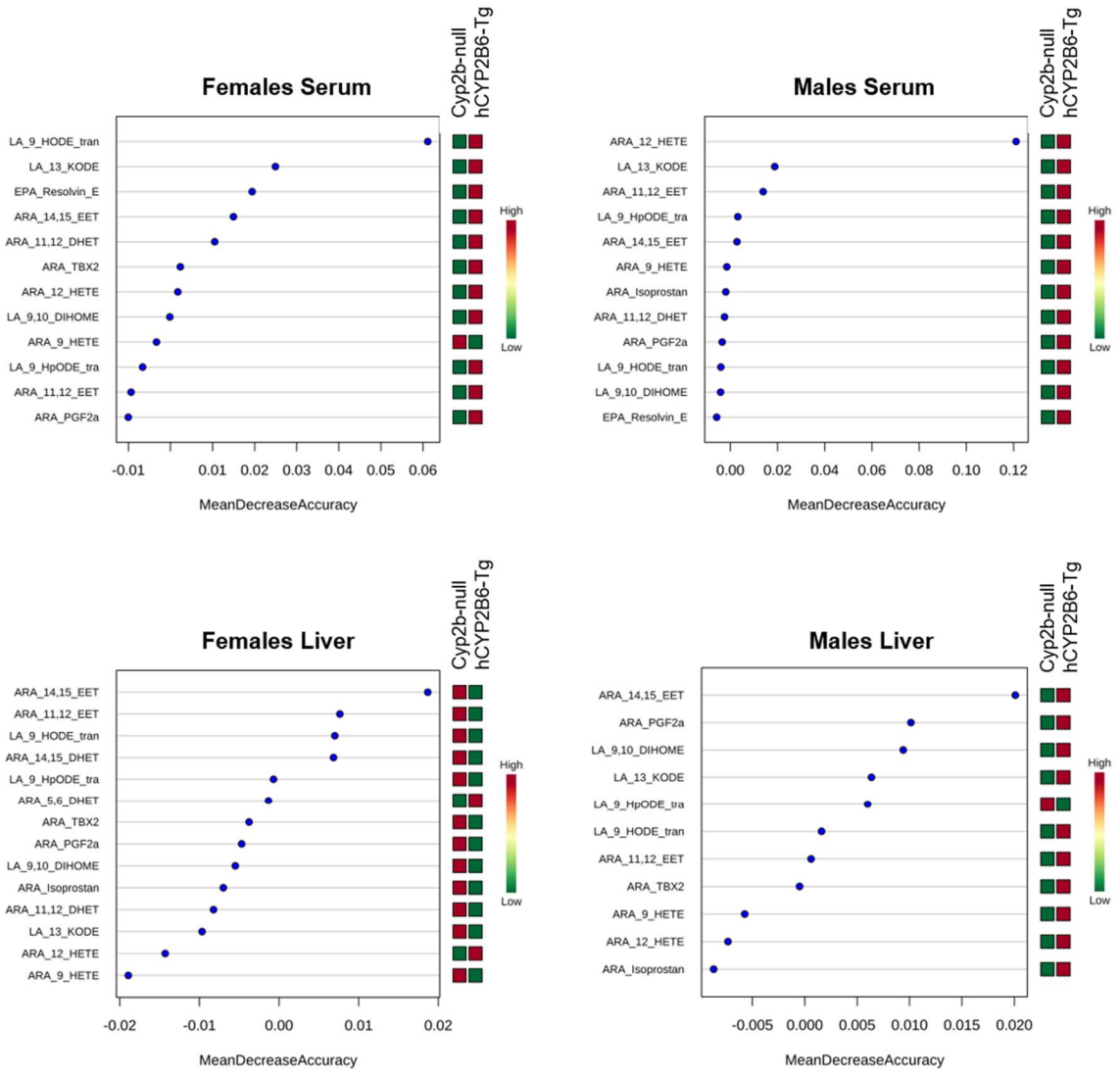

Figure 5.5. Random forest analysis of lipid metabolites by tissue type in female and male mice. Important lipid metabolites identified by random forest analysis between Cyp2b-null and hCYP2B6-Tg mice in serum or liver tissue.

The anti-inflammatory signaling molecule, AA 14,15-EET was ranked the most predictive lipid metabolite in hepatic tissue in female and male hCYP2B6-Tg mice (**Fig. 5.5**). Interestingly, AA 14,15-EET was the only statistically different oxylipin by unpaired Student's t-tests between Cyp2b-null and hCYP2B6-Tg female mice in serum, and there were no significant changes in oxylipin concentrations between HFD-fed Cyp2b-null and hCYP2B6-Tg mice in the liver. While individual hepatic oxylipin differences were small or not significant, the total average concentration of oxylipins in the liver significantly increased in male hCYP2B6-Tg mice (**Table 5.3**).

Table 5.3. Total average of oxylipin metabolites measured in liver and serum of HFD-fed Cyp2b-null and hCYP2B6-Tg mice.

	Serum		Liver	
	Cyp2b-null	**hCYP2B6-Tg**	**Cyp2b-null**	**hCYP2B6-Tg**
Females	0.002521 ± 0.0005892	0.003214 ± 0.0007361	0.007582 ± 0.001603	0.004072 ± 0.000926
Males	0.002238 ± 0.0005311	0.005842 ± 0.002113	0.002008 ± 0.0004811	0.004106 ± 0.0008813*

Data are presented as mean (ng/μL) ± SEM. Statistical significance was determined by unpaired Student's t-tests (n=5). * indicates a p-value < 0.05.

Hepatic pro-inflammatory response metabolites, LA 9--hydroxyoctadecadienoic acid (LA 9-HODE) (females) and AA 12-hydroxyeicosatetraenoic acid (AA 12-HETE) (males), followed by LA 13-HODE derivative, 13-keto-9Z,11E-octadecadienoic acid (LA 13-KODE), were identified as the most predictive lipid metabolites in serum of female and male mice (**Fig. 5.5**). With the exception of AA 12-HETE, these metabolites and

others were also different by Student's t-tests (**Table 5.4**). LA 9,10-dihydroxyoctadec-12-enoic acid (DiHOME) a hydrolase metabolite of 9,10-epoxy-12Z-octadecenoic acid (EpOME), LA 9-HODE and LA 13-KODE, as well as AA 14,15-epoxyeicosatrienoic acid (AA 14,15-EET) and ALA isoprostane all increased in the serum of female hCYP2B6-Tg mice (**Table 5.4A**). These PUFA metabolites also increased in the serum of male hCYP2B6-Tg mice but not significantly. The only lipid metabolite to significantly increase in the presence of CYP2B6 in the serum of male mice was AA thromboxane B2 (TXB2) (**Table 5.4B**). Total average oxylipin concentrations in serum samples increased, but not significantly, in both female and male hCYP2B6-Tg mice compared to Cyp2b-null mice (**Table 5.3**).

Table 5.4. Measured serum and liver lipid metabolite concentrations in Cyp2b-null and hCYP2B6-Tg female (A) and male (B) mice fed a HFD for 16 weeks.
A.

	Serum		Liver	
Oxylipin Species	**Cyp2b-null**	**hCYP2B6-Tg**	**Cyp2b-null**	**hCYP2B6-Tg**
AA 14,15-EET	3.444E-06 ± 2.11E-06	2.909E-05 ± 2.946E-06**	0.0008699 ± 0.0004062	0.0003727 ± 0.000219
AA 11,12-EET	0.001911 ± 0.0003876	0.002914 ± 0.001033	0.007769 ± 0.002561	0.003422 ± 0.001977
AA 9-HETE	0.008382 ± 0.005741	0.007522 ± 0.003799	0.01077 ± 0.005417	0.006018 ± 0.002752
AA 12-HETE	0.0004833 ± 9.685E-05	0.001130 ± 0.0003599	0.002732 ± 0.0008528	0.001756 ± 0.001041
AA 11,12-DHET	0.01543 ± 0.003179	0.02971 ± 0.006977	0.02317 ± 0.009411	0.01133 ± 0.00699
AA PGE2	0.0047044 ± 0.001773	0 ± 0*	0.0002838 ± 0.0002838	0 ± 0
AA PGF2a	0.003416 ± 0.0008837	0.005472 ± 0.001738	0.04234 ± 0.02609	0.02244 ± 0.01324
AA TXB2	6.141E-05 ± 2.902E-05	0.0001025 ± 4.572E-05	0.001356 ± 0.000447	0.0006450 ± 0.0004188
LA 9-HODE	0.001124 ± 0.0001462	0.004251 ± 0.0009221*	0.03462 ± 0.0141	0.01603 ± 0.009448
LA 9-HpODE	0.02914 ± 0.002886	0.02957 ± 0.004296	0.03637 ± 0.01197	0.03278 ± 0.004932
LA 13-KODE	0.0003835 ± 6.357E-05	0.001051 ± 0.0001858**	0.007301 ± 0.00389	0.002536 ± 0.001444
LA 9,10-DiHOME	9.894E-05 ± 4.307E-05	0.000345 ± 8.309E-05*	0.002194 ± 0.0008728	0.0008417 ± 0.0005167
EPA Resolvin	0.002928 ± 0.0001994	0.004320 ± 0.0006148	0.0007463 ± 0.0004635	0.0003922 ± 0.0002707
ALA 9-HOTrE	0 ± 0	0.0001253 ± 0.0001253	0.0006108 ± 0.0002531	0.0002325 ± 0.0002325
ALA Isoprostane	0 ± 0	0.0002449 ± 6.423E-05**	0.008005 ± 0.003746	0.003327 ± 0.001886

B.

	Serum		Liver	
Oxylipin Species	**Cyp2b-null**	**hCYP2B6-Tg**	**Cyp2b-null**	**hCYP2B6-Tg**
AA 14,15-EET	1.281E-05 ± 4.445E-06	3.707E-05 ± 2.216E-05	8.732E-05 ± 2.825E-05	0.0003897 ± 0.0002161
AA 11,12-EET	0.002183 ± 0.0006091	0.006343 ± 0.003742	0.0009780 ± 0.0003435	0.004964 ± 0.002834
AA 9-HETE	0.003868 ± 0.001342	0.01030 ± 0.003904	0.006016 ± 0.001504	0.01118 ± 0.003558
AA 12-HETE	0.0004491 ± 0.0001189	0.002130 ± 0.001214	0.0006437 ± 0.000258	0.002592 ± 0.001547
AA 11,12-DHET	0.01763 ± 0.00509	0.04130 ± 0.02508	0.002351 ± 0.001458	0.01177 ± 0.006342
AA PGE2	0.002081 ± 0.0008876	0.002618 ± 0.001158	0.0004154 ± 0.0004154	0 ± 0
AA PGF2a	0.001286 ± 0.0008909	0.007236 ± 0.003804	0.005866 ± 0.002478	0.02343 ± 0.01314
AA TXB2	0 ± 0	0.0001574 ± 5.767E-05*	0.0002758 ± 0.0001044	0.00140 ± 0.0008361
LA 9-HODE	0.001534 ± 0.0005044	0.004277 ± 0.00226	0.004474 ± 0.001505	0.01805 ± 0.01013
LA 9-HpODE	0.02545 ± 0.002158	0.02385 ± 0.007709	0.02616 ± 0.00340	0.02363 ± 0.004619
LA 13-KODE	0.0005594 ± 0.0001023	0.001398 ± 0.0008135	0.0006725 ± 0.0001771	0.002463 ± 0.001289
LA 9,10-DiHOME	9.070E-05 ± 4.131E-05	0.0002486 ± 0.0001336	0.0003869 ± 0.000138	0.001156 ± 0.0006744
EPA Resolvin	0.003274 ± 0.000697	0.003091 ± 0.0008124	0 ± 0	0 ± 0
ALA 9-HOTrE	0 ± 0	0 ± 0	0 ± 0	0.0004337 ± 0.000286
ALA Isoprostane	0.0001335 ± 5.946E-05	0.0003280 ± 0.000126	0.0008786 ± 0.000269	0.003881 ± 0.002122

Data are presented as mean (ng/μL) ± SEM. Statistical significance was determined by unpaired Student's t-tests (n=5). * indicates a p-value < 0.05 and ** indicates a p-value < 0.01.

5.3.6 Gene expression differences between HFD-fed Cyp2b-null and hCYP2B6-Tg mice:

RNAseq was performed on liver samples to examine the effect of CYP2B6 on global hepatic gene expression compared to Cyp2b-null mice during HFD treatment

(**S5.2**). Gene ontology (GO) enrichment chord plots were used to display the relationship between differentially expressed genes and enriched biological process GO terms (**S5.3**). Several circadian rhythm-associated genes were up-regulated in HFD-fed hCYP2B6-Tg mice compared to Cyp2b-null mice (**Fig. 5.6**). Circadian regulation plays an important role in liver metabolism and metabolic disease (Shi et al., 2019). Female and to a lesser extent, male hCYP2B6-Tg mice had several perturbed protein processing and phosphorylation associated genes. Previous RNAseq data generated in our lab determined Cyp2b-null mice have increased endoplasmic reticulum stress compared to wild-type mice (Heintz et al., 2019). Consistent with these results, female and to a lesser extent, male hCYP2B6-Tg mice had several perturbed protein processing and phosphorylation associated genes compared to Cyp2b-null mice. In addition, female hCYP2B6-Tg mice had several down-regulated genes involved in lipid synthesis, notably *Angptl8*, a critical modulator of serum triglyceride levels (Luo & Peng, 2018) (**Fig. 5.6**). Interestingly in males, *Cyp2b10* was the second highest induced gene (logFC=6.19) in HFD-fed hCYP2B6-Tg compared to Cyp2b-null mice (**S5.2**). Cyp2b10 is the murine ortholog to human CYP2B6 and 74% identical. Based on alignment program settings and sequencing variation (i.e. number of SNPs), CYP2B reads were aligned to Cyp2b10 on the reference genome (**S5.4**). Furthermore, the epidermal growth factor receptor (*Egfr*) was down-regulated (logFC = -1.34) in male hCYP2B6-Tg mice compared to Cyp2b-null mice. The down-regulation of EGFR provides a mechanism for the activation of CAR and subsequent induction of Cyp2b10/CYP2B6 (Mutoh et al., 2013). Conversely, *Cyp2b10*

was not differentially expressed in females, probably because *Egfr* was up-regulated (logFC = 0.77) in female hCYP2B6-Tg mice.

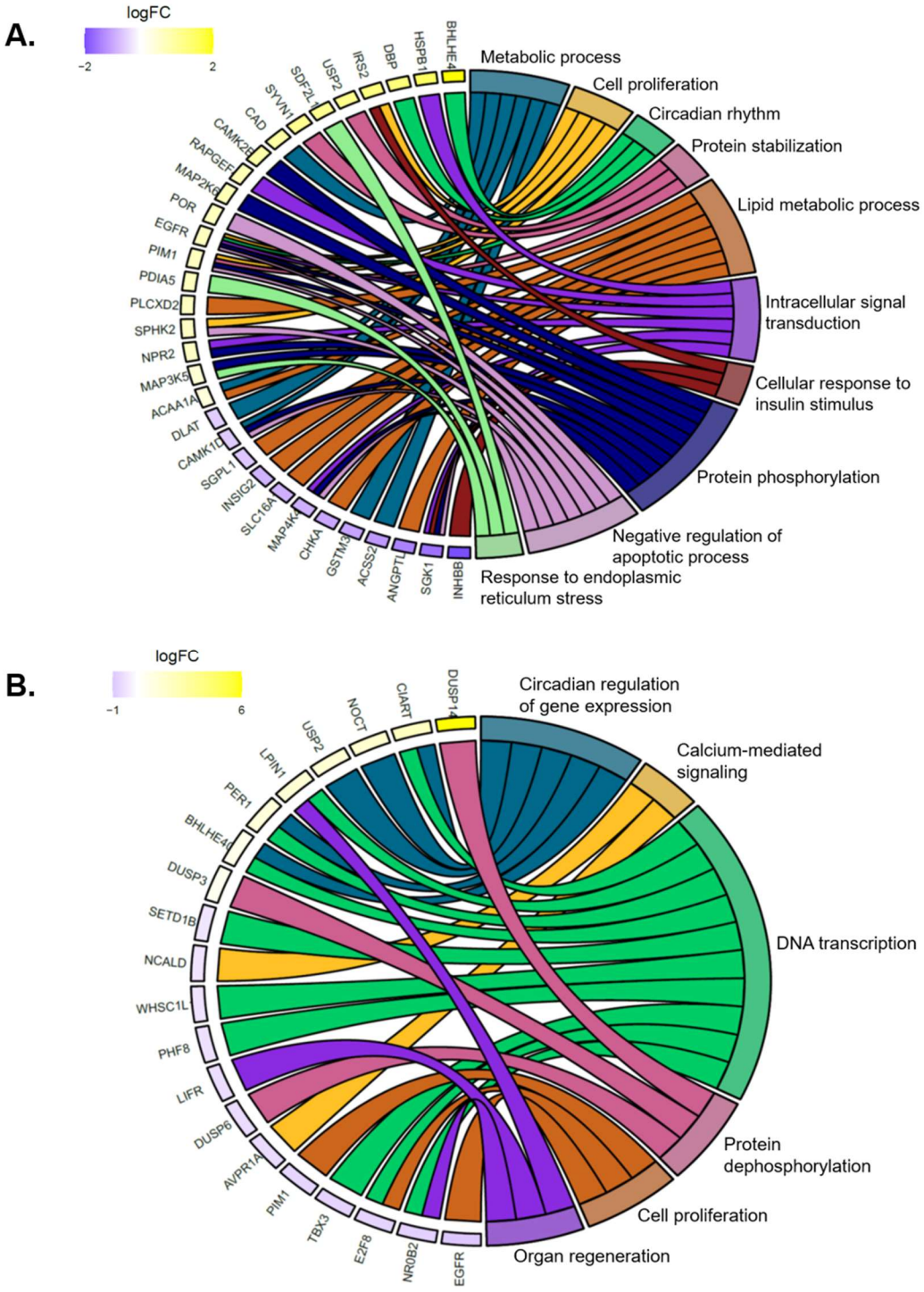

Figure 5.6. Chord plots displaying relationships between RNAseq gene expression data and gene ontology. Chord plots were used to display the relationship between enriched GO terms and differential gene expression data in female (A) and male (B) mice.

To determine associations between physiological parameters, serum lipids, serum and liver oxylipin species, and differentially expressed genes between HFD-fed Cyp2b-null and hCYP2B6-Tg mice, hierarchical cluster analysis was performed using the top 50 measured variables from female and male mice (**Fig. 5.7).** There was clear separation by genotype in females, with hierarchical clustering showing that in addition to differentially expressed genes, serum-associated variables make up the most distinguishing factors between genotypes in female mice (**Fig. 5.7A**). HFD-fed hCYP2B6-Tg female mice were associated with an increase in several serum oxylipins, LDL, and HDL as well as more differentially expressed genes than Cyp2b-null females. Fewer serum parameters, TAG, VLDL, and two AA serum oxylipin species (AA-TBX2; AA-PGE2) (role in inflammation) were increased in HFD-fed Cyp2b-null female mice (**Fig. 5.7A**).

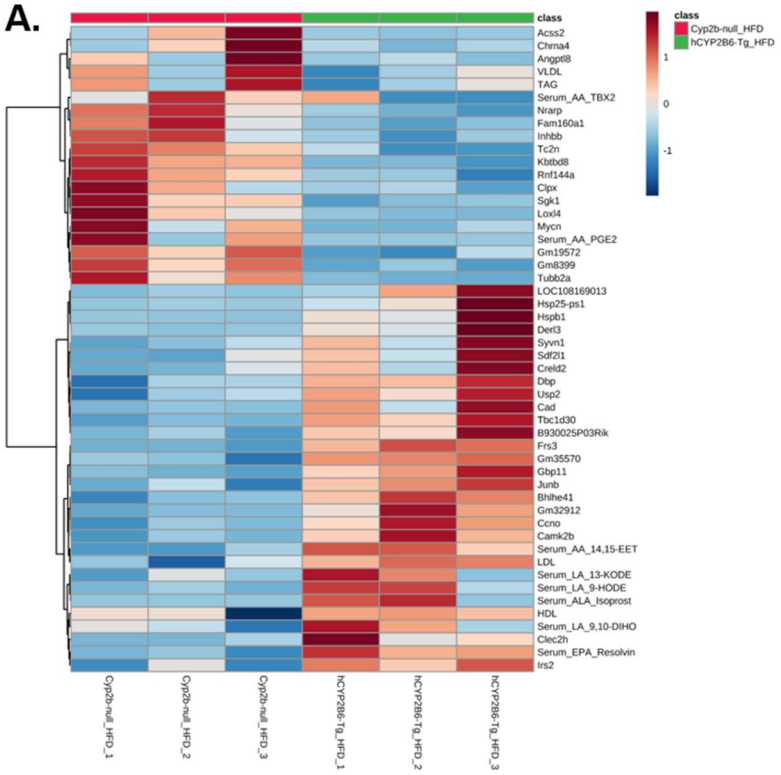
A.
class
Acss2
Chrna4
Angptl8
VLDL
TAG
Serum_AA_TBX2
Nrarp
Fam160a1
Inhbb
Tc2n
Kbtbd8
Rnf144a
Clpx
Sgk1
Loxl4
Mycn
Serum_AA_PGE2
Gm19572
Gm8399
Tubb2a
LOC108169013
Hsp25-ps1
Hspb1
Derl3
Syvn1
Sdf2l1
Creld2
Dbp
Usp2
Cad
Tbc1d30
B930025P03Rik
Frs3
Gm35570
Gbp11
Junb
Bhlhe41
Gm32912
Ccno
Camk2b
Serum_AA_14,15-EET
LDL
Serum_LA_13-KODE
Serum_LA_9-HODE
Serum_ALA_Isoprost
HDL
Serum_LA_9,10-DIHO
Clec2h
Serum_EPA_Resolvin
Irs2
Cyp2b-null_HFD_1
Cyp2b-null_HFD_2
Cyp2b-null_HFD_3
hCYP2B6-Tg_HFD_1
hCYP2B6-Tg_HFD_2
hCYP2B6-Tg_HFD_3
class
Cyp2b-null_HFD
hCYP2B6-Tg_HFD
1
0
-1

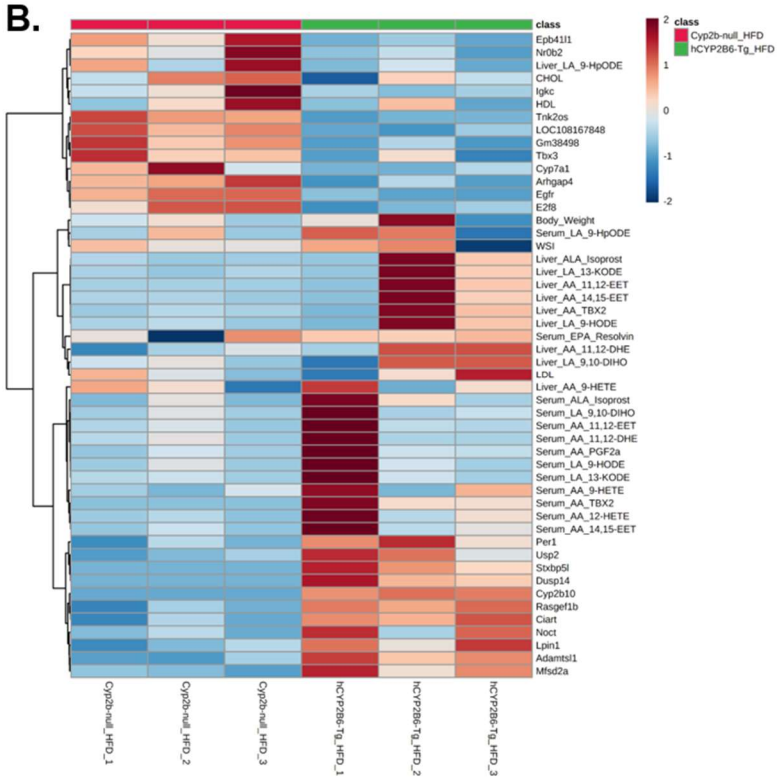
B.
class
Epb41l1
Nr0b2
Liver_LA_9-HpODE
CHOL
Igkc
HDL
Tnk2os
LOC108167848
Gm38498
Tbx3
Cyp7a1
Arhgap4
Egfr
E2f8
Body_Weight
Serum_LA_9-HpODE
WSI
Liver_ALA_Isoprost
Liver_LA_13-KODE
Liver_AA_11,12-EET
Liver_AA_14,15-EET
Liver_AA_TBX2
Liver_LA_9-HODE
Serum_EPA_Resolvin
Liver_AA_11,12-DHE
Liver_LA_9,10-DIHO
LDL
Liver_AA_9-HETE
Serum_ALA_Isoprost
Serum_LA_9,10-DIHO
Serum_AA_11,12-EET
Serum_AA_11,12-DHE
Serum_AA_PGF2a
Serum_LA_9-HODE
Serum_LA_13-KODE
Serum_AA_9-HETE
Serum_AA_TBX2
Serum_AA_12-HETE
Serum_AA_14,15-EET
Per1
Usp2
Stxbp5l
Dusp14
Cyp2b10
Rasgef1b
Ciart
Noct
Lpin1
Adamtsl1
Mfsd2a
Cyp2b-null_HFD_1
Cyp2b-null_HFD_2
Cyp2b-null_HFD_3
hCYP2B6-Tg_HFD_1
hCYP2B6-Tg_HFD_2
hCYP2B6-Tg_HFD_3
class
Cyp2b-null_HFD
hCYP2B6-Tg_HFD
2
1
0
-1
-2

Figure 5.7. Hierarchical cluster analysis comparing measured variables between HFD-fed hCYP2B6-Tg and Cyp2b-null mice. Hierarchical cluster analysis determining the top 50 measured variables associated with HFD-fed Cyp2b-null or hCYP2B6-Tg female (A) or male (B) mice visualized in heatmaps. Variables include serum lipids, WAT somatic index (WSI), body weight, serum and liver oxylipin species, and differentially expressed genes (logFC >1.0 or <1.0).

Samples also clustered by genotype in male mice, but with more variability than females (**Fig. 5.7B**). Interestingly, HFD-fed Cyp2b-null males were associated with an increase in serum cholesterol and HDL and only one liver oxylipin metabolite. Conversely, hCYP2B6-Tg counterparts were correlated with an increase in WSI, LDL, and numerous serum and liver oxylipin species (**Fig. 5.7B**). In addition, an increase in circadian rhythm-related genes in hCYP2B6-Tg mice was a prominent differentiating factor between genotype clusters in both female and male mice (**Fig. 5.7**).

5.4 Discussion

Female hCYP2B6-Tg mice gained less weight than Cyp2b-null counterparts after 16 weeks of HFD treatment. The difference in weight was not as great and the duration of the study was longer than previously conducted when comparing Cyp2b-null and WT mice (Heintz et al., 2019). This suggests that human CYP2B6 is an anti-obesity enzyme,

but not with the efficacy of the murine Cyp2b enzymes. In addition, the sexual dimorphic effects of human CYP2B6 and murine Cyp2b's were flipped, as Cyp2b-null male mice weighed much more than WT mice (Heintz et al., 2019), but it was Cyp2b-null female mice that weighed more than hCYP2B6-Tg mice (**Fig. 5.3**).

In addition to body weight, hCYP2B6-Tg females also decreased WAT mass 27%, but not significantly, when compared to Cyp2b-null mice. While 27% is not statistically significant, a 27% drop in WAT mass is biologically impressive. Genes that play a role in adipocyte lipid accumulation, *Angptl8* (Y. Zhang et al., 2016), and differentiation (*Slc16a1*) (Petersen et al., 2017) were concurrently down-regulated in hCYP2B6-Tg female mice, as well as acyl-coA synthetase short chain family member 2 (*Acss2*), which has been found to promote the systemic storage of fats under HFD conditions in mice (Huang et al., 2018). Additionally, previous studies have found serum TAG, VLDL and *Angptl8* expression to be positively correlated in humans and mice (Chung et al., 2016; R. Zhang, 2012). These variables were also increased and grouped together by hierarchical cluster analysis in HFD-fed Cyp2b-null female mice. Female RNAseq results also indicate disruption of circadian rhythm genes, which often regulate lipid distribution (S. Liu et al., 2013) as well as effects on lipid metabolism/cholesterol/bile acid pathways (*Insig2*) (Yabe, Komuro, Liang, Goldstein, & Brown, 2003) and energy utilization (*Sgk1*) (Lang & Voelkl, 2013).

Concentrations of specific oxylipin metabolites were significantly increased in the serum of hCYP2B6-Tg females, which corresponds well with their signaling role and obesity-associated effects observed in the physiological and transcriptomic results of

HFD-fed hCYP2B6-Tg female mice. These altered oxylipin species do not share one specific role, as AA-14,15-EET is anti-inflammatory (Jiang et al., 2014), while LA-9-HODE and 13-KODE are agonists of the pain receptor, transient receptor potential vanilloid 1 (TRPV1) and likely inflammatory (Patwardhan, Scotland, Akopian, & Hargreaves, 2009). Furthermore, hierarchical cluster analysis showed changes in AA-14,15-EET are associated with genes involved in proliferation (*Ccno, Frs3, Junb*) (Passegué, Jochum, Behrens, Ricci, & Wagner, 2002; Valencia et al., 2011; Villa et al., 2017) and LA-9-HODE and 13-KODE, which are closely associated with each other, are associated with genes involved in insulin signaling (*Irs2, Clec2h*) (Hines et al., 2011). Changes between HFD-fed hCYP2B6-Tg and Cyp2b-null female mice suggest CYP2B6 affected lipid distribution from the liver to other tissues.

In contrast to females, there was no change in weight between genotypes in HFD-fed male mice, although male hCYP2B6-Tg mice exhibited increased glucose sensitivity and higher liver triglyceride levels compared to Cyp2b-null males. High fat diets often cause a shift from normal triglyceride synthesis to bioactive lipid intermediates that can induce endoplasmic reticulum (ER) stress and cause lipotoxicity (Fuchs & Sanyal, 2012); however, lipotoxic ER stress was not observed in male hCYP2B6-Tg mice. We suspect that the increase in inert hepatic triglycerides provided lipotoxic protection from other fatty acid-derived species (Cusi, 2009; Jou, Choi, & Diehl, 2008). Additionally, the downregulation of *Egfr* in male hCYP2B6-Tg provides a mechanism for the up-regulation of Cyp2b10 (Mutoh et al., 2013) and potentially explains the physiological and

lipid metabolism differences between male and female hCYP2B6-Tg mice, as *Egfr* was up-regulated in females.

Differences between male hCYP2B6-Tg and Cyp2b-null mice were predominantly liver-based effects. In addition to increased liver triglyceride accumulation and glucose sensitivity, HFD-fed hCYP2B6-Tg males also increased total average concentrations of hepatic oxylipin species compared to Cyp2b-null counterparts. Increased levels of oxylipin metabolites of ALA and LA have been previously associated with soybean oil-induced fatty liver and obesity in mice (Deol et al., 2017). Additionally, similar to females, hCYP2B6-Tg male mice also experienced perturbations in circadian rhythm-associated genes that are important mediators of hepatic lipid homeostasis (Shi et al., 2019).

In humans, excess intrahepatic fat and visceral adipose tissue (VAT) have been associated with perturbed glucose and lipid metabolism. VAT is highly lipolytic and increases levels of free fatty acids in the liver, causing enhanced gluconeogenesis and hepatic insulin resistance (Bugianesi, McCullough, & Marchesini, 2005). Additionally, it has been shown that adults and children with NAFLD have impaired glucose tolerance in equal proportions to the degree of steatosis (Bedogni et al., 2012; Gastaldelli et al., 2007). In this study HFD-fed hCYP2B6-Tg male mice simultaneously increased hepatic triglycerides and glucose uptake compared to Cyp2b-null mice, which is unusual but not unprecedented (Xu et al., 2005) as other studies have shown that NAFLD can be protective (Raubenheimer, Nyirenda, & Walker, 2006). Differences are also potentially due to the differing roles of human versus murine CYP2B, as CAR activation in murine

models inhibits gluconeogenesis, lipogenesis and fatty acid synthesis, but in human hepatocytes CAR was only found to inhibit gluconeogenesis (Lynch et al., 2014), and RNAseq suggests the potential for CAR activation based on decreased *Egfr* and *Cyp7a1*, and increased CYP2B6/*Cyp2b10* (**Fig. 5.6**) (Mutoh et al., 2013). Interestingly, decreased *Egfr* and *Cyp7a1* were associated with decreased serum cholesterol and HDL (**Fig. 5.7**) Furthermore, AA-14,15-EET and other CYP-derived EETs (Gangadhariah et al., 2017) contribute positively to insulin sensitivity. Taken together, there appears to be several pieces of evidence that suggest a role positive role for CYP2B6 in glucose tolerance.

Although AA and DHA had the lowest IC50 values compared to the other PUFAs measured by concentration-dependent response curves, ALA was the predominant substrate metabolized by CYP2B6 *in vitro* followed by LA and AA when adequate substrate was provided. CYP2B6 oxylipin metabolites were produced in the 9- and 13-positions at high concentrations, especially 9-HOTrE followed by 13-HOTrE. The oxylipin 13-HOTrE is known for its role in suppression of inflammation (N. Kumar et al., 2016; Schulze-Tanzil et al., 2002), and although the biological effect of the previously determined lipoxygenase product 9-HOTrE (M. Liu et al., 2013) is not established, it is predicted to share a similar anti-inflammatory role (J. Zhang et al., 2017). Conversely, important or significantly altered PUFA metabolites from liver and serum samples of HFD-fed hCYP2B6-Tg mice suggests CYP2B6 primarily metabolizes the n-6 PUFAs, LA and AA *in vivo*, in the 9- and 13- positions. This change in substrate preference is most likely attributed to the available concentrations of the different PUFAs and their affinity for CYP2B6 (**Fig. 5.1**). The HFD provided has nearly10X more n-6 than n-3

PUFAs as the main source of PUFAs in the HFD treatment was soybean oil, which is approximately 55% LA and only 7% ALA (Clemente & Cahoon, 2009). In addition, ALA had a much lower affinity to CYP2B6 compared to AA according to concentration-dependent response curve results, indicating more ALA would need to be present for metabolism to occur.

In conclusion, the data presented indicates CYP2B6 is an anti-obesity enzyme, but to a lesser degree than murine Cyp2b enzymes. CYP2B6 metabolizes PUFAs *in vitro* and *in vivo* preferentially in the 9- and 13- positions on LA and ALA and produces several important anti-inflammatory mediators of metabolic disease, as well as some inflammatory oxylipins. In addition, HFD-fed hCYP2B6-Tg male and female mice were less susceptible to development of metabolic disease compared to Cyp2b-null mice through different mechanisms as female mice showed reduced body weight and males increased glucose sensitivity. Overall, this study provides putative mechanisms by which CYP2B6 acts as an anti-obesity/anti-metabolic disease enzyme and suggests how chemical inhibition or polymorphic loss of CYP2B6 could increase diet-induced obesity and metabolic disease through reduced production of important oxylipins and changes in circadian-mediated regulation of lipid metabolism and distribution.

Acknowledgements

This study was primarily supported by NIH grant R15ES017321 with assistance from the Emory Integrated Lipidomics Core (EILC), which is subsidized by the Emory University School of Medicine and is one of the Emory Integrated Core Facilities. Additional

support was provided by the Georgia Clinical & Translational Science Alliance of the National Institutes of Health under Award Number UL1TR002378. Transcriptomic support was provided by Dr. Rooksana E. Noorai and the Clemson University Genomics and Bioinformatics Facility through the National Institute of General Medical Sciences Grant: P20GM109094.

References

Abe, T., Takahashi, M., Kano, M., Amaike, Y., Ishii, C., Maeda, K., . . . Yoshinari, K. (2017). Activation of nuclear receptor CAR by an environmental pollutant perfluorooctanoic acid. *Arch Toxicol, 91*(6), 2365-2374. doi:10.1007/s00204-016-1888-3

Acevedo, R., Parnell, P. G., Villanueva, H., Chapman, L. M., Gimenez, T., Gray, S. L., & Baldwin, W. S. (2005). The contribution of hepatic steroid metabolism to serum estradiol and estriol concentrations in nonylphenol treated MMTVneu mice and its potential effects on breast cancer incidence and latency. *Journal of Applied Toxicology, 25*(5), 339-353. doi:10.1002/jat.1078

Audet-Walsh, É., & Anderson, A. (2009). Dexamethasone Induction of Murine CYP2B Genes Requires the Glucocorticoid Receptor. *Drug Metabolism and Disposition, 37*(3), 580. doi:10.1124/dmd.108.022772

Ayala, J. E., Samuel, V. T., Morton, G. J., Obici, S., Croniger, C. M., Shulman, G. I., . . . McGuinness, O. P. (2010). Standard operating procedures for describing and performing metabolic tests of glucose homeostasis in mice. *Disease Models & Mechanisms, 3*(9-10), 525-534. doi:10.1242/dmm.006239

Baldwin, W. S., & Roling, J. A. (2009). A concentration addition model for the activation of the constitutive androstane receptor by xenobiotic mixtures. *Toxicol Sci, 107*(1), 93-105. doi:10.1093/toxsci/kfn206

Bedogni, G., Gastaldelli, A., Manco, M., De Col, A., Agosti, F., Tiribelli, C., & Sartorio, A. (2012). Relationship between fatty liver and glucose metabolism: A cross-sectional study in 571 obese children. *Nutrition, Metabolism and Cardiovascular Diseases, 22*(2), 120-126. doi:https://doi.org/10.1016/j.numecd.2010.05.003

Benet, M., Lahoz, A., Guzmán, C., Castell, J. V., & Jover, R. (2010). CCAAT/Enhancer-binding Protein α (C/EBPα) and Hepatocyte Nuclear Factor 4α (HNF4α) Synergistically Cooperate with Constitutive Androstane Receptor to Transactivate the Human Cytochrome P450 2B6 (CYP2B6) Gene: APPLICATION TO THE DEVELOPMENT OF A METABOLICALLY COMPETENT HUMAN HEPATIC CELL MODEL. *Journal of Biological Chemistry, 285*(37), 28457-28471. doi:10.1074/jbc.M110.118364

Breiman, L. (2001). Random Forests. *Machine Learning, 45*(1), 5-32. doi:10.1023/A:1010933404324

Bugianesi, E., McCullough, A. J., & Marchesini, G. (2005). Insulin resistance: A metabolic pathway to chronic liver disease. *Hepatology, 42*(5), 987-1000. doi:10.1002/hep.20920

Capdevila, J. H., Karara, A., Waxman, D. J., Martin, M. V., Falck, J. R., & Guengerich, F. P. (1990). Cytochrome P-450 enzyme-specific control of the regio- and enantiofacial selectivity of the microsomal arachidonic acid epoxygenase. *Journal of Biological Chemistry, 265*(19), 10865-10871.

Chung, H. S., Lee, M. J., Hwang, S. Y., Lee, H. J., Yoo, H. J., Seo, J.-A., . . . Choi, K. M. (2016). Circulating angiopoietin-like protein 8 (ANGPTL8) and ANGPTL3 concentrations in relation to anthropometric and metabolic profiles in Korean children: a prospective cohort study. *Cardiovascular Diabetology, 15*(1), 1. doi:10.1186/s12933-015-0324-y

Clemente, T. E., & Cahoon, E. B. (2009). Soybean oil: genetic approaches for modification of functionality and total content. *Plant Physiol, 151*(3), 1030-1040. doi:10.1104/pp.109.146282

Cusi, K. (2009). Role of insulin resistance and lipotoxicity in non-alcoholic steatohepatitis. *Clin Liver Dis, 13*(4), 545-563. doi:10.1016/j.cld.2009.07.009

Damiri, B., & Baldwin, W. S. (2018). Cyp2b-Knockdown Mice Poorly Metabolize Corn Oil and Are Age-Dependent Obese. *Lipids, 53*(9), 871-884. doi:10.1002/lipd.12095

Deol, P., Fahrmann, J., Yang, J., Evans, J. R., Rizo, A., Grapov, D., . . . Sladek, F. M. (2017). Omega-6 and omega-3 oxylipins are implicated in soybean oil-induced obesity in mice. *Scientific Reports, 7*(1), 12488. doi:10.1038/s41598-017-12624-9

Dong, B., Saha, P. K., Huang, W., Chen, W., Abu-Elheiga, L. A., Wakil, S. J., . . . Moore, D. D. (2009). Activation of nuclear receptor CAR ameliorates diabetes and fatty liver disease. *PNAS, 106*(44), 18831-18836.

Du, L., Yermalitsky, V., Ladd, P. A., Capdevila, J. H., Mernaugh, R., & Keeney, D. S. (2005). Evidence that cytochrome P450 CYP2B19 is the major source of epoxyeicosatrienoic acids in mouse skin. *Archives of Biochemistry and Biophysics, 435*(1), 125-133. doi:https://doi.org/10.1016/j.abb.2004.11.023

Dvorak, Z., Modriansky, M., Pichard-Garcia, L., Balaguer, P., Vilarem, M. J., Ulrichova, J., . . . Pascussi, J. M. (2003). Colchicine down-regulates cytochrome P450 2B6, 2C8, 2C9, and 3A4 in human hepatocytes by affecting their glucocorticoid receptor-mediated regulation. *Mol Pharmacol, 64*(1), 160-169. doi:10.1124/mol.64.1.160

Finn, R. D., Henderson, C. J., Scott, C. L., & Wolf, C. R. (2009). Unsaturated fatty acid regulation of cytochrome P450 expression via a CAR-dependent pathway. *Biochem. J., 417*, 43-54.

Foxenberg, R. J., McGarrigle, B. P., Knaak, J. B., Kostyniak, P. J., & Olson, J. R. (2007). Human hepatic cytochrome p450-specific metabolism of parathion and chlorpyrifos. *Drug Metab Dispos, 35*(2), 189-193. doi:10.1124/dmd.106.012427

Fuchs, M., & Sanyal, A. J. (2012). Lipotoxicity in NASH. *J Hepatol, 56*(1), 291-293. doi:10.1016/j.jhep.2011.05.019

Gangadhariah, M. H., Dieckmann, B. W., Lantier, L., Kang, L., Wasserman, D. H., Chiusa, M., . . . Luther, J. M. (2017). Cytochrome P450 epoxygenase-derived epoxyeicosatrienoic acids contribute to insulin sensitivity in mice and in humans. *Diabetologia, 60*(6), 1066-1075. doi:10.1007/s00125-017-4260-0

Gastaldelli, A., Cusi, K., Pettiti, M., Hardies, J., Miyazaki, Y., Berria, R., . . . DeFronzo, R. A. (2007). Relationship Between Hepatic/Visceral Fat and Hepatic Insulin Resistance in Nondiabetic and Type 2 Diabetic Subjects. *Gastroenterology, 133*(2), 496-506. doi:https://doi.org/10.1053/j.gastro.2007.04.068

Hales, C. M., Carroll, M. D., Fryar, C. D., & Ogden, C. L. (2020). *Prevalence of obesity and severe obesity among adults: United States, 2017–2018*.

Hashita, T., Sakuma, T., Akada, M., Nakajima, A., Yamahara, H., Ito, S., . . . Nemoto, N. (2008). Forkhead Box A2–Mediated Regulation of Female-Predominant Expression of the Mouse Cyp2b9 Gene. *Drug Metabolism and Disposition, 36*(6), 1080. doi:10.1124/dmd.107.019729

Heintz, M. M., Kumar, R., Rutledge, M. M., & Baldwin, W. S. (2019). Cyp2b-null male mice are susceptible to diet-induced obesity and perturbations in lipid homeostasis. *The Journal of Nutritional Biochemistry, 70*, 125-137. doi:https://doi.org/10.1016/j.jnutbio.2019.05.004

Heintz, M. M., McRee, R., Kumar, R., & Baldwin, W. S. (2020). Gender differences in diet-induced steatotic disease in Cyp2b-null mice. *PLOS ONE, 15*(3), e0229896-e0229896. doi:10.1371/journal.pone.0229896

Hernandez, J. P., Mota, L. C., & Baldwin, W. S. (2009). Activation of CAR and PXR by Dietary, Environmental and Occupational Chemicals Alters Drug Metabolism, Intermediary Metabolism, and Cell Proliferation. *Current Pharmacogenomics Personal Medicine, 7*(2), 81-105. doi:10.2174/187569209788654005

Hernandez, J. P., Mota, L. C., Huang, W., Moore, D. D., & Baldwin, W. S. (2009). Sexually dimorphic regulation and induction of P450s by the constitutive androstane receptor (CAR). *Toxicology, 256*(1), 53-64. doi:https://doi.org/10.1016/j.tox.2008.11.002

Hines, I. N., Hartwell, H. J., Feng, Y., Theve, E. J., Hall, G. A., Hashway, S., . . . Rogers, A. B. (2011). Insulin Resistance and Metabolic Hepatocarcinogenesis with Parent-of-Origin Effects in A×B Mice. *Am J Pathol, 179*(6), 2855-2865. doi:10.1016/j.ajpath.2011.08.014

Hodgson, E., & Rose, R. L. (2007). The importance of cytochrome P450 2B6 in the human metabolism of environmental chemicals. *Pharmacology & Therapeutics, 113*(2), 420-428. doi:https://doi.org/10.1016/j.pharmthera.2006.10.002

Hoek-van den Hil, E. F., van Schothorst, E. M., van der Stelt, I., Swarts, H. J., van Vliet, M., Amolo, T., . . . Keijer, J. (2015). Direct comparison of metabolic health effects of the flavonoids quercetin, hesperetin, epicatechin, apigenin and anthocyanins in high-fat-diet-fed mice. *Genes Nutr, 10*(4), 469. doi:10.1007/s12263-015-0469-z

Hongbing, W., & Masahiko, N. (2003). Transcriptional Regulation of Cytochrome P450 2B Genes by Nuclear Receptors. *Current Drug Metabolism, 4*(6), 515-525. doi:http://dx.doi.org/10.2174/1389200033489262

Huang da, W., Sherman, B. T., & Lempicki, R. A. (2009a). Bioinformatics enrichment tools: paths toward the comprehensive functional analysis of large gene lists. *Nucleic Acids Res, 37*(1), 1-13. doi:10.1093/nar/gkn923

Huang da, W., Sherman, B. T., & Lempicki, R. A. (2009b). Systematic and integrative analysis of large gene lists using DAVID bioinformatics resources. *Nat Protoc, 4*(1), 44-57. doi:10.1038/nprot.2008.211

Huang, Z., Zhang, M., Plec, A. A., Estill, S. J., Cai, L., Repa, J. J., . . . Tu, B. P. (2018). ACSS2 promotes systemic fat storage and utilization through selective regulation of genes involved in lipid metabolism. *Proceedings of the National Academy of Sciences, 115*(40), E9499-E9506. doi:10.1073/pnas.1806635115

Huber, W., Carey, V. J., Gentleman, R., Anders, S., Carlson, M., Carvalho, B. S., . . . Morgan, M. (2015). Orchestrating high-throughput genomic analysis with Bioconductor. *Nature Methods, 12*, 115. doi:10.1038/nmeth.3252

Jiang, J.-x., Zhang, S.-j., Liu, Y.-n., Lin, X.-x., Sun, Y.-h., Shen, H.-j., . . . Xie, Q.-m. (2014). EETs alleviate ox-LDL-induced inflammation by inhibiting LOX-1 receptor expression in rat pulmonary arterial endothelial cells. *European Journal of Pharmacology, 727*, 43-51. doi:https://doi.org/10.1016/j.ejphar.2014.01.045

Jou, J., Choi, S. S., & Diehl, A. M. (2008). Mechanisms of disease progression in nonalcoholic fatty liver disease. *Semin Liver Dis, 28*(4), 370-379. doi:10.1055/s-0028-1091981

Keeney, D. S., Skinner, C., Wei, S., Friedberg, T., & Waterman, M. R. (1998). A Keratinocyte-specific Epoxygenase, CYP2B12, Metabolizes Arachidonic Acid with Unusual Selectivity, Producing a Single Major Epoxyeicosatrienoic Acid. *Journal of Biological Chemistry, 273*(15), 9279-9284. doi:10.1074/jbc.273.15.9279

Kumar, N., Gupta, G., Anilkumar, K., Fatima, N., Karnati, R., Reddy, G. V., . . . Reddanna, P. (2016). 15-Lipoxygenase metabolites of α-linolenic acid, [13-(S)-HPOTrE and 13-(S)-HOTrE], mediate anti-inflammatory effects by inactivating NLRP3 inflammasome. *Scientific Reports, 6*(1), 31649. doi:10.1038/srep31649

Kumar, R., Litoff, E. J., Boswell, W. T., & Baldwin, W. S. (2018). High fat diet induced obesity is mitigated in Cyp3a-null female mice. *Chem Biol Interact, 289*, 129-140. doi:10.1016/j.cbi.2018.05.001

Kumar, R., Mota, L. C., Litoff, E. J., Rooney, J. P., Boswell, W. T., Courter, E., . . . Baldwin, W. S. (2017). Compensatory changes in CYP expression in three different toxicology mouse models: CAR-null, Cyp3a-null, and Cyp2b9/10/13-null mice. *PLOS ONE, 12*(3), e0174355. doi:10.1371/journal.pone.0174355

Lamba, V., Lamba, J., Yasuda, K., Strom, S., Davila, J., Hancock, M. L., . . . Schuetz, E. G. (2003). Hepatic CYP2B6 Expression: Gender and Ethnic Differences and Relationship to CYP2B6 Genotype and CAR (Constitutive Androstane Receptor) Expression. *Journal of Pharmacology and Experimental Therapeutics, 307*(3), 906. doi:10.1124/jpet.103.054866

Lang, F., & Voelkl, J. (2013). Therapeutic potential of serum and glucocorticoid inducible kinase inhibition. *Expert Opinion on Investigational Drugs, 22*(6), 701-714. doi:10.1517/13543784.2013.778971

Leung, A., Trac, C., Du, J., Natarajan, R., & Schones, D. E. (2016). Persistent Chromatin Modifications Induced by High Fat Diet. *J Biol Chem, 291*(20), 10446-10455. doi:10.1074/jbc.M115.711028

Li, C.-C., Lii, C.-K., Liu, K.-L., Yang, J.-J., & Chen, H.-W. (2007). DHA down-regulates phenobarbital-induced cytochrome P450 2B1 gene expression in rat primary hepatocytes by attenuating CAR translocation. *Toxicology and applied pharmacology, 225*(3), 329-336. doi:https://doi.org/10.1016/j.taap.2007.08.009

Li, L., Li, D., Heyward, S., & Wang, H. (2016). Transcriptional Regulation of CYP2B6 Expression by Hepatocyte Nuclear Factor 3β in Human Liver Cells. *PLOS ONE, 11*(3), e0150587-e0150587. doi:10.1371/journal.pone.0150587

Liu, M., Chen, P., Véricel, E., Lelli, M., Béguin, L., Lagarde, M., & Guichardant, M. (2013). Characterization and biological effects of di-hydroxylated compounds deriving from the lipoxygenation of ALA. *J Lipid Res, 54*(8), 2083-2094. doi:10.1194/jlr.M035139

Liu, S., Brown, J. D., Stanya, K. J., Homan, E., Leidl, M., Inouye, K., . . . Lee, C.-H. (2013). A diurnal serum lipid integrates hepatic lipogenesis and peripheral fatty acid use. *Nature, 502*(7472), 550-554. doi:10.1038/nature12710

Luo, M., & Peng, D. (2018). ANGPTL8: An Important Regulator in Metabolic Disorders. *Frontiers in endocrinology, 9*, 169-169. doi:10.3389/fendo.2018.00169

Lynch, C., Pan, Y., Li, L., Heyward, S., Moeller, T., Swaan, P. W., & Wang, H. (2014). Activation of the constitutive androstane receptor inhibits gluconeogenesis without affecting lipogenesis or fatty acid synthesis in human hepatocytes. *Toxicol Appl Pharmacol, 279*(1), 33-42. doi:10.1016/j.taap.2014.05.009

Masuoka, H. C., & Chalasani, N. (2013). Nonalcoholic fatty liver disease: an emerging threat to obese and diabetic individuals. *Annals of the New York Academy of Sciences, 1281*(1), 106-122. doi:10.1111/nyas.12016

Mo, S. L., Liu, Y. H., Duan, W., Wei, M. Q., Kanwar, J. R., & Zhou, S. F. (2009). Substrate specificity, regulation, and polymorphism of human cytochrome P450 2B6. *Curr Drug Metab, 10*(7), 730-753.

Mutoh, S., Sobhany, M., Moore, R., Perera, L., Pedersen, L., Sueyoshi, T., & Negishi, M. (2013). Phenobarbital indirectly activates the constitutive active androstane receptor (CAR) by inhibition of epidermal growth factor receptor signaling. *Science signaling, 6*(274), ra31-ra31. doi:10.1126/scisignal.2003705

Naudin, C. R., Maner-Smith, K., Owens, J. A., Wynn, G. M., Robinson, B. S., Matthews, J. D., . . . Jones, R. M. (2020). Lactococcus Lactis subsp. cremoris Elicits

Protection Against Metabolic Changes Induced by a Western-style Diet. *Gastroenterology*. doi:https://doi.org/10.1053/j.gastro.2020.03.010

Nebert, D. W., & Russell, D. W. (2002). Clinical importance of the cytochromes P450. *The Lancet, 360*(9340), 1155-1162. doi:https://doi.org/10.1016/S0140-6736(02)11203-7

Passegué, E., Jochum, W., Behrens, A., Ricci, R., & Wagner, E. F. (2002). JunB can substitute for Jun in mouse development and cell proliferation. *Nature Genetics, 30*(2), 158-166. doi:10.1038/ng790

Patwardhan, A. M., Scotland, P. E., Akopian, A. N., & Hargreaves, K. M. (2009). Activation of TRPV1 in the spinal cord by oxidized linoleic acid metabolites contributes to inflammatory hyperalgesia. *Proceedings of the National Academy of Sciences, 106*(44), 18820-18824. doi:10.1073/pnas.0905415106

Petersen, C., Nielsen, M. D., Andersen, E. S., Basse, A. L., Isidor, M. S., Markussen, L. K., . . . Pedersen, S. F. (2017). MCT1 and MCT4 Expression and Lactate Flux Activity Increase During White and Brown Adipogenesis and Impact Adipocyte Metabolism. *Scientific Reports, 7*(1), 13101. doi:10.1038/s41598-017-13298-z

Raubenheimer, P. J., Nyirenda, M. J., & Walker, B. R. (2006). A Choline-Deficient Diet Exacerbates Fatty Liver but Attenuates Insulin Resistance and Glucose Intolerance in Mice Fed a High-Fat Diet. *Diabetes, 55*(7), 2015-2020. doi:10.2337/db06-0097

Renaud, H. J., Cui, J. Y., Khan, M., & Klaassen, C. D. (2011). Tissue Distribution and Gender-Divergent Expression of 78 Cytochrome P450 mRNAs in Mice. *Toxicological Sciences, 124*(2), 261-277. doi:10.1093/toxsci/kfr240

Robinson, J. T., Thorvaldsdóttir, H., Winckler, W., Guttman, M., Lander, E. S., Getz, G., & Mesirov, J. P. (2011). Integrative genomics viewer. *Nature biotechnology, 29*(1), 24-26. doi:10.1038/nbt.1754

Schmidt, A. M., Sengupta, N., Saski, C. A., Noorai, R. E., & Baldwin, W. S. (2017). RNA sequencing indicates that atrazine induces multiple detoxification genes in Daphnia magna and this is a potential source of its mixture interactions with other chemicals. *Chemosphere, 189*, 699-708. doi:10.1016/j.chemosphere.2017.09.107

Schulze-Tanzil, G., de, S. P., Behnke, B., Klingelhoefer, S., Scheid, A., & Shakibaei, M. (2002). Effects of the antirheumatic remedy hox alpha--a new stinging nettle leaf extract--on matrix metalloproteinases in human chondrocytes in vitro. *Histol Histopathol, 17*(2), 477-485. doi:10.14670/hh-17.477

Shi, D., Chen, J., Wang, J., Yao, J., Huang, Y., Zhang, G., & Bao, Z. (2019). Circadian Clock Genes in the Metabolism of Non-alcoholic Fatty Liver Disease. *Frontiers in Physiology, 10*(423). doi:10.3389/fphys.2019.00423

Snider, N. T., Nast, J. A., Tesmer, L. A., & Hollenberg, P. F. (2009). A Cytochrome P450-Derived Epoxygenated Metabolite of Anandamide Is a Potent Cannabinoid Receptor 2-Selective Agonist. *Mol Pharmacol, 75*(4), 965. doi:10.1124/mol.108.053439

Sridar, C., Snider, N. T., & Hollenberg, P. F. (2011). Anandamide Oxidation by Wild-Type and Polymorphically Expressed CYP2B6 and CYP2D6. *Drug Metabolism and Disposition, 39*(5), 782. doi:10.1124/dmd.110.036707

Tang, J., Cao, Y., Rose, R. L., Brimfield, A. A., Dai, D., Goldstein, J. A., & Hodgson, E. (2001). Metabolism of chlorpyrifos by human cytochrome P450 isoforms and human, mouse, and rat liver microsomes. *Drug Metab Dispos, 29*(9), 1201-1204.

Tillman, M. C., Imai, N., Li, Y., Khadka, M., Okafor, C. D., Juneja, P., . . . Ortlund, E. A. (2020). Allosteric regulation of Thioesterase Superfamily Member 1 by free fatty acids and lysophosphatidylcholine. *bioRxiv*, 2020.2002.2018.954917. doi:10.1101/2020.02.18.954917

Valencia, T., Joseph, A., Kachroo, N., Darby, S., Meakin, S., & Gnanapragasam, V. J. (2011). Role and expression of FRS2 and FRS3 in prostate cancer. *BMC Cancer, 11*(1), 484. doi:10.1186/1471-2407-11-484

Villa, M., Gialitakis, M., Tolaini, M., Ahlfors, H., Henderson, C. J., Wolf, C. R., . . . Stockinger, B. (2017). Aryl hydrocarbon receptor is required for optimal B-cell proliferation. *The EMBO Journal, 36*(1), 116-128. doi:10.15252/embj.201695027

Wei, P., Zhang, J., Egan-Hafley, M., Liang, S., & Moore, D. D. (2000). The nuclear receptor CAR mediates specific xenobiotic induction of drug metabolism. *Nature, 407*(6806), 920-923. doi:10.1038/35038112

Wei, Y., Wu, H., Li, L., Liu, Z., Zhou, X., Zhang, Q., . . . Ding, X. (2012). Generation and Characterization of a CYP2A13/2B6/2F1-Transgenic Mouse Model. *Drug Metabolism and Disposition, 40*(6), 1144-1150. doi:10.1124/dmd.112.044826

Wencke, W., Sánchez-Cabo, F., & Ricote, M. (2015). GOplot: an R package for visually combining expression data with functional analysis.

Wiwi, C. A., Gupte, M., & Waxman, D. J. (2004). Sexually dimorphic P450 gene expression in liver-specific hepatocyte nuclear factor 4alpha-deficient mice. *Mol Endocrinol, 18*(8), 1975-1987. doi:10.1210/me.2004-0129

Wolfrum, C., Asilmaz, E., Luca, E., Friedman, J. M., & Stoffel, M. (2004). Foxa2 regulates lipid metabolism and ketogenesis in the liver during fasting and in diabetes. *Nature, 432*, 1027. doi:10.1038/nature03047 https://www.nature.com/articles/nature03047#supplementary-information

Wu, Y., Chitranshi, P., Loukotkova, L., Gamboa da Costa, G., Beland, F. A., Zhang, J., & Fang, J. L. (2017). Cytochrome P450-mediated metabolism of triclosan attenuates its cytotoxicity in hepatic cells. *Arch Toxicol, 91*(6), 2405-2423. doi:10.1007/s00204-016-1893-6

Xia, J., & Wishart, D. S. (2002). Using MetaboAnalyst 3.0 for Comprehensive Metabolomics Data Analysis. In *Current Protocols in Bioinformatics*: John Wiley & Sons, Inc.

Xu, A., Lam, M. C., Chan, K. W., Wang, Y., Zhang, J., Hoo, R. L. C., . . . Lam, K. S. L. (2005). Angiopoietin-like protein 4 decreases blood glucose and improves glucose tolerance but induces hyperlipidemia and hepatic steatosis in mice. *Proceedings of the National Academy of Sciences, 102*(17), 6086-6091. doi:10.1073/pnas.0408452102

Yabe, D., Komuro, R., Liang, G., Goldstein, J. L., & Brown, M. S. (2003). Liver-specific mRNA for Insig-2 down-regulated by insulin: Implications for fatty acid synthesis. *Proceedings of the National Academy of Sciences, 100*(6), 3155-3160. doi:10.1073/pnas.0130116100

Zanger, U. M., & Klein, K. (2013). Pharmacogenetics of cytochrome P450 2B6 (CYP2B6): advances on polymorphisms, mechanisms, and clinical relevance. *Front Genet, 4*, 24. doi:10.3389/fgene.2013.00024

Zhang, J., Yang, Q., Li, J., Zhong, Y., Zhang, L., Huang, Q., . . . Cai, C. (2017). Distinct differences in serum eicosanoids in healthy, enteritis and colorectal cancer individuals. *Metabolomics, 14*(1), 4. doi:10.1007/s11306-017-1293-9

Zhang, R. (2012). Lipasin, a novel nutritionally-regulated liver-enriched factor that regulates serum triglyceride levels. *Biochem Biophys Res Commun, 424*(4), 786-792. doi:https://doi.org/10.1016/j.bbrc.2012.07.038

Zhang, Y., Li, S., Donelan, W., Xie, C., Wang, H., Wu, Q., . . . Yang, L.-J. (2016). Angiopoietin-like protein 8 (betatrophin) is a stress-response protein that down-regulates expression of adipocyte triglyceride lipase. *Biochimica et Biophysica Acta (BBA) - Molecular and Cell Biology of Lipids, 1861*(2), 130-137. doi:https://doi.org/10.1016/j.bbalip.2015.11.003

Supplementary Materials

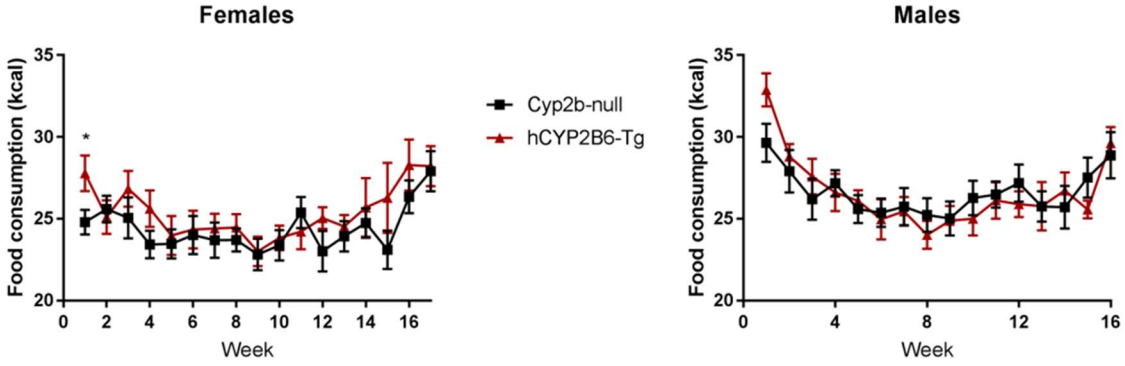

Supplementary File 5.1. Feed consumption of Cyp2b-null and hCYP2B6-Tg mice during 16-weeks of high-fat diet treatment. Female and male feed consumption was measured by weighing the food every alternate day. Data are presented as mean calories ± SEM. Statistical significance was determined by unpaired Student's t-tests (n=8). * indicates a p-value < 0.05.

Supplementary File 5.2. Differentially expressed gene lists of female and male HFD-fed hCYP2B6-Tg mice compared to HFD-fed Cyp2b-null mice.

Supplementary File 5.3. GO term enrichment analysis list of up and down-regulated genes in female and male HFD-fed hCYP2B6-Tg mice compared to HFD-fed Cyp2b-null mice.

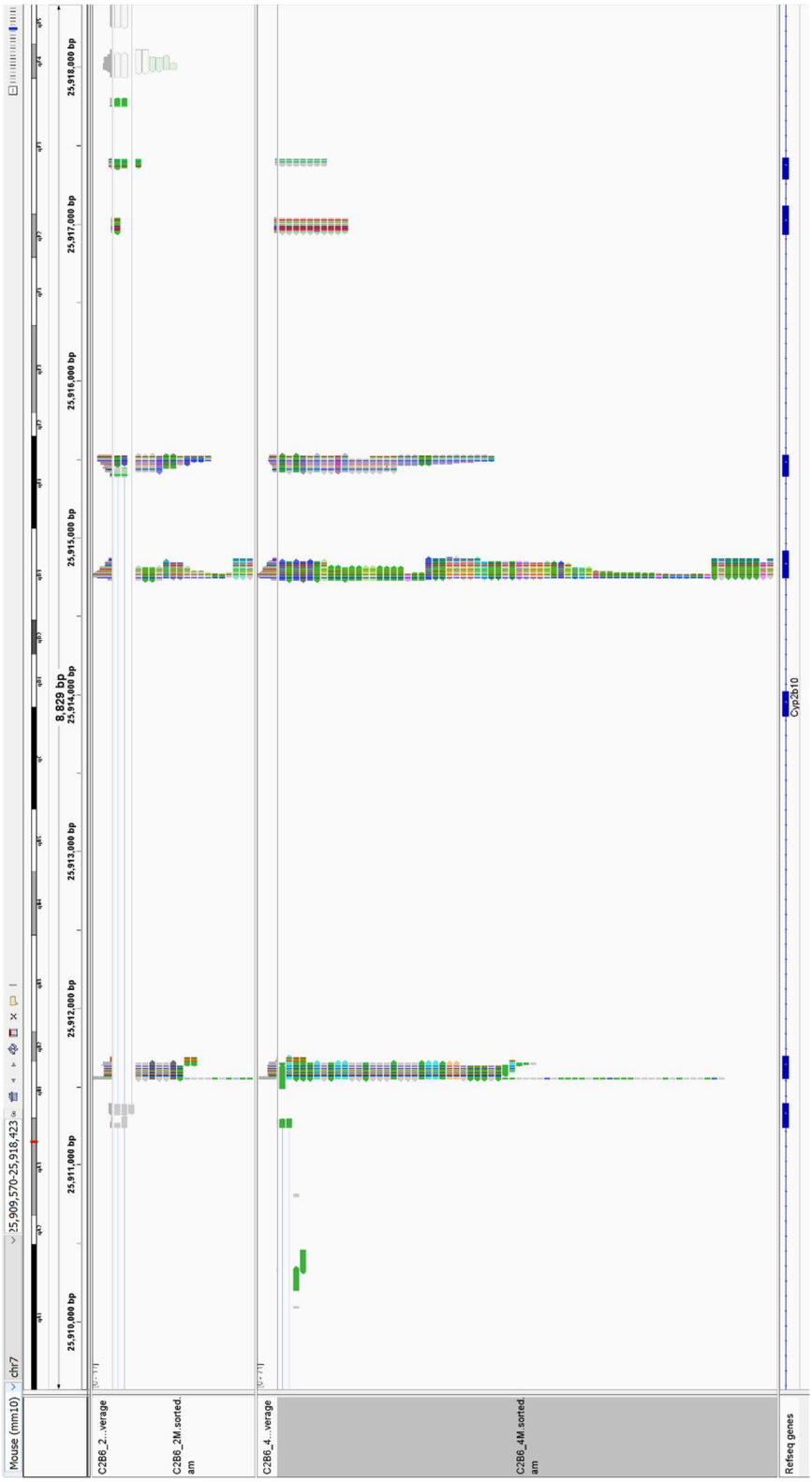
Mouse (mm10)
chr7
25,909,570-25,918,423
25,910,000 bp
25,911,000 bp
25,912,000 bp
25,913,000 bp
8,829 bp
25,914,000 bp
25,915,000 bp
25,916,000 bp
25,917,000 bp
25,918,000 bp
C2B6_2...verage
C2B6_2M.sorted.bam
C2B6_4...verage
C2B6_4M.sorted.bam
Refseq genes
Cyp2b10

Supplementary File 5.4. CYP2B6 alignment to Cyp2b10 on mouse reference genome. Alignment of male hCYP2B6-Tg bam files to mouse reference genome using IGV viewer (Robinson et al., 2011). The high number single nucleotide polymorphisms (SNPs) within the exon regions of Cyp2b10 is provides evidence of the human CYP2B6 misalignment to mouse Cyp2b10.

CHAPTER SIX

DISCUSSION

The purpose of this research was to determine the role of CYP2B in unsaturated fatty acid metabolism, obesity and nonalcoholic fatty liver disease (NAFLD). Our previously generated Cyp2b-null mouse model (R. Kumar et al., 2017) was used to continue to study the role of Cyp2b in NAFLD and progression to nonalcoholic steatohepatitis (NASH), as well as changes to the hepatic lipidome. In addition, CYP2B6 containing baculosomes and a newly generated humanized-CYP2B6-Tg mouse model were also used to determine the metabolic role of human CYP2B6 *in vitro* and *in vivo*, respectively.

Cyp2b-null male, but not female, mice are diet-induced obese, with increased accumulation of liver triglycerides and decreased serum triglycerides in both normal diet (ND)- and high fat diet (HFD)-fed Cyp2b-null male mice (Data by R. Kumar). The purpose of Aim 1 was to identify differentially expressed genes involved in energy and fatty acid metabolism in HFD-fed Cyp2b-null mice by RNA sequencing (RNAseq). Analysis of global hepatic gene expression using hierarchical clustering showed that ND-fed Cyp2b-null male mice share a similar hepatic gene expression profile to HFD-fed WT male mice, as samples from these groups clustered together. Venn diagrams confirmed that these two experimental groups share over 40% of each group's total number of differentially expressed genes, indicating that the Cyp2b-null genotype causes effects similar to that of a HFD-treatment potentially due to increased liver triglycerides in the

ND-fed Cyp2b-null male mice. In addition, shared GO terms, and similarly perturbed KEGG pathways also present evidence that ND-fed Cyp2b-null male mice have similar gene expression changes to HFD-fed WT mice, clearly indicating perturbations in lipid utilization and metabolism.

Conversely, significantly fewer genes were altered in female mice. Hierarchical clustering showed samples grouped by diet and not genotype. These gene expression results demonstrate the lack of response to the Cyp2b knockout and to a lesser extent, HFD, in female mice compared to male mice, similar to the physiological results from this study (Data by R. Kumar). Pre-menopausal female mice are generally considered partially resistant to obesity (Hong, Stubbins, Smith, Harvey, & Nunez, 2009; Spruiell et al., 2014). This resistance was also observed in our study and indicates that the sexually dimorphic Cyp2b9 and Cyp2b13 enzymes (Hernandez, Mota, Huang, Moore, & Baldwin, 2009; Wiwi, Gupte, & Waxman, 2004) are not the reason for the sexual dimorphism in obesity. However, the transcription factors that regulate Cyp2b including CAR, PXR, and FoxA2 may be partially responsible for the murine female resistance to obesity; as these transcription factors are important in lipid metabolism regulation and predominantly female expressed (Hashita et al., 2008; Hernandez et al., 2009; Ledda-Columbano et al., 2003; Spruiell et al., 2014).

The key findings from Aim 1 show perturbed lipid signaling regardless of diet in Cyp2b-null mice, supporting that hepatic murine Cyp2b genes are important in fatty acid metabolism and obesity. Although Cyp2b-null mice showed greater triglyceride accumulation and increased NAFLD, they showed very little hepatic inflammation,

suggesting Cyp2b-null mice may be protected from developing NASH. The purpose of Aim 2 was to determine whether a lack of Cyp2b worsens or remediates the pathological effects of NASH.

After 8 weeks of choline-deficient, L-amino acid-defined high fat diet (CDAHFD) treatment, female Cyp2b-null mice had lower white adipose tissue and liver mass, as well as a lower total body weight than their CDAHFD-fed WT counterparts. CDAHFD-fed Cyp2b-null females also exhibited significantly decreased levels of serum markers of liver injury including ALT, AST, and ALP and liver triglycerides compared to WT mice. Increased levels of liver inflammation marker, C-reactive protein, corticosterone, the main glucocorticoid in rodents, and transcriptomic up-regulation of glucocorticoid-mediated KEGG pathway genes including *Tnfrsf18* and *Calml4* and immunosuppressive gene *Tgfb2* (Yoshimura & Muto, 2011) in Cyp2b-null females, suggest protection from liver damage is due to glucocorticoid-mediated repression of immune responses, resulting in less inflammation.

In contrast, CDAHFD-fed male mice experienced diet-induced weight loss and increased serum markers of liver injury regardless of genotype. CDAHFD-fed Cyp2b-null males had increased serum creatine kinase levels by a 1.5-fold compared to all other groups, suggesting that CDAHFD treatment caused damage to Cyp2b-null males in other tissues, such as cardiac or skeletal muscle, in addition to liver (Yen et al., 2017). Liver steatosis also increased in CDAHFD-fed male mice, with higher liver triglyceride levels in Cyp2b-null compared to WT mice. In addition, numerous genes associated with fatty acid metabolism were down-regulated in CDAHFD-fed WT male mice compared to ND-

fed counterparts, and these genes were further down-regulated in CDAHFD-fed Cyp2b-null male mice, suggesting greater steatosis in the CDAHFD-fed Cyp2b-null male mice, which concurred with hepatic triglyceride levels. Although fibrosis was heavily induced by CDAHFD treatment in both sexes, there were few differences in fibrosis markers between CDAHFD-fed genotypes, except for slightly lower hydroxyproline levels in the livers of Cyp2b-null female mice.

These results show that Cyp2b-null female mice are protected from diet-induced steatosis and to a lesser extent diet-induced NASH. In Cyp2b-null males, very few differences in NASH markers were observed while NAFLD increased, corroborating with results in Aim 1. These studies indicate a role for Cyp2b in fatty liver disease that differs based on gender, probably due to the highly sexually dimorphic nature of murine hepatic Cyp2b members (Hernandez et al., 2009; Ledda-Columbano et al., 2003; Renaud, Cui, Khan, & Klaassen, 2011; Wiwi et al., 2004). Overall, results from Aim 2 confirm that increased NAFLD development does not necessarily lead to progressive NASH. Often NASH patients have little or no liver steatosis, in fact, only 10-20% of patients with NAFLD progress to NASH primarily due to failure of antilipotoxic protection (Tilg & Moschen, 2010).

Previous observations have indicated that Cyp2b-KD mice developed age-onset obesity in males with a significant lesser effect in females (Damiri & Baldwin, 2018). In addition, Cyp2b-null male mice are more susceptible to obesity than WT mice when fed a HFD as determined in Aim 1. The hepatic phospholipid profile has not been investigated in Cyp2b-null mice. The purpose of Aim 3 was to determine changes in the hepatic

phospholipid profile of healthy, obese and old Cyp2b-null male mice. Phospholipid species were identified and quantified from the livers of male Cyp2b-null and WT young (4.5 mo) ND and HFD-fed mice and old (9 mo) mice by LC-MS/MS.

Age had the strongest effect on the hepatic phospholipid profile, followed by a HFD and then a loss of Cyp2b in male mice. The effect of age also superseded the effect of HFD on the blood lipidome of female mice (9). Principle component analysis (PCA) showed lipid profiles from ND-fed young mice, especially WT, were associated with more n-3 fatty acids, including α-linolenic acid (ALA) and docosahexaenoic acid (DHA) which help to maintain healthy lipid homeostasis in both humans (Amigó et al., 2020; Catapano et al., 2016) and mice (Pauter et al., 2014). Interestingly, the lipid profile from ND-fed Cyp2b-null mice was situated between ND-fed WT and HFD-fed groups on the PCA plot, concurring with triglyceride levels and findings from Aim 1. Age increased total and LDL-cholesterol, as previously found in both humans and rodents (18, 19), and these biomarkers were further exacerbated in old Cyp2b-null mice. In addition, total body and liver weight, serum VLDL, TAG, and ALT levels were all significantly higher in old Cyp2b-null mice compared to WT counterparts as well as all other featured groups. PCA results conclude old WT and Cyp2b-null mice are associated with unhealthy physiological, serum, and lipid profiles that contribute to an increased risk of metabolic disease and obesity (31, 32). The combination of age and a lack of Cyp2b enhanced adverse effects, as it resulted in dyslipidemia and liver injury in old Cyp2b-null mice. These findings suggest accelerated aging and metabolic disease in Cyp2b-null mice.

The purpose of Aim 4 was to investigate the role of human CYP2B6 in polyunsaturated fatty acid (PUFA) metabolism *in vitro* and *in vivo*. Using CYP2B6 containing baculosomes, several PUFAs including arachidonic acid (AA), linoleic acid (LA), DHA, and ALA were identified as endogenous inhibitors of human CYP2B6 with IC50's below 10μM. However, these endogenous inhibitors have 10-15x's less affinity to CYP2B6 compared to known xenobiotic inhibitors of CYP2B6, such as nonylphenol (Hernandez et al., 2007). In addition, these PUFAs are also metabolized by CYP2B6, with a greater than 20-fold preference for the metabolism of α-linolenic acid to 9-HOTrE and to a lesser extent 13-HOTrE. This high concentration of a lipid metabolite suggests the potential for 9-HOTrE as an important signaling molecule.

When investigating the role of CYP2B6 *in vivo* during a 16-week HFD treatment, hCYP2B6-Tg mice, females and to a lesser extent males, reduced weight gain. However, male mice increased liver triglycerides compared to HFD-fed Cyp2b-null mice. This lipid accumulation in the liver is suspected to be protective against metabolic disease (at least initially) in hCYP2B6-Tg mice based on glucose sensitivity, as an increase in inert hepatic triglycerides can provide lipotoxic protection from other fatty acid-derived species (Cusi, 2009; Jou, Choi, & Diehl, 2008). Unexpectedly, lipidomic analysis of serum and liver samples revealed that most significantly altered PUFA metabolites in either tissue were LA or AA oxylipin metabolites, also primarily in the 9- and 13-positions. These results are most likely attributed to the high-fat diet which had a much greater ratio of n-6 to n-3 PUFAs available for metabolism as the main source of PUFAs in the diet was soybean oil (Clemente & Cahoon, 2009).

Differential gene expression revealed several up-regulated circadian rhythm-associated genes in HFD-fed hCYP2B6-Tg mice compared to Cyp2b-null mice. Circadian genes are important regulators of hepatic lipid homeostasis (Shi et al., 2019) and lipid distribution (Liu et al., 2013). The epidermal growth factor receptor *(Egfr*) was down-regulated in male HFD-fed hCYP2B6-Tg mice compared to Cyp2b-null mice. The down-regulation of EGFR provides a mechanism for the activation of CAR and subsequent induction of *Cyp2b10*/CYP2B6 (Mutoh et al., 2013). Conversely, Cyp2b10 was not differentially expressed in females, as *Egfr* was up-regulated in female hCYP2B6-Tg mice, potentially explaining the physiological and lipid metabolism differences between male and female hCYP2B6-Tg mice.

Overall, human CYP2B6 is an anti-obesity enzyme that metabolizes PUFAs but is not as effective as murine Cyp2b9 or Cyp2b10 in reversing diet-induced obesity (Aim 1). With advancements in detection methods, the number of endo- and xenobiotic substrates of CYP2B6 is increasing (Wang & Tompkins, 2008), including over 60 clinical drugs (Mo et al., 2009), numerous environmental toxicants (Hodgson & Rose, 2007), as well as steroids, bile acids and fatty acids (Mo et al., 2009). Findings from Aim 4 define a mechanism by which chemical inhibition of CYP2B6 can increase diet-induced obesity and metabolic disorders through reduced production of important oxylipins and changes in circadian-mediated regulation of lipid metabolism and distribution.

Future studies

Based on the findings from Aim 4, CYP2B6 metabolizes PUFAs into lipid metabolites that are important mediators of pro- and anti-inflammation such as LA-9-

HODE and 13-KODE (*in vivo*), and ALA-13-HOTrE (*in vitro*) (N. Kumar et al., 2016; Warner et al., 2017). Future research examining the roles of ALA, LA, and AA CYP2B6 metabolites as signaling molecules, especially in 9- and 13- positions, should be further investigated *in vitro* (initially) using cells from a variety of tissues including liver, adipose, and skeletal muscle. Lipid metabolites are endogenous ligands of several cell-surface and nuclear receptors, such as peroxisome proliferator-activated receptors (PPARs), which are present in many cell types and act as moderators of systemic and cellular metabolic functions in different tissues (Wahli & Michalik, 2012). Results from this work could potentially identify key signaling metabolites that are important in treating metabolic diseases.

In addition, our hCYP2B6-Tg mouse model can be used to study interactions between chemical inhibitors of CYP2B6 and HFD treatment. Perfluorooctanesulfonic acid (PFOS) is an anthropogenic fluorosurfactant and a persistent organic pollutant found worldwide. Exposure to PFOS disrupts normal hepatic lipid metabolism and causes steatosis in animal models (Das et al., 2017; Wan et al., 2012). Furthermore, fatty liver induces Cyp2b in PFOS-exposed models (Dong et al., 2016). Initial *in vitro* studies conducted in our lab have determined PFOS is an inhibitor of CYP2B6. Research is currently underway to test whether Cyp2b-null or hCYP2B6-Tg mice are more sensitive to NAFLD following exposure to PFOS.

Conclusion

Over one third of adults are considered overweight worldwide and 13% are obese (WHO, 2020). Furthermore, global prevalence of NAFLD is about 25%, with the

prevalence of obesity in over 50% and 81% of NAFLD and NASH patients, respectively (Younossi et al., 2016). As rates of obesity and diabetes increase worldwide, it is predicted that NAFLD will also become even more prevalent. Findings from this work support the importance of considering exposure to environmental toxicants as a contributing factor to the development of obesity and fatty liver disease. The inhibition of key detoxification enzymes, such as CYP2B6, by pesticides, pharmaceuticals, or dietary fats may perturb lipid homeostasis and metabolism based on studies using our Cyp2b-null and hCYP2B6-Tg mouse models.

This research also enforces the value of investigating gender differences in metabolic and liver disease studies (Durazzo et al., 2014; Ohta et al., 2014). Our results differed by gender, most likely due to the sexually dimorphic expression of murine Cyp2b members in both of our mouse models. Human CYP2B6 expression is also sexually dimorphic, as it is predominantly expressed in females (Lamba et al., 2003). Although the exact role of CYP2B6 in NAFLD and NASH has yet to be determined (Fisher et al., 2009; Gao et al., 2016), CYP2B6 polymorphisms also need to be considered in terms of susceptibility to fatty liver disease, as CYP2B6 is one of the most polymorphic CYP genes in humans (Zanger & Klein, 2013).

In addition, there are numerous interspecies similarities and differences with regards to species-specific CYP isoform composition, expression and catalytic activities (Martignoni, Groothuis, & de Kanter, 2006). Our work established a significant difference in the role of fatty acid metabolism between murine Cyp2b and human CYP2B6, as murine Cyp2b decreases, while human CYP2B6 increases lipid

accumulation in the liver. Additionally, we have also determined using both *in vitro* and *in vivo* models that PUFAs, especially LA, and ALA, are metabolized preferentially in the 9- and 13- positions by CYP2B6. These results as well as others previously discussed, validate our recently established hCYP2B6-Tg mouse model as a relevant tool for studying functions of CYP2B6 in human liver.

References

Amigó, N., Akinkuolie, A. O., Chiuve, S. E., Correig, X., Cook, N. R., & Mora, S. (2020). Habitual Fish Consumption, n‐3 Fatty Acids, and Nuclear Magnetic Resonance Lipoprotein Subfractions in Women. *Journal of the American Heart Association, 9*(5), e014963. doi:doi:10.1161/JAHA.119.014963

Catapano, A. L., Graham, I., De Backer, G., Wiklund, O., Chapman, M. J., Drexel, H., . . . Cooney, M. T. (2016). 2016 ESC/EAS Guidelines for the Management of Dyslipidaemias. *Eur Heart J, 37*(39), 2999-3058. doi:10.1093/eurheartj/ehw272

Clemente, T. E., & Cahoon, E. B. (2009). Soybean oil: genetic approaches for modification of functionality and total content. *Plant Physiol, 151*(3), 1030-1040. doi:10.1104/pp.109.146282

Cusi, K. (2009). Role of insulin resistance and lipotoxicity in non-alcoholic steatohepatitis. *Clin Liver Dis, 13*(4), 545-563. doi:10.1016/j.cld.2009.07.009

Damiri, B., & Baldwin, W. S. (2018). Cyp2b-Knockdown Mice Poorly Metabolize Corn Oil and Are Age-Dependent Obese. *Lipids, 53*(9), 871-884. doi:10.1002/lipd.12095

Das, K. P., Wood, C. R., Lin, M. T., Starkov, A. A., Lau, C., Wallace, K. B., . . . Abbott, B. D. (2017). Perfluoroalkyl acids-induced liver steatosis: Effects on genes controlling lipid homeostasis. *Toxicology, 378*, 37-52. doi:https://doi.org/10.1016/j.tox.2016.12.007

Dong, H., Curran, I., Williams, A., Bondy, G., Yauk, C. L., & Wade, M. G. (2016). Hepatic miRNA profiles and thyroid hormone homeostasis in rats exposed to dietary potassium perfluorooctanesulfonate (PFOS). *Environmental Toxicology and Pharmacology, 41*, 201-210. doi:https://doi.org/10.1016/j.etap.2015.12.009

Durazzo, M., Belci, P., Collo, A., Prandi, V., Pistone, E., Martorana, M., . . . Bo, S. (2014). Gender specific medicine in liver diseases: a point of view. *World journal of gastroenterology, 20*(9), 2127-2135. doi:10.3748/wjg.v20.i9.2127

Fisher, C. D., Lickteig, A. J., Augustine, L. M., Ranger-Moore, J., Jackson, J. P., Ferguson, S. S., & Cherrington, N. J. (2009). Hepatic cytochrome P450 enzyme alterations in humans with progressive stages of nonalcoholic fatty liver disease. *Drug metabolism and disposition: the biological fate of chemicals, 37*(10), 2087-2094. doi:10.1124/dmd.109.027466

Gao, J., Zhou, J., He, X.-P., Zhang, Y.-F., Gao, N., Tian, X., . . . Qiao, H.-L. (2016). Changes in cytochrome P450s-mediated drug clearance in patients with hepatocellular carcinoma in vitro and in vivo: a bottom-up approach. *Oncotarget, 7*(19), 28612-28623. doi:10.18632/oncotarget.8704

Hashita, T., Sakuma, T., Akada, M., Nakajima, A., Yamahara, H., Ito, S., . . . Nemoto, N. (2008). Forkhead Box A2–Mediated Regulation of Female-Predominant Expression of the Mouse Cyp2b9 Gene. *Drug Metabolism and Disposition, 36*(6), 1080. doi:10.1124/dmd.107.019729

Hernandez, J. P., Huang, W., Chapman, L. M., Chua, S., Moore, D. D., & Baldwin, W. S. (2007). The environmental estrogen, nonylphenol, activates the constitutive androstane receptor. *Toxicol Sci, 98*(2), 416-426. doi:10.1093/toxsci/kfm107

Hernandez, J. P., Mota, L. C., Huang, W., Moore, D. D., & Baldwin, W. S. (2009). Sexually dimorphic regulation and induction of P450s by the constitutive androstane receptor (CAR). *Toxicology, 256*(1), 53-64. doi:https://doi.org/10.1016/j.tox.2008.11.002

Hodgson, E., & Rose, R. L. (2007). The importance of cytochrome P450 2B6 in the human metabolism of environmental chemicals. *Pharmacology & Therapeutics, 113*(2), 420-428. doi:https://doi.org/10.1016/j.pharmthera.2006.10.002

Hong, J., Stubbins, R. E., Smith, R. R., Harvey, A. E., & Nunez, N. P. (2009). Differential susceptibility to obesity between male, female and ovariectomized female mice. *Nutr J, 8*, 11. doi:10.1186/1475-2891-8-11

Jou, J., Choi, S. S., & Diehl, A. M. (2008). Mechanisms of disease progression in nonalcoholic fatty liver disease. *Semin Liver Dis, 28*(4), 370-379. doi:10.1055/s-0028-1091981

Kumar, N., Gupta, G., Anilkumar, K., Fatima, N., Karnati, R., Reddy, G. V., . . . Reddanna, P. (2016). 15-Lipoxygenase metabolites of α-linolenic acid, [13-(S)-HPOTrE and 13-(S)-HOTrE], mediate anti-inflammatory effects by inactivating NLRP3 inflammasome. *Scientific Reports, 6*(1), 31649. doi:10.1038/srep31649

Kumar, R., Mota, L. C., Litoff, E. J., Rooney, J. P., Boswell, W. T., Courter, E., . . . Baldwin, W. S. (2017). Compensatory changes in CYP expression in three different toxicology mouse models: CAR-null, Cyp3a-null, and Cyp2b9/10/13-null mice. *PLOS ONE, 12*(3), e0174355. doi:10.1371/journal.pone.0174355

Lamba, V., Lamba, J., Yasuda, K., Strom, S., Davila, J., Hancock, M. L., . . . Schuetz, E. G. (2003). Hepatic CYP2B6 Expression: Gender and Ethnic Differences and Relationship to CYP2B6 Genotype and CAR (Constitutive Androstane Receptor) Expression. *Journal of Pharmacology and Experimental Therapeutics, 307*(3), 906. doi:10.1124/jpet.103.054866

Ledda-Columbano, G. M., Pibiri, M., Concas, D., Molotzu, F., Simbula, G., Cossu, C., & Columbano, A. (2003). Sex difference in the proliferative response of mouse hepatocytes to treatment with the CAR ligand, TCPOBOP. *Carcinogenesis, 24*(6), 1059-1065. doi:10.1093/carcin/bgg063

Liu, S., Brown, J. D., Stanya, K. J., Homan, E., Leidl, M., Inouye, K., . . . Lee, C.-H. (2013). A diurnal serum lipid integrates hepatic lipogenesis and peripheral fatty acid use. *Nature, 502*(7472), 550-554. doi:10.1038/nature12710

Martignoni, M., Groothuis, G. M., & de Kanter, R. (2006). Species differences between mouse, rat, dog, monkey and human CYP-mediated drug metabolism, inhibition and induction. *Expert Opin Drug Metab Toxicol, 2*(6), 875-894. doi:10.1517/17425255.2.6.875

Mo, S. L., Liu, Y. H., Duan, W., Wei, M. Q., Kanwar, J. R., & Zhou, S. F. (2009). Substrate specificity, regulation, and polymorphism of human cytochrome P450 2B6. *Curr Drug Metab, 10*(7), 730-753.

Mutoh, S., Sobhany, M., Moore, R., Perera, L., Pedersen, L., Sueyoshi, T., & Negishi, M. (2013). Phenobarbital indirectly activates the constitutive active androstane receptor (CAR) by inhibition of epidermal growth factor receptor signaling. *Science signaling, 6*(274), ra31-ra31. doi:10.1126/scisignal.2003705

Ohta, T., Katsuda, Y., Miyajima, K., Sasase, T., Kimura, S., Tong, B., & Yamada, T. (2014). Gender differences in metabolic disorders and related diseases in Spontaneously Diabetic Torii-Lepr(fa) rats. *Journal of diabetes research, 2014*, 841957-841957. doi:10.1155/2014/841957

Pauter, A. M., Olsson, P., Asadi, A., Herslöf, B., Csikasz, R. I., Zadravec, D., & Jacobsson, A. (2014). Elovl2 ablation demonstrates that systemic DHA is endogenously produced and is essential for lipid homeostasis in mice. *J Lipid Res, 55*(4), 718-728. doi:10.1194/jlr.M046151

Renaud, H. J., Cui, J. Y., Khan, M., & Klaassen, C. D. (2011). Tissue Distribution and Gender-Divergent Expression of 78 Cytochrome P450 mRNAs in Mice. *Toxicological Sciences, 124*(2), 261-277. doi:10.1093/toxsci/kfr240

Shi, D., Chen, J., Wang, J., Yao, J., Huang, Y., Zhang, G., & Bao, Z. (2019). Circadian Clock Genes in the Metabolism of Non-alcoholic Fatty Liver Disease. *Frontiers in Physiology, 10*(423). doi:10.3389/fphys.2019.00423

Spruiell, K., Richardson, R. M., Cullen, J. M., Awumey, E. M., Gonzalez, F. J., & Gyamfi, M. A. (2014). Role of pregnane X receptor in obesity and glucose homeostasis in male mice. *J Biol Chem, 289*(6), 3244-3261. doi:10.1074/jbc.M113.494575

Tilg, H., & Moschen, A. R. (2010). Evolution of inflammation in nonalcoholic fatty liver disease: the multiple parallel hits hypothesis. *Hepatology, 52*(5), 1836-1846. doi:10.1002/hep.24001

Wahli, W., & Michalik, L. (2012). PPARs at the crossroads of lipid signaling and inflammation. *Trends in Endocrinology & Metabolism, 23*(7), 351-363. doi:https://doi.org/10.1016/j.tem.2012.05.001

Wan, H. T., Zhao, Y. G., Wei, X., Hui, K. Y., Giesy, J. P., & Wong, C. K. C. (2012). PFOS-induced hepatic steatosis, the mechanistic actions on β-oxidation and lipid transport. *Biochimica et Biophysica Acta (BBA) - General Subjects, 1820*(7), 1092-1101. doi:https://doi.org/10.1016/j.bbagen.2012.03.010

Wang, H., & Tompkins, L. M. (2008). CYP2B6: New Insights into a Historically Overlooked Cytochrome P450 Isozyme. *Current Drug Metabolism, 9*, 598-610.

Warner, D. R., Liu, H., Miller, M. E., Ramsden, C. E., Gao, B., Feldstein, A. E., . . . Kirpich, I. A. (2017). Dietary Linoleic Acid and Its Oxidized Metabolites Exacerbate Liver Injury Caused by Ethanol via Induction of Hepatic Proinflammatory Response in Mice. *Am J Pathol, 187*(10), 2232-2245. doi:10.1016/j.ajpath.2017.06.008

WHO. (2020). Obesity and overweight. Retrieved from

Wiwi, C. A., Gupte, M., & Waxman, D. J. (2004). Sexually dimorphic P450 gene expression in liver-specific hepatocyte nuclear factor 4alpha-deficient mice. *Mol Endocrinol, 18*(8), 1975-1987. doi:10.1210/me.2004-0129

Yen, C.-H., Wang, K.-T., Lee, P.-Y., Liu, C.-C., Hsieh, Y.-C., Kuo, J.-Y., . . . Lam, C. S. P. (2017). Gender-differences in the associations between circulating creatine kinase, blood pressure, body mass and non-alcoholic fatty liver disease in

asymptomatic asians. *PLOS ONE, 12*(6), e0179898. doi:10.1371/journal.pone.0179898

Yoshimura, A., & Muto, G. (2011). TGF-beta function in immune suppression. *Curr Top Microbiol Immunol, 350*, 127-147. doi:10.1007/82_2010_87

Younossi, Z. M., Koenig, A. B., Abdelatif, D., Fazel, Y., Henry, L., & Wymer, M. (2016). Global epidemiology of nonalcoholic fatty liver disease—Meta-analytic assessment of prevalence, incidence, and outcomes. *Hepatology, 64*(1), 73-84. doi:10.1002/hep.28431

Zanger, U. M., & Klein, K. (2013). Pharmacogenetics of cytochrome P450 2B6 (CYP2B6): advances on polymorphisms, mechanisms, and clinical relevance. *Front Genet, 4*, 24. doi:10.3389/fgene.2013.00024